Effects of antifungals and long-term macrophage exposure on *Candida* species: mode of action and fungal response

Dissertation

To fulfil the

requirements for the degree of

„doctor rerum naturalium“ (Dr. rer. nat.)

FRIEDRICH-SCHILLER-
UNIVERSITÄT
JENA

Submitted to the Council of the Faculty
of Biological Sciences
of the Friedrich Schiller University Jena

by Diplom-Biochemiker Daniel Fischer

born on 25st February 1989 in Halberstadt

Angaben zu den Gutachtern

Erstgutachter

Prof. Dr. Bernhard Hube

Lehrstuhl für Mikrobielle Pathogenität, Friedrich-Schiller-Universität Jena

Zweitgutachterin

Prof. Dr. Erika Kothe

Lehrstuhl für Mikrobielle Kommunikation, Friedrich-Schiller-Universität Jena

Externe Gutachterin

Prof. Dr. Carolina H. Pohl-Albertyn

Lehrstuhl “Pathogenic Yeasts”, University of the Free State, Bleomfontein, South Africa

Datum der öffentlichen Verteidigung

26.04.2021

15:00 – 17:00 Uhr

This thesis was prepared at the “Leibniz Institute for Natural Product Research and Infection Biology e. V. – Hans Knöll Institute”, Jena in the Department of Microbial Pathogenicity Mechanisms (MPM) under the supervision of Prof. Bernhard Hube.

This thesis was mainly financed by budget resources of the Department of Microbial Pathogenicity Mechanisms (MPM) of the Leibniz Institute for Natural Product Research and Infection Biology e. V. – Hans Knöll Institute. Minor contributions from other resources are indicated appropriately on the corresponding manuscripts.

Table of content

Summary

Pathogenic fungi of humans and plants are an important, yet frequently underestimated problem in the medical care system and in agriculture. Especially fungi which are pathogenic for humans might become even more relevant in the near future: anthropogenic climate change and the use of clinical antimycotic compound classes in agriculture promote selection mechanisms which enhance the probability that new and/or resistant fungal species or strains will cause infections in humans. Still, only few treatment options for fungal infections are available today. In this work, a two-pronged approach was followed:

A) A diversification of agriculturally and clinically used antimycotics could contribute to better clinical treatment options: by directly enhancing the available clinical treatment options and/or by introducing antimycotics with a different mode of action into agriculture, which should alter selection pressures for environmentally derived fungal pathogens. This should lead to less frequent appearances of environmental fungal pathogens with resistances in the clinic. To this end, the mode of action and possible applications of the new antifungal jagaricin were investigated in this study. As its mode of action, lysis of susceptible biological membranes by formation of large lesions which allow Ca^{2+} flux was identified. Correspondingly, tolerance of the fungus towards jagaricin was determined to a large part by its ability to detect jagaricin-induced Ca^{2+} influx. This relied mainly on the calcineurin signalling pathway, which was required to initiate adequate membrane repair processes. The application spectrum of jagaricin in its unmodified form was found to be limited to agricultural applications, as jagaricin was found to be toxic for human, but not plant cells.

B) A comprehensive understanding of the interactions of human pathogenic fungi with the human immune system during antimycotic treatment can allow the development of targeted treatment strategies. This requires knowledge of both, the immune system components which determine the interaction on the host side and the selection pressures exerted by antifungal treatment and immune reactions which act on the fungal pathogen. It has been shown before that immune evasion is of great importance in *Candida glabrata* infection processes. Especially its interaction with mononuclear cells plays a key role: *C. glabrata* exhibited a comparatively high affinity to these immune cells in several *in vitro* and *in vivo* infection models and has been shown to survive and replicate within their phagosomes, probably by interfering with phagolysosome maturation. However, previous models were not able to reflect long-term persistence of *C. glabrata* yeasts in macrophages as part of its immune evasion process. This scientific model gap was closed with the methods developed in this work, and important fungal mechanisms and contributing factors were characterized by large scale approaches

(transcriptome, mutant library screening). Among the most important results, *C. glabrata* was found to be under constant stress in the phagosome within the week-long investigation period. Accordingly, fungal factors which are important for the entry into, maintenance of, and exit from cellular quiescence were found to be critical for persistence of *C. glabrata* in macrophages. Correspondingly, large energy-consuming processes like the gene expression apparatus were continuously downregulated in *C. glabrata* yeasts, at least on the transcriptional level. A continuously applied long-term treatment with antimycotics (caspofungin, amphotericin B) *in vitro* was not able to fully eradicate *C. glabrata* yeasts from human macrophages, which points to a possible clinical relevance of yeasts which persist in a cellular quiescent state in macrophages. Specific aspects of the quiescent cellular state of *C. glabrata* in macrophages were investigated or discussed further, e.g. the role of the protectant molecule trehalose and its metabolism, the phosphate metabolism, and the potential function of the yet unidentified sexual cycle of *C. glabrata* in macrophages. Thereby, the new long-term model revealed potential explanations on why clinical treatment of *C. glabrata* infections is often difficult and on the potential evolutionary selection paths of *C. glabrata* in a clinical infection.

Both approaches which were employed in this study – the investigation of a potential drug, which was discovered from interactions of fungi with their environment, and the study of pathogenicity mechanisms of yeasts – have the potential to expand our knowledge on the interactions of fungi with their environment. This knowledge can be used in the future to treat pathogenic fungi and improve existing treatment strategies.

Zusammenfassung

Human- und pflanzenpathogene Pilze sind ein bedeutendes, aber oft unterschätztes Problem in Gesundheitswesen und Landwirtschaft. Besonders die Bedeutung humanpathogener Pilze könnte in naher Zukunft noch zunehmen: der anthropogene Klimawandel und der Einsatz von auch in der Klinik verwendeten Antimykotikaklassen in der Landwirtschaft fördert Selektionsmechanismen, die das Auftreten neuer und/oder resistenter Pilzspezies und -stämme wahrscheinlicher machen. Dennoch stehen weiterhin nur wenige Behandlungsmöglichkeiten für Mykosen zur Verfügung. In dieser Arbeit wurde nun ein mehrgleisiger Lösungsansatz verfolgt.

A) Eine Diversifizierung der landwirtschaftlich und klinisch eingesetzten Antimykotika könnte dazu beitragen, dass Behandlungsmöglichkeiten in der Klinik verbessert werden: sowohl durch mehr verfügbare klinische Behandlungsoptionen und/oder durch Nutzung von Antimykotika in der Landwirtschaft mit anderem Wirkmechanismus als in der Klinik, was zu einem anderen Selektionsdruck auf Umweltpathogene führt. Letzteres sollte zu einem verringerten Auftreten antimykotikaresistenter Umwelt-Pilzpathogenen in der Klinik führen. Zu diesem Zweck wurde in dieser Arbeit der Wirkmechanismus und das Anwendungsspektrum des neuen Antimykotikums Jagaricin untersucht. Als Wirkmechanismus konnte die Lyse von empfänglichen Biomembranen durch die Erzeugung großer, Ca^{2+}-durchlässiger Läsionen identifiziert werden. Entsprechend ist die pilzliche Jagaricin-Toleranz wesentlich davon bestimmt, Jagaricin-verursachten Ca^{2+}-Influx über den Calcineurin-Signalweg wahrzunehmen, um adäquate Membranreparaturprozesse einleiten zu können. Das Anwendungsspektrum von Jagaricin wäre nach diesen Ergebnissen in seiner unveränderten Form wurde auf landwirtschaftliche Anwendungen eingeschränkt, da sich Jagaricin als toxisch für humane, aber nicht pflanzliche Zellen herausgestellt hat.

B) Ein genaueres Verständnis der Interaktion humanpathogener Pilze mit dem menschlichen Immunsystem im Kontext einer antimykotischen Behandlung kann die Entwicklung gezielterer Behandlungsstrategien ermöglichen. Dies benötigt insbesondere Kenntnisse über die Bestandteile des menschlichen Immunsystems, die die Interaktion bestimmen und die durch antimykotische Behandlung und Immunreaktion auf das Pilzpathogen wirkende Selektion.

Für die humanpathogene Hefe *Candida glabrata* konnte in vorangegangenen Arbeiten gezeigt werden, dass Immunevasion von zentraler Bedeutung im Infektionsprozess ist. Dabei kommt der Interaktion mit mononukleären Zellen eine Schlüsselrolle zu, da *C. glabrata* eine relativ hohe Affinität zu diesen Immunzellen in mehreren *in vitro* und *in vivo*-Infektionsmodellen aufwies und in deren Phagosom mutmaßlich durch Interferenz mit dem Phagolysosom-Reifungsprozess überleben und sich vermehren

kann. Bisherige Modelle waren aber nicht in der Lage, über einen längeren Zeitraum die Persistenz von *C. glabrata*-Hefen in Makrophagen als Teil des Immunevasionsprozesses abzubilden. Diese Modelllücke wurde im Rahmen dieser Arbeit geschlossen und zentrale Mechanismen und Faktoren auf der Pilzseite durch Verwendung von breit angelegten Analysemethoden (Transkriptom, Mutantenbibliothek-Screening) charakterisiert. Als zentrales Ergebnis konnte herausgearbeitet werden, dass *C. glabrata* auch über den eine Woche langen Untersuchungszeitraum im Phagosom von Makrophagen unter anhaltendem Stress steht und entsprechend Faktoren für die Einleitung, die Aufrechterhaltung und den Exit aus einem zellulären Ruhestatus entscheidend sind für die Persistenz von *C. glabrata* in Makrophagen. Passend dazu sind große energiezehrende Prozesse wie Genexpression auf transkriptioneller Ebene in den Hefen durchgängig herunterreguliert. Eine durchgängig aufrechterhaltene langfristige Behandlung mit Antimykotika (Caspofungin, Amphotericin B) war *in vitro* nicht in der Lage, *C. glabrata*-Hefen vollständig aus humanen Makrophagen zu entfernen, was auf eine klinische Relevanz dieser in Makrophagen in einem zellulären Ruhezustand persistierenden Hefen hinweist. Einige speziellere Aspekte des zellulären Ruhestatus von *C. glabrata* in Makrophagen wurden weiter untersucht bzw. diskutiert (z.B. die Rolle des Protektants Trehalose und seines Metabolismus, der Phosphatmetabolismus und die mögliche Funktion des noch unbekannten sexuellen Zyklus von *C. glabrata* in Makrophagen). Damit konnten mit dem neuen Langzeitmodell weitere wichtige Anhaltspunkte gewonnen werden, warum die klinische Behandlung von *C. glabrata*-Infektionen oft schwierig ist und in welchen evolutionären Selektionspfaden sich *C. glabrata*-Hefen während einer klinischen Infektion bewegen.

Beide in dieser Studie verwendeten Ansätze – die Untersuchung potentieller Wirkstoffe, die aus der Interaktion von Pilzen mit ihrer Umgebung stammen und die Untersuchung von Pathogenitätsmechanismen von Hefen – sollen letztlich über die Studie von Interaktionen von Pilzen mit ihrer Umgebung Wissen zu generieren, dass sich zur Behandlung von Pilzpathogenen einsetzen lässt und damit zur Verbesserung der Behandlungsstrategien beitragen könnte.

1 Introduction

1.1 Unique features and the environment define the fungal interactome

The fungal kingdom encompasses an estimated 2.2 to 3.8 million species (Hawksworth and Lücking 2017), suggesting by sheer numbers that large phenotypic and genetic diversity will exist among the species. Nevertheless, all fungi share some common characteristics restricting or predetermining their interactions with other organisms to certain outcomes. These common characteristics include e.g. a near-universal incorporation of ergosterol into membranes, strict heterotrophy, and a rigid chitin-containing cell wall. The morphology of fungi can mostly be divided into hyphal and filamentous structures, yeasts, and spores. Larger networks or functional structures can emerge exclusively via hyphae formation, e.g. in the case of fruiting body formation. Some examples might illustrate how these typical characteristics determine possible interaction outcomes: The heterotrophic lifestyle requires that the fungus searches out its nutrient source while the rigid cell wall and lack of motility structures (with the notable exception of chytridimycota) limit its mobility primarily to growth. Therefore, fungi developed a plethora of strategies involving abiotic factors as well as biotic interaction partners to deal with these limitations or even turn them into an advantage. E.g., the formation of vast numbers of spores which are widely distributed by ejection mechanisms or external factors like wind or animals ensure that fungi reach new substrates for renewed growth. Other fungi manage to socialize with other organisms like plants or termites which provide them with a constant nutrient supply, rendering own mobility unnecessary for the length of the interaction.

Accordingly, fungi are known to play parts in all types of inter-organismal interactions: competition (e.g. with other microorganisms in soil), predation (e.g. yeasts as prey for amoebae, carnivorous fungi as predator of nematodes (Pramer 1964), parasitism and pathogenic interactions (e.g. plant- or animal-infecting fungal pathogens as parasites and bacteria-infected mushroom caps as hosts), commensalism (e.g. certain yeasts in the gut of animals), amensalism (e.g. allergic reactions provoked by moulds) and mutualism (e.g. mycorrhiza, fungi hosting endosymbiotic bacteria). Each interaction in their specific environments puts special demands on the fungal partner. For example, the ability to survive within a human host as commensal or pathogen strictly requires the ability to grow at 37°C. The temperature optimum of most fungi lies in the range of 12 – 30°C, with only a few species being able to grow beyond 35°C (Robert and Casadevall 2009). Endothermic regulation of body temperature thereby (partially) explains how mammals and birds were able to restrict the number of their fungal pathogens to several hundreds, while the number of fungal pathogens of insects and plants have been

estimated to be between 10,000 to 50,000, or even (in the tropics) 270,000 species (Hawksworth and Rossman 1997; Robert and Casadevall 2009). However, global warming might redefine this game (Garcia-Solache and Casadevall 2010); evolutionary adaptation to higher temperatures is likely not per se impossible for most fungi, but is restricted by the niches they inhabit with their lower temperature. A raising mean temperature in many biotopes may make the step to life in mammals easier in the future, which was suggested as a reason for the appearance of *C. auris* as a global pathogen of humans (Casadevall, Kontoyiannis, and Robert 2019; Jackson *et al.* 2019; Misseri, Ippolito, and Cortegiani 2019).

In summary, generic fungal and the species-specific attributes in particular determine whether and how a certain fungal species will be able to react, adapt, and evolve in interaction with another organism. If these interactions happen frequently, the adaptive traits get fixed within the population in the long run.

1.2 Reasons for studying fungal competitive and predator-prey interactions

Knowledge about interactions of fungi with other organisms can have significant value for human health. Especially parasitic or pathogenic interactions are of importance: first, knowledge about virulence factors and pathogenicity mechanisms allows to develop treatment strategies. Human-pathogenic fungi cause billions of infections each year. While most of them are topical, systemic fungal infections cause roughly one and a half million deaths per year worldwide (Brown *et al.* 2012). In addition, fungal phytopathogens can cause devastating losses of crop yields (Maarten J. Chrispeels 2003; Meena and Kanwar 2015; Doehlemann *et al.* 2017), and pathogens of fungi can significantly lower the yield in mushroom farms (Kobayashi and Crouch 2009; Largeteau and Savoie 2010). Second, many fungi as well as their interaction partners deploy biologically active molecules – e.g. secondary metabolites, peptides or enzymes – as part of competitive or predator-prey interactions. These molecules, often evolved from microbiological competition, are of outstanding interest for development of future therapeutics: for example, a significant proportion of antibiotics in use today comes from or was inspired by secondary metabolism of microbes which interact with fungi or from the fungal partner in this interaction (Netzker *et al.* 2018).

1.3 Fungi in parasitic and pathogenic interactions: fungi as host

Fungi are not only infectious agents, but can themselves be infected by a broad variety of organisms like (myco)viruses, bacteria or other fungi. In addition, many other organisms like animals, insects or slime moulds feed on fungi, and plants like the non-

photosynthetic bird´s-nest orchid parasitize on fungi. In contrast to animals and plants, knowledge about fungal immunity is limited and in part controversially debated. Similar to innate immunity in animals and plants, physical barriers and defence molecules certainly do play a role: interaction with bacteria has been shown to lead to induction of secondary metabolite clusters (Schroeckh *et al.* 2009; Brakhage 2013; Ipcho *et al.* 2016; Künzler 2018; Netzker *et al.* 2018; Stroe *et al.* 2020; Jomori *et al.* 2020), and at least one study reported transcriptional induction of iron scavenging mechanisms and secondary metabolite clusters in response to bacterial microbe-associated molecular patterns (MAMPs) (Ipcho *et al.* 2016).

Mushroom-infecting bacteria

In addition to parasitic insects and other fungi, several bacterial species are among the most important pests in commercial mushroom cultivation (Kobayashi and Crouch 2009; Largeteau and Savoie 2010). These include e.g. the causative agents of brown blotch disease, *Pseudomonas tolaasii* and *Pseudomonas reactans*, and the causative agent of soft rot disease, *Janthinobacterium agaricidamnosum*. The *Pseudomonas* species both possess membrane-active virulence factors: WLIP (White Line Inducing Principle; *P. reactans*) and tolaasin (*P. tolaasii*) (Coraiola *et al.* 2006; Scherlach *et al.* 2013), while lesions on mushroom tissue elicited by *J. agaricidamnosum* are caused by its virulence factor jagaricin (Graupner *et al.* 2012). Aside from mushroom cultivation, not much is known about mushroom cap infections by bacteria or other organisms in the natural environment.

Jagaricin belongs to the class of lipopeptides (Graupner *et al.* 2012). These molecules are composed of a lipid chain linked to a linear or cyclic peptide moiety. Such a chemical configuration is associated with activity on membranes, but action towards cell wall biosynthetic enzymes has also been described for similar molecules (Denning 2003; Zhao *et al.* 2017). The cell wall and membrane have been used as targets for the development of antifungal drugs in the past: all three classes of antimycotics (azoles, echinocandins, polyenes) in use today for treatment of invasive fungal infections act either directly on or via biosynthetic enzymes of these targets – this limitation to few targets is due to the limited set of cellular differences between fungal and mammalian cells. Since some lipopeptides are already in clinical use due to their antifungal or antibacterial properties (e.g. echinocandins, polymyxins, daptomycin), examination of further, newly identified members of this molecule class could be promising. Jagaricin has been shown to have activity against medically relevant fungal pathogens (Graupner *et al.* 2012), warranting further investigations into its mode of action and application possibilities.

1.4 Fungi in parasitic and pathogenic interactions: fungal pathogens

Diseases caused by fungi

Research on pathogenic fungi today focuses on fungi which infect humans, as this has immediate implications for human health. Another focus are phytopathogenic fungi that can cause devastating crop yield losses in agriculture (Maarten J. Chrispeels 2003; Meena and Kanwar 2015; Doehlemann *et al.* 2017). In human infections by fungi, one has to distinguish between topical and systemic manifestations. While topical infections can be further classified into superficial, cutaneous, and subcutaneous, depending on the amount and depth of dermal and underlying tissue involved, systemic infections (i.e. spreading in most or all organs) are typically classified as being caused by either primary or opportunistic fungal pathogens. While the former have the potential to infect healthy individuals, the latter normally cause disease "only" in the immunocompromised. Typically the primary fungal pathogens can be found within the order Onygenales (*Histoplasma* spp., *Coccidioides* spp.). *Cryptococcus* spp. cause disease in healthy as well as immunocompromised individuals, while typical opportunistic pathogens (causing infection only in immunocompromised patients) include e.g. *Candida* spp. and *Aspergillus* spp. (e.g. reviewed in (Köhler *et al.* 2017)).

Candida spp. differ from e.g. *Aspergillus* spp. in their association with the human host: while *Candida* spp. typically are commensals, *Aspergillus* spp. come from the environment. This also becomes apparent in the transmission routes: spores of *Aspergillus* spp. typically enter the human host via the respiratory system and cause primarily lung infections, while *Candida* spp. can breach human epidermal barriers, causing superficial infections on skin, oral, and vaginal tissue, or even systemic infections by translocation through the gastrointestinal tract barrier. While transmission routes are comparatively well investigated for *C. albicans* (Allert *et al.* 2018), the species most frequently responsible for Candidiasis, these are unknown so far for many other *Candida* species like *C. glabrata* (Brunke and Hube 2013). Although both species bear the same generic name, *C. glabrata* is actually only distantly related to *C. albicans* and rather related to the baker's yeast, *Saccharomyces cerevisiae* (Kurtzman and Robnett 1997; Dujon *et al.* 2004; Butler *et al.* 2009). In this regard, it is perhaps unsurprising that both *Candida* species show quite distinct biological behaviours. This includes morphotypes – *C. albicans* can grow as yeast (and variations thereof), pseudohyphae, and hyphae, and it also forms chlamydospores (Noble, Gianetti, and Witchley 2017), while *C. glabrata* mainly grows as yeast (and variations thereof) and rarely in pseudohyphal form (Csank and Haynes 2000; Lachke *et al.* 2002; Sasani *et al.* 2016). Another difference is their sexual behaviour – *C. albicans* can undergo a parasexual cycle that is induced by switching mechanisms (Hull, Raisner, and Johnson 2000; Magee

and Magee 2000; Miller and Johnson 2002; Bennett and Johnson 2003), while mating of *C. glabrata* has never been shown directly despite the presence of mating gene orthologues within its genome (Wong *et al.* 2003; Srikantha, Lachke, and Soll 2003; Muller *et al.* 2008) and indications of mating in the environment (Carreté *et al.* 2018). As a last example, they differ in terms of aggressivity in confrontation with the host (immune system). The first line of immune defence against pathogens is built by epithelial barriers as well as cellular (mainly phagocytes like neutrophils and mononuclear cells) and molecular components of the innate immune system. Phagocytic cells exhibit different behaviours according to their function in the immune system: neutrophils are recruited mainly within the first hours of the infection and aggressively fight against invading pathogens by secretion of antimicrobial molecules, neutrophil extracellular trap (NET) formation and/or phagocytosis (Brinkmann *et al.* 2004; Urban *et al.* 2006; Timár, Lőrincz, and Ligeti 2013). In contrast, monocytes follow a time-delayed but long-lasting kinetic and remain up to weeks, while resident tissue macrophages and dendritic cells permanently screen their environment to detect threats early (pages 64/65 in (Murphy *et al.* 2009)). All mononuclear cells mainly fight invaders by phagocytosis, followed by antigen presentation for initiation of adaptive immunity (pages 64/65 and 240-247 in (Murphy *et al.* 2009)), although similar to NET formation, the formation of macrophage extracellular traps (METs) has been described (Doster *et al.* 2018). In both cases, phagocytosis aims at destroying the pathogen by creation of a hostile environment including restriction of nutrients and trace metals, direct pathogen attack by generation of reactive species, antimicrobial peptides and exposure to degradative enzymes (Flannagan, Heit, and Heinrichs 2015; Erwig and Gow 2016; Sprenger *et al.* 2018; Piacenza, Trujillo, and Radi 2019; Uribe-Querol and Rosales 2020). Phagosomes mature into phagolysosomes by fusion with endosomal and lysosomal vesicles, a process which potentially can be hijacked by pathogens (Haas 2007; Erwig and Gow 2016; Levin, Grinstein, and Canton 2016; Pradhan *et al.* 2019; Uribe-Querol and Rosales 2020). While the neutrophil phagosome has an alkaline pH, the phagosome of mononuclear cells is acidified (Thomas, Lehrer, and Rest 1988; Erwig and Gow 2016; Piacenza, Trujillo, and Radi 2019). In order to cause infection, fungal pathogens have to find a strategy to overcome or deal with these obstacles.

For example, *C. albicans* reacts to immune cells by hyphal growth (e.g. when engulfed in macrophages) (Vázquez-Torres and Balish 1997; Lorenz, Bender, and Fink 2004) and secretion of a membrane pore-forming toxin, Candidalysin (Moyes *et al.* 2016; Kasper *et al.* 2018; König, Hube, and Kasper 2020), as well as lipases and proteases (Borg-von Zepelin *et al.* 1998; Naglik *et al.* 2004; Paraje *et al.* 2008; Paraje *et al.* 2009), which generally leads to host tissue damage and a strong immune response (Moyes *et al.*

2016; Swidergall *et al.* 2019; Ho *et al.* 2019; Ho *et al.* 2020). In contrast, *C. glabrata* uses an immune evasion strategy (Jacobsen *et al.* 2010; Seider *et al.* 2011; Seider *et al.* 2014; Kasper, Seider, and Hube 2015), as shown by much less damage to host cells *in vitro* (Seider *et al.* 2011) and its low virulence in systemic murine infection models compared to *C. albicans*, although it can persist for weeks in both, immunocompetent and immunocompromised mice (Brieland *et al.* 2001; Jacobsen *et al.* 2010; Cheng *et al.* 2014). *C. glabrata* has exhibited a higher affinity to mononuclear cells than other *Candida* spp. in several *in vitro* and *in vivo* infection models (Brieland *et al.* 2001; Jacobsen *et al.* 2010; Cheng *et al.* 2014; Duggan *et al.* 2015), and is able to survive and replicate within these immune cells (Otto and Howard 1976; Kaur, Ma, and Cormack 2007; Roetzer *et al.* 2010; Seider *et al.* 2011). While *in vitro* and *ex vivo* models are available for investigations into the short-term interaction of *C. glabrata* with macrophages, none of these models can represent a persistent intracellular state simply due to the limitation of yeast overgrowth within two to three days within these models.

1.5 Antifungal resistance causes treatment failure in the clinic

Modern medicine has increased the number of immunocompromised patients at risk for these opportunistic fungi, and widespread use of antifungals in the clinic, but also in agriculture, has led to the emergence and spread of resistant and less susceptible species (Verweij *et al.* 2009; Arendrup and Patterson 2017; Perlin, Rautemaa-Richardson, and Alastruey-Izquierdo 2017). This is well-documented for azoles in commensal (Pfaller 2012) and environmental fungal species (Verweij *et al.* 2009; Howard and Arendrup 2011), as well as for echinocandins and sporadically for polyenes for commensals (Pfaller *et al.* 2012; Perlin, Rautemaa-Richardson, and Alastruey-Izquierdo 2017). Resistances can also develop during long-term treatment (Cowen *et al.* 2014; Jensen *et al.* 2015; Perlin 2015). This manifests e.g. as acquired resistance against azoles in *C. albicans*, a shift from *C. albicans* to less susceptible non-*C. albicans* *Candida* species – e.g. *C. glabrata* – as the causative pathogens in Candidiasis (Pfaller 2012; Perlin, Rautemaa-Richardson, and Alastruey-Izquierdo 2017), and recently as increasing echinocandin resistance found in *C. glabrata* (Alexander *et al.* 2013; Perlin, Rautemaa-Richardson, and Alastruey-Izquierdo 2017) and the rise of the frequently multi drug-resistant pathogen, *C. auris* (Chowdhary, Sharma, and Meis 2017). Inefficacy of one or several antimycotics causes considerable treatment challenges given that only three classes of antimycotics – azoles, echinocandins and polyenes – are currently available for treatment of systemic fungal infections. This partially explains why death rates remain unacceptably high for invasive fungal infections (Berman and Krysan 2020). An improvement of this situation requires – apart from introduction of new antifungals –

an improved understanding what causes clinical treatment failure, how resistance develops or where it comes from and the development of prevention strategies.

1.6 Resistance, tolerance, persistence and quiescence of fungal pathogens

Since there is some persisting confusion on the use of the term “resistance” in the literature, and it is often confounded with concepts like “tolerance”, a clarification of terms is necessary. The meaning of “resistance” depends, among others, on the author’s intentions and scientific background. In general, resistance could be defined as the ability of a treated species to grow without reduction in its growth rate in the presence of an inhibitory substance. It is often mediated by mechanisms like enhanced drug efflux or target changes. Apart from the basic resistance level which is further defined by drug kinetics, a fungal strain under antimycotic treatment can gain further resistance which will lead to a shift towards a higher drug concentration which is necessary to inhibit fungal growth, typically in strict defined standard *in vitro* assays. These are generally used to define the minimal inhibitory concentration (MIC) needed for inhibition of fungal growth. For clinicians, the most important information is whether the respective clinical isolate can still be inhibited by application levels of the drug which can still be tolerated by the patient. Therefore, clinically approved drugs most often have established breakpoint concentrations which classify if a given clinical isolate is still treatable. In contrast, basic researchers often employ a different use of the term resistance, here in the sense that e.g. a certain mutant is “more resistant” or “more susceptible” towards the drug in comparison to the wild type.

In contrast to resistance, tolerance towards an antimycotic is linked to an altered cellular state or cell cycle progression which allows (slowed down) growth even “in the presence of an antifungal drug at concentrations above the MIC” (Berman and Krysan 2020), which becomes visible only if e.g. an antimycotic assay is incubated longer than the standard 24 hours used for definition of resistance. Importantly, tolerance against antifungals typically relies on central (stress) signalling pathways like the calcineurin pathway. Therefore, inhibition of these pathways is a possible way to abolish fungal tolerance (e.g. reviewed in (Berman and Krysan 2020)).

Finally, entry into persistence allows a small part of the population (for fungicidal drugs typically less than 1 %) to survive in a quiescent, non-growing state even under high antimycotic concentrations (exceeding even tolerance levels). Only after removal of the drug, these cells might be able to restart growth (LaFleur, Kumamoto, and Lewis 2006; Khot *et al.* 2006; Lewis 2010; Wuyts, Van Dijck, and Holtappels 2018; Berman and Krysan 2020). Persistence is not inheritable but a stochastic process: a population grown

from survivor cells (= persister cells) incubated with the same conditions as the initial population will show the same rate of persister cell formation (LaFleur, Kumamoto, and Lewis 2006; Wuyts, Van Dijck, and Holtappels 2018). However, multiple rounds of treatment and population re-growth from persister cells can lead to enrichment of isolates with enhanced persister cell formation rates (Lafleur, Qi, and Lewis 2010).

A prerequisite for persistence is quiescence. In short, quiescence can be defined as "reversible absence of proliferation" (Sagot and Laporte 2019) and in yeast is typically linked to a strong reduction of important energy-consuming processes like protein biosynthesis (Boucherie 1985; Fuge, Braun, and Werner-Washburne 1994; Ju and Warner 1994; DeRisi, Iyer, and Brown 1997). Quiescence must be differentiated from senescence (non-reversible absence of proliferation), which is complicated by the fact that a quiescent cell can become senescent with time. However, quiescence alone is not sufficient to explain the survival of yeast persister cells. The conditions which led to the induction of quiescence (like lack of a certain nutrient) have a strong influence on its characteristics, and even within the same environment, individual cells can display heterogeneous properties (Gray *et al.* 2004; Coller, Sang, and Roberts 2006; Boer *et al.* 2010; Klosinska *et al.* 2011; Laporte *et al.* 2011; Palková, Wilkinson, and Váchová 2014; Miles and Breeden 2017; Laporte *et al.* 2017; Laporte *et al.* 2018). In fact, the decision to enter quiescence is taken before the "last" cell cycle has been completed (Argüello-Miranda *et al.* 2018) and e.g. build-up of the reserve carbohydrate glycogen in yeast batch-cultures is triggered before onset of glucose exhaustion, followed by onset of trehalose accumulation as well as triglyceride and steryl ester accumulation in lipid droplets during the diauxic shift (reviewed in (François and Parrou 2001)).

Accordingly, the transition into, maintenance of and exit from quiescence are tightly regulated processes which develop along certain guard rails like the cAMP-PKA and mTOR pathway in yeast, which integrates diverse metabolic cues such as availability of nitrogen and fermentable carbon sources. Inactivation of these pathways is required for proper entry into quiescence, while activation of these pathways is required for exit from quiescence (reviewed in (De Virgilio 2012)). In contrast, the Snf1 kinase pathway is dispensable under ideal growth conditions, but controls several key traits during the diauxic shift which prepare the cell for quiescence. Accordingly, cells without Snf1 rapidly lose viability during the stationary phase (Thompson-Jaeger *et al.* 1991; De Virgilio 2012).

Various further metabolites, metabolic pathways and storage molecules affect quiescence: intracellular trehalose for example stabilizes protein structures (Singer and Lindquist 1998; Jain and Roy 2009; Goldberg *et al.* 2009; Kyryakov *et al.* 2012), but is also suggested to fuel glycolysis for a rapid exit from quiescence ((Laporte *et al.* 2017)

and reviewed in (Valcourt *et al.* 2012)). This is important since flux through glycolysis is strictly required for exit from quiescence (Laporte *et al.* 2011). As a last example, the loss of polyphosphate-degrading enzymes has been shown to lead to loss of cell viability in the stationary phase (Sethuraman, Rao, and Kornberg 2001). In addition to cessation of growth and cell division, quiescent yeast cells exhibit a broad shut-down of cellular metabolism and gene expression (e.g. reviewed in (De Virgilio 2012; Sagot and Laporte 2019)). This is linked to formation of storage bodies which protect biomolecules from stress or sequester away critical regulators of cellular metabolism. Their targets include e.g. mRNA (cytosolic P-bodies, stress granules), enzymes (cytosolic filaments), cytoskeleton components (cytosolic actin bodies, nuclear microtubule bundles), specific protein complexes (cytosolic proteasome storage granules [PSG], cytosolic heat shock protein granules) as well as the reorganization of mitochondria into cortical vesicles, chromosome condensation and formation of telomeric hyper-clusters and relocation of Hsp90 to the nucleus (reviewed in (Sagot and Laporte 2019)). In addition, cell wall remodelling controlled by the cell wall integrity (CWI) pathway is critical for maintaining viability of quiescent cells (Krause and Gray 2002; Levin 2005). Some of these structures are also triggered by stress conditions independently of entry into quiescence (Laporte *et al.* 2018; Sagot and Laporte 2019). In total these phenotypic and functional alterations enable quiescent cells to maintain viability especially in the long-run better than proliferating cells, even if they are exposed to diverse stressors like antimycotic treatment (e.g. (Allen *et al.* 2006) and reviewed in (Lewis 2010; Bojsen, Regenberg, and Folkesson 2017; Berman and Krysan 2020)).

In summary, tolerance and persistence can explain clinical treatment failure of *in vitro* susceptible fungal strains (Bojsen, Regenberg, and Folkesson 2017; Berman and Krysan 2020). It has been proposed that resistant strains can emerge from drug tolerant and persistent variants, as selection for resistance can act on such a surviving population (Cowen and Lindquist 2005; Berman and Krysan 2020).

1.7 Antifungal resistance and fungal evolution: mechanisms and driving forces

What, then, drives and determines resistance development, especially in a clinical context? The likelihood of resistance acquisition is largely linked to the mode of action – it is more likely for fungistatic drugs like azoles than for fungicidal drugs like polyenes – as well as length of exposure (Berman and Krysan 2020). Fungal infections can be prolonged and often temporarily symptom-free (e.g. reactivation of *C. neoformans* infections established early in childhood) or become chronic (e.g. chronic mucocutaneous candidiasis) if a subpopulation of the infecting fungus adopts a

(persisting) state which the immune system either tolerates or is not able to eliminate (Alvarez-Rueda *et al.* 2012; Coelho, Bocca, and Casadevall 2014; Jabra-Rizk *et al.* 2016; Misme-Aucouturier *et al.* 2017). Similarly, fungi that reside in niches where antifungal concentrations reach only low effective levels, e.g. in biofilms or in the gall bladder, can develop resistance (Taff *et al.* 2013; Hsieh, Brunke, and Brock 2017). Therefore, identification and evaluation of possible reservoirs – like the putative intracellular persistence of *C. glabrata* within macrophages – is critical to ensure treatment success. Apart from fungal evolution during antifungal treatment, evolutionary processes prior to infection can influence infection outcome. In general, the ability to cause infections of humans is thought to have evolved in natural reservoirs. In this model, environmental species evolve in an "environmental virulence school" (Casadevall 2008; Bliska and Casadevall 2009) while commensals pass through a "commensal virulence school" (Hube 2009). Both hypotheses posit that conditions and the biotic and abiotic interactions in their environments trained these species to gain critical properties needed for virulence. A good example is the ability to survive within phagocytic immune cells: while environmental fungi like *Aspergillus* spp. are exposed to amoebae within soil (Novohradská, Ferling, and Hillmann 2017), commensal fungi like *Candida* spp. might face occasionally confrontation with macrophages which continuously sample the gastrointestinal tract (Hube 2009). In both cases, fungal cells resistant to such occasional attacks have a selection advantage in the long term. Altered selection pressures within the environment – e.g. antibiotic treatment, immunosuppression or altered host diets for commensals, antifungal treatment of crops or temperature increase due to climate change for environmental species – therefore will lead to novel adaptations or shifts in species distribution patterns. In consequence, the effects of such changes will be visible in the clinic.

1.8 Aims

This study's aim is to investigate two types of interactions of fungi with other organisms which have potential consequences for clinical applications: First, an antifungal substance which is produced by bacteria preying on fungi, jagaricin, will be evaluated for its efficacy against fungal pathogens of humans. Second, the ability of the yeast pathogen, *C. glabrata*, to persist within human macrophages during infection will be characterized as an example for direct human-fungal interactions. Both approaches complement each other, as the latter will reveal potential modes for the development of resistances, while the former will help to find ways to counteract these. In detail, the following specific aims will be addressed in this work:

- Determination of the mode of action of the novel antifungal jagaricin and the possible tolerance and resistance mechanisms of pathogenic fungi
- Assessment of possible applications for jagaricin
- Establishment of the first model for studies of long-term interactions of human macrophages with a fungal pathogen
- First identification of strategies and genes required for the ability of *C. glabrata* to persist within human macrophages
- Discussion of microevolution in infection processes under antimycotic treatment

2 Manuscripts

2.1 Manuscript I

Disruption of Membrane Integrity by the Bacterium-Derived Antifungal Jagaricin

Daniel Fischer, Guido Gessner, Taicia Pacheco Fill, Robert Barnett, Kyrylo Tron, Katharina Dornblut, Florian Kloss, Pierre Stallforth, Bernhard Hube, Stefan H. Heinemann, Christian Hertweck, Kirstin Scherlach and Sascha Brunke

Antimicrob Agents Chemother **63**:e00707-19.
DOI: https://doi.org/10.1128/AAC.00707-19.

Summary:
This study investigated the mode of action of jagaricin, a virulence factor of the bacterium *Janthinobacterium agaricidamnosum* known to be responsible for mushroom soft rot disease. In addition to its role as a virulence factor, jagaricin is of special interest given its reported antifungal activity against fungal pathogens of humans. In this manuscript, it is shown by electrophysiological methods that jagaricin exerts its function by inducing a breakdown of the plasma membrane chemiosmotic potential. In agreement with this observation, a transcriptome analysis of *Candida albicans* showed that the yeast responds to jagaricin by shutting down membrane-potential driven transport processes. Measurement of intracellular Ca^{2+} levels revealed that jagaricin-mediated membrane breakdown leads to rapid Ca^{2+} influx suggesting formation of large-sized membrane lesions. This matches with data from *Candida* mutants, which show that the Ca^{2+}-sensing calcineurin pathway is essential for tolerance to sublethal jagaricin levels.
Further investigations into jagaricin´s possible applications showed that the antifungal in its unmodified form is toxic for human cells, as indicated e.g. by its haemolytic activity, but it could be used against phytopathogens in agriculture, since it does not affect plant growth.

Own Contribution:
Daniel Fischer designed the study and planned, performed, evaluated and interpreted the following experiments: *C. albicans* PI assay, susceptibility tests of *C. albicans* and *C. glabrata* mutants and clinical isolates, *C. albicans* transcriptomic response, hemolysis assay and checkerboard assays. Daniel Fischer further initiated, discussed and evaluated the following experiments: *Dictyostelium discoideum*, phytopathogenic fungi and plant susceptibility testing; Patch clamp assays, Ca^{2+} influx assays with Fura-2-AM,

a black lipid membrane assay and CMC measurements.
Daniel Fischer generated and/or compiled all figures, coordinated the experimental work between groups, and wrote the manuscript.

Estimated authors' contributions:

Daniel Fischer	55%
Guido Gessner	5%
Taicia Pacheco Fill	4%
Robert Barnett	2%
Kyrylo Tron	2%
Katharina Dornblut	2%
Florian Kloss	1%
Pierre Stallforth	1%
Bernhard Hube	2%
Stefan H. Heinemann	2%
Christian Hertweck	2%
Kirstin Scherlach	7%
Sascha Brunke	15%

Prof. Bernhard Hube

AMERICAN SOCIETY FOR MICROBIOLOGY | Antimicrobial Agents and Chemotherapy®

MECHANISMS OF ACTION: PHYSIOLOGICAL EFFECTS

Disruption of Membrane Integrity by the Bacterium-Derived Antifungal Jagaricin

Daniel Fischer,[a] Guido Gessner,[b] Taicia Pacheco Fill,[c]* Robert Barnett,[d] Kyrylo Tron,[b]* Katharina Dornblut,[c] Florian Kloss,[e] Pierre Stallforth,[d] Bernhard Hube,[a,f] Stefan H. Heinemann,[b] Christian Hertweck,[c,f] Kirstin Scherlach,[c] Sascha Brunke[a]

[a]Department of Microbial Pathogenicity Mechanisms, Leibniz Institute for Natural Product Research and Infection Biology–Hans Knöll Institute, Jena, Germany
[b]Center for Molecular Biomedicine, Department of Biophysics, Friedrich Schiller University Jena and Jena University Hospital, Jena, Germany
[c]Department of Biomolecular Chemistry, Leibniz Institute for Natural Product Research and Infection Biology–Hans Knöll Institute, Jena, Germany
[d]Junior Research Group Chemistry of Microbial Communication, Leibniz Institute for Natural Product Research and Infection Biology–Hans Knöll Institute, Jena, Germany
[e]Transfer Group Antiinfectives, Leibniz Institute for Natural Product Research and Infection Biology–Hans Knöll Institute, Jena, Germany
[f]Faculty of Biological Sciences, Friedrich Schiller University Jena, Jena, Germany

ABSTRACT Jagaricin is a lipopeptide produced by the bacterial mushroom pathogen *Janthinobacterium agaricidamnosum*, the causative agent of mushroom soft rot disease. Apart from causing lesions in mushrooms, jagaricin is a potent antifungal active against human-pathogenic fungi. We show that jagaricin acts by impairing membrane integrity, resulting in a rapid flux of ions, including Ca^{2+}, into susceptible target cells. Accordingly, the calcineurin pathway is required for jagaricin tolerance in the fungal pathogen *Candida albicans*. Transcriptional profiling of pathogenic yeasts further revealed that jagaricin triggers cell wall strengthening, general shutdown of membrane potential-driven transport, and the upregulation of lipid transporters, linking cell envelope integrity to jagaricin action and resistance. Whereas jagaricin shows hemolytic effects, it exhibited either no or low plant toxicity at concentrations at which the growth of prevalent phytopathogenic fungi is inhibited. Therefore, jagaricin may have potential for agricultural applications. The action of jagaricin as a membrane-disrupting antifungal is promising but would require modifications for use in humans.

KEYWORDS *Candida albicans*, jagaricin, mode of action, calcium influx, membrane integrity, pathogenic fungi, susceptibility testing

Historically, natural interactions between microbes and other organisms have proven to be the best source of antimicrobial compounds, and even human ingenuity cannot normally compete with billions of years of evolution (1). Antagonistic interactions between species often drive this evolution toward production of biologically highly active compounds. Recently, we described such an interaction by showing that the mushroom pathogen *Janthinobacterium agaricidamnosum* employs a novel cyclic lipopeptide, jagaricin, to cause soft rot disease of *Agaricus bisporus*. We further found that jagaricin is also active against common human-pathogenic fungi, such as *Candida albicans* and *Aspergillus fumigatus*, whereas bacteria are not affected (2). Identification of novel antifungal compounds—ideally with a novel mode of action—is desperately needed, because fungal diseases kill as many people as, e.g., tuberculosis, and invasive fungal infections are often associated with high mortality rates (3). The situation is further exacerbated by the emergence of drug-resistant fungal isolates in hospitals, exemplified recently by *Candida auris* (3, 4). Furthermore, fungal pathogens cause severe losses in agriculture (5–7), while the use of the same compound classes of antifungals in agriculture and medicine might lead to the emergence of resistant strains (8). This poses a significant challenge to the identification of new scaffolds for agricul-

Citation Fischer D, Gessner G, Fill TP, Barnett R, Tron K, Dornblut K, Kloss F, Stallforth P, Hube B, Heinemann SH, Hertweck C, Scherlach K, Brunke S. 2019. Disruption of membrane integrity by the bacterium-derived antifungal jagaricin. Antimicrob Agents Chemother 63:e00707-19. https://doi.org/10.1128/AAC.00707-19.

Address correspondence to Kirstin Scherlach, kirstin.scherlach@leibniz-hki.de, or Sascha Brunke, sascha.brunke@leibniz-hki.de.

* Present address: Taicia Pacheco Fill, Laboratório de Biossíntese e Bioprospecção de Produtos Naturais (IQ-B-200), Instituto de Química-Departamento de Química Orgânica, Universidade Estadual de Campinas-UNICAMP, Barão Geraldo, Campinas, Brazil; Kyrylo Tron, Institute for Physiology II, Jena University Hospital, Friedrich Schiller, University Jena, Jena, Germany.

Received 3 April 2019
Returned for modification 25 April 2019
Accepted 14 June 2019
Accepted manuscript posted online 24 June 2019
Published 23 August 2019

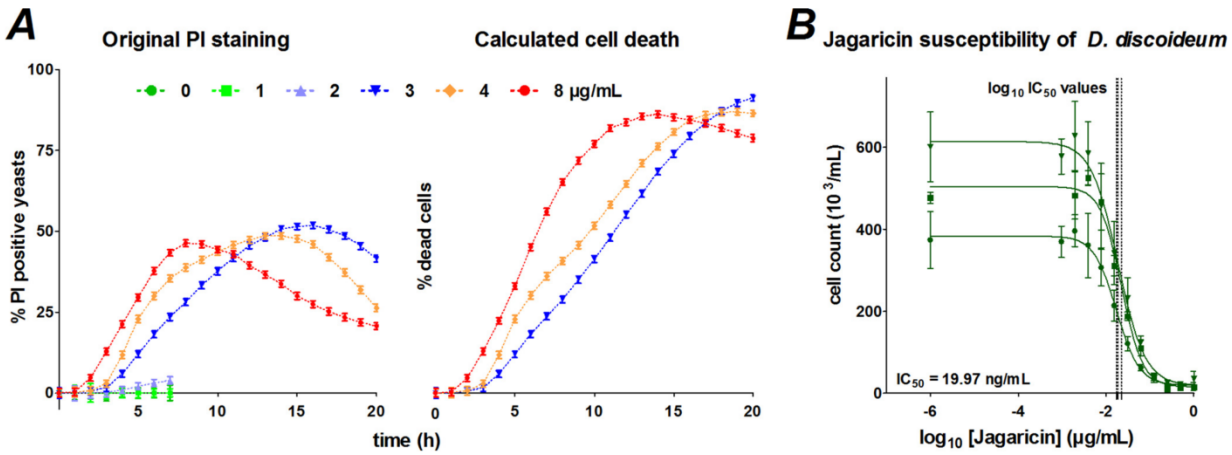

FIG 1 Susceptibility analysis *D. discoideum* and killing of *C. albicans*. (A) Killing of *C. albicans* by jagaricin. (Left) Transient positive staining of *C. albicans* yeasts by PI indicates recent cell death; (right) extrapolated cumulative cell death of the population based on PI staining kinetics obtained at the respective jagaricin concentration (see Materials and Methods). At low jagaricin concentrations (0, 1, and 2 μg/ml), yeast growth made analysis impossible after 7 h for the original PI staining and prohibited the obtainment of PI staining kinetics. Geometric means of three biological replicates for either the % PI positive cells (left) or the % dead cells (right) $\pm$ the geometric standard deviations are plotted. (B) Jagaricin susceptibility of *D. discoideum*. Jagaricin showed strong inhibitory activity toward *D. discoideum* (IC_{50} = 19.97 ng/ml; $\log_{10}$ IC_{50} = -1.70 ± 0.21). Individual $\log_{10}$ IC_{50} values are marked on the *x* axis. Three biological replicates with weighted arithmetic means of three technical replicates $\pm$ the standard deviations are plotted.

tural use with distinct structures and mechanisms of action compared to drugs in current clinical use.

Lipopeptides consist of a linear or cyclic peptide moiety covalently linked to a lipid chain, resulting in typically amphiphilic characteristics and, depending on the ratio of hydrophobic to hydrophilic molecule parts, a tendency for self-aggregation and the formation of micelles, vesicles, or nanofibers (9). In general, biologically active lipopeptides can originate from natural sources, such as jagaricin, but especially membrane-active lipopeptides can also be artificially generated by linkage of a peptide with a lipid chain (10). Lipopeptides have been described to have (among others) surfactant, antibacterial, antifungal, antiviral and cytotoxic properties (see, for example, references 6, 9, and 10), and often have an effect on the integrity of membranes (e.g., fengycin, surfactin, and iturin; all from *Bacillus* spp. [11]) or by inhibiting cell wall biosynthetic enzymes of fungi (e.g., echinocandins [12]). Accordingly, some lipopeptides, such as polymyxins, caspofungin, micafungin, and daptomycin, are now in clinical use (13), and biologically derived lipopeptides continue to be a prolific source of inspiration for drug discovery. Here, we evaluate the lipopeptide jagaricin in regard to its mode of action, primary biological activities, and selectivity, and we suggest potential uses for this antifungal agent. We show that jagaricin most likely exerts its function by the formation of membrane pores, leading to nonreversible breakdown of the membrane potential as well as Ca^{2+} influx and consequently to cell death.

RESULTS

Jagaricin is a fungicidal compound. Fungal growth inactivation by antifungals can be roughly categorized into fungicidal and fungistatic, and this classification helps to guide the search for possible modes of action. We therefore determined killing of a very common human-pathogenic fungus, *C. albicans*, by jagaricin using propidium iodide (PI) staining, which allows detection of dead cells via fluorescence. After jagaricin application, we found strongly fluorescent yeast cells in defined growth medium (SD) (Fig. 1A), suggesting a general fungicidal mechanism. Accordingly, in control experiments, we found a corresponding reduction in CFU numbers after jagaricin exposure (data not shown). Notably, isolated killing of *C. albicans* cells was observed even at otherwise permissive jagaricin levels (Fig. 1A).

Jagaricin targets determined via *C. albicans* and *C. glabrata* mutant and species comparison. In a first step to investigate the mechanism of action, we aimed to narrow down the potential fungal targets of jagaricin. Jagaricin inhibited growth of all tested fungal species (2), which makes fungus-specific cell wall structures or ergosterol-containing membranes potential targets of its action. We therefore tested *Dictyostelium discoideum*, an ergosterol-containing social amoeba lacking a cell wall, for its susceptibility. Since jagaricin was highly active against *D. discoideum* (Fig. 1B), we concluded that the cell wall is not the primary target.

To further identify the potential targets and mode of action of jagaricin, we performed a selected library screen with mutants of the common fungal pathogens *C. albicans* and *C. glabrata* as model organisms. The mutants were chosen based on their function in central signaling pathways or function in membrane or cell wall synthesis, allowing us to infer potential cellular target processes (Fig. 2). In accordance with the hypothesis that jagaricin does not target the fungal cell wall, *Candida* deletion mutants of the protein kinase C pathway (controlling cell wall integrity) showed no altered susceptibility toward jagaricin (*Cgrom2*Δ, *Cgslt2*Δ, *Cgrlm*1, *Carlm1*Δ, and *Camkk2*Δ) or only a slight increase in susceptibility (*Camkc1*Δ). Similarly, no effect was observed with mutants of cell wall-synthesizing enzymes (*Cgfks2*Δ, *Cgfks3*Δ, and *Casun41*Δ). In contrast, deletion of components of the calcineurin pathway (involved in general cell integrity) resulted in strongly increased jagaricin susceptibility in *C. albicans* (*Cacrz1*Δ, *Cacmp1*Δ, and *Camid1*Δ), but led to no effect in *C. glabrata* (*Cgmid1*Δ). The Hog1 mitogen-activated protein (MAP) kinase pathway is responsible, among others, for osmotic stress tolerance. Deletion of its core components (*Capbs2*Δ, *Cassk2*Δ, and *Cahog1*Δ) led to pronounced growth defects in the presence of jagaricin, although this was not the case for other sensors or effectors of the osmotic and/or oxidative stress response (*Cgskn7*Δ, *Caskn7*Δ, *Casko1*Δ, and *Cachk1*Δ). Interestingly, deletions of two of three tested genes encoding inositol polyphosphate phosphatases (*Cginp53*Δ and *Cainp51*Δ; Fig. 2B) led to higher resistance to jagaricin (no effect for *Cginp51*Δ), while a *Cgslm1*Δ strain (lacking a homolog of a phosphatidylinositol-4,5-bisphosphate binding protein) was hypersusceptible. These genes are linked to cell membrane organization via their role in regulation of actin cytoskeleton organization and endocytosis. In summary, these results strongly suggest that jagaricin might affect fungal cell membrane integrity, leading to osmotic stress.

In case of an intracellular target, drug tolerance in fungi is often mediated by active drug efflux. We therefore tested a number of clinical isolates with known enhanced Cdr or Mdr efflux phenotypes, deletion mutants of known drug transporters and their regulators, as well as gain-of-function strains of drug transporter regulators (*Ca*Tac1 and *Ca*Mrr1). Deletion of individual drug transporter genes did not increase jagaricin susceptibility (*Cgpdr1*Δ, *Cgprd17*Δ, *Casnq2*Δ, *Cacdr1*Δ, *Cgcdr1*Δ, and *Cgsnq2*Δ), and this was the same for both Cdr- and Mdr-based increased efflux (in clinical isolates EU0992, EU0989, EU0999, and EU0981). Similarly, *C. albicans* strains with synthetic gain-of-function mutations in the regulator genes *MRR1* or *TAC1*, which cause upregulation of the transporters Mdr1 or Cdr1/Cdr2, respectively, had no effect on jagaricin susceptibility. Also, deletion of the same drug transporter regulator genes had no effect (*Camrr1*Δ, *Camrr2*Δ, and *Catac1*Δ). In summary, susceptibility toward jagaricin is not affected by the investigated drug transporters, indicating that jagaricin is either not transported outside or—more likely—does not act on a cytoplasmatic target but rather directly on the plasma membrane.

If jagaricin acts on the plasma membrane, the membrane composition should influence susceptibility. Since ergosterol and the ergosterol biosynthesis pathway are well-known targets of antifungal compounds, we continued our mutant analysis in this context (Fig. 2). Deletion of *ERG5* did not significantly change susceptibility in *C. albicans* and *C. glabrata*, and a defect of the Erg6-mediated step (clinical *C. albicans* isolate EU0136) in ergosterol biosynthesis similarly did not result in a difference of jagaricin susceptibility compared to the *C. albicans* reference strain SC5314. In contrast, clinical isolates harboring disruptive mutations in the *ERG3* gene (*C. albicans* EU0012

A

Name	ORF	2 µg/mL jagaricin A (600 nm) % Wt	2 µg/mL jagaricin Growth speed Index	0 µg/mL jagaricin A (600 nm) % Wt	0 µg/mL jagaricin Growth speed Index
Sphingolipid + Inositol metabolism and signaling					
ISC1	CAGL0E06556g	96,3	-0,40	87,4	-0,31
IRS4	CAGL0M03157g	99,6	-0,04	98,3	0,00
INP53	**CAGL0B04631g**	92,0	-0,03	87,5	-0,04
INP51	CAGL0J02134g	94,2	0,00	97,1	0,02
OPI1	orf19.1543	98,9	-0,12	96,8	0,04
INO4	orf19.837.1	84,7	-0,38	95,2	-0,03
FGR22	orf19.1586	99,0	-0,03	102,0	0,04
STT4	orf19.1814	94,6	-0,37	102,0	0,01
DPL1	orf19.6951	97,9	-0,12	99,0	-0,18
HET1	orf19.6327	99,4	0,03	97,1	-0,08
MTS1	orf19.4831	94,1	-0,02	95,0	-0,07
INO1	orf19.7585	99,1	0,21	98,6	0,12
KCS1	orf19.1007	102,0	0,17	100,3	0,02
INP51	**orf19.1373**	87,8	0,41	96,5	0,09
SLD1	orf19.260	91,0	-0,23	96,6	0,11
Calcineurin signaling and related pathway					
MID1	CAGL0M03597g	100,0	-0,06	97,6	0,08
CRZ1	orf19.7359	14,9	-1,42	98,2	0,06
MID1	orf19.3212	20,5	-1,23	97,8	0,01
CMP1	orf19.6033	1,2	-1,33	97,5	0,09
Osmotic/Oxidative stress response (signaling pathway)					
SKN7	CAGL0F09097g	97,6	0,07	99,3	0,08
PBS2	orf19.7388	82,5	-0,88	89,8	-0,22
SSK2	orf19.11257	72,3	-1,15	90,4	-0,20
HOG1	orf19.895	23,8	-1,30	96,8	0,00
SKO1	orf19.1032	103,2	-0,13	99,0	-0,12
SKN7	orf19.971	102,6	0,07	95,5	0,08
CHK1	orf19.896	98,5	0,00	94,2	-0,02
PKC signaling pathway (cell [wall] stress response)					
ROM2	CAGL0G04873g	102,1	-0,04	99,4	0,00
RLM1	CAGL0H05621g	97,8	0,09	95,6	0,04
SLT2	CAGL0J00539g	103,0	-0,08	101,2	0,06
RLM1	orf19.4662	97,5	0,05	92,6	0,02
MKK2	orf19.6889	97,9	0,15	99,5	0,07
MKC1	orf19.7523	93,5	-0,48	100,4	-0,13
cAMP-PKA signaling pathway					
BCY1	CAGL0I05236g	61,8	-0,07	64,6	0,27
TPK2	orf19.2277	108,0	-0,29	102,2	-0,08
TPK1	orf19.4892	104,6	0,01	98,6	0,01
EFG1	orf19.610	87,5	-0,89	84,0	-0,36
Drug efflux transporter (regulation)					
PDR1	CAGL0A00451g	101,7	0,02	99,7	0,04
PDR17	CAGL0J08074g	98,9	-0,09	96,8	0,02
QDR2	CAGL0G08624g	99,4	-0,05	98,6	-0,02
CDR1	CAGL0M01760g	109,6	0,38	99,3	0,06
SNQ2	CAGL0I04862g	109,2	0,38	98,9	0,02
TAC1	orf19.3188	102,0	0,07	99,6	-0,01
MRR2	orf19.6182	99,8	0,02	99,0	0,02
MRR1	orf19.7372	99,9	0,01	97,4	0,04
SNQ2	orf19.5759	100,5	0,00	95,8	-0,03
CDR1	orf19.6000	107,1	0,37	103,8	0,16
TAC1 GOF allele 5	orf19.3188	93,1	-0,07	90,6	0,02
MRR1 GOF allele 3	orf19.7372	92,9	-0,19	97,7	0,02
EU0992: clinical isolate (Cdr-Efflux phenotype)		89,9	0,28	94,9	0,05
EU0989: clinical isolate (Cdr-Efflux phenotype)		53,8	-0,24	81,6	0,09
EU0981: clinical isolate (Mdr-Efflux phenotype)		101,9	0,37	99,9	-0,04
EU0999: clinical isolate (Mdr-Efflux phenotype)		98,6	0,16	94,4	-0,11
TORC2 signaling pathway					
SLM1	CAGL0G02827g	57,0	-1,49	93,3	-0,12
SLM2	CAGL0G01386g	98,5	-0,02	99,0	0,00
Membrane: Ergosterol biosynthesis (regulation) and flippases					
ERG5	CAGL0M07656g	101,2	-0,36	101,2	0,04
UPC2B	CAGL0F07865g	97,5	0,14	94,7	0,12
ERG5	orf19.5178	89,0	-0,21	92,1	-0,06
UPC2	orf19.391	96,7	-0,13	96,6	-0,10
UPC2 GOF allele 3	orf19.391	13,2	-1,16	89,2	-0,02
EU0012: clinical isolate (Erg3 deficiency)		0,1	-1,79	100,6	0,12
EU1008: clinical isolate (Erg3 deficiency)		0,2	-1,98	109,3	0,12
EU0136: clinical isolate (Erg6 deficiency)		62,0	-0,30	68,8	-0,62
NEO1	orf19.783	88,0	0,13	92,6	0,15
Others					
SNF5	orf19.5871	5,6	-0,51	37,1	-0,43
FKS2	CAGL0K04037g	99,7	0,07	97,5	0,04
FKS3	CAGL0M13827g	100,7	0,12	99,4	0,06
SUN41	orf19.3642	97,9	-0,22	99,2	0,09
IRE1	orf19.5068	96,1	-0,28	91,6	-0,04
CEK1	orf19.2886	101,3	-0,04	95,5	0,02
CPP1	orf19.4866	100,4	-0,13	101,5	0,02
MSB2	orf19.1490	94,0	-0,10	94,6	0,04

B

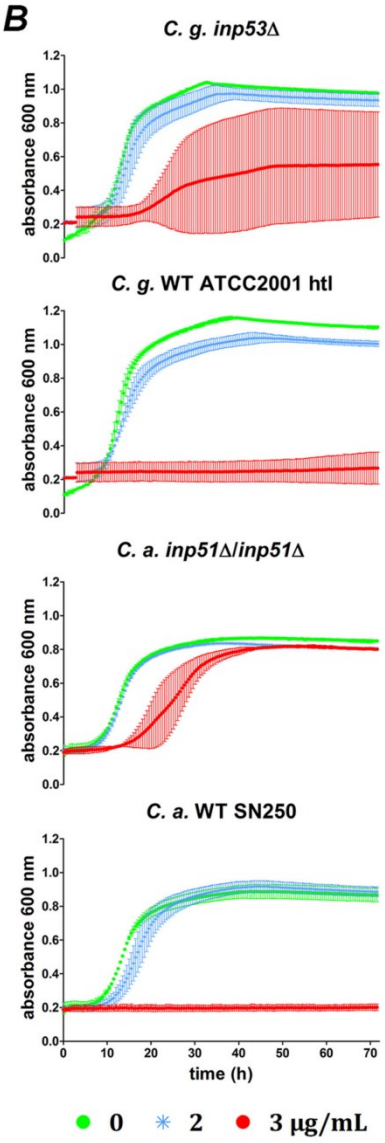

FIG 2 Jagaricin susceptibility of selected *C. albicans* (black, orf19.nnn) and *C. glabrata* (light blue, CAGL0nnn) mutants. Jagaricin effects on selected *C. albicans* and *C. glabrata* mutants are shown. The growth of *Candida* strains at 3 μg/ml (growth-inhibiting), 2 μg/ml

(Continued on next page)

and EU1008) showed strongly reduced jagaricin tolerance. Finally, a gain-of-function mutation in the ergosterol biosynthesis regulator *UPC2* (showing increased Erg11 expression and plasma membrane ergosterol levels [14–16]) of *C. albicans* led to high susceptibility toward jagaricin, whereas a *UPC2* deletion did not affect jagaricin susceptibility. Although these results do not necessarily indicate a highly specific binding of jagaricin to ergosterol, they imply a role of sterol levels and membrane composition for jagaricin susceptibility.

***C. albicans* transcriptome changes in the presence of jagaricin.** We continued to assess the physiological effects of jagaricin on *C. albicans* by transcriptional profiling of yeasts exposed to the antifungal. To this end, we obtained transcriptomes from a short-term (30 min) exposure to nontoxic jagaricin levels (1 μg/ml, 5×10^6 yeasts/ml) and from a culture growing in a jagaricin concentration still permitting growth (0.5 μg/ml, 2.5×10^5 yeasts/ml, sampled at an optical density at 600 nm (OD_{600}) of 0.5.

Short-term transcriptomic response. The short-term transcriptional response of *C. albicans* toward jagaricin was analyzed via Gene Ontology term (GO-term) enrichment to determine global functional patterns. Our data show clear hallmarks of a general cell wall repair and strengthening response (Fig. 3; see also Fig. S1A and B and Table S1A in the supplemental material), suggesting that jagaricin affects the integrity of the cellular envelope. Furthermore, a loss of membrane chemiosmotic potential is indicated by these two transcriptional events: (i) a downregulation of secondary active transmembrane transporter genes (Fig. 4) and (ii) a downregulation of the gene for the major plasma membrane H^+-ATPase, Pma1 (Fig. 4A; see Table S1A in the supplemental material). Against the general downregulation of ion transporter genes, certain Ca^{2+} transporter genes, such as *PMC1*, which codes for a Ca^{2+}-detoxifying vacuolar ATPase, were strongly upregulated (Fig. 4B). We also observed an upregulation of the gene for the central transcription factor of the calcineurin pathway, *CRZ1*, and of *RCN1*, a calcineurin regulator (17, 18) whose expression has been shown to be upregulated by calcineurin at least in *S. cerevisiae* (19) and humans (20). Together, this indicates an increased intracellular Ca^{2+} level and calcineurin activity. This is in agreement with our mutant-based finding that Crz1 is required for *C. albicans* jagaricin tolerance. In contrast to the general trend of downregulation of transporter-coding genes, gene set enrichment analysis (GSEA) revealed the enrichment of the set "aminophospholipid transporter activity" among jagaricin-associated genes (Fig. S1F and Table S1A) due to several upregulated transmembrane lipid transporter genes (*RTA2*, *RTA3*, *RTA4*, and a potential orthologue of *DRS25*). Furthermore, the transcriptional response includes downregulation of cell cycle processes, especially those associated with mitosis, and fatty acid biosynthesis (Fig. 3; see also Fig. S1B and Table S1A).

Amphotericin B exposure to *C. albicans* is known to elevate transcript levels of genes encoding potassium (*HAK1*), as well as sodium (*ENA21*) transporters (21). Both were also upregulated under jagaricin treatment. Furthermore, amphotericin B application to fungal cells has been shown to lead to oxidative stress (21, 22). Interestingly, jagaricin treatment led to transcriptional upregulation of a specific set of oxidative stress-related genes, namely, those which are mainly involved in cell envelope-associated oxidative stress responses (*SOD5*, *PST3*, and *YCP4*).

Transcriptomes during growth under growth permissive jagaricin levels. The transcriptomic response of exponentially growing cells under 0.5 μg/ml jagaricin was

FIG 2 Legend (Continued)
(growth-permissive), and 0 μg/ml jagaricin was recorded in individual wells of a 96-well plate by measuring absorbance at 600 nm every 30 min over a period of 3 days under continuous incubation in an enzyme-linked immunosorbent assay reader. (A) The *A* (600 nm) % WT was calculated as the geometric mean of three biological replicates. The growth speed index is $-\log_2$ of the maximum $t_{1/2}$ ratio of the mutant and reference strain, where the maximum $t_{1/2}$ is the time to half-maximal *A* (600 nm) value; negative values indicate slower and positive values faster growth than the wild type; the arithmetic means of three biological replicates are shown. The individual origins of the strains are listed in Table S2. Genes depicted in boldface showed "stable growth" (for the definition, see Materials and Methods) at the otherwise growth-inhibiting jagaricin concentration of 3 μg/ml. (B) Individual growth curves of these mutants (and the corresponding *C. glabrata* [ATCC 2001 hlt] and *C. albicans* [SN250] reference strains) are shown. Arithmetic means of *A* (600 nm) values of three biological replicates ± the standard deviations are shown.

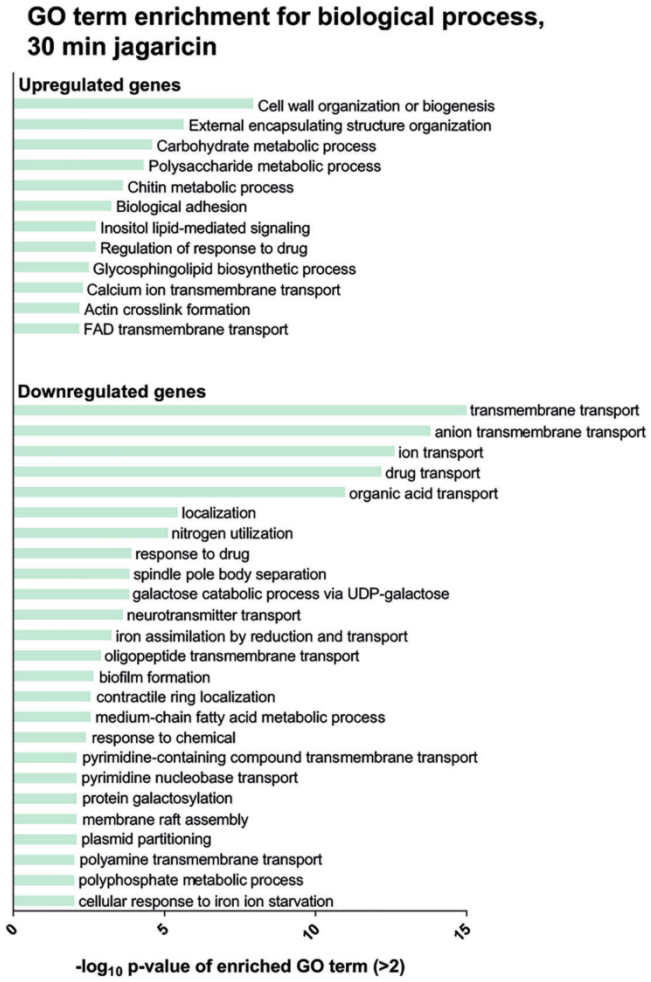

FIG 3 Enriched GO-terms upon exposure to jagaricin. Global short-term transcriptional response of *C. albicans* to a 30-min exposure to nontoxic jagaricin levels. GO-terms in the "biological process" domain were summarized by Revigo (66) for upregulated (top) and downregulated (bottom) genes (cutoff $-\log_{10} P > 2$).

less pronounced than the short-term response. In general, plasma membrane transport processes were upregulated (compare GO-term analyses, see Fig. S1C and S1D and Table S1B), in part contrasting their downregulation in the short-term experiment and possibly indicating a compensatory response. Notably, among downregulated genes, mitochondrion-associated GO-terms were partially enriched (e.g., GO:0005746: mitochondrial respiratory chain; Revigo summary $\log_{10} P = -1.8593$), suggesting that low levels of jagaricin interfere either directly or indirectly with mitochondrial function. Analogous effects have been observed for the surfactants cetyltrimethylammonium bromide (CTAB) and sodium dodecyl sulfate (SDS) (23).

The growth of *C. albicans* in the presence of the ergosterol biosynthesis inhibitor ketoconazole is known to induce ergosterol biosynthesis genes, while amphotericin B treatment leads to the downregulation of *ERG3* and *ERG11* transcription (21). Similarly, jagaricin exposure affected ergosterol biosynthesis by upregulation of the gene for the main regulator of the ergosterol biosynthesis, *UPC2*, in the short-term and downregulation in the growth-phase response (see Tables S1A and S1B in the supplemental material). As revealed by GSEA (Fig. S1F and Table S1B) and GO-term analysis (Fig. S1D

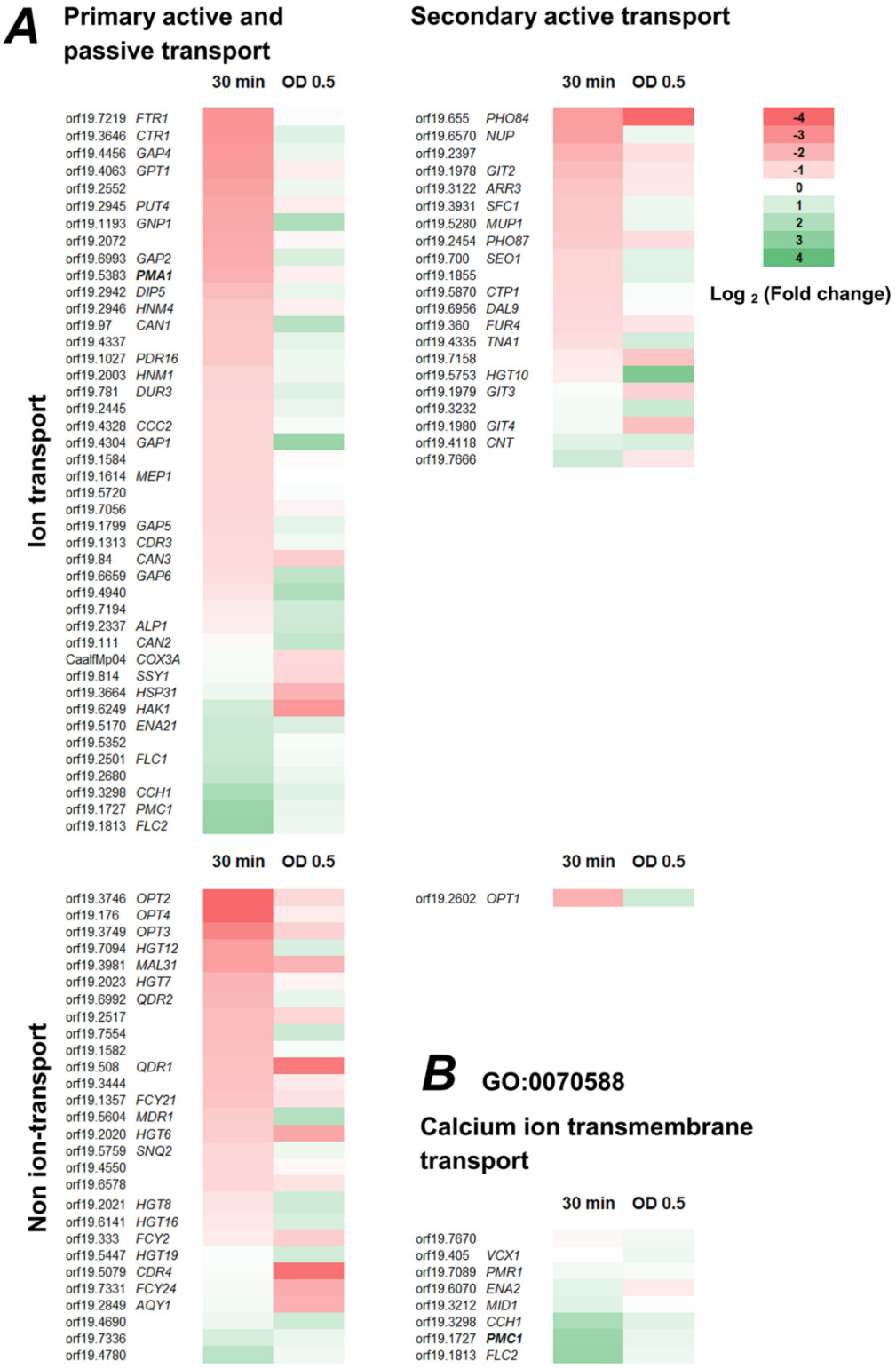

FIG 4 Transcriptomic response: regulation of transporters. The regulation of transporter genes in response to short-term (i.e., after 30 min) jagaricin exposure or jagaricin exposure during growth phase (grown to an OD_{600} of 0.5) was assessed. Genes

(Continued on next page)

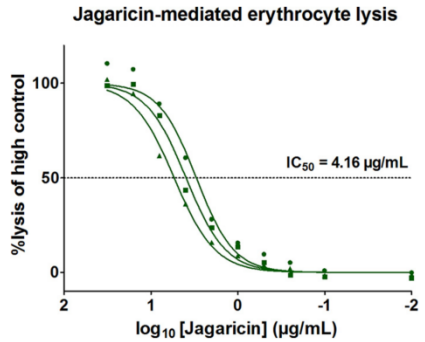

FIG 5 Erythrocyte lysis. Jagaricin lyses human erythrocytes. A total of 10^7 erythrocytes were incubated with various amounts of jagaricin for 1 h, and the OD_{541} of the supernatant was determined. Three biological replicates with two technical replicates each resulted in a weighted mean IC_{50} of 4.16 μg/ml ($\log_{10} IC_{50} = 0.62 \pm 0.18$).

and Table S1B), the latter was accompanied by the downregulation of several ergosterol biosynthesis genes (*ERG1*, *ERG3*, and *ERG11*; Table S1B).

Jagaricin effects on plasma membrane resistance and Ca^{2+} influx. These results indicated that jagaricin might interfere with membrane integrity. We thus tested artificial and natural membrane systems, where jagaricin showed no effect on the integrity of an artificial membrane based on soybean asolectin, even at 4 μg/ml (data not shown), but exhibited a significant lytic activity toward human erythrocytes with a half-maximal inhibitory concentration (IC_{50}) of 4.16 μg/ml (Fig. 5). This indicated that a membrane compound or property is required that is present in mammalian and fungal cells (and lacking in the investigated artificial membrane model). Our previous data hinted at an interference with the chemiosmotic potential, and we thus tested the ability of jagaricin to elicit ion fluxes through the plasma membrane of human HEK293T cells using patch-clamp assays (Fig. 6A). A few minutes after jagaricin application, we consistently observed a sudden and irreversible onset of a transmembrane current. Both the delay of the onset and the magnitude of the current were found to be concentration dependent. This would be consistent with an accumulation of jagaricin in the membrane, followed by breakdown of the plasma membrane chemiosmotic potential.

To test whether the possible cation influx into HEK293T cells included Ca^{2+} ions as indicated by our previous results, we measured intracellular Ca^{2+} levels using a fluorescent reporter assay (Fura-2-AM; Fig. 6B). At 5 μg/ml jagaricin, similar to the patch-clamp results, we observed a lag time, followed by a fast Ca^{2+} influx that plateaued within about 1 min and remained at this level for the duration of the experiment. At a lower concentration of 1 μg/ml, the lag time was considerably prolonged, and the intracellular Ca^{2+} levels increased more slowly. Drawing from these data from experimentally accessible mammalian cells and our previous data, we conclude that jagaricin likely also mediates Ca^{2+} influx in *C. albicans* in an analogous manner.

We were interested whether jagaricin causes this Ca^{2+} influx via the activation of membrane-spanning Ca^{2+} transporters or channels, as suggested recently for another bioactive lipopeptide, orfamide A (24). For this, we blocked Ca^{2+}-specific transport by addition of Cd^{2+}, which, however, did not block the jagaricin-mediated Ca^{2+} influx into HEK293T cells (see Fig. S2 in the supplemental material). Altogether, our results are in

FIG 4 Legend (Continued)
upregulated under jagaricin treatment are indicated in green; downregulated genes are indicated in red. (A) Depicted genes were selected according to an annotated function as transporter gene and a >2-fold up- or downregulation for at least one time point. (B) Against the general trend toward transporter downregulation, Ca^{2+} transporters are upregulated in the short-term response.

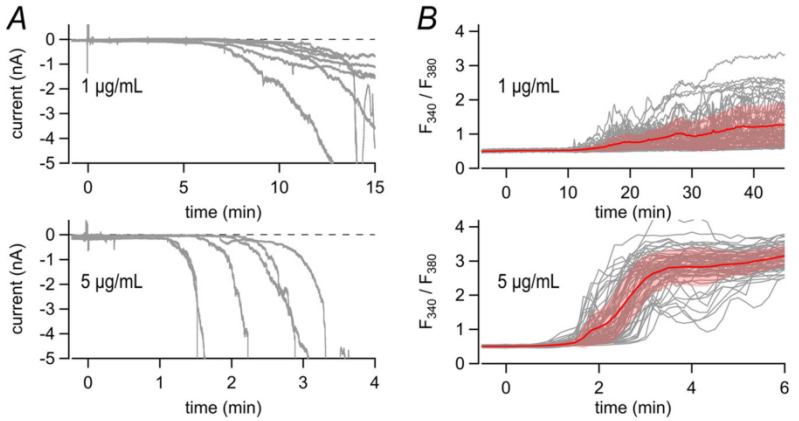

FIG 6 Ion fluxes in human cells upon jagaricin exposure. Jagaricin effects on HEK293T cells were assessed. (A) Whole-cell patch-clamp recordings of HEK293T cells. Cells were voltage clamped at −40 mV. The resulting current is shown for individual cells. Downward deflection indicates the inward flux of cations or the outward flux of anions. Jagaricin was applied at time point zero (top, 1 μg/ml; bottom, 5 μg/ml). (B) HEK293T cells were loaded with the Ca^{2+} indicator Fura-2-AM. The intracellular free Ca^{2+} concentration was determined from the fluorescence ratio of the dye at 340 and 380 nm (F340/F380) and is plotted as a function of time. Individual cell traces are superimposed (gray); the red trace indicates the mean, with shading indicating the standard deviations. Jagaricin application was as described for panel A. A representative graph of five independent experiments is shown for each jagaricin concentration.

best agreement with a model where jagaricin creates membrane lesions large enough to allow diffusion even of strongly hydrated ions such as Ca^{2+}.

One possible scenario for the action of a lipopeptide against membranes is the "micellar mechanism," the solubilization of host membrane parts into mixed micelles (25). We found that jagaricin forms micelles only at concentrations exceeding 176 μg/ml (Fig. S3), arguing for a different mode of action at biologically relevant concentrations.

Cooperative effects with commonly used antifungals. Based on the possible mechanisms of action, we continued testing for cooperative effects with other clinically used drugs. Synergistic interactions among drugs can help to reduce the side effects of a single drug at high doses and enables the investigation of further mechanistic relationships. We therefore tested the combined action of jagaricin with one representative each of the three major antimycotic compound classes that target cell wall and plasma membrane (the polyene amphotericin B, the echinocandin caspofungin, and the azole clotrimazole). We measured growth at 24 and 48 h and estimated potential synergism or antagonism by calculating the fractional inhibitory concentration index (ΣFICI). While this index indicated indifferent interactions ($\Sigma FICI > 0.5$ but ≤ 4) of jagaricin with all three tested antimycotics at 24 h, the addition of clotrimazole restored *Candida* growth at the otherwise fungicidal jagaricin concentration of 4 μg/ml at 48 h (Fig. 7A). Time-resolved growth curves show that this growth in the presence of clotrimazole appears mainly after 24 h of incubation (Fig. 7B). Similarly, at a normally toxic amphotericin B level of 1 μg/ml, addition of low levels of jagaricin allowed for (barely detectable) growth, again visible at 48 h (Fig. 7A).

Potential application spectrum of jagaricin. So far, our investigations into the effectiveness and mode of action of jagaricin focused on human-pathogenic fungi. Phytopathogens are another major class of fungi which are responsible for large economic losses in crops. New and dedicated fungicides for agriculture could help to reduce these losses and limit the transfer of resistance against clinically used drugs to human pathogens. We therefore tested the susceptibility of a range of important phytopathogenic fungi (*Alternaria alternata*, *Penicillium digitatum*, *Penicillium italicum*, *Colletotrichum gloeosporioides*, *Geotrichum candidum*, *Botrytis cinerea*, and *Fusarium graminearum*) and found them all susceptible to jagaricin at an MIC range of 0.1 to 5 μg/ml, comparable to our data on human pathogens (Fig. 8). Importantly, when we

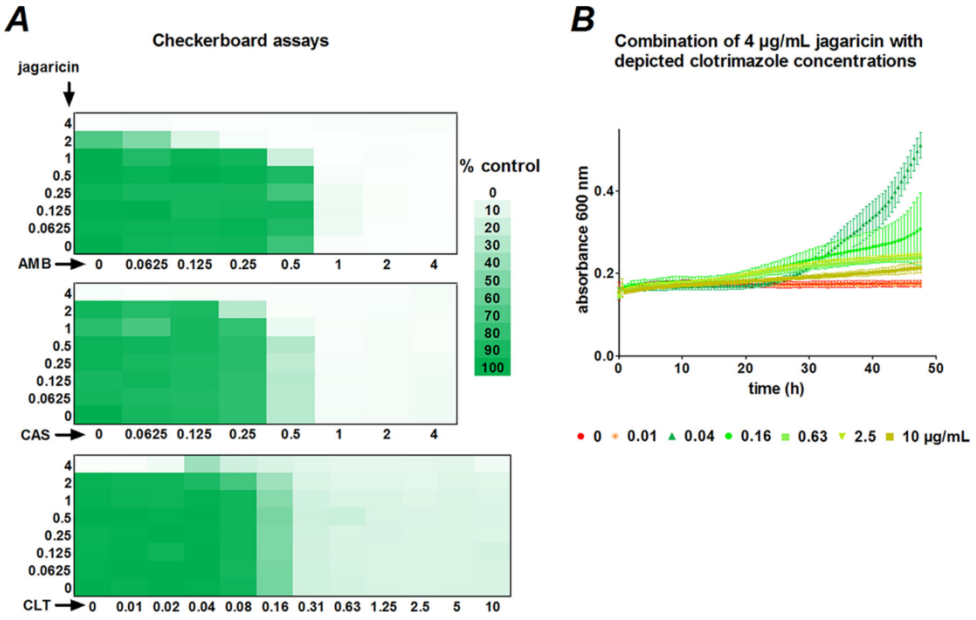

FIG 7 Checkerboard assay. Cooperative tests of jagaricin action with amphotericin B (AMB), caspofungin (CAS), or clotrimazole (CLT) after 2 days of incubation; compound concentrations are given in μg/ml. (A) While fractional inhibitory concentration index (ΣFICI) calculation after 1 day of incubation showed indifferent interactions between jagaricin and each of the three tested antimycotics, clotrimazole restored some growth at the otherwise fully growth-inhibiting jagaricin concentration of 4 μg/ml, seen here after 2 days of incubation. Similarly, low levels of jagaricin allowed (very limited) growth at the otherwise toxic amphotericin B concentration of 1 μg/ml over 2 days. (B) Individual growth curves of selected clotrimazole concentrations from panel A with 4 μg/ml jagaricin are shown. The data points represent the arithmetic means of three biological replicates $\pm$ the standard deviations.

tested the plant model hosts, *Sinapis alba* and *Lepidium sativum*, we detected no inhibition of germination even at 5 μg/ml jagaricin, the highest concentration in this range (Fig. 8). Only in the absence of light, there was an intermediate reduction of 40.4% in root growth observed for *S. alba*, but there was no reduction independent of light for *L. sativum*. In summary, these data seem very promising for future, more detailed investigations into the application of jagaricin against phytopathogenic fungi.

DISCUSSION

Cell integrity disturbing lipopeptides generally act either by direct membrane disruption or by targeting cell wall-synthesizing enzymes (reviewed in reference 10). Here, we investigated the mode of action of the recently discovered lipopeptide, jagaricin, on fungal and mammalian cells and found that it disrupts membrane integrity, leading to a permanent depolarization of the plasma membrane. In mammalian and likely fungal cells, this is accompanied by an influx of Ca^{2+} and, most likely, other ions. We found that the drop in membrane resistance, as well as the influx of Ca^{2+}, was rapid and nonreversible in a mammalian cell line. Furthermore, we demonstrated that Ca^{2+} influx was not inhibited in the presence of Cd^{2+}, a potent blocker of Ca^{2+} channels, suggesting the formation of pores within the plasma membrane that are large enough to allow unspecific Ca^{2+} flow and do not seal spontaneously. This resembles the activity of other membrane-permeabilizing agents, such as fengycins, which also lead to the formation of large pores (26, 27). In contrast, e.g., amphotericin B creates smaller, defined pores allowing ions and smaller metabolites to pass, in particular K^+ (28, 29), and the antibacterial lipopeptide daptomycin forms K^+-selective pores (30; for a review, see reference 31). Importantly, we observed a strong effect on fungal and human cell membranes but no evident toxicity toward bacteria (2) and only

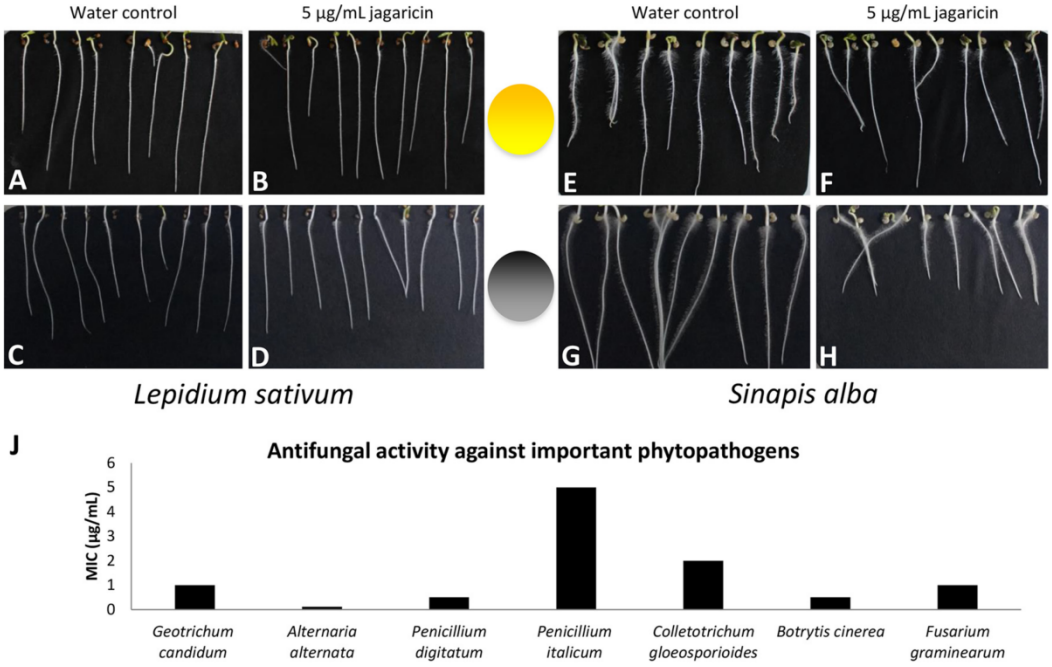

FIG 8 Susceptibility tests for application (plants and phytopathogenic fungi). Phytotoxicity assays with jagaricin were performed. *Lepidium sativum* (left) or *Sinapis alba* (right) seedlings were grown in the presence (top) or absence (bottom) of light in substrate containing distilled water (control; A, C, E, and G) or jagaricin at 5 μg/ml (B, D, F, and H). In general, 5 μg/ml jagaricin caused no inhibition of seed germination; root length was only inhibited with *Sinapis alba* in the absence of light (root growth inhibition = 40.4%). (J) Jagaricin shows low MICs for different phytopathogenic fungi. The bars represent the arithmetic means of two biological replicates.

specific and limited toxicity toward plants (Fig. 8). Based on the data presented here, which mechanisms could therefore best explain the membrane disruption effect of jagaricin as well as its specificity?

The social amoeba, fungal, and mammalian cell death (including hemolysis) seems to be mediated by membrane disruption. Our transcriptional and electrophysiological data demonstrate this for fungi and a human cell line, and the influx of Ca^{2+} directly observed in human cells was reflected by the calcineurin-related transcriptional events in fungal cells. We therefore propose that the mechanisms are conceptually similar for fungal and mammalian cells.

Similar to other lipopeptides, jagaricin starts to form micelles at its critical micellar concentration (CMC) value of 176 μg/ml (Fig. S3), 2 to 3 orders of magnitude higher than the concentrations required for biological activity. We therefore conclude that the "micellar mechanism," the solubilization of part of the host membrane into mixed micelles (as defined in reference 25), is unlikely to play a major role for jagaricin action. Based on the structure of jagaricin, we assume that rather the lipid tail is anchored into the membrane, while the peptide part is at least partially exposed to the outside. In this regard, it is interesting to note that all polar side chains of the jagaricin molecule (Fig. 9) that are able to participate in hydrogen bond interactions (hydroxyl group of the fatty acid, D-allo-Thr-4, L-allo-Thr-9, and L-His-10) cluster around the hydrophobic ring-closing ester moiety (L-Thr-3 and its neighbor Dhb-2), separating the hydrophobic tail from a second hydrophobic cluster (D-Tyr-5, Dhb-6, D-Gln-7, and Gly-8). This may result in a three-dimensional structure with the hydrophilic parts located within the phospholipid head layer and the hydrophobic peptide cluster and lipid chain located in the lipophilic part of the membrane. Notably, the lipid chain of the jagaricin molecule is rather short; such a conformation would therefore exert a strong bending stress toward the local membrane environment but might also trigger self-aggregation of jagaricin molecules. In general, aggregate formation within fungal membranes has been sug-

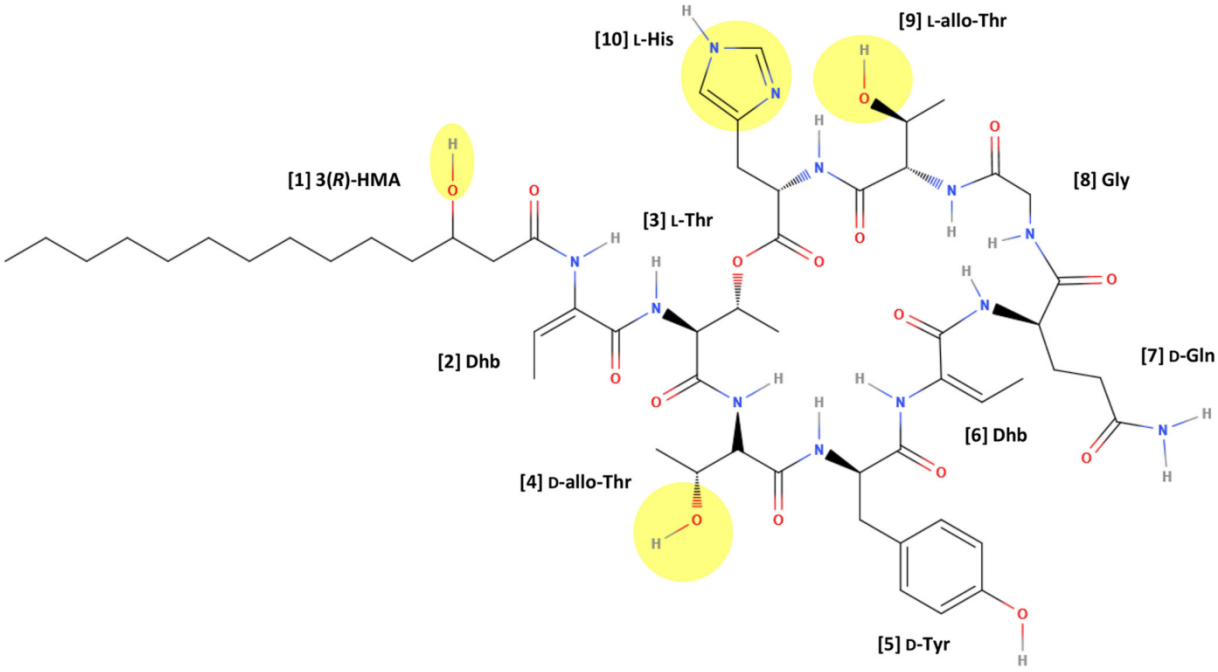

FIG 9 Polarity distribution within the jagaricin molecule. The structure and distribution of polar and apolar parts within the jagaricin molecule are depicted. Polar functional groups are highlighted in light yellow.

gested as crucial for the antifungal action of the *Bacillus* lipopeptide classes of fengycins and iturins (26, 27, 32–35). This phenomenon is explained by the combined effect of aggregates of, e.g., inverted-cone shaped lipopeptides on the local membrane bending, while monomers are typically insufficient to significantly alter local membrane structures. Fengycin aggregate formation was found to be triggered by immiscibility of the lipopeptide with the target membrane (27, 35, 36). This also explains the missing activity of fengycin against bacteria, since fengycin can readily interact with their large amounts of phosphatidylethanolamine, thus mixing with membrane components and inhibiting formation of biologically active aggregates (35). In fungal membranes, phosphatidylcholine and fengycin do not interact, and aggregate formation takes place. Thus, contrary to intuition, the presence of an avid binding partner in a membrane can actually diminish the effect of an intercalating agent. In the case of jagaricin, we can speculate whether aggregate formation in membranes is relevant to its biological activity and which possible role sterols may play in the biological activity of jagaricin.

Interestingly, organisms containing cholesterol (mammals) and ergosterol (fungi and social amoebae) were targeted, while bacteria (containing no sterols) and plants, whose membranes typically contain a diverse mixture of sterols (mainly phytosterols, with cholesterol typically accounting only for 1 to 2% of total sterols [37]), remained largely unaffected. When we investigated the ergosterol metabolism in yeasts, we observed both positive and negative effects on jagaricin susceptibility: strains defective at different steps of ergosterol biosynthesis (*Caerg5*Δ, *Cgerg5*Δ, and a clinical *C. albicans* isolate with deficiency at Erg6) showed no altered susceptibility toward jagaricin, while clinical isolates deficient for Erg3 showed reduced jagaricin tolerance. These strains are known to accumulate episterol, ergosta-7-enol, and ergosta-7,22-dienol instead of ergosterol under typical culture conditions (38, 39). Such compounds could potentially serve as a jagaricin interaction partner as well or better than ergosterol to explain this phenotype. Importantly, these compounds do not have the same detrimental effect as 14α-methylergosta-8,24(28)-dien-3β,6α-diol to the organism (40), which accumulates in membranes of azole-treated yeasts and increases their fluidity (40). Since we ob-

served a rescue of yeast growth when clotrimazole was added together with otherwise toxic jagaricin levels, it seems possible that such a more fluid membrane decreases the activity of jagaricin, for example via reduced aggregation or faster closing of lesions formed by jagaricin. Indeed, it is known that higher plasma membrane sterol levels (and concomitant decreased fluidity) prolong the lifetime of opened pore states for iturins (32, 33). We similarly observed that the *UPC2* gain-of-function strain, with its increased ergosterol plasma membrane levels (14–16), was hypersusceptible to jagaricin.

Furthermore, transcription of the regulator of ergosterol biosynthesis in *C. albicans*, *UPC2*, itself was upregulated upon short-term exposure to jagaricin, possibly indicating membrane stress. However, it was downregulated, together with some ergosterol biosynthesis genes (*ERG1*, *ERG3*, and *ERG11*), under longer-term growth permissive jagaricin treatment. This would lower the ergosterol levels and thus jagaricin susceptibility. Whether or not this happened as a direct response to the action of jagaricin will be interesting to study in the future, for example, to determine whether this mechanism could be inhibited to enhance the antifungal action of jagaricin. In summary, we conclude that composition and levels of membrane sterols can influence jagaricin susceptibility, and a reduction of ergosterol biosynthesis rates might enable yeasts to grow in the presence of otherwise toxic jagaricin levels—interestingly the opposite of a classical azole resistance mechanism.

So far, we have discussed the direct interaction of jagaricin with the plasma membrane. But what are the consequences of this interaction for susceptible target cells? Lesions caused by jagaricin are likely large, since they allow the transit of large hydrated ions like Ca^{2+}, and nonselective, since the influx of Ca^{2+} was not inhibited by Cd^{2+} in a mammalian cell line. As a result, these ion fluxes will lead to the breakdown of the plasma membrane potential. This would lead to increased osmosensitivity, and in fact deletion of essentially any of the MAP kinases of the high osmolarity glycerol pathway resulted in a decreased jagaricin resistance. This is similar to iturins which have been shown to provoke osmotic stress in the fungal phytopathogen *Verticillium dahliae*, and fungal resistance toward iturins depends on Hog1 activation (41). In conclusion, we hypothesize that the breakdown of plasma membrane potential, together with the intracellular accumulation of Ca^{2+}, aided by osmotic stress and possibly ROS generation, will in sum lead to fungal cell death.

Our data using growth permissive jagaricin concentrations revealed important hints regarding the molecular events triggered by jagaricin in fungi: during exposure, we found transcriptional indications of a shutdown of mitochondria function, which could hint toward a disruption of mitochondrial membrane potential by sublethal jagaricin levels, similar to the surfactants SDS and CTAB (23) or feasibly apoptotic processes under disrupted Ca^{2+} homeostasis (42). Are mitochondria thus a relevant target for jagaricin toxicity? Loss of mitochondrial membrane potential will disrupt ATP generation, and we would expect a pronounced reduction of energy-consuming cellular processes such as transcription, translation, amino acid biosynthesis, and fatty acid synthesis. Except for the transcriptional downregulation of fatty acid biosynthesis in the short-term transcriptomic response, we did not observe such reductions neither in the transcriptional short-term nor in the growth response. We therefore propose that the observed transcriptional shutdown of plasma membrane transport processes, as well as the downregulation of the gene for the main electrogenic proton pump, Pma1 (43), in *C. albicans* is caused by the loss of the plasma membrane chemiosmotic potential and Ca^{2+} influx rather than by ATP level reduction. In support of this view, Ca^{2+}-dependent calcineurin signaling is known to control Pma1 activity in *S. cerevisiae* (44, 45). Furthermore, a subinhibitory jagaricin concentration elicited limited cell death in a subpopulation of *C. albicans* cells as shown by PI staining, although the majority continued to grow (Fig. 1A).

Interestingly, during our screening we found two deletion mutants with increased resistance toward jagaricin, both lacking genes for inositol polyphosphate phosphatases (*cginp53*Δ and *cainp51*Δ [but not *cginp51*Δ]). Both enzymes dephosphorylate inositol phosphates, including PIP_2, which is located in the inner membrane leaflet and

known to play a pivotal role in actin cytoskeleton organization, endocytosis, and integrity of the cell envelope as a membrane anchor for proteins (46, 47). This complements the observed hypersusceptibility of *Cgslm1*Δ, a *C. glabrata* mutant lacking the homolog of the *S. cerevisiae* PIP_2-binding protein Slm1. The latter is known to regulate actin cytoskeleton organization in response to stress (48). In summary, this membrane-bound regulator of endocytosis and actin polymerization is proposed to play an important role in withstanding jagaricin, again linking membrane composition to jagaricin susceptibility.

Permanently elevated intracellular Ca^{2+} levels, breakdown of plasma membrane potential and membrane pores all together disrupt the cell's highly ordered state. Elevated cytosolic Ca^{2+} levels alter the localization of cationic proteins away from the cytoplasm-facing membrane leaflet (49), and Ca^{2+} influx through membrane lesions also triggers the onset of local membrane repair processes (50). Therefore, the transcriptional upregulation of phospholipid translocases could counteract jagaricin action in two ways: first, directly via promotion of (e.g., endosome-driven) membrane repair processes (51, 52) and, second, by potentially increasing negatively charged phospholipids in the cytoplasmic leaflet of the plasma membrane to restore protein organization. This could provide an additional explanation for the resistance phenotype of the inositol polyphosphate phosphatases, since an elevated level of highly phosphorylated inositol phosphates would have the same effect. Interestingly, of the three most strongly upregulated jagaricin phospholipid translocases, Rta2 and Rta4 are targets of calcineurin regulation and upregulated under extracellular Ca^{2+} stress (53, 54), and Rta3 has been shown to regulate membrane asymmetry in *C. albicans* (55). Therefore, membrane asymmetry regulation in response to elevated cytosolic Ca^{2+} levels might (partially) restore cell homeostasis under the severe stress induced by jagaricin.

Overall, these proposed mechanisms render jagaricin an interesting candidate for a fungicide directly targeting the membrane. However, its lytic effect on erythrocytes seems to prohibit its use in mammals in its unmodified form. Potentially, chemical modification could be used to increase its specificity. One possible aim of further optimization should be increased self-aggregation within ergosterol-containing membranes over cholesterol-containing membranes, if aggregates in fact represent the active forms of jagaricin. Jagaricin derivatives with decreased overall toxicity could potentially be combined with non-azole ergosterol biosynthesis inhibitors which increase sterol by-products to enhance its efficacy, similar to what we observed for the Erg3-deficient *C. albicans* strains with jagaricin.

As an interesting feature, we observed broad activity against phytopathogenic fungi, but no or very specific and limited detrimental effects on their host plants: all tested phytopathogens were susceptible in a comparable concentration range, while plant root growth was either unaffected (*L. sativum*) or only affected under one experimental condition (*S. alba*). Despite modern crop management, phytopathogenic fungi still cause devastating yield losses (5–7, 56), and agricultural use of substance classes also in use for human disease treatment is controversial (8, 57). As biotechnological production of jagaricin appears feasible, further optimization of fermentation conditions of *Janthinobacterium agaricidamnosum* and future process development will enable the production of ample amounts for agricultural uses.

Interestingly, *Bacillus* species producing various amounts of surfactins, iturins, and fengycins are used as biocontrol species in agriculture instead of the purified compounds (58), which have been reported to stimulate the plant defense against pathogens in addition to their direct antimicrobial action (58). *Janthinobacteria* are commonly found in soil (59, 60) raising the question whether jagaricin-related compounds that have coevolved in symbiotic bacterium-plant interactions exist. Therefore, *Janthinobacteria* might merit further investigations to elucidate their potential as biocontrol species.

In summary, we showed that jagaricin is an example for a virulence factor developed by a pathogenic bacterium against its mushroom host that exerts its function by disrupting cell membranes. We found a certain degree of species specificity and suggest that this is at least partly based on membrane composition. Interestingly, the

target and the mode of action of jagaricin are superficially similar to toxins of other mushroom-infecting bacteria such as tolaasin from *Pseudomonas tolaasii* (61, 62) and WLIP from *Pseudomonas reactans* (61). This kind of interorganism interaction could thus be an interesting source to identify new antifungals for human medicine. Jagaricin and its future derivatives are therefore candidates with great potential as antifungal agents.

MATERIALS AND METHODS

Yeast growth conditions. Yeasts were routinely streaked on YPD (1% yeast extract, 2% peptone, 2% glucose; pH 7) agar and incubated 1 to 2 days at 30°C. Yeast cultures were stored at 4°C for up to 1 month. Yeast cultures were routinely grown overnight in YPD (1% yeast extract, 1% peptone, 2% glucose; pH ≈ 6) at 30°C with shaking (180 rpm).

Yeast strains. For the PI assay, the transcriptome analysis and the combinatorial drug tests, the *C. albicans* reference strain SC5314 was used. For *C. albicans* and *C. glabrata* strains used in the mutant test screening, see Table S1B in the supplemental material.

Chemicals and media. A total of 500 ml of 2× SD (pH 6) (+ CSM) (+ uridine) liquid medium, 6.7 g of YNB without amino acids (Difco, catalog no. 291940, 100 g), and optionally 0.395 g of complete supplement mixture (CSM, Formedium, catalog no. DCS0019) were dissolved in 400 ml of double-distilled water, adjusted to pH 6 with NaOH, and autoclaved. Then, 100 ml of autoclaved 20% (wt/vol) glucose solution was added. When required, 5 ml of water was replaced by an autoclaved uridine (5 mg/ml; Carl Roth, catalog no. 0714.3) solution added after autoclaving to reach 50 μg/ml.

Jagaricin powder was dissolved at a concentration of 1 mg/ml in 10% ethanol by sonication, aliquoted, and stored at −80°C until usage. Aliquots were thawed immediately before use. Amphotericin B (Sigma, catalog no. A4888, 100 mg) powder was dissolved in dimethyl sulfoxide (DMSO) to give a stock solution of 10 mg/ml, aliquoted, and stored at 4°C in the dark for a maximum of 6 months. Aliquots were thawed immediately before use. Caspofungin diacetate (Sigma, catalog no. 32343, 10 mg) was dissolved in sterile phosphate-buffered saline (PBS) to give a final concentration of 20 mg/ml, aliquoted, and stored at −20°C. Aliquots were thawed immediately before use. Clotrimazole powder (Bayer) was dissolved at 1 mg/ml in 10% ethanol to yield a cloudy stock solution, which cleared upon further dilutions. Aliquots were stored at −80°C and thawed immediately before use.

Jagaricin production and purification. A cryostock of *Janthinobacterium agaricidamnosum* DSM 9628 (~0.5 ml) was used to inoculate 50 ml of sterile nutrient broth (1 g/liter beef extract, 2 g/liter yeast extract, 5 g/liter peptone, 5 g/liter NaCl), and the culture was grown at 25°C for 20 h at 150 rpm. Five Erlenmeyer flasks containing 200 ml of a suitable sterile growth medium (5 g/liter glycerol, 10 g/liter glucose, 10 g/liter yeast extract, 5 g/liter sodium glutamate, 3 g/liter $CaCO_3$; after sterilization, 2 ml/liter trace element solution, containing 4 g/liter $CaCl_2 \cdot 2H_2O$, 1 g/liter iron(III) citrate·H_2O, 0.2 g/liter $MnSO_4$, 0.1 g/liter $ZnCl_2$, 0.03 g/liter $CoCl_2 \cdot 6H_2O$, 0.04 g/liter $CuSO_4 \cdot 5H_2O$, 0.03 g/liter $Na_2MoO_4 \cdot 2H_2O$, and 0.06 g/liter $Na_2B_4O_7 \cdot 10H_2O$ was added, and the pH was adjusted to 6.8 using NaOH) were inoculated with 1 ml of the preculture. The cultures were grown at 25°C for 20 h at 150 rpm. Fermentation was performed at a 30-liter scale using the same medium and 0.167 g/liter antifoaming agent SAG471. The fermenter was inoculated with 800 ml of the preculture. The pH was regulated in a range of 6.2 to 7.8, and the temperature was set to 23°C. The culture was aerated with a sterile airflow of 5 to 10 liters/min and a stirrer speed of 200 to 500 rpm to reach a saturation of >20% O_2. The fermentation was stopped after 51 h. Then, 15 liters of the fermentation broth was twice extracted with ethyl acetate (27 and 15 liters), and the collected extracts were concentrated to dryness. The residue was taken up in methanol (20 ml), and ice-cold ethyl acetate (40 ml) was added. The mixture was sonicated and stirred until a homogeneous slurry was obtained. The solid was removed by filtration and washed with small portions of ice-cold ethyl acetate and dried under reduced pressure. A portion of the solid (50 mg) was treated with methanol (~1 ml), centrifuged to remove undissolved material, and the supernatant was subjected to preparative high-pressure liquid chromatography (Macherey & Nagel Nucleodur C_{18} column [5 μm, 40 by 250 mm]; gradient, 25 to 75% acetonitrile with 0.1% trifluoroacetic acid; flow, 30 ml/min) to obtain pure jagaricin (28 mg).

***Candida* mutant susceptibility testing.** Yeast overnight cultures were harvested by centrifugation for 1 min at 5,000 × *g*, washed twice with distilled water, and resuspended in 1 volume of distilled water. Yeast cells were then diluted 1:100 in 2× SD plus CSM medium and adjusted to 5×10^5 yeast cells/ml. All dilutions were stored on ice to prevent further yeast growth. Jagaricin stock solutions were diluted to 6 or 4 μg/ml in 1% ethanol. For the assay, 100 μl of yeast cells was mixed with 100 μl of jagaricin or control solution in a 96-well plate (TPP, catalog no. 92696), resulting in 5×10^4 cells per well in 1× SD plus CSM plus 0.5% ethanol (pH 6). Each strain was tested at 3, 2, and 0 μg/ml jagaricin in technical duplicates for each of three biological replicates. For growth curve measurements, the plate was covered with sealing foil (Excel Scientific, STR-SEAL-PLT), transferred to a microplate reader (Tecan Infinite M200; i-control software), and incubated for 3 days at 30°C, with absorbance measurements at 600 nm (A_{600}) every 30 min after 10 s of orbital shaking.

Occasional, late-onset residual growth occurred even at the usually toxic dose of 3 μg/ml jagaricin. If all or the majority of strains showed unexpected fast growth at 3 μg/ml jagaricin, the assays were excluded from further analysis, and new biological replicates were performed with a fresh jagaricin aliquot (in a total of two cases). Stable growth of a mutant at 3 μg/ml jagaricin was defined as detectable growth in at least two of three biological replicates and a maximum change in A of $\Delta A = \max(A - A_{background}) \geq 0.15$ (the mean of three biological replicates). We used the growth curve data to calculate

the relative A_{max} as follows: relative A_{max} (%) = (ΔA [mutant]/ΔA [wild type]) × 100. The relative half-maximal time ($t_{1/2}$) was defined as the $-\log_2$ value of the ratio of the wild type and mutant $t_{1/2}$ values.

Transcriptome analysis. For RNA isolation *C. albicans* SC5314 was grown in YPD overnight, 1 ml of this culture harvested by centrifugation (10,000 × *g*, 1 min), washed twice with distilled water, and used to inoculate a second YPD culture at OD_{600} of 0.1 in 5 to 10 ml of YPD, which was grown at 30°C and 180 rpm until reaching an OD_{600} of 1 to 4. Cells were pelleted (10,000 × *g*, 1 min), washed twice with distilled water, and adjusted to either 10^7 ml^{-1} or 5×10^5 ml^{-1} in 2× SD (pH 6) for short-term exposure to and growth in jagaricin, respectively.

For short-term exposure, yeasts were mixed 1:1 with jagaricin or control solution to reach 5×10^6 yeast cells/ml in SD (pH 6) plus 0.05% ethanol with (1 μg/ml) or without jagaricin in 5 ml and then incubated at 30°C and 180 rpm. Yeast cells were harvested for RNA isolation after 30 min, and continued yeast viability was ascertained by CFU plating. Higher concentrations of jagaricin (5 μg/ml) consistently led to cell death (data not shown).

For the transcriptome response of *C. albicans* cells growing in the presence of jagaricin, yeasts were mixed with jagaricin, respectively, control solution to reach 2.5×10^5 yeast cells/ml in SD (pH 6) plus 0.05% ethanol with (0.5 μg/ml) or without jagaricin in 15 ml, followed by incubation at 30°C and 180 rpm. We found that 0.5 μg/ml jagaricin in this assay increased the lag time by several hours but did not influence the final growth rate. Samples were taken at the early growth phase at an OD_{600} of 0.5. Three biological replicates were performed for each condition.

RNA was then isolated using an RNeasy minikit (Qiagen) and Cy5-labeled cRNA (Cy5 CTP; GE Healthcare) generated using a QuickAmp labeling kit (Agilent). Samples were cohybridized with a common Cy3-labeled reference (RNA from mid-log-phase-grown *C. albicans* SC5314 [63]) on Agilent arrays (AMADID 026869), scanned in a GenePix 4200AL with GenePix Pro 6.1 (Auto PMT; pixel size, 5 μm), and analyzed with GeneSpring 14.8 (Agilent), GSEA v2.2.0 (Broad Institute) (64, 65), and Revigo (66).

Hemolysis assay. Blood for hemolysis assays was taken from healthy volunteers with written informed consent according to the principles expressed in the Declaration of Helsinki. The blood donation protocol and use of blood were approved by the institutional ethics committee of the University Hospital Jena (permission number 2207-01/08). Blood was collected using EDTA-containing S-Monovette tubes (Sarstedt). Portions (1 ml) were centrifuged for 5 min and 1,000 × *g* at room temperature, washed with 500 μl of Dulbecco PBS (DPBS; Gibco), and resuspended in 300 μl of DPBS. The erythrocyte cell count was determined using an Auto BC-5300 Vet hematology analyzer and adjusted to 5×10^8 ml^{-1} in DPBS. The hemolysis assay was performed with 20 μl of erythrocyte solution in a total volume of 150 μl with variable jagaricin concentrations and 0.5% (vol/vol) ethanol. For the high control [HC], 130 μl of double-distilled water was used; for the low control [LC], 118 μl of DPBS, 4.5 μl of water, and 7.5 μl of 10% (vol/vol) ethanol were added (the same as for the jagaricin diluent). The mixtures were incubated 1 h at 30°C and centrifuged 3 min and 1,000 × *g* at room temperature, and the supernatant was immediately transferred to a 96-well plate for absorbance determination at 541 nm in a Tecan Infinite M200 microplate reader (using i-control software). Individual hemolysis rates were calculated as follows: the % lysis of HC = $[(A_{sample} - A_{LC})/(A_{HC} - A_{LC})] \times 100$ in two technical replicates. The normalized lysis values were plotted against the inverse logarithmic concentration of the compound to determine the IC_{50} value using Prism (v7; GraphPad). The assay was repeated three times to obtain the weighted mean and error of the $\log_{10}$ IC_{50}, as described previously (67).

***C. albicans* PI assay.** Yeast overnight cultures of *C. albicans* SC5314 were harvested for 1 min at 5,000 × *g*, washed twice with distilled water, resuspended in either 2× SD or 2× PBS (pH 7.4) at 5×10^5 ml^{-1}, and kept on ice until the start of the assay. Portions (100 μl/well) were then pipetted into a 96-well plate (TPP) with 1 μl of propidium iodide (PI) solution (1 mg/ml), and the cells were allowed to settle for 15 min. Then, 100 μl of jagaricin solution was added to a final concentration of 0 to 8 μg/ml jagaricin (containing 0.1% [vol/vol] ethanol). Immediately after jagaricin addition, the plate was imaged hourly with a CellDiscoverer 7 microscope and ZEN 2.3 software (Zeiss) at 30°C for 20 h; three biological replicates were performed. The images were analyzed by automatic detection in ImageJ (68–70), with yeasts and PI-positive signals defined as signal intensities of greater than or equal to the means plus 3× standard deviation in the contrast enhanced bright-field or fluorescence channel, respectively. A fraction of yeasts lost the PI signal over time. The fraction size and decay time of PI signal were thus separately determined with 150 yeasts in 3, 4, and 8 μg/ml jagaricin and used to correct the loss of PI signal of the respective jagaricin concentrations during longer measurements.

Cooperative drug tests. Overnight cultures of *C. albicans* SC5314 were harvested for 1 min at 5000 g, washed twice and resuspended in distilled water, and adjusted to 5×10^5 ml^{-1} and kept on ice until start of the assay. Jagaricin and other drugs (clotrimazole, caspofungin or amphotericin B) were diluted from stocks with double-distilled water to appropriate concentrations. Assays were performed as follows: 100 μl of yeasts were mixed with 50 μl each of jagaricin and combinatorial drug in a microplate well (TPP, Ref. no. 92696) to a final 2.5×10^4 cells per well in 1× SD (pH 6) plus 0.05% (vol/vol) ethanol (amphotericin B, caspofungin) or 0.15% (vol/vol) ethanol (clotrimazole), and 0.05% (vol/vol) DMSO (amphotericin B). The plate was covered with a gas-permeable sealing foil (4titude; product code 4ti-0516/96) and absorbance at 600 nm determined every 30 min in a Tecan infinite M200 microplate reader (software: i-control) set to 30°C for a total duration of 48 h. Three biological replicates were performed for each combination scenario. For $\sum$FICI calculations, MIC95 was used for jagaricin, AMB and CAS, while MIC75 was applied for CLT.

Growth inhibition assay *D. discoideum*. A total of 3,000 *D. discoideum* cells (AX2) were cultured at 22°C as triplicates in 96-well plates (Sarstedt) in 200 μl of HL5 medium containing 1% DMSO (Carl Roth) and a 2-fold serial dilution of jagaricin from 1 μg/ml down to 0.1 ng/ml; the positive growth control

lacked jagaricin. After 72 h, the cell concentration was determined at a size range of 7.6 to 17.6 μm with a CASYCell Counter and an Analyser system (model TT [Roche Innovatis AG]; equipped with a 60-μm capillary). The viable cell concentration was plotted against the logarithmic concentration of the compound to determine the IC_{50} value using Prism. The assay was repeated three times to obtain the weighted mean and error of the $\log_{10}$ IC_{50}, as described previously (67).

$[Ca^{2+}]_i$ and patch-clamp measurements. HEK293T cells were obtained from the German Collection of Microorganisms and Cell Cultures (DSMZ, Braunschweig, Germany) and maintained in DMEM/F-12 (Dulbecco modified Eagle medium: nutrient mixture F-12; Life Technologies, Darmstadt, Germany) supplemented with 10% fetal calf serum (Biochrom, Berlin, Germany) at 37°C in a 95% air–5% CO_2 atmosphere and saturated humidity. Measurements of intracellular free Ca^{2+} levels ($[Ca^{2+}]_i$) were performed as described previously (71) with slight modifications: HEK293T cells were loaded with 1 μM Fura-2-AM (Life Technologies) in complete culture medium for about 20 min at 37°C. The cells were washed, and recording was performed in a HEPES-buffered solution containing 150 mM NaCl, 2 mM KCl, 1.5 mM $CaCl_2$, 1 mM $MgCl_2$, and 10 mM HEPES (pH 7.4) at room temperature. In control experiments, the specific Ca^{2+} transport was blocked by the addition of 0.1 mM $CdCl_2$ to the recording buffer. Fluorescence was measured using a microscopy-based system after alternating the illumination at 340 or 380 nm with a sample rate of 0.1 Hz. The data were analyzed using TILLvisION software (TILL Photonics, Gräfelfing, Germany). The 340-nm/380-nm ratio of the background-corrected fluorescence signal was calculated on a single-cell level and plotted as a function of time for 60 to 100 cells per experiment in at least five independent experiments for each condition.

Currents were recorded from HEK293T cells in the whole-cell configuration of the patch-clamp method using an EPC-10 amplifier (HEKA Elektronik, Lambrecht, Germany), operated with PatchMaster software (HEKA; for further details, see reference 72). Cells were clamped to −40 mV, while jagaricin was applied by complete bath exchange. Solutions were as follows (in mM): internal (pipette), 140 KCl, 10 EGTA, and 10 HEPES (pH 7.4 with KOH); and external (bath), 146 NaCl, 4 KCl, 2 $CaCl_2$, 2 $MgCl_2$, and 10 HEPES (pH 7.4 with NaOH).

Black lipid membranes. Planar lipid bilayers of asolectin from soybean (Sigma, catalog no. 11145-50G), dissolved in D-decane (10 mg of lipid per ml of solvent), were formed on a 1-mm-diameter Teflon septum with both bath chambers containing 100 mM KCl and 10 mM Tris-HCl (pH 8.0). The membrane current was measured with a Turbo TEC-10CD amplifier (NPI Electronic GmbH, Tamm, Germany), combined with repetitive stimulation with voltage ramps from –50 to 50 mV (see reference 73). Jagaricin was applied on both sides of the membrane up to a final concentration of 4 μg/ml; amphotericin B (2 μg/ml) and gramicidin A (1 nM) served as positive controls.

Plant susceptibility testing. Jagaricin phytotoxicity was investigated at 5 μg/ml using Phytotest-kit (MicroBioTests, Inc.) with two plants according to the manufacturer's instructions: *Lepidium sativum* and *Sinapis alba* were incubated at 25°C in the presence or absence of light for 72 h in three or two biological replicates, respectively, and evaluated for inhibition of seed germination and root length.

Susceptibility test of phytopathogenic fungi. Antifungal activity was determined in broth dilution according to CLSI reference method M38-A2, with slight modifications, for the major agricultural phytopathogens *Alternaria alternata*, *Penicillium digitatum*, *Penicillium italicum*, *Geotrichum candidum*, *Colletrothricum gloeosporioides*, *Fusarium graminearum*, and *Botrytis cinerea*. The tests were performed in 96-well plates in duplicate, with 195 μl of RPMI 1640 medium per well supplemented from a jagaricin stock solution (1.28 mg/ml dissolved in 5% DMSO) to reach a final concentration range of 20 to 0.08 μg/ml. Then, 5 μl of each fungal species was added to reach 5×10^4 CFU/ml, followed by incubation for 48 h at 30°C. As a positive control, ketoconazole (50 μg/ml) was used, and 5% DMSO in RPMI 1640 medium served as the negative control.

Critical micellar concentration (CMC) determination. Measurements were performed as described previously (74). Fluorescence measurements were performed on a Jasco FP6200 instrument using 10-mm fused silica cuvettes. Excitation was carried out at 331.5 nm, and emission spectra were recorded at 340 to 450 nm. I_1/I_3 ratios were calculated from the intensities at 374 nm (1) and 386 nm (3). The matrix solution was prepared from ultrapure water (Thermo GenPure system) containing approximately 2 μM pyrene. Pyrene (≈0.4 mg) was taken up in 20% ethanol using an ultrasonic bath (80°C) and diluted with water to give a final ethanol content of 0.5%. To this solution, defined volumes of a suitable stock solution of jagaricin (1, 10, or 100 mg/ml in methanol) were added to give final volumes of 4 ml and total methanol contents of <2%, preferably <0.5%. Individual samples for each data point were prepared, gently mixed, and incubated for at least 30 min at room temperature prior to fluorescence measurement.

Statistical analysis. Experiments were performed in biological replicates from independent samples ($n \geq 3$) unless stated otherwise (see "Plant susceptibility testing"). All experiments were performed unblinded. Data points in graphs represent either (weighted) arithmetic or geometric means (see individual graphs) ± the standard deviations. Data were analyzed using GraphPad Prism 7 (GraphPad Software, Inc., La Jolla), ImageJ (68–70), Excel 2010, GeneSpring GX (v14.8; Agilent Technologies, Inc., Santa Clara, CA), GSEA v2.2.0 (Broad Institute) (64, 65), and Revigo (66). Where applicable, samples were tested for significance ($P < 0.05$) using a two-sided *t* test, and GO-term enrichment was determined by using the Fisher exact test.

Data availability. All relevant data are available by request from the authors, with the restriction of data that would compromise the confidentiality of blood donors. The microarray data are available in the ArrayExpress database at EMBL-EBI (www.ebi.ac.uk/arrayexpress) under accession number E-MTAB-7718.

SUPPLEMENTAL MATERIAL

Supplemental material for this article may be found at https://doi.org/10.1128/AAC.00707-19.

SUPPLEMENTAL FILE 1, PDF file, 2.1 MB.
SUPPLEMENTAL FILE 2, XLSX file, 1.8 MB.
SUPPLEMENTAL FILE 3, XLSX file, 1.7 MB.
SUPPLEMENTAL FILE 4, XLSX file, 0.02 MB.

ACKNOWLEDGMENTS

We thank Vito Valiante and Jakob Weber for sharing unpublished results and helpful discussions, Dominique Sanglard and Oliver Bader for kindly providing some strains for the mutant analysis, Karin Martin for performing and optimizing the jagaricin preparation, Nadja Jablonowski, Daniela Schulz, and Dorothee Eckhardt for technical help with the *Candida* mutant tests, and Ankido Gustin for technical help with the *C. albicans* killing assay.

D.F., B.H., and S.B. have been supported by the Cluster of Excellence "Balance of the Microverse" of the Friedrich Schiller University Jena and by the Leibniz Science Campus "InfectoOptics" and Collaborative Research Centre/Transregio 124–"FungiNet" (project C1) of the Deutsche Forschungsgemeinschaft. S.H.H. has been supported by the German Federal Ministry of Research and Education (Competence Cluster for Nutrition and Cardiovascular Health—nutriCARD, grant 01EA1411A). R.B. was a member of the Jena School for Microbial Communication. F.K. has been supported by InfectControl 2020 (FKZ 03ZZ0803A). The work of C.H., K.S., K.D., and T.P.F. has been supported by the SFB 1127 ChemBioSys. T.P.F. has been supported by a Capes-Humboldt research fellowship. The funders had no role in study design, data collection and interpretation, or the decision to submit the work for publication.

D.F. performed experiments (*C. albicans* killing, *Candida* mutant screen, *C. albicans* transcriptome analysis, hemolysis assay, and the cooperative drug test), analyzed the data, wrote the manuscript, and prepared the figures. G.G. and K.T. performed patch clamp assays and measurements of intracellular free Ca^{2+} levels, analyzed the data, and edited the manuscript. T.P.F. performed susceptibility tests of phytopathogenic fungi and plant susceptibility testing, analyzed the data, and edited the manuscript. R.B. and P.S. performed the *D. discoideum* susceptibility test, analyzed the data, and edited the manuscript. F.K. and K.S. isolated and provided jagaricin. F.K. performed the CMC determination, analyzed the data, and edited the manuscript. K.D., B.H., and C.H. discussed and interpreted the data and edited the manuscript. S.H.H. discussed the data, edited the manuscript, designed parts of the study (patch clamp assays and intracellular calcium measurements), and prepared the corresponding figures. K.S. and S.B. conceived and designed the study, K.S. edited the manuscript, and S.B. cowrote the manuscript.

We declare no competing interests.

REFERENCES

1. Newman DJ, Cragg GM. 2012. Natural products as sources of new drugs over the 30 years from 1981 to 2010. J Nat Prod 75:311–335. https://doi.org/10.1021/np200906s.
2. Graupner K, Scherlach K, Bretschneider T, Lackner G, Roth M, Gross H, Hertweck C. 2012. Imaging mass spectrometry and genome mining reveal highly antifungal virulence factor of mushroom soft rot pathogen. Angew Chem Int Ed Engl 51:13173–13177. https://doi.org/10.1002/anie.201206658.
3. Brown GD, Denning DW, Gow NA, Levitz SM, Netea MG, White TC. 2012. Hidden killers: human fungal infections. Sci Transl Med 4:165rv113.
4. Chowdhary A, Sharma C, Meis JF. 2017. *Candida auris*: a rapidly emerging cause of hospital-acquired multidrug-resistant fungal infections globally. PLoS Pathog 13:e1006290. https://doi.org/10.1371/journal.ppat.1006290.
5. Chrispeels MJ, Sadava DE. 2003. Plants, genes, and crop biotechnology, 2nd ed. Jones & Bartlett Publishers, Sudbury, MA.
6. Meena KR, Kanwar SS. 2015. Lipopeptides as the antifungal and antibacterial agents: applications in food safety and therapeutics. Biomed Res Int 2015:473050. https://doi.org/10.1155/2015/473050.
7. Doehlemann G, Okmen B, Zhu W, Sharon A. 2017. Plant pathogenic fungi. Microbiol Spectr 5:703–726.
8. Verweij PE, Snelders E, Kema GH, Mellado E, Melchers WJ. 2009. Azole resistance in *Aspergillus fumigatus*: a side-effect of environmental fungicide use? Lancet Infect Dis 9:789–795. https://doi.org/10.1016/S1473-3099(09)70265-8.
9. Hamley IW. 2015. Lipopeptides: from self-assembly to bioactivity. Chem Commun 51:8574–8583. https://doi.org/10.1039/c5cc01535a.
10. Mangoni ML, Shai Y. 2011. Short native antimicrobial peptides and engineered ultrashort lipopeptides: similarities and differences in cell specificities and modes of action. Cell Mol Life Sci 68:2267–2280. https://doi.org/10.1007/s00018-011-0718-2.
11. Zhao H, Shao D, Jiang C, Shi J, Li Q, Huang Q, Rajoka MSR, Yang H, Jin

M. 2017. Biological activity of lipopeptides from *Bacillus*. Appl Microbiol Biotechnol 101:5951–5960. https://doi.org/10.1007/s00253-017-8396-0.
12. Denning DW. 2003. Echinocandin antifungal drugs. Lancet 362: 1142–1151. https://doi.org/10.1016/S0140-6736(03)14472-8.
13. Koh JJ, Lin S, Beuerman RW, Liu S. 2017. Recent advances in synthetic lipopeptides as anti-microbial agents: designs and synthetic approaches. Amino Acids 49:1653–1677. https://doi.org/10.1007/s00726-017-2476-4.
14. Lohberger A, Coste AT, Sanglard D. 2014. Distinct roles of *Candida albicans* drug resistance transcription factors TAC1, MRR1, and UPC2 in virulence. Eukaryot Cell 13:127–142. https://doi.org/10.1128/EC.00245-13.
15. Flowers SA, Barker KS, Berkow EL, Toner G, Chadwick SG, Gygax SE, Morschhauser J, Rogers PD. 2012. Gain-of-function mutations in UPC2 are a frequent cause of ERG11 upregulation in azole-resistant clinical isolates of *Candida albicans*. Eukaryot Cell 11:1289–1299. https://doi.org/10.1128/EC.00215-12.
16. Dunkel N, Liu TT, Barker KS, Homayouni R, Morschhäuser J, Rogers PD. 2008. A gain-of-function mutation in the transcription factor Upc2p causes upregulation of ergosterol biosynthesis genes and increased fluconazole resistance in a clinical *Candida albicans* isolate. Eukaryot Cell 7:1180–1190. https://doi.org/10.1128/EC.00103-08.
17. Hilioti Z, Gallagher DA, Low-Nam ST, Ramaswamy P, Gajer P, Kingsbury TJ, Birchwood CJ, Levchenko A, Cunningham KW. 2004. GSK-3 kinases enhance calcineurin signaling by phosphorylation of RCNs. Genes Dev 18:35–47. https://doi.org/10.1101/gad.1159204.
18. Reedy JL, Filler SG, Heitman J. 2010. Elucidating the *Candida albicans* calcineurin signaling cascade controlling stress response and virulence. Fungal Genet Biol 47:107–116. https://doi.org/10.1016/j.fgb.2009.09.002.
19. Kingsbury TJ, Cunningham KW. 2000. A conserved family of calcineurin regulators. Genes Dev 14:1595–1604.
20. Fuentes JJ, Genesca L, Kingsbury TJ, Cunningham KW, Perez-Riba M, Estivill X, de la Luna S. 2000. DSCR1, overexpressed in Down syndrome, is an inhibitor of calcineurin-mediated signaling pathways. Hum Mol Genet 9:1681–1690. https://doi.org/10.1093/hmg/9.11.1681.
21. Liu TT, Lee RE, Barker KS, Lee RE, Wei L, Homayouni R, Rogers PD. 2005. Genome-wide expression profiling of the response to azole, polyene, echinocandin, and pyrimidine antifungal agents in *Candida albicans*. Antimicrob Agents Chemother 49:2226–2236. https://doi.org/10.1128/AAC.49.6.2226-2236.2005.
22. Mesa-Arango AC, Trevijano-Contador N, Román E, Sánchez-Fresneda R, Casas C, Herrero E, Argüelles JC, Pla J, Cuenca-Estrella M, Zaragoza O. 2014. The production of reactive oxygen species is a universal action mechanism of amphotericin B against pathogenic yeasts and contributes to the fungicidal effect of this drug. Antimicrob Agents Chemother 58:6627–6638. https://doi.org/10.1128/AAC.03570-14.
23. Yu Q, Zhang B, Ma F, Jia C, Xiao C, Zhang B, Xing L, Li M. 2015. Novel mechanisms of surfactants against *Candida albicans* growth and morphogenesis. Chem Biol Interact 227:1–6. https://doi.org/10.1016/j.cbi.2014.12.014.
24. Aiyar P, Schaeme D, Garcia-Altares M, Carrasco Flores D, Dathe H, Hertweck C, Sasso S, Mittag M. 2017. Antagonistic bacteria disrupt calcium homeostasis and immobilize algal cells. Nat Commun 8:1756. https://doi.org/10.1038/s41467-017-01547-8.
25. Patel H, Huynh Q, Bärlehner D, Heerklotz H. 2014. Additive and synergistic membrane permeabilization by antimicrobial (lipo)peptides and detergents. Biophys J 106:2115–2125. https://doi.org/10.1016/j.bpj.2014.04.006.
26. Deleu M, Paquot M, Nylander T. 2008. Effect of fengycin, a lipopeptide produced by *Bacillus subtilis*, on model biomembranes. Biophys J 94: 2667–2679. https://doi.org/10.1529/biophysj.107.114090.
27. Patel H, Tscheka C, Edwards K, Karlsson G, Heerklotz H. 2011. All-or-none membrane permeabilization by fengycin-type lipopeptides from *Bacillus subtilis* QST713. Biochim Biophys Acta 1808:2000–2008. https://doi.org/10.1016/j.bbamem.2011.04.008.
28. Baginski M, Resat H, Borowski E. 2002. Comparative molecular dynamics simulations of amphotericin B-cholesterol/ergosterol membrane channels. Biochim Biophys Acta 1567:63–78. https://doi.org/10.1016/s0005-2736(02)00581-3.
29. de Kruijff B, Gerritsen WJ, Oerlemans A, Demel RA, van Deenen LL. 1974. Polyene antibiotic-sterol interactions in membranes of *Acholeplasma laidlawii* cells and lecithin liposomes. I. Specificity of the membrane permeability changes induced by the polyene antibiotics. Biochim Biophys Acta 339:30–43. https://doi.org/10.1016/0005-2736(74)90330-7.
30. Allen NE, Hobbs JN, Alborn WE, Jr. 1987. Inhibition of peptidoglycan biosynthesis in gram-positive bacteria by LY146032. Antimicrob Agents Chemother 31:1093–1099. https://doi.org/10.1128/AAC.31.7.1093.
31. Taylor SD, Palmer M. 2016. The action mechanism of daptomycin. Bioorg Med Chem 24:6253–6268. https://doi.org/10.1016/j.bmc.2016.05.052.
32. Maget-Dana R, Ptak M. 1990. Iturin lipopeptides: interactions of mycosubtilin with lipids in planar membranes and mixed monolayers. Biochim Biophys Acta 1023:34–40. https://doi.org/10.1016/0005-2736(90)90006-a.
33. Maget-Dana R, Ptak M, Peypoux F, Michel G. 1985. Pore-forming properties of iturin A, a lipopeptide antibiotic. Biochim Biophys Acta 815: 405–409. https://doi.org/10.1016/0005-2736(85)90367-0.
34. Harnois I, Genest D, Brochon JC, Ptak M. 1988. Micellization and interactions with phospholipid vesicles of the lipopeptide iturin A, as monitored by time-resolved fluorescence of a D-tyrosyl residue. Biopolymers 27:1403–1413. https://doi.org/10.1002/bip.360270907.
35. Sur S, Romo TD, Grossfield A. 2018. Selectivity and mechanism of fengycin, an antimicrobial lipopeptide, from molecular dynamics. J Phys Chem B 122:2219–2226. https://doi.org/10.1021/acs.jpcb.7b11889.
36. Nazari M, Kurdi M, Heerklotz H. 2012. Classifying surfactants with respect to their effect on lipid membrane order. Biophys J 102:498–506. https://doi.org/10.1016/j.bpj.2011.12.029.
37. Moreau RA, Whitaker BD, Hicks KB. 2002. Phytosterols, phytostanols, and their conjugates in foods: structural diversity, quantitative analysis, and health-promoting uses. Prog Lipid Res 41:457–500. https://doi.org/10.1016/S0163-7827(02)00006-1.
38. Kelly SL, Lamb DC, Kelly DE, Manning NJ, Loeffler J, Hebart H, Schumacher U, Einsele H. 1997. Resistance to fluconazole and cross-resistance to amphotericin B in *Candida albicans* from AIDS patients caused by defective sterol Δ5,6-desaturation. FEBS Lett 400:80–82. https://doi.org/10.1016/S0014-5793(96)01360-9.
39. Chau AS, Gurnani M, Hawkinson R, Laverdiere M, Cacciapuoti A, McNicholas PM. 2005. Inactivation of sterol Δ5,6-desaturase attenuates virulence in *Candida albicans*. Antimicrob Agents Chemother 49: 3646–3651. https://doi.org/10.1128/AAC.49.9.3646-3651.2005.
40. Abe F, Usui K, Hiraki T. 2009. Fluconazole modulates membrane rigidity, heterogeneity, and water penetration into the plasma membrane in *Saccharomyces cerevisiae*. Biochemistry 48:8494–8504. https://doi.org/10.1021/bi900578y.
41. Han Q, Wu F, Wang X, Qi H, Shi L, Ren A, Liu Q, Zhao M, Tang C. 2015. The bacterial lipopeptide iturins induce *Verticillium dahliae* cell death by affecting fungal signaling pathways and mediate plant defence responses involved in pathogen-associated molecular pattern-triggered immunity. Environ Microbiol 17:1166–1188. https://doi.org/10.1111/1462-2920.12538.
42. Carraro M, Bernardi P. 2016. Calcium and reactive oxygen species in regulation of the mitochondrial permeability transition and of programmed cell death in yeast. Cell Calcium 60:102–107. https://doi.org/10.1016/j.ceca.2016.03.005.
43. Monk BC, Kurtz MB, Marrinan JA, Perlin DS. 1991. Cloning and characterization of the plasma membrane H^+-ATPase from *Candida albicans*. J Bacteriol 173:6826–6836. https://doi.org/10.1128/jb.173.21.6826-6836.1991.
44. Velivela SD, Kane PM. 2018. Compensatory Internalization of Pma1 in V-ATPase mutants in *Saccharomyces cerevisiae* requires calcium- and glucose-sensitive phosphatases. Genetics 208:655–672. https://doi.org/10.1534/genetics.117.300594.
45. Withee JL, Sen R, Cyert MS. 1998. Ion tolerance of *Saccharomyces cerevisiae* lacking the Ca^{2+}/CaM-dependent phosphatase (calcineurin) is improved by mutations in URE2 or PMA1. Genetics 149:865–878.
46. Strahl T, Thorner J. 2007. Synthesis and function of membrane phosphoinositides in budding yeast, *Saccharomyces cerevisiae*. Biochim Biophys Acta 1771:353–404. https://doi.org/10.1016/j.bbalip.2007.01.015.
47. Delage E, Puyaubert J, Zachowski A, Ruelland E. 2013. Signal transduction pathways involving phosphatidylinositol 4-phosphate and phosphatidylinositol 4,5-bisphosphate: convergences and divergences among eukaryotic kingdoms. Prog Lipid Res 52:1–14. https://doi.org/10.1016/j.plipres.2012.08.003.
48. Audhya A, Loewith R, Parsons AB, Gao L, Tabuchi M, Zhou H, Boone C, Hall MN, Emr SD. 2004. Genome-wide lethality screen identifies new PI4,5P2 effectors that regulate the actin cytoskeleton. EMBO J 23: 3747–3757. https://doi.org/10.1038/sj.emboj.7600384.
49. Yeung T, Gilbert GE, Shi J, Silvius J, Kapus A, Grinstein S. 2008. Membrane phosphatidylserine regulates surface charge and protein localization. Science 319:210–213. https://doi.org/10.1126/science.1152066.

50. Radulovic M, Stenmark H. 2018. ESCRTs in membrane sealing. Biochem Soc Trans 46:773–778. https://doi.org/10.1042/BST20170435.
51. Romero M, Keyel M, Shi G, Bhattacharjee P, Roth R, Heuser JE, Keyel PA. 2017. Intrinsic repair protects cells from pore-forming toxins by microvesicle shedding. Cell Death Differ 24:798–808. https://doi.org/10.1038/cdd.2017.11.
52. Muthusamy BP, Natarajan P, Zhou X, Graham TR. 2009. Linking phospholipid flippases to vesicle-mediated protein transport. Biochim Biophys Acta 1791:612–619. https://doi.org/10.1016/j.bbalip.2009.03.004.
53. Karababa M, Valentino E, Pardini G, Coste AT, Bille J, Sanglard D. 2006. CRZ1, a target of the calcineurin pathway in *Candida albicans*. Mol Microbiol 59:1429–1451. https://doi.org/10.1111/j.1365-2958.2005.05037.x.
54. Jia XM, Wang Y, Jia Y, Gao PH, Xu YG, Wang L, Cao YY, Cao YB, Zhang LX, Jiang YY. 2009. RTA2 is involved in calcineurin-mediated azole resistance and sphingoid long-chain base release in *Candida albicans*. Cell Mol Life Sci 66:122–134. https://doi.org/10.1007/s00018-008-8409-3.
55. Srivastava A, Sircaik S, Husain F, Thomas E, Ror S, Rastogi S, Alim D, Bapat P, Andes DR, Nobile CJ, Panwar SL. 2017. Distinct roles of the 7-transmembrane receptor protein Rta3 in regulating the asymmetric distribution of phosphatidylcholine across the plasma membrane and biofilm formation in *Candida albicans*. Cell Microbiol 19:e12767. https://doi.org/10.1111/cmi.12767.
56. Bebber DP, Gurr SJ. 2015. Crop-destroying fungal and oomycete pathogens challenge food security. Fungal Genet Biol 74:62–64. https://doi.org/10.1016/j.fgb.2014.10.012.
57. Berger S, El Chazli Y, Babu AF, Coste AT. 2017. Azole resistance in *Aspergillus fumigatus*: a consequence of antifungal use in agriculture? Front Microbiol 8:1024. https://doi.org/10.3389/fmicb.2017.01024.
58. Ongena M, Jacques P. 2008. Bacillus lipopeptides: versatile weapons for plant disease biocontrol. Trends Microbiol 16:115–125. https://doi.org/10.1016/j.tim.2007.12.009.
59. Sabri NSA, Zakaria Z, Mohamad SE, Jaafar AB, Hara H. 2018. Importance of soil temperature for the growth of temperate crops under a tropical climate and functional role of soil microbial diversity. Microbes Environ 33:144–150. https://doi.org/10.1264/jsme2.ME17181.
60. Gillis M, Logan NA. 2015. Janthinobacterium. *In* Whitman WB (ed), Bergey's manual of systematics of archaea and bacteria. John Wiley & Sons, Inc, New York, NY.
61. Coraiola M, Lo Cantore P, Lazzaroni S, Evidente A, Iacobellis NS, Dalla Serra M. 2006. WLIP and tolaasin I, lipodepsipeptides from *Pseudomonas reactans* and *Pseudomonas tolaasii*, permeabilize model membranes. Biochim Biophys Acta 1758:1713–1722. https://doi.org/10.1016/j.bbamem.2006.06.023.
62. Jo G, Hwang D, Lee S, Woo Y, Hyun J, Yong Y, Kang K, Kim DW, Lim Y. 2011. In silico study of the ion channel formed by tolaasin I produced by *Pseudomonas tolaasii*. J Microbiol Biotechnol 21:1097–1100. https://doi.org/10.4014/jmb.1103.03026.
63. Wächtler B, Wilson D, Haedicke K, Dalle F, Hube B. 2011. From attachment to damage: defined genes of *Candida albicans* mediate adhesion, invasion and damage during interaction with oral epithelial cells. PLoS One 6:e17046. https://doi.org/10.1371/journal.pone.0017046.
64. Subramanian A, Tamayo P, Mootha VK, Mukherjee S, Ebert BL, Gillette MA, Paulovich A, Pomeroy SL, Golub TR, Lander ES, Mesirov JP. 2005. Gene set enrichment analysis: a knowledge-based approach for interpreting genome-wide expression profiles. Proc Natl Acad Sci U S A 102:15545–15550. https://doi.org/10.1073/pnas.0506580102.
65. Mootha VK, Lindgren CM, Eriksson KF, Subramanian A, Sihag S, Lehar J, Puigserver P, Carlsson E, Ridderstrale M, Laurila E, Houstis N, Daly MJ, Patterson N, Mesirov JP, Golub TR, Tamayo P, Spiegelman B, Lander ES, Hirschhorn JN, Altshuler D, Groop LC. 2003. PGC-1alpha-responsive genes involved in oxidative phosphorylation are coordinately downregulated in human diabetes. Nat Genet 34:267–273. https://doi.org/10.1038/ng1180.
66. Supek F, Bošnjak M, Škunca N, Šmuc T. 2011. REVIGO summarizes and visualizes long lists of gene ontology terms. PLoS One 6:e21800. https://doi.org/10.1371/journal.pone.0021800.
67. Jones DC, Hallyburton I, Stojanovski L, Read KD, Frearson JA, Fairlamb AH. 2010. Identification of a kappa-opioid agonist as a potent and selective lead for drug development against human African trypanosomiasis. Biochem Pharmacol 80:1478–1486. https://doi.org/10.1016/j.bcp.2010.07.038.
68. Schindelin J, Arganda-Carreras I, Frise E, Kaynig V, Longair M, Pietzsch T, Preibisch S, Rueden C, Saalfeld S, Schmid B, Tinevez JY, White DJ, Hartenstein V, Eliceiri K, Tomancak P, Cardona A. 2012. Fiji: an open-source platform for biological-image analysis. Nat Methods 9:676–682. https://doi.org/10.1038/nmeth.2019.
69. Schneider CA, Rasband WS, Eliceiri KW. 2012. NIH Image to ImageJ: 25 years of image analysis. Nat Methods 9:671–675. https://doi.org/10.1038/nmeth.2089.
70. Schindelin J, Rueden CT, Hiner MC, Eliceiri KW. 2015. The ImageJ ecosystem: an open platform for biomedical image analysis. Mol Reprod Dev 82:518–529. https://doi.org/10.1002/mrd.22489.
71. Schmidt J, Friebel K, Schönherr R, Coppolino MG, Bosserhoff AK. 2010. Migration-associated secretion of melanoma inhibitory activity at the cell rear is supported by KCa3.1 potassium channels. Cell Res 20:1224–1238. https://doi.org/10.1038/cr.2010.121.
72. Gessner G, Macianskiene R, Starkus JG, Schönherr R, Heinemann SH. 2010. The amiodarone derivative KB130015 activates hERG1 potassium channels via a novel mechanism. Eur J Pharmacol 632:52–59. https://doi.org/10.1016/j.ejphar.2010.01.010.
73. Jadhav KB, Stein C, Makarewicz O, Pradel G, Lichtenecker RJ, Sack H, Heinemann SH, Arndt HD. 2017. Bioactivity of topologically confined gramicidin A dimers. Bioorg Med Chem 25:261–268. https://doi.org/10.1016/j.bmc.2016.10.033.
74. Basu Ray G, Chakraborty I, Moulik SP. 2006. Pyrene absorption can be a convenient method for probing critical micellar concentration (CMC) and indexing micellar polarity. J Colloid Interface Sci 294:248–254. https://doi.org/10.1016/j.jcis.2005.07.006.

Supplement Figure 1 (Transcriptomic analysis)

Figure legend

Suppl. Fig. 1A – 1D. Global view on short-term (30 min exposure; 1A and 1B) and growth-phase (OD 0.5; 1C and 1D) *C. albicans* transcriptomic response to non-toxic jagaricin exposure. Graphs show Revigo(1)-summarized GO terms enriched within genes upregulated (1A, 1C) or downregulated (1B, 1D) by jagaricin (Cut-off $-\log_{10}$ p-value > 2; all categories).

Suppl. 1A: Revigo summary of enriched GO terms within jagaricin upregulated genes (30 min)

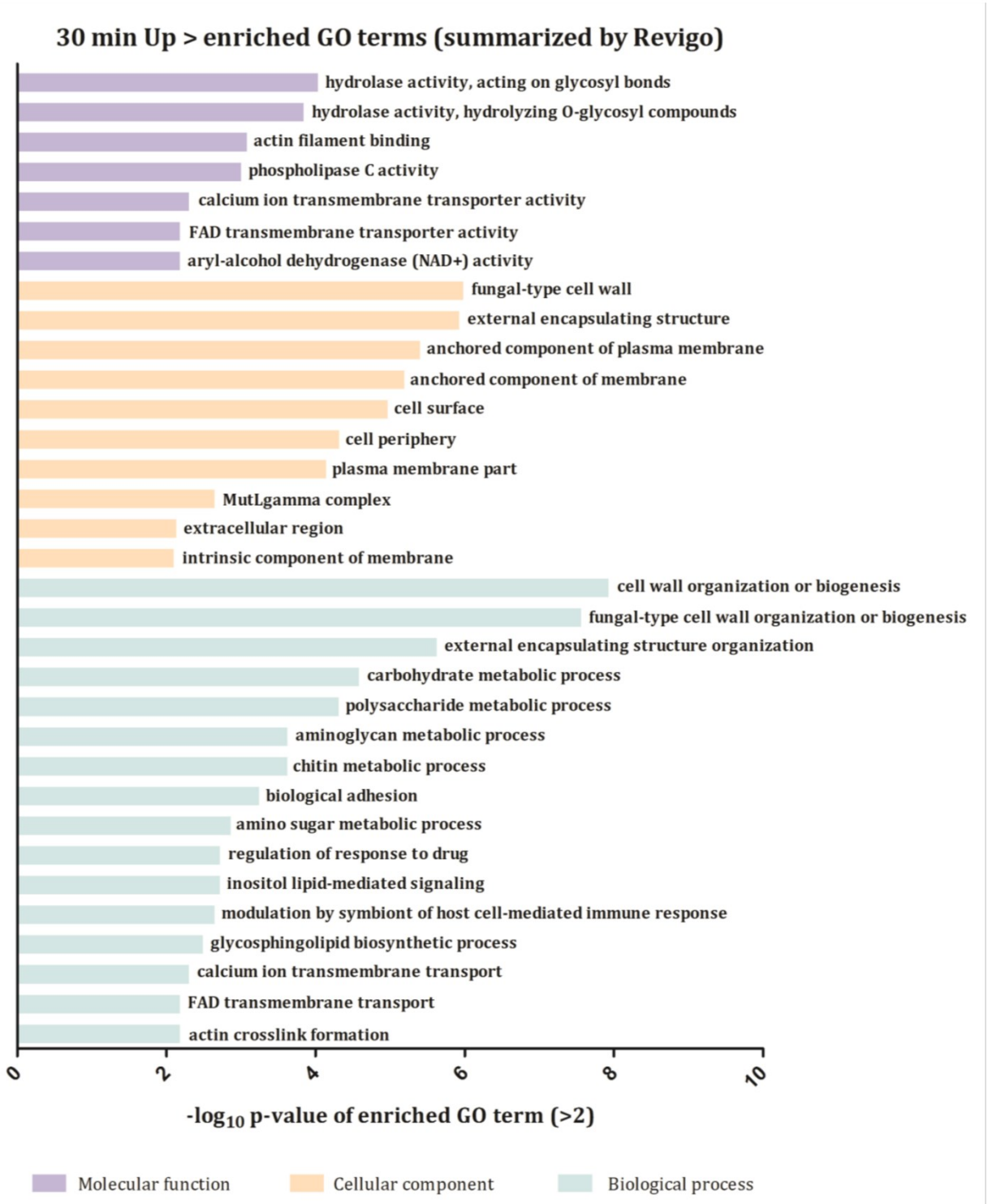

Suppl. 1B: Revigo summary of enriched GO terms within jagaricin downregulated genes (30 min)

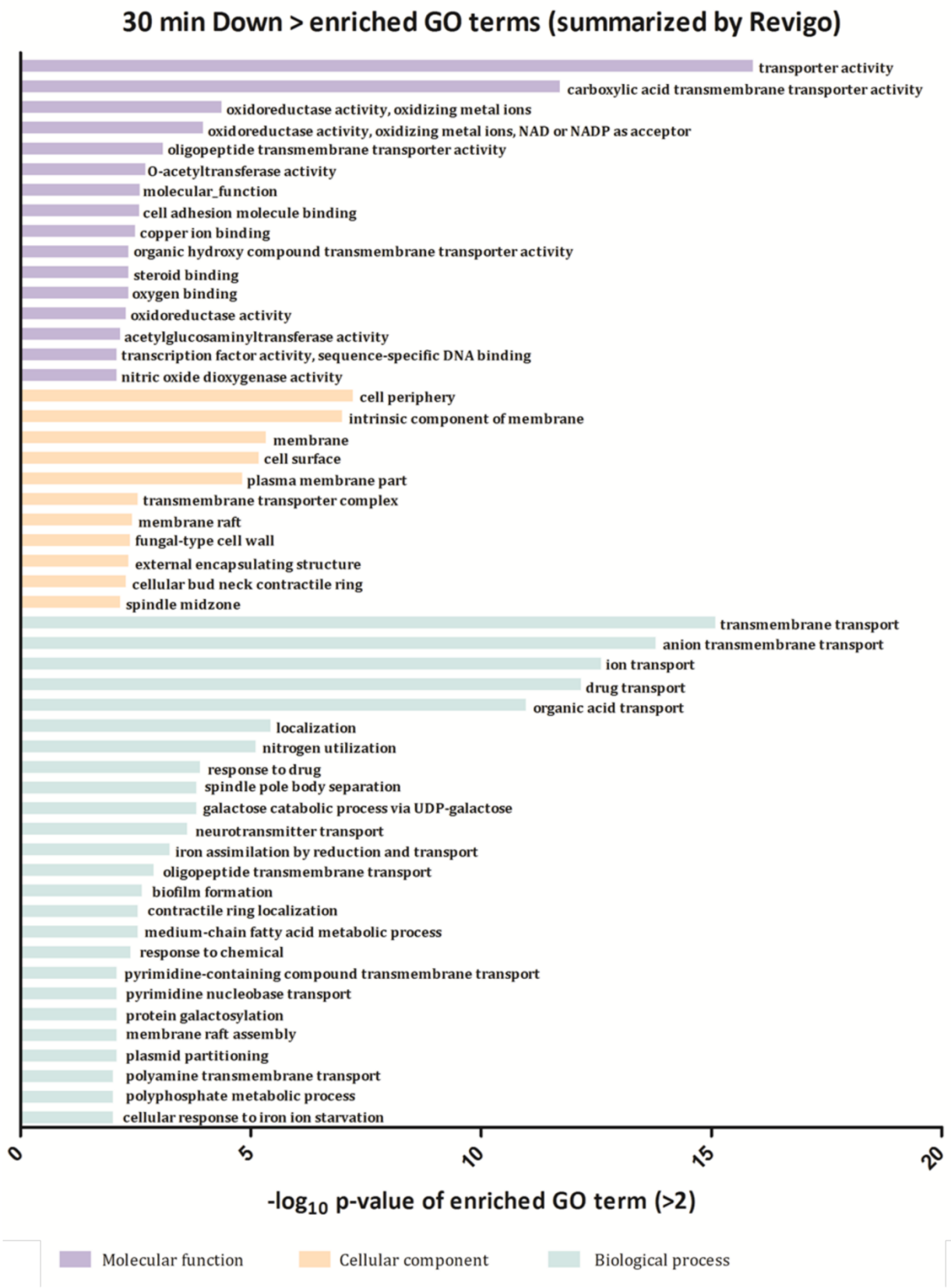

Suppl. 1C: Revigo summary of enriched GO terms within jagaricin upregulated genes (OD 0.5)

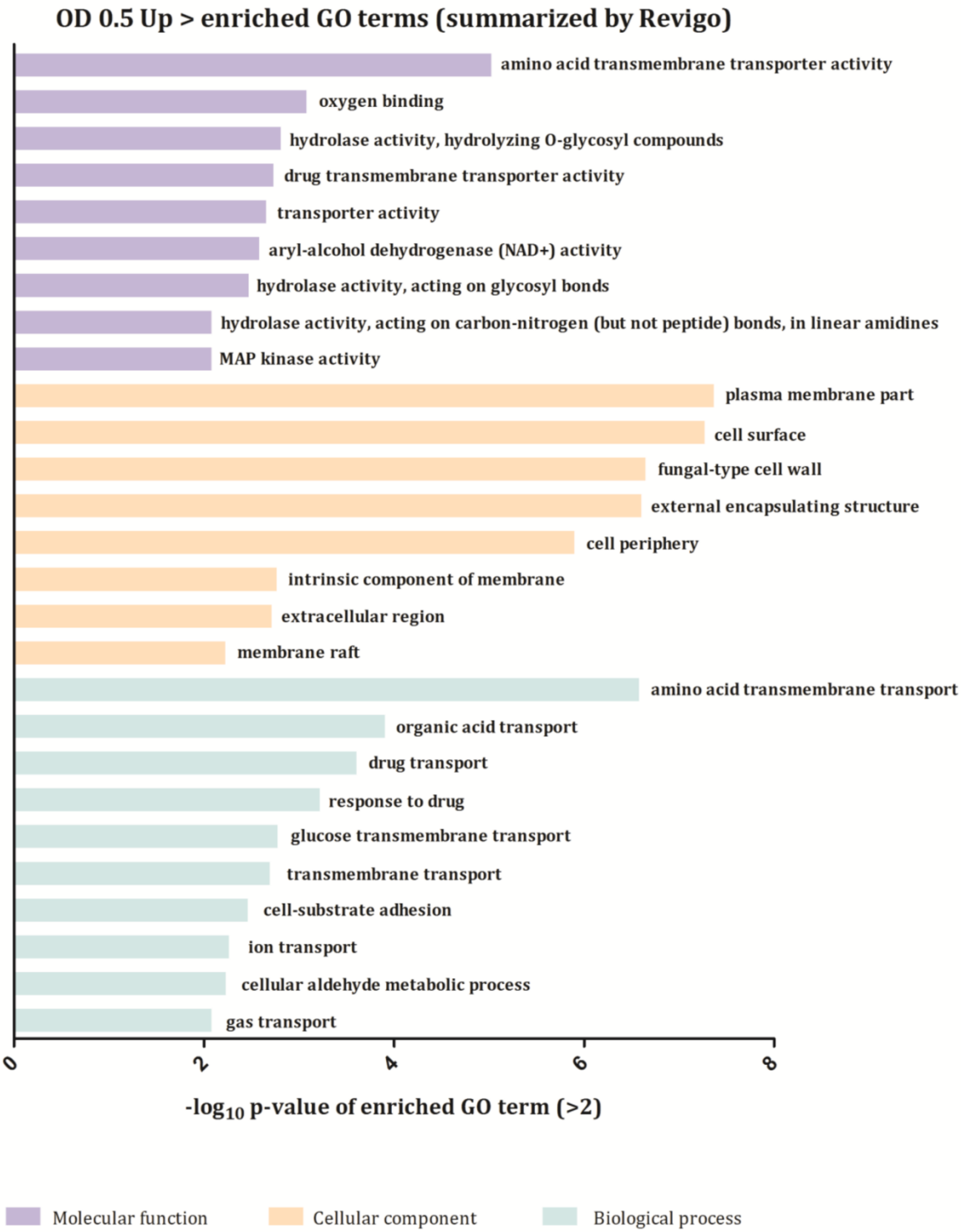

Suppl. 1D: Revigo summary of enriched GO terms within jagaricin downregulated genes (OD 0.5)

Figure legend

Suppl. Fig. 1E-1F. GSEA plots of individual GSEA terms. For details on GSEA analysis, compare the sheet "Overview table" in Suppl. Table 1A or 1B.

Suppl. Fig. 1E: GSEA plot "Aminophospholipid transporter activity" (30 min, enriched in jagaricin upregulated genes)

GeneSet	AMINOPHOSPHOLIPID TRANSPORTER ACTIVITY_MOL
Enrichment Score (ES)	0,8755
Normalized Enrichment Score (NES)	1,9399
Nominal p-value	0,0000
FDR q-value	0,0393
FWER p-Value	0,5790

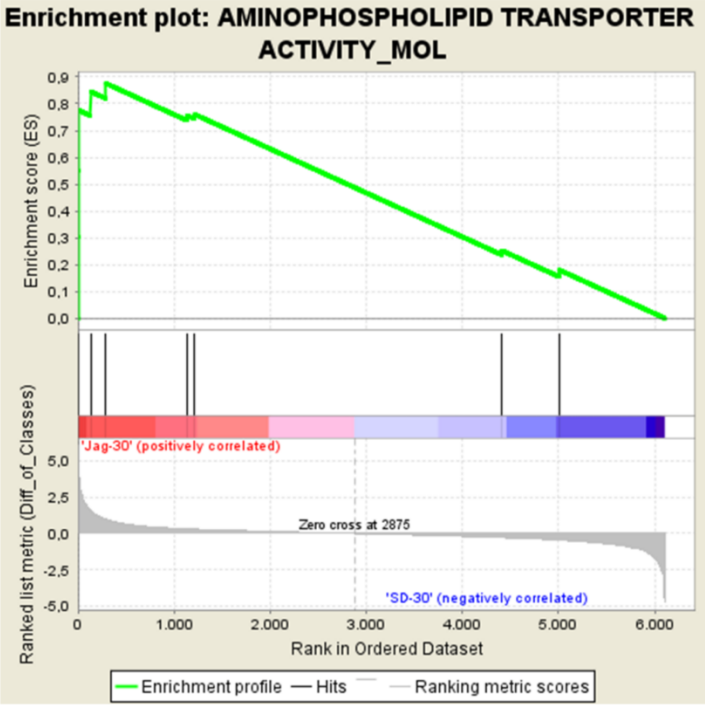

PROBE	DESCRIPTION (from dataset)	RANK IN GENE LIST	RANK METRIC SCORE	RUNNING ES	CORE ENRICHMENT
orf19.6595	RTA4	3	5,317	0,303	Yes
orf19.24	n/a	7	4,374	0,552	Yes
orf19.23	n/a	13	3,903	0,775	Yes
orf19.2680	n/a	131	1,574	0,845	Yes
orf19.783	n/a	292	0,989	0,876	Yes
orf19.6224	n/a	1135	0,324	0,756	No
orf19.6778	n/a	1216	0,300	0,760	No
orf19.932	n/a	4408	-0,282	0,253	No
orf19.323	n/a	5007	-0,447	0,180	No

Suppl. Fig. 1F: GSEA plot "Ergosterol biosynthetic process" (OD 0.5, enriched in jagaricin downregulated genes)

GeneSet	ERGOSTEROL BIOSYNTHETIC PROCESS_BIO
Enrichment Score (ES)	-0,7372
Normalized Enrichment Score (NES)	-2,0136
Nominal p-value	0,0000
FDR q-value	0,0092
FWER p-Value	0,2670

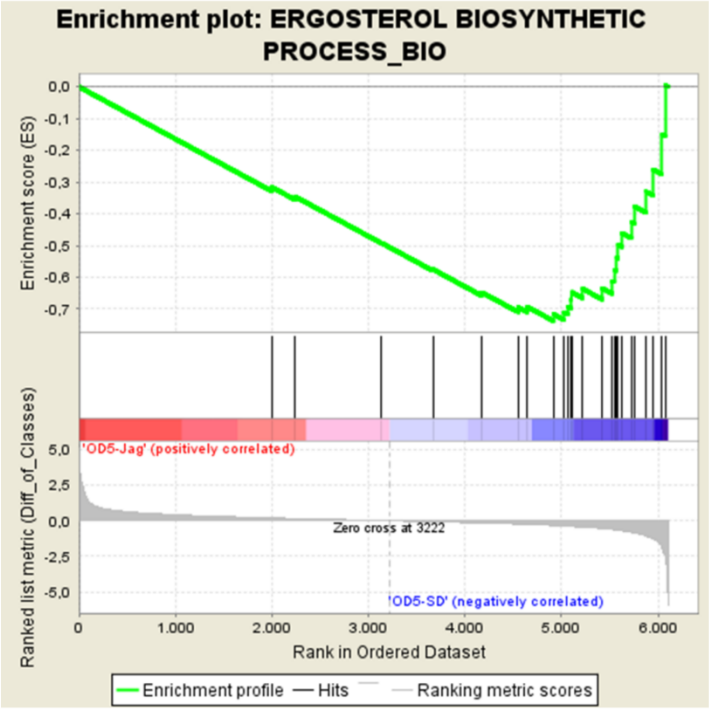

PROBE	DESCRIPTION (from dataset)	RANK IN GENE LIST	RANK METRIC SCORE	RUNNING ES	CORE ENRICHMENT
orf19.4809	n/a	1997	0,196	-0,316	No
orf19.3507	MCR1	2242	0,156	-0,346	No
orf19.1031	HMG1	3136	0,015	-0,492	No
orf19.4606	ERG8	3668	-0,070	-0,575	No
orf19.6026	ERG2	4169	-0,164	-0,647	No
orf19.3240	ERG27	4550	-0,237	-0,694	No
orf19.2672	NCP1	4645	-0,263	-0,693	No
orf19.5379	ERG4	4914	-0,338	-0,716	Yes
orf19.5178	ERG5	5025	-0,376	-0,710	Yes
orf19.1570	ERG7	5065	-0,387	-0,692	Yes
orf19.2775	IDI1	5101	-0,401	-0,672	Yes
orf19.4491	ERG20	5104	-0,402	-0,647	Yes
orf19.1598	n/a	5219	-0,456	-0,637	Yes
orf19.7312	ERG13	5421	-0,552	-0,635	Yes
orf19.7049	CYB5	5526	-0,613	-0,613	Yes
orf19.2016	ERG28	5545	-0,629	-0,576	Yes
orf19.1591	ERG10	5573	-0,652	-0,539	Yes
orf19.3616	ERG9	5587	-0,664	-0,499	Yes
orf19.3732	ERG25	5624	-0,695	-0,460	Yes
orf19.1631	n/a	5722	-0,801	-0,426	Yes
orf19.2909	ERG26	5755	-0,845	-0,377	Yes
orf19.922	ERG11	5879	-1,055	-0,330	Yes
orf19.767	ERG3	5950	-1,277	-0,261	Yes
orf19.406	ERG1	6042	-1,995	-0,149	Yes
orf19.4631	ERG251	6074	-2,500	0,005	Yes

Supplement Fig. 2: Cd^{2+} addition to Fura-2-AM assay

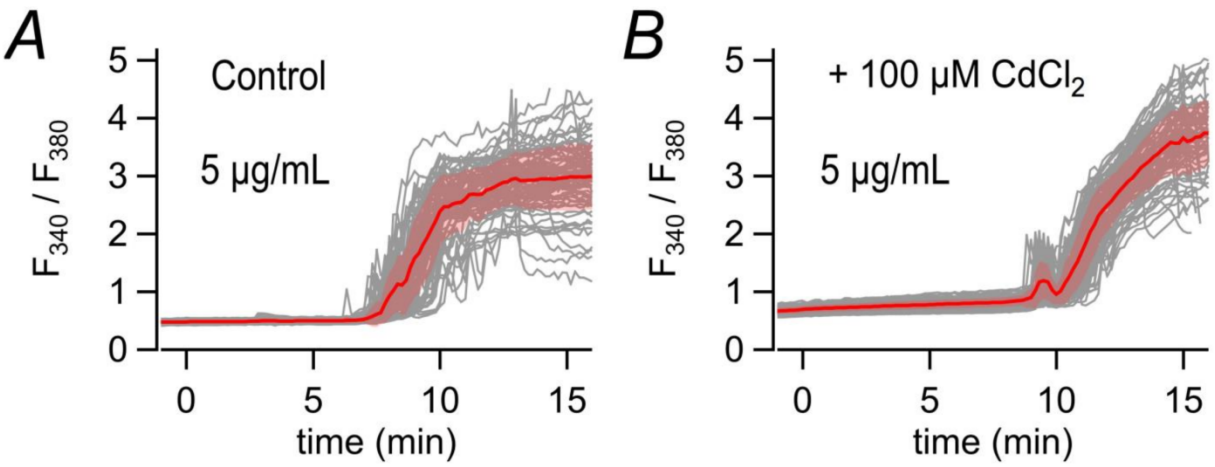

Figure legend

Suppl. Fig. 2. Jagaricin-mediated Ca^{2+} influx into HEK293T cells cannot be inhibited by Cd^{2+}. A) HEK293T cells were loaded with the Ca^{2+}-sensitive dye Fura-2-AM and the ratio of fluorescence at 340 and 380 nm (F340 / F380) was measured as an indicator of the intracellular free Ca^{2+} concentration and plotted as a function of time. Traces from individual cells are superimposed (grey); the red trace is the mean, the shading indicates ± SD. 5 µg/mL jagaricin was applied at time zero. B) Same procedure as in A), but with addition of Cd^{2+} at time point zero. A representative graph of five independent experiments is shown in each panel.

Supplement Fig. 3: CMC determination by continuous fluorescence measurement of pyrene emission

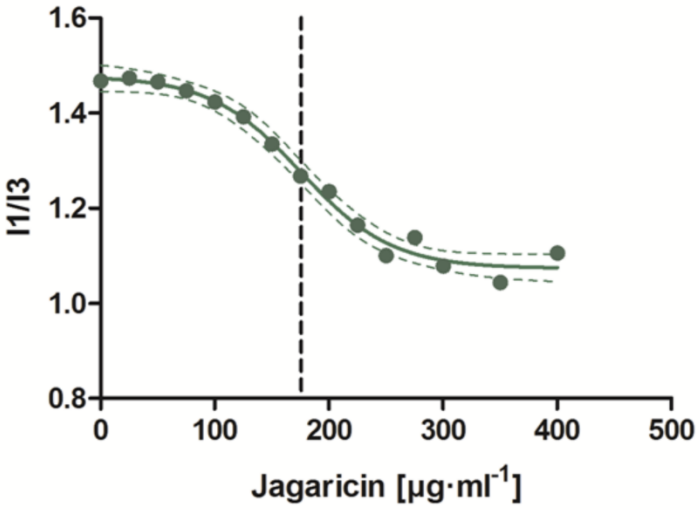

Figure legend

Suppl. Fig. 3. The CMC of jagaricin is 176 µg/mL speaking against a micellar mechanism of action against fungi. CMC value was calculated as described in (2). Curve was fitted using GraphPad Prism 7.

Commentary to Suppl. Table 2 (List of mutants, clinical isolates and wild types respective reference strains)

Strains originate from supplementary references (3-19). The yet unpublished clinical isolates EU0992, EU0989, EU0981, EU0999 and EU0136 were a kind gift from Oliver Bader (phenotypes were told by personal communication) and sampled as part of the EURESFUN (European Resistance Fungal Network) project.

Supplementary References

1. **Supek F, Bošnjak M, Škunca N, Šmuc T.** 2011. REVIGO summarizes and visualizes long lists of gene ontology terms. PLoS One **6:**e21800.
2. **Basu Ray G, Chakraborty I, Moulik SP.** 2006. Pyrene absorption can be a convenient method for probing critical micellar concentration (cmc) and indexing micellar polarity. J Colloid Interface Sci **294:**248-254.
3. **Lohberger A, Coste AT, Sanglard D.** 2014. Distinct roles of Candida albicans drug resistance transcription factors TAC1, MRR1, and UPC2 in virulence. Eukaryot Cell **13:**127-142.
4. **Schwarzmüller T, Ma B, Hiller E, Istel F, Tscherner M, Brunke S, Ames L, Firon A, Green B, Cabral V, Marcet-Houben M, Jacobsen ID, Quintin J, Seider K, Frohner I, Glaser W, Jungwirth H, Bachellier-Bassi S, Chauvel M, Zeidler U, Ferrandon D, Gabaldon T, Hube B, d'Enfert C, Rupp S, Cormack B, Haynes K, Kuchler K.** 2014. Systematic phenotyping of a large-scale Candida glabrata deletion collection reveals novel antifungal tolerance genes. PLoS Pathog **10:**e1004211.
5. **Noble SM, French S, Kohn LA, Chen V, Johnson AD.** 2010. Systematic screens of a Candida albicans homozygous deletion library decouple morphogenetic switching and pathogenicity. Nat Genet **42:**590-598.
6. **Homann OR, Dea J, Noble SM, Johnson AD.** 2009. A phenotypic profile of the Candida albicans regulatory network. PLoS Genet **5:**e1000783.
7. **Nobile CJ, Mitchell AP.** 2009. Large-scale gene disruption using the UAU1 cassette. Methods Mol Biol **499:**175-194.
8. **Martel CM, Parker JE, Bader O, Weig M, Gross U, Warrilow AG, Rolley N, Kelly DE, Kelly SL.** 2010. Identification and characterization of four azole-resistant erg3 mutants of Candida albicans. Antimicrob Agents Chemother **54:**4527-4533.
9. **Sonneborn A, Bockmühl DP, Gerads M, Kurpanek K, Sanglard D, Ernst JF.** 2000. Protein kinase A encoded by TPK2 regulates dimorphism of Candida albicans. Mol Microbiol **35:**386-396.
10. **Bockmühl DP, Krishnamurthy S, Gerads M, Sonneborn A, Ernst JF.** 2001. Distinct and redundant roles of the two protein kinase A isoforms Tpk1p and Tpk2p in morphogenesis and growth of Candida albicans. Mol Microbiol **42:**1243-1257.
11. **Hiller E, Heine S, Brunner H, Rupp S.** 2007. Candida albicans Sun41p, a putative glycosidase, is involved in morphogenesis, cell wall biogenesis, and biofilm formation. Eukaryot Cell **6:**2056-2065.
12. **Lo HJ, Köhler JR, DiDomenico B, Loebenberg D, Cacciapuoti A, Fink GR.** 1997. Nonfilamentous C. albicans mutants are avirulent. Cell **90:**939-949.
13. **Kumamoto CA.** 2005. A contact-activated kinase signals Candida albicans invasive growth and biofilm development. Proc Natl Acad Sci U S A **102:**5576-5581.
14. **Noble SM, Johnson AD.** 2005. Strains and strategies for large-scale gene deletion studies of the diploid human fungal pathogen Candida albicans. Eukaryot Cell **4:**298-309.
15. **Davis DA, Bruno VM, Loza L, Filler SG, Mitchell AP.** 2002. Candida albicans Mds3p, a conserved regulator of pH responses and virulence identified through insertional mutagenesis. Genetics **162:**1573-1581.

16. **Fonzi WA, Irwin MY.** 1993. Isogenic strain construction and gene mapping in Candida albicans. Genetics **134:**717-728.
17. **Fradin C, De Groot P, MacCallum D, Schaller M, Klis F, Odds FC, Hube B.** 2005. Granulocytes govern the transcriptional response, morphology and proliferation of Candida albicans in human blood. Mol Microbiol **56:**397-415.
18. **Wilson RB, Davis D, Mitchell AP.** 1999. Rapid hypothesis testing with Candida albicans through gene disruption with short homology regions. J Bacteriol **181:**1868-1874.
19. **Moyes DL, Wilson D, Richardson JP, Mogavero S, Tang SX, Wernecke J, Höfs S, Gratacap RL, Robbins J, Runglall M, Murciano C, Blagojevic M, Thavaraj S, Förster TM, Hebecker B, Kasper L, Vizcay G, Iancu SI, Kichik N, Hader A, Kurzai O, Luo T, Krüger T, Kniemeyer O, Cota E, Bader O, Wheeler RT, Gutsmann T, Hube B, Naglik JR.** 2016. Candidalysin is a fungal peptide toxin critical for mucosal infection. Nature **532:**64-68.

Complete supplemental material for this article may be found at: https://aac.asm.org/content/63/9/e00707-19/figures-only#fig-data-additional-files and is included in the enclosed **CD ROM (folder: Jagaricin)**. Tables S1A, S1B and S2 are Excel files and were therefore not included in the printed version.

2.2 Manuscript II

Fine-Scale Chromosomal Changes in Fungal Fitness

Daniel Fischer, Bernhard Hube and Sascha Brunke

Curr Fungal Infect Rep (2014) **8**:171–178.
DOI 10.1007/s12281-014-0179-9
Fine-Scale Chromosomal Changes in Fungal Fitness | SpringerLink

Summary:
Like all forms of life on earth, fungal pathogens are under continuous selection pressure in ever-changing environments. This review summarizes the current knowledge on typical fungal microevolution strategies – with a focus on small scale genetic exchanges – which may be important to understand the progression of human fungal diseases. Important parameters which determine this process are discussed: selection pressures prior to and during infection, infection routes, organ specificities, antifungal drug treatment, and genetic diversity of the infecting fungus or fungal population. In sum, fungal microevolution influences the outcome of fungal infections and therefore needs to be taken into account also in clinical settings, but a deeper understanding of these processes may also provide us with new clinical intervention possibilities.

Own Contribution:
Daniel Fischer conducted literature research, generated the figure, and wrote the manuscript.

Estimated authors' contributions:

Daniel Fischer	70%
Bernhard Hube	10%
Sascha Brunke	20%

Prof. Bernhard Hube

Curr Fungal Infect Rep (2014) 8:171–178
DOI 10.1007/s12281-014-0179-9

TRANSLATIONAL RESEARCH (R WHEELER, SECTION EDITOR)

Fine-Scale Chromosomal Changes in Fungal Fitness

Daniel Fischer · Bernhard Hube · Sascha Brunke

Published online: 13 March 2014

Abstract Fungi are frequently exposed to changing environments and must adapt continuously to retain their fitness. This is especially true when changes occur rapidly and toward harsher conditions – a situation, for example, encountered by pathogenic fungi when they infect a host and during the different stages of infections. Here we provide an overview of the role of small-scale genetic exchanges for the fitness of human pathogenic fungi. These alterations can influence host-fungus interactions, and hence the outcome of an infection. We present recent experiments and observations dealing with the importance of the genetic diversity and previous selection pressures of the infecting pool. In addition, we discuss the role of specific niches and disease progression as well as antifungal treatment on fungal microevolution in vivo. We conclude that different mechanisms of small-scale genetic changes allow pathogenic fungi to increase their fitness in the host, and can thus alter the course of infections.

Keywords Microevolution · Adaptation mechanism · Fungal pathogenesis · Loss of heterozygosity (LOH) · Drug resistance · Selection pressure · Evolution mechanisms · Virulence · Candida · Cryptococcus · Recurrent infection · Loss/gain-of-function mutation · Compensatory mutation · Phenotypic change · Host-pathogen interaction · Commensalism · Bloodstream infection · Mutator strains · Mutation frequency

D. Fischer · B. Hube · S. Brunke (✉)
Department of Microbial Pathogenicity Mechanisms, Leibniz Institute for Natural Product Research and Infection Biology – Hans Knoell Institute Jena (HKI), Beutenbergstraße 11a, 07745 Jena, Germany
e-mail: sascha.brunke@hki-jena.de

B. Hube · S. Brunke
Integrated Research and Treatment Center, Sepsis und Sepsisfolgen, Center for Sepsis Control and Care (CSCC), Universitätsklinikum Jena, Jena, Germany

B. Hube
Friedrich Schiller University, Jena, Germany

Introduction

Fungi can be found in a broad range of different environments. With a predicted 5.1 million species, they have colonized nearly all available habitats on earth [1]. In fact, nearly all higher plants benefit from their association with mycorrhizal fungi [2], and in mutualistic relationships of fungi with algae as lichen, they thrive even in hostile environments. Interestingly, several thousand fungal species are associated with animals, and at least 150–400 of these are known to cause disease in humans, yet they are often underappreciated as pathogens [3]. In sheer number, fungi pose a severe threat to human health globally [3]. In addition, fungal plant pathogens cause severe losses in crops worldwide and have a major impact on both the economy and nutrition for a growing world population [4]. All of these fungi have adapted and must continue to adapt to their respective hosts.

Mutations are the building blocks from which phenotypic variations of organisms arise. Selection then acts on these variations. During evolution, mutation and selection will lead to an ever better adaptation of organisms to their environment, be it decaying wood, compost piles, living plants, or a human body. Many different genetic mechanisms to generate diversity have been recognized in the past, from single nucleotide exchanges to gross chromosomal rearrangements. In this review, we will focus on small-scale changes that occur in the genome of pathogenic fungi and how this affects their fitness in the human host.

Chromosomal alterations can include many forms, and the border between large- and small-scale changes is difficult to define. Clearly, whole chromosome or even genome ploidy

changes can be considered large-scale changes, and these events have been crucial in the evolution of some fungal lineages; duplicated genes are free to evolve novel functions due to their redundancy. For example *Saccharomyces cerevisiae* and *Candida glabrata* both derive from a common ancestor that experienced a whole-genome duplication event [5, 6]. Aneuploidies are driving, via gene dosis effects, many types of immediate adaptations – for example, via duplicated metabolic genes for increased fitness with certain nutrient sources, or increased export of toxic substances like drugs (see below).

For diploid fungi like *C. albicans*, LOH is an important mechanism for both small-scale and large-scale chromosomal changes. The genome of the sequenced *C. albicans* strain SC5314 harbors approximately 60,000 SNPs [7], where a single nucleotide differs between the two alleles of a chromosome. This heterozygosity provides the cell with a pool of potentially useful alleles. In an LOH event, mechanisms like gene conversion, break-induced replication, or chromosome loss lead to the removal of one allele [8]. The remaining recessive or gene dosis-dependent alleles can then influence the phenotype. LOH rates were found to be in the range of approximately 10^{-6} to 10^{-7}/cell division under non-stressful conditions, depending upon the individual locus [9••].

In comparison, spontaneous mutation rates (e.g., 3.3 x 10^{-10} for haploid [10] and 2.9 x 10^{-10} for diploid baker yeast [11]) are significantly less frequent. They encompass single nucleotide exchanges, and deletions and insertions of single or very few bases (indels) in the chromosome. Like the large-scale changes, these can have severe effects on gene function and expression, and hence the fitness of an organism, in a changing environment.

Certain features are known to increase the rate of occurrence of these chromosomal alterations. Repetitive sequences found in minisatellites can expand or contract, but also locally increase the rate of chromosomal translocations and non-disjunctions. The telomeric region in particular is highly variable, which seems to be especially relevant for the continuing evolution of *C. glabrata* (see below). Furthermore, tRNA genes, as points of frequent collision between the gene transcription and DNA replication machinery, are common starting points for LOH events [12, 13]. In addition, the unusual mating and chromosome reduction systems of some pathogenic fungi, such as the parasexual cycle of *C. albicans*, seem to favor chromosomal recombinations and aneuploidies [14]. Finally, loss-of-function mutations in the DNA repair machinery itself can increase the number of nucleotide mutation events per generation, leading to a 'hypermutator' state from which novel genotypes and phenotypes arise at a higher rate.

Evolution of Fungal Pathogens in a Clinical Context

For pathogens, increased fitness – and hence increased survival and/or growth rates in the host – is often (but not always) associated with increased virulence. A broad range of small- and large-scale alterations have been observed in fungal pathogens; their precise causative mechanism often depends upon the specific conditions. Our goal here is to provide insight into which adaptation mechanisms might be of importance for different fungal pathogens when facing the host (Fig. 1).

The size of the infecting population determines the genetic diversity from which adaptation, and the resulting increased fitness, can arise. *C. albicans*, for example, exists as commensal in the human vaginal and gastrointestinal tract, which can serve as a source of infection [15]. During infection, comparatively few cells enter the bloodstream via mucosal lesions or by invasive growth and/or induced endocytosis of hyphae through epithelial cells [16, 17], or are present on catheters

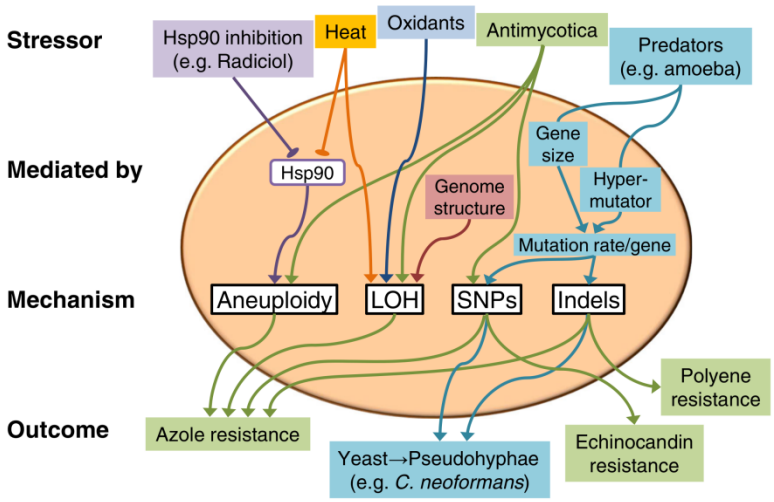

Fig. 1 An overview of the stressors and mechanisms discussed in this review. The arrows indicate exemplary ways for fungal adaptation to stress, but are not meant as a comprehensive overview of all possible adaptation mechanisms. For details, see main text

(for a review, see [18]). This leads to a genetic bottleneck effect in comparison to the total colonizing population. In fact, *C. albicans* bloodstream infections generally seem to derive from a single strain, and sequential isolates from one patient commonly derive from a single progenitor [19, 20]. It is unclear, however, whether these derive from a single or multiple infection event from the colonizing pool. Furthermore, *C. albicans* experiences microevolution events – e.g., LOH – during the colonization of the gastrointestinal and vaginal tracts [21, 22]. Therefore, distinguishing between microevolution events in the infecting versus the commensal population is difficult in cases of recurrent candidiasis. The situation is similar for other *Candida* species, including the haploid *C. glabrata* [23, 24].

Other fungal pathogens such as *Cryptococcus neoformans* and *Aspergillus fumigatus* enter the body via the lung by inhalation of spores. This primary lung infection can then directly develop into an invasive infection or can be completely cleared, or as in the case of *C. neoformans*, the fungus can establish a latent infection [25, 26]. A bloodstream infection of immunocompromised patients can then occur through reactivation of the latent infection. This suggests that many *C. neoformans* populations in bloodstream infection have already been under a microevolutionary selection process in the host environment. One indication of this, for example, is the fact that environmental *C. neoformans* isolates are not as virulent as clinical isolates in animal models, as they persist in the lung rather than cause disease [27–29], which would seem to suggest that the microevolutionary adaptation of the environmental strains is relevant to establish disease. As an alternative explanation, it may be that only a subset of environmental strains are pre-adapted to cause disease, whereas all clinical isolates have necessarily passed through this test of fitness.

Microevolution in the Host and Niche Specificities

For human pathogens, microevolution is known to take place in the patient. This has been demonstrated in the past with a diverse range of fungal pathogens, such as *C. albicans* [30], *C. dubliniensis* [31], *C. glabrata* [23], and *C. neoformans* [32, 33].

After infection, the first selective pressure results from the different environments in the target organs. Nutrient availability and physical properties, but also type and timing of immune system activation, can differ significantly between organs. As an example, the immune response in the murine kidney during systemic *C. albicans* infection is delayed in comparison to other colonized organs like spleen and liver [34]. Concomitantly, while fungal load increases in the kidney, in most other organs it declines over time until the fungi are cleared [35]. Hence, the different organs present very different ecological niches and likely favor different genetic alterations for different evolutionary trajectories.

In addition, microorganisms may be more or less (pre-)adapted to certain organs or niches before the actual infection commences. This is especially true for opportunistic pathogens, and the degree of adaptation can be estimated by the rate of genetic and phenotypic alterations of the fungus in a specific organ. By repeatedly transferring *C. albicans* from the spleen of infected mice to the bloodstream of healthy animals, Cheng and colleagues reported the appearance of a stable respiration-deficient isolate with altered carbon utilization, delayed filamentation initiation, reduced in vitro growth, and decreased virulence in a mouse model of disseminated candidiasis [36]. The isolate showed significant reduced fungal load in the kidney but was able to persist without killing the host. Additionally, it displayed enhanced resistance against oxidative stress [36]. These strong phenotypic changes betray the need for *C. albicans* to adapt during prolonged spleen colonization, which is consistent with the fact that *C. albicans* is normally cleared rapidly from the spleen during infection [34, 35].

Further microevolution studies of *C. albicans* investigated genetic alterations due to passages through murine kidneys. Forche and colleagues observed microevolutionary events after a single renal passage [37]. These included primarily large-scale LOH events and karyotypic alterations, accompanied by phenotypic changes such as an increased rate of wrinkled colonies [37]. In contrast, in our lab we found no obvious phenotypic changes in the *C. albicans* type strain SC5314, even after a series of eight passages through murine kidneys. We concluded that *C. albicans* is already well-adapted to the environment of the murine kidney [38••], in keeping with the fact that kidneys are the main target organ during mouse infection [34].

This apparent contradiction is probably best explained by differences in experimental setup. Forche and colleagues isolated their strains from moribund mice. In contrast, we used strains from mostly healthy animals, exposed to a low infection dose. The result was likely different selection scenarios for fungal fitness in the host: fast growth in disrupted tissue and growth accompanied by little damage, respectively. In combination with the previously described spleen passage experiment, these data thus illustrate that overall fungal fitness depends on both the organ and the stage of infection.

How can the genetic basis for these niche-specific adaptations be determined? The recent advent of fast and affordable genomic sequencing offers many new opportunities, many of which have already been utilized for answers to this question. Analyzing two serial *C. neoformans* isolates from an HIV patient, representing an initial and relapse episode of cryptococcal meningoencephalitis, Ormerod and colleagues observed several phenotypic changes, including differences in melanization, capsule size, and carbon source usage as well as

an altered virulence [39••]. They then employed whole-genome sequencing to show that the strains were, in fact, closely related. Both were independently derived from a common ancestor, likely the initial infecting strain [39••]. The sequences revealed that the phenotypic differences were due primarily to a small change in the genome, a frameshift mutation that led to a truncation of the transcriptional regulator protein Avc1 (atrioventricular canal 1). Changes in the copy number of the left and right arms of chromosome 12 were also observed. Interestingly, however, the overall virulence of the second "relapse" isolate was reduced, likely reflecting a niche specificity for the brain from which the strain was isolated. The adaptation may be associated with a fitness cost in the transit into organs and growth inside the different tissues. Further corroborating the concept of in vivo adaptation was the observation of a moderate increase in resistance to fluconazole, the treatment drug for the patient [39••].

In addition to adaptation to specific organ niches, interaction with host immune cells can determine the fitness of the fungus in the host. As an example, *C. glabrata* is primarily surrounded by mononuclear cells in systemic mice infections [40], and in addition, is able to survive and replicate inside macrophages in vitro [41, 42]. In a long-term in vitro evolution experiment, we observed that *C. glabrata* was able to adapt to macrophages with little genetic alteration. At the same time, macrophage adaptation led to altered organ-specific fitness, leading to an increase in total virulence (unpublished data).

When Mankind Intervenes: Antifungal Treatment

In the last decades, the well-rehearsed interaction between humans as host and selected fungi as pathogens has witnessed the appearance of a new player: the broad use of antimycotics. After initial successes, inherently resistant species have begun appearing more and more in the clinical setting (reviewed in [43]), and importantly, initially susceptible species have developed antifungal resistance (reviewed in [44]).

Antifungal treatment leads to additional genetic bottlenecks during infection when large proportions of the fungal population are removed either directly by the drug or indirectly by reduced growth and destruction by the host. Mutants directly relevant for resistance are strongly selected for, but unrelated mutations can also become enriched via genetic drift, either by genetic association with relevant mutations or when the fungus resides in a niche unreachable by antimycotics.

In extreme cases, multiple rounds of recurrent infection and pathogen adaptation through microevolution can occur. This phenomenon was described by Singh-Babak and colleagues for a case of recurrent *C. glabrata* candidiasis [45••]. The patient was treated several times with caspofungin, and seven sequential isolates were taken in a time frame of 10 months. Again, all originated from the same progenitor strain. In the series of isolates, two stepwise increases in caspofungin resistance were observed: first, a slight increase due to a mutation in the *CDC6* gene, and a second, more significant increase mediated by a mutation in the echinocandin target protein Fks2. This mutation was associated with a fitness cost, however, under conditions without echinocandin treatment [45••]. A similar fitness cost effect has been observed for homozygous mutations leading to amino acid exchanges in the hot-spot *FKS1* gene of *C. albicans* [46, 47]. In the case of *C. glabrata*, the fitness cost was then compensated in later isolates by an additional mutation in the *CDC55* gene [45••]. Such compensatory mutations are well-described in bacterial microevolution systems (for a review, see [48]). In fungi, these compensatory mutations have not yet been well investigated. In addition to the study of Singh-Babak et al., compensatory mutations have been investigated for *C. albicans* in the presence of fluconazole [49, 50].

The emergence of resistance has been described for azoles, echinocandins, and polyenes, the three clinically relevant classes of antifungal drugs. *Candida* strains resistant to the polyene amphotericin B are still rarely found in patients, and the increased resistance is generally due to loss-of-function mutations of genes in the ergosterol biosynthetic pathway [51–56]. The rarity of such isolates may be attributable to the high fitness costs associated with the resistance mechanisms under in vivo and in vivo-like conditions [56].

In contrast, clinical resistance against echinocandins is more common. Among *Candida* species, this is particularly true for the non-*albicans* species such as *C. glabrata* and *C. krusei* [57]. Thus far, the only known genetic bases of this resistance mechanism are amino acid exchanges or deletions inside of hot-spot regions of the target proteins Fks1 and Fks2 [58].

For azoles, typical resistance mechanisms in *Candida* species with clinical significance are mutations in the ergosterol biosynthetic pathway and the induction of *CDR* or *MDR* genes, coding for ABC transporters and facilitators for drug export, respectively [59]. Most common are point mutations in the gene of the lanosterol demethylase Erg11 that reduce the binding capacity of this enzyme to azoles [60]. Overexpression of *ERG11* (e.g., by gain-of-function mutations due to distinct single amino acid exchanges in the transcriptional factor Upc2) results in higher minimal inhibitory concentrations of the drug [61]. Mutations in *ERG3* to a non-functional state can alleviate the toxic side effects of Erg11 inhibition [62, 63] and thereby increase the fitness of the mutant strain again under these conditions. Finally, the formation of an additional isochromosome [i(5 L)] by segmental aneuploidy has been described for *C. albicans* [64, 65]. This neochromosome mediates azole resistance through additional copies of *ERG11* and *TAC1*, which codes for an activator of *CDR* genes [66]. A gain-of-function mutation leading to

hyperactivation of Tac1 can be enhanced by homozygosity of the hyperactive *TAC1* allele [66, 67]. Mutations in other activators of *CDR* or *MDR*, such as a hyperactivating amino acid exchange in the *MDR1*-regulator Mrr1 [68], have a similar effect, consequently leading to azole resistance.

In general, these mutations are rare and come with an initial fitness cost, and combining two or more antifungals should therefore significantly lower the chance for developing resistances, as this would require multiple independent mutations [69]. Combining inhibitors of the chaperone Hsp90 with azole drugs, for example, can have this effect. Rapid selection for azole resistance selects for mutants minimizing the toxicity for the cell (e.g., loss-of-function of *ERG3*) [63]. These mutants depend on Hsp90 function and are therefore sensitive to Hsp90 inhibitors as well as calcineurin inhibitors [70]. In contrast, gradual selection leads to azole resistance mechanisms that are Hsp90-independent [70], such as gain-of-function of Pdr1 through point mutations near the activation domain of the protein [71]. To study the evolution against an antifungal drug combination, Hill and colleagues experimentally evolved *C. albicans* and *S. cerevisiae* populations harboring *ERG3* loss-of-function mutations or deletions in the presence of both an azole and either a calcineurin or an Hsp90 inhibitor [72••]. The study showed several pathways leading to resistance against the drug combinations: 1) point mutations that alleviated or prevented the effect of the Hsp90 and calcineurin inhibitors by modifying either the target proteins or their binding to the effector proteins (*ScHSC82*, *CaHSP90*, *ScFPR1*), 2) point mutations that led to independence from Hsp90 function (*ScPDR1, ScMOT3*, *CaLCB1*), and 3) extensive aneuploidies of several chromosome and chromosome parts which were observed in four of the experimental *C. albicans* lineages [72••].

Interestingly, Hsp90 stress itself is known to induce aneuploidy (and hence allow more rapid adaptation), as illustrated by the drastic enhanced chromosomal instability in the presence of the Hsp90 inhibitor radicicol [73]. Compromising Hsp90 function has additionally been shown to release prestored genetic variability, as variants of Hsp90 client proteins are no longer forcibly refolded [70, 74]. As such, Hsp90 plays a major role in relaying a strong environmental stress to an increased rate of chromosomal alterations or phenotypic realization of these, and hence faster evolutionary adaptation.

A similar mechanism linking low fitness to increased evolution rates in a given environment is the stress induction of LOH events that have been described in *C. albicans* [9••]. Interestingly, the specific type of stress was found to be crucial for the LOH mechanism; temperature stress and fluconazole exposure led to an increased rate of whole-chromosome LOH accompanied by aneuploidy [9••]. Oxidative stress, however, caused an increase of short-tract LOH events rather than large-tract LOH or chromosome-wide LOH events. These stress-induced LOH events may indeed help the fungus to adapt to the host during infections [9••], but are also observed during commensal growth [75]. Of course, in obligatory haploid species like *C. glabrata*, LOH events cannot occur and hence do not play a role in adaptation.

Pathogen Evolution Outside the Human Host

Thus far we have focused on genetic alterations and their implication for the fitness of fungal pathogens inside the host. But adaptation to the host or host-like conditions can also happen outside the body, in a process that can be thought as an "environmental virulence school" [76–78]. As an example, the relatively high fitness of *C. neoformans* in the phagosomes of immune cells with their oxidative and nitrosative stress may have developed due to the exposure of the fungus to environmental amoebae. In the natural soil reservoir of *C. neoformans,* amoeba take up the fungus as a food source, but some strains are able to replicate inside of amoebae and break out, similar to the interaction of *C. neoformans* with host immune cells [76].

Stable morphological switches of fungi in relatively short time frames are generally thought to be mediated by epigenetic events. A counterexample was found in *C. neoformans*, where co-incubation with amoebae led to a morphological switch from yeasts to a pseudohyphal strain, thereby preventing uptake of the fungus [79, 80]. Magditch et al. demonstrated that this yeast-to-pseudohyphae switch of *C. neoformans* was due to point mutations and indels in several genes of the RAM pathway, which regulates Ace2 activity and cellular morphogenesis, among other functions [81, 82••]. Ace2 activity is required for correct septum destruction during cytokinesis [83]. The high frequency of switching is explained in one case by a previous hypermutator phenotype, and generally by the comparatively large total size of the RAM pathway genes as a target for mutations [82••]. Interestingly, there are significant variations in the fitness of these evolved *C. neoformans* strains depending upon the model. For example, while the pseudohyphal strains showed improved survival against their natural predators, amoeba, they were attenuated in virulence in a mouse infection model [79, 82••, 83–85].

Conclusions

In conclusion, it is evident that fungi are under constant evolutionary pressure, and for fungal pathogens, this pressure is frequently due to changes in their habitat – for example, coming from a commensal state in the gastrointestinal tract or in soil into the host during a pathogenic life phase. In the last decades, antifungal drug usage in particular has altered the interaction between fungal pathogens and the human host. This has led to shifts in the pathogen pool composition, with

previously uncommon fungal species gaining foothold as pathogens and with development of resistances to antifungal drugs [43, 44].

The mechanisms leading to a higher fitness due to chromosomal alterations differ between short- and long-term reactions and between different environmental or stress conditions, as well as between species. Knowing which mechanism is most relevant for any given condition (e.g., antifungal drug exposure) and how it affects the general fitness of the pathogen may be helpful in reducing or potentially even preventing these events (Fig. 1). For *C. albicans,* the most common stress-induced short-term adaptation mechanisms seems to be LOH and aneuploidy [9••, 73]. In the haploid state of *S. cerevisiae*, and in haploid fungi in general, LOH is impossible and aneuploidy is less common [86]; hence these fungi most likely have to adapt in different ways.

While the link between external stress and chromosomal alterations in stress-inducible mechanisms of *C. albicans* make biological sense, there are conditions where these mechanisms cannot lead to an increased fitness. This appears to be the case, for example, in echinocandin resistance of *C. albicans* and *C. glabrata*, which is mediated primarily by *FKS1* and *FKS2* mutations [58], as well as for polyene resistance by loss of function of ergosterol biosynthetic pathway genes [51–56]. Aneuploidy has never been described in these cases, suggesting that this mechanism does not confer any selective advantage.

In summary, what role do fine-scale chromosomal alterations play in fungal evolution and fitness in the host? The examples above show that fine-scale changes can have significant and biologically relevant phenotypic effects. These include resistance to different stressors such as antifungal drug exposure or important morphological and metabolic changes. Initial beneficial mutations are often associated with fitness costs unrelated to the selection stress, which often leads to additional compensatory mutations. When fungi are faced with strong selection (e.g., by exposure to antifungals) fast adaptation is necessary. Spontaneous mutation rates are less frequent than LOH rates, for example, and therefore LOH seems better suited for a fast increase in fitness. However, mutation rates can also be increased by (e.g., a hypermutator state) a large total coding size for the relevant genes and by the location (e.g., in the (sub)telomeric region) or the presence of repetitive sequences. These factors enhance the potential of to achieving a crucial increase in fitness under selection pressure. Overall, small-scale chromosomal alterations play a central role in the adaptation of the fungal pathogen to its host, and hence can play an important role in development and persistence of disease.

Acknowledgments We thank the team "Microevolution" of the department MPM, and especially Anja Lüttich and Katja Seider for helpful discussions. Our own work was supported by the Center for Sepsis Control and Care – CSCC (FKZ 01EO1002) and by the Deutsche Forschungsgemeinschaft (Hu 528 17–1) within the DACH program.

Compliance with Ethics Guidelines

Conflict of Interest D. Fischer declares no conflicts of interest.
B. Hube declares no conflicts of interest.
S. Brunke declares no conflicts of interest.

Human and Animal Rights and Informed Consent All studies by the authors involving animal subjects were performed after approval by the appropriate institutional review boards.

References

Papers of particular interest, published recently, have been highlighted as:
•• Of major importance

1. Blackwell M. The fungi: 1, 2, 3 … 5.1 million species? Am J Bot. 2011;98(3):426–38.
2. Bonfante P, Genre A. Mechanisms underlying beneficial plant-fungus interactions in mycorrhizal symbiosis. Nat Commun. 2010;1:48.
3. Brown GD et al. Hidden killers: human fungal infections. Sci Transl Med. 2012;4(165):165rv13.
4. Palumbi SR. Humans as the world's greatest evolutionary force. Science. 2001;293(5536):1786–90.
5. Kellis M, Birren BW, Lander ES. Proof and evolutionary analysis of ancient genome duplication in the yeast *Saccharomyces cerevisiae*. Nature. 2004;428(6983):617–24.
6. Dujon B et al. Genome evolution in yeasts. Nature. 2004;430(6995):35–44.
7. Jones T et al. The diploid genome sequence of *Candida albicans*. Proc Natl Acad Sci U S A. 2004;101(19):7329–34.
8. Selmecki A, Forche A, Berman J. Genomic plasticity of the human fungal pathogen *Candida albicans*. Eukaryot Cell. 2010;9(7):991–1008.
9.•• Forche A, et al. Stress alters rates and types of loss of heterozygosity in Candida albicans. MBio. 2011;2(4). doi:10.1128/mBio.00129-11. *First description that LOH can be induced by stress in C. albicans; shows that different types of stress lead to specific LOH events, ranging from short range to whole chromosomes*.
10. Lynch M et al. A genome-wide view of the spectrum of spontaneous mutations in yeast. Proc Natl Acad Sci U S A. 2008;105(27):9272–7.
11. Nishant KT et al. The baker's yeast diploid genome is remarkably stable in vegetative growth and meiosis. PLoS Genet. 2010;6(9):e1001109. doi:10.1371/journal.pgen.1001109.
12. Deshpande AM, Newlon CS. DNA replication fork pause sites dependent on transcription. Science. 1996;272(5264):1030–3.
13. Prado F, Aguilera A. Impairment of replication fork progression mediates RNA polII transcription-associated recombination. EMBO J. 2005;24(6):1267–76.
14. Forche A et al. The parasexual cycle in *Candida albicans* provides an alternative pathway to meiosis for the formation of recombinant strains. PLoS Biol. 2008;6(5):e110. doi:10.1371/journal.pbio.0060110.
15. Miranda LN et al. *Candida* colonisation as a source for candidaemia. J Hosp Infect. 2009;72(1):9–16.
16. Zakikhany K et al. In vivo transcript profiling of *Candida albicans* identifies a gene essential for interepithelial dissemination. Cell Microbiol. 2007;9(12):2938–54.

17. Dalle F et al. Cellular interactions of *Candida albicans* with human oral epithelial cells and enterocytes. Cell Microbiol. 2010;12(2): 248–71.
18. Walraven CJ, Lee SA. Antifungal lock therapy. Antimicrob Agents Chemother. 2013;57(1):1–8.
19. Da Matta DA et al. Multilocus sequence typing of sequential *Candida albicans* isolates from patients with persistent or recurrent fungemia. Med Mycol. 2010;48(5):757–62.
20. Shin JH et al. Molecular epidemiological analysis of bloodstream isolates of *Candida albicans* from a university hospital over a five-year period. J Microbiol. 2005;43(6):546–54.
21. Bougnoux ME et al. Multilocus sequence typing reveals intrafamilial transmission and microevolutions of *Candida albicans* isolates from the human digestive tract. J Clin Microbiol. 2006;44(5):1810–20.
22. Schroppel K et al. Evolution and replacement of *Candida albicans* strains during recurrent vaginitis demonstrated by DNA fingerprinting. J Clin Microbiol. 1994;32(11):2646–54.
23. Shin JH et al. Changes in karyotype and azole susceptibility of sequential bloodstream isolates from patients with *Candida glabrata* candidemia. J Clin Microbiol. 2007;45(8):2385–91.
24. Enache-Angoulvant A et al. Multilocus microsatellite markers for molecular typing of *Candida glabrata*: application to analysis of genetic relationships between bloodstream and digestive system isolates. J Clin Microbiol. 2010;48(11):4028–34.
25. Garcia-Hermoso D, Janbon G, Dromer F. Epidemiological evidence for dormant *Cryptococcus neoformans* infection. J Clin Microbiol. 1999;37(10):3204–9.
26. Goldman DL et al. Serologic evidence for *Cryptococcus neoformans* infection in early childhood. Pediatrics. 2001;107(5):E66.
27. Hasenclever HF, Emmons CW. The prevalence and mouse virulence of *cryptococcus neoformans* strains isolated from urban areas. Am J Hyg. 1963;78:227–31.
28. Fromtling RA, Abruzzo GK, Ruiz A. Virulence and antifungal susceptibility of environmental and clinical isolates of *Cryptococcus neoformans* from Puerto Rico. Mycopathologia. 1989;106(3):163–6.
29. Litvintseva AP, Mitchell TG. Most environmental isolates of *Cryptococcus neoformans* var. grubii (serotype A) are not lethal for mice. Infect Immun. 2009;77(8):3188–95.
30. Sampaio P et al. New microsatellite multiplex PCR for *Candida albicans* strain typing reveals microevolutionary changes. J Clin Microbiol. 2005;43(8):3869–76.
31. Fleischhacker M, Pasligh J, Moran G, Ruhnke M. Longitudinal genotyping of Candida dubliniensis isolates reveals strain maintenance, microevolution, and the emergence of itraconazole resistance. J Clin Microbiol. 2010;48(5):1643–50.
32. Brandt ME et al. Molecular subtypes and antifungal susceptibilities of serial *Cryptococcus neoformans* isolates in human immunodeficiency virus-associated Cryptococcosis. Cryptococcal Disease Active Surveillance Group. J Infect Dis. 1996;174(4):812–20.
33. Sullivan D et al. Persistence, replacement, and microevolution of Cryptococcus neoformans strains in recurrent meningitis in AIDS patients. J Clin Microbiol. 1996;34(7):1739–44.
34. Lionakis MS, Lim JK, Lee CC, Murphy PM. Organ-specific innate immune responses in a mouse model of invasive candidiasis. J Innate Immun. 2011;3(2):180–99.
35. MacCallum DM, Odds FC. Temporal events in the intravenous challenge model for experimental *Candida albicans* infections in female mice. Mycoses. 2005;48(3):151–61.
36. Cheng S et al. Uncoupling of oxidative phosphorylation enables *Candida albicans* to resist killing by phagocytes and persist in tissue. Cell Microbiol. 2007;9(2):492–501.
37. Forche A et al. Evolution in *Candida albicans* populations during a single passage through a mouse host. Genetics. 2009;182(3):799–811.
38.•• Lüttich A, Brunke S, Hube B, Jacobsen ID. Serial passaging of *Candida albicans* in systemic murine infection suggests that the wild type strain SC5314 is well adapted to the murine kidney. PLoS One. 2013;8(5):e64482. doi:10.1371/journal.pone.0064482. *Demonstrates that C. albicans is likely pre-adapted to colonize the murine kidney as main target organ. In comparing with other passaging experiments, suggests in vivo microevolution of C. albicans is determined by target organ and stage of disease progression.*
39.•• Ormerod KL et al. Comparative genomics of serial isolates of cryptococcus neoformans reveals gene associated with carbon utilization and virulence. G3 (Bethesda). 2013. doi:10.1534/g3.113.005660. *Shows adaptation mechanisms of C. neoformans during colonization of the brain; decreased virulence of the derived strain in a lung inhalation model of mice suggests niche-specific microevolution.*
40. Jacobsen ID et al. *Candida glabrata* persistence in mice does not depend on host immunosuppression and is unaffected by fungal amino acid auxotrophy. Infect Immun. 2010;78(3):1066–77.
41. Kaur R, Ma B, Cormack BP. A family of glycosylphosphatidylinositol-linked aspartyl proteases is required for virulence of *Candida glabrata*. Proc Natl Acad Sci U S A. 2007;104(18):7628–33.
42. Seider K et al. The facultative intracellular pathogen *Candida glabrata* subverts macrophage cytokine production and phagolysosome maturation. J Immunol. 2011;187(6):3072–86.
43. Pfaller MA, Diekema DJ. Rare and emerging opportunistic fungal pathogens: concern for resistance beyond *Candida albicans* and Aspergillus fumigatus. J Clin Microbiol. 2004;42(10):4419–31.
44. Pfaller MA. Antifungal drug resistance: mechanisms, epidemiology, and consequences for treatment. Am J Med. 2012;125(1 Suppl): S3–S13.
45.•• Singh-Babak SD et al. Global analysis of the evolution and mechanism of echinocandin resistance in *Candida glabrata*. PLoS Pathog. 2012;8(5):e1002718. doi:10.1371/journal.ppat.1002718. *Follows multiple steps of microevolution of C. glabrata during recurrent candidiasis in one patient; nvestigates mechanisms for caspofungin resistance; shows compensatory mutations abolish the fitness costs of the echinocandin resistance mutation.*
46. Ben-Ami R et al. Fitness and virulence costs of *Candida albicans* FKS1 hot spot mutations associated with echinocandin resistance. J Infect Dis. 2011;204(4):626–35.
47. Ben-Ami R, Kontoyiannis DP. Resistance to echinocandins comes at a cost: the impact of FKS1 hotspot mutations on *Candida albicans* fitness and virulence. Virulence. 2012;3(1):95–7.
48. Andersson DI, Hughes D. Antibiotic resistance and its cost: is it possible to reverse resistance? Nat Rev Microbiol. 2010;8(4):260–71.
49. Cowen LE, Kohn LM, Anderson JB. Divergence in fitness and evolution of drug resistance in experimental populations of *Candida albicans*. J Bacteriol. 2001;183(10):2971–8.
50. Cowen LE et al. Population genomics of drug resistance in *Candida albicans*. Proc Natl Acad Sci U S A. 2002;99(14):9284–9.
51. Kelly SL et al. Resistance to fluconazole and cross-resistance to amphotericin B in *Candida albicans* from AIDS patients caused by defective sterol delta5,6-desaturation. FEBS Lett. 1997;400(1):80–2.
52. Sanglard D et al. *Candida albicans* mutations in the ergosterol biosynthetic pathway and resistance to several antifungal agents. Antimicrob Agents Chemother. 2003;47(8):2404–12.
53. Vandeputte P et al. A nonsense mutation in the ERG6 gene leads to reduced susceptibility to polyenes in a clinical isolate of *Candida glabrata*. Antimicrob Agents Chemother. 2008;52(10):3701–9.
54. Martel CM et al. A clinical isolate of *Candida albicans* with mutations in ERG11 (encoding sterol 14alpha-demethylase) and ERG5 (encoding C22 desaturase) is cross resistant to azoles and amphotericin B. Antimicrob Agents Chemother. 2010;54(9):3578–83.

55. Hull CM et al. Two clinical isolates of *Candida glabrata* exhibiting reduced sensitivity to amphotericin B both harbor mutations in ERG2. Antimicrob Agents Chemother. 2012;56(12):6417–21.
56. Vincent BM et al. Fitness trade-offs restrict the evolution of resistance to amphotericin B. PLoS Biol. 2013;11(10):e1001692. doi: 10.1371/journal.pbio.1001692.
57. Eschenauer GA, et al. Real-world experience with echinocandin MICs against Candida species: A multi-center study of hospitals that routinely perform susceptibility testing of bloodstream isolates. Antimicrob Agents Chemother. 2014;
58. Beyda ND, Lewis RE, Garey KW. Echinocandin resistance in Candida species: mechanisms of reduced susceptibility and therapeutic approaches. Ann Pharmacother. 2012;46(7–8):1086–96.
59. Perea S et al. Prevalence of molecular mechanisms of resistance to azole antifungal agents in *Candida albicans* strains displaying high-level fluconazole resistance isolated from human immunodeficiency virus-infected patients. Antimicrob Agents Chemother. 2001;45(10):2676–84.
60. Morio F et al. Screening for amino acid substitutions in the *Candida albicans* Erg11 protein of azole-susceptible and azole-resistant clinical isolates: new substitutions and a review of the literature. Diagn Microbiol Infect Dis. 2010;66(4):373–84.
61. Flowers SA et al. Gain-of-function mutations in UPC2 are a frequent cause of ERG11 upregulation in azole-resistant clinical isolates of *Candida albicans*. Eukaryot Cell. 2012;11(10):1289–99.
62. Kelly SL et al. Mode of action and resistance to azole antifungals associated with the formation of 14 alpha-methylergosta-8,24(28)-dien-3 beta,6 alpha-diol. Biochem Biophys Res Commun. 1995;207(3):910–5.
63. Watson PF et al. Defective sterol C5-6 desaturation and azole resistance: a new hypothesis for the mode of action of azole antifungals. Biochem Biophys Res Commun. 1989;164(3):1170–5.
64. Selmecki A, Forche A, Berman J. Aneuploidy and isochromosome formation in drug-resistant *Candida albicans*. Science. 2006;313(5785):367–70.
65. Coste A et al. Genotypic evolution of azole resistance mechanisms in sequential *Candida albicans* isolates. Eukaryot Cell. 2007;6(10): 1889–904.
66. Coste AT et al. TAC1, transcriptional activator of CDR genes, is a new transcription factor involved in the regulation of *Candida albicans* ABC transporters CDR1 and CDR2. Eukaryot Cell. 2004;3(6):1639–52.
67. Coste A et al. A mutation in Tac1p, a transcription factor regulating CDR1 and CDR2, is coupled with loss of heterozygosity at chromosome 5 to mediate antifungal resistance in *Candida albicans*. Genetics. 2006;172(4):2139–56.
68. Morschhäuser J et al. The transcription factor Mrr1p controls expression of the MDR1 efflux pump and mediates multidrug resistance in *Candida albicans*. PLoS Pathog. 2007;3(11):e164. doi:10.1371/journal.ppat.0030164.
69. zur Wiesch PA et al. Population biological principles of drug-resistance evolution in infectious diseases. Lancet Infect Dis. 2011;11(3):236–47.
70. Cowen LE, Lindquist S. Hsp90 potentiates the rapid evolution of new traits: drug resistance in diverse fungi. Science. 2005;309(5744): 2185–9.
71. Anderson JB et al. Mode of selection and experimental evolution of antifungal drug resistance in Saccharomyces cerevisiae. Genetics. 2003;163(4):1287–98.
72.•• Hill JA et al. Genetic and genomic architecture of the evolution of resistance to antifungal drug combinations. PLoS Genet. 2013;9(4): e1003390. doi:10.1371/journal.pgen.1003390. *Shows that adaptation to antifungal drug combinations is possible, though likely to a lesser extent than to a single compound; gives mechanistic insights into how resistance to antifungal drug combinations can be mediated.*
73. Chen G, Bradford WD, Seidel CW, Li R. Hsp90 stress potentiates rapid cellular adaptation through induction of aneuploidy. Nature. 2012;482(7384):246–50.
74. Taipale M, Jarosz DF, Lindquist S. HSP90 at the hub of protein homeostasis: emerging mechanistic insights. Nat Rev Mol Cell Biol. 2010;11(7):515–28.
75. Diogo D, Bouchier C, d'Enfert C, Bougnoux ME. Loss of heterozygosity in commensal isolates of the asexual diploid yeast *Candida albicans*. Fungal Genet Biol. 2009;46(2):159–68.
76. Steenbergen JN, Shuman HA, Casadevall A. *Cryptococcus neoformans* interactions with amoebae suggest an explanation for its virulence and intracellular pathogenic strategy in macrophages. Proc Natl Acad Sci U S A. 2001;98(26):15245–50.
77. Casadevall A. Evolution of intracellular pathogens. Annu Rev Microbiol. 2008;62:19–33.
78. Bliska JB, Casadevall A. Intracellular pathogenic bacteria and fungi–a case of convergent evolution? Nat Rev Microbiol. 2009;7(2):165–71.
79. Neilson JB, Ivey MH, Bulmer GS. *Cryptococcus neoformans*: pseudohyphal forms surviving culture with Acanthamoeba polyphaga. Infect Immun. 1978;20(1):262–6.
80. Bunting LA, Neilson JB, Bulmer GS. *Cryptococcus neoformans*: gastronomic delight of a soil ameba. Sabouraudia. 1979;17(3):225–32.
81. Nelson B et al. RAM: a conserved signaling network that regulates Ace2p transcriptional activity and polarized morphogenesis. Mol Biol Cell. 2003;14(9):3782–803.
82.•• Magditch DA, Liu TB, Xue C, Idnurm A. DNA mutations mediate microevolution between host-adapted forms of the pathogenic fungus *Cryptococcus neoformans*. PLoS Pathog. 2012;8(10): e1002936. doi:10.1371/journal.ppat.1002936. *Determines the genetic basis for fitness changes of a fungus in interaction with natural predators. Demonstrates high-rate phenotypic switching through small-scale chromosomal changes.*
83. Dohrmann PR et al. Parallel pathways of gene regulation: homologous regulators SWI5 and ACE2 differentially control transcription of HO and chitinase. Genes Dev. 1992;6(1):93–104.
84. Fromtling RA, Blackstock R, Hall NK, Bulmer GS. Immunization of mice with an avirulent pseudohyphal form of *Cryptococcus neoformans*. Mycopathologia. 1979;68(3):179–81.
85. Neilson JB, Fromtling RA, Bulmer GS. Pseudohyphal forms of *Cryptococcus neoformans*: decreased survival in vivo. Mycopathologia. 1981;73(1):57–9.
86. Zhu J et al. Karyotypic determinants of chromosome instability in aneuploid budding yeast. PLoS Genet. 2012;8(5):e1002719. doi: 10.1371/journal.pgen.1002719.

2.3 Manuscript III

A model of long-term *Candida glabrata*-macrophage interaction links quiescence with intramacrophagal persistence

Daniel Fischer, Marcel Sprenger, Jörg Linde, Bernhard Hube, Sascha Brunke

In preparation for submission to *mSphere*.

Summary:
Different fungal pathogens interact preferentially with different host (immune) cells and the different kinds of interactions determine disease outcomes. *Candida glabrata* has been shown in several *in vitro* and *in vivo* experimental settings to interact preferentially with mononuclear cells. Since *C. glabrata* is known to modify phagolysosome maturation *in vitro* and can thereby survive and replicate inside of macrophages, the outcome of this interaction is likely to have a strong impact on outcome of *C. glabrata* infections. This work, like previous studies, proposes that *in vivo* a part of this interaction consists of a long-term residence of *C. glabrata* yeasts within mononuclear cells, a scenario which would be especially relevant in chronic or recurrent diseases. Until now, such a scenario could not be modelled, as *C. glabrata*-macrophage models are typically characterized by fast intracellular yeast replication followed by bursting of the macrophage within roughly two days. Here, we established the – to our best knowledge – first *C. glabrata*-macrophage model(s) which represent this "missing part of the whole story". By combining data from a barcode sequencing-based *C. glabrata* mutant library screen and a *C. glabrata* transcriptome analysis, we identified several factors and processes which are critical for persistence in macrophages. Among them, several regulators of yeast quiescence were found, implying a role of this process in long-term survival within macrophage. In addition, constant antimycotic treatment was found to be insufficient for complete eradication of intramacrophagal *C. glabrata*. This proves that persistence in macrophages is possible even in the face of antifungal treatment, probably involving quiescent yeasts. Furthermore, *C. glabrata* transcriptionally induced genes involved in the mating response, an unexpected finding in a yeast whose sexual cycle was never observed, and which warrants further investigations. In summary, our results support the idea that *C. glabrata* can use mononuclear cells as a niche for persistence during (long-term) infections, and the methods and models developed in the study will allow future, deeper investigations of this topic.

Own Contribution:

Daniel Fischer planned, performed (with technical help), evaluated, and interpreted all experiments, generated all figures, and wrote the manuscript. The Bar-Seq data analysis pipeline was established by Sascha Brunke and Jörg Linde together with Daniel Fischer. Most of the new mutant strains first described in this study were created by Daniel Fischer, with technical help for the barcoded reference strains and with the exception of *C. glabrata* ATCC2001 yeGFP.

Estimated authors' contributions:

Daniel Fischer	74%
Marcel Sprenger	2%
Jörg Linde	1%
Bernhard Hube	3%
Sascha Brunke	20%

Prof. Bernhard Hube

A model of long-term *Candida glabrata*-macrophage interaction links quiescence with intramacrophagal persistence

Authors

Daniel Fischer, Marcel Sprenger, Jörg Linde, Bernhard Hube, Sascha Brunke

Abstract

The yeast *Candida glabrata* is a facultative pathogen of humans. In mice models of infection, *C. glabrata* shows low virulence, but can persist over long periods in infected organs. During experimental infections *in vitro* and *in vivo*, *C. glabrata* is predominantly in association with mononuclear cells and it has been shown that the fungus can survive and replicate within macrophages. This has led to the hypothesis that *C. glabrata* might hide within mononuclear cells for immune evasion. However, no models were available up to now to investigate the long-term intramacrophagal persistence of *C. glabrata*. Here, we present a new *C. glabrata* macrophage model which allows following its life inside macrophages over several days. This model, together with large-scale approaches – a Bar-Seq based mutant library screen and transcriptomes of *C. glabrata* – allowed us to identify several critical fungal stress adaptation factors and processes for intramacrophagal persistence, many linked to quiescence regulation in yeast. Importantly, *C. glabrata* inside of macrophages were not eradicated completely by treatment with antifungal agents such as amphotericin B or caspofungin. These findings support the hypothesis that *C. glabrata* might use macrophages as persistence niche and possibly as a starting point to cause re-infection of the host.

Abbreviations

human monocyte derived macrophages (hMDMs); colony forming unit (cfu)

Introduction

Candida glabrata is a facultative human-pathogenic hemiascomycete closely related to the baker´s yeast *Saccharomyces cerevisiae* (Kurtzman and Robnett 1997; Dujon *et al.* 2004; Butler *et al.* 2009). Although *C. glabrata* is considered to be mostly harmless for healthy individuals, it frequently causes superficial infections and can become a serious threat in immunocompromised, especially elderly individuals (Fidel, Vazquez, and Sobel 1999; Diekema *et al.* 2002; Weinberger *et al.* 2005; Li, Redding, and Dongari-Bagtzoglou 2007). In this patient population, *C. glabrata* can give rise to systemic infections with potentially fatal outcome due to sepsis (Perlroth, Choi, and Spellberg 2007). There are some special characteristics of *C. glabrata* when compared e.g. to *Candida albicans*, the most prominent *Candida* species. In the clinical setting, *C. glabrata* often has a higher

intrinsic resistance towards azoles and can quickly acquire resistance against azoles (Pfaller *et al.* 2011; Pfaller *et al.* 2012; Farmakiotis, Tarrand, and Kontoyiannis 2014; McCarty and Pappas 2016), but also echinocandins (Pfaller *et al.* 2011; Pfaller *et al.* 2012; Alexander *et al.* 2013; Farmakiotis, Tarrand, and Kontoyiannis 2014), and much less frequently to polyenes (Vandeputte *et al.* 2007; Vandeputte *et al.* 2008), which is associated with a higher rate of treatment failure. In its morphology, *C. glabrata* is limited to yeasts (and potentially pseudohyphae (Csank and Haynes 2000)) – in stark contrast to the polymorphic *C. albicans* whose morphological flexibility is fundamental for its ability to infect mammalian hosts (Sudbery 2011). It also lacks an orthologue of the candidalysin toxin-encoding ECE1 gene of *C. albicans* and typically causes only little damage to human epithelial and immune cells, with a limited inflammatory response *in vitro* (Aybay and Imir 1996; Filler *et al.* 1996; Schaller *et al.* 2002; Li and Dongari-Bagtzoglou 2007; Seider *et al.* 2011) and *in vivo* (Brieland *et al.* 2001; Arendrup, Horn, and Frimodt-Møller 2002; Jacobsen *et al.* 2010).

Consequently, in comparison to *C. albicans*, *C. glabrata* is typically much less virulent in murine infection models (Brieland *et al.* 2001; Cheng *et al.* 2014). However, *C. glabrata* has been shown to persist at appreciable numbers, but without clinical symptoms for weeks in different organs of immunocompromised as well as immunocompetent mice, both in a model of disseminated (Brieland *et al.* 2001; Jacobsen *et al.* 2010) and intra-abdominal candidiasis (Cheng *et al.* 2014). In both models *C. glabrata* was found associated with mononuclear cells (Brieland *et al.* 2001; Jacobsen *et al.* 2010; Cheng *et al.* 2014). An *in vitro* study with different fungal species showed preferential uptake of *C. glabrata* by monocytes (Duggan *et al.* 2015), and in an *ex vivo* model of human bloodstream infections, *C. glabrata* was more often associated with monocytes than other *Candida* species (P. Kämmer *et al.*, mBio, accepted). Importantly, *C. glabrata* has also been shown to survive and replicate within macrophages *in vitro* (Otto and Howard 1976; Kaur, Ma, and Cormack 2007; Roetzer *et al.* 2010; Seider *et al.* 2011), and for these reasons we and others previously discussed macrophages as a potential site for *C. glabrata* immune evasion and persistence (Seider *et al.* 2011; Kasper, Seider, and Hube 2015).

In addition to the previously mentioned resistance to antifungals, otherwise susceptible fungal cells can also enter a non-susceptible, quiescent state under certain circumstances. This has been shown e.g. for planktonic, quiescent *S. cerevisiae* cells, which in this state are not susceptible to voriconazole and caspofungin (Bojsen, Regenberg, and Folkesson 2014). Thus, subpopulations of infecting fungi can potentially survive in an antifungal-tolerant state and outlast treatment to re-establish infection afterwards (e.g. reviewed in (Berman and Krysan 2020)). Therefore, it seems possible

that *C. glabrata* cells can remain in macrophages for long periods of time, where they adopt this quiescent state and thus are protected from both immune assaults and antifungals.

Investigations into yeast-host interactions on longer time scales have been performed in different mice models (Jacobsen *et al.* 2010; Cheng *et al.* 2014) or in a granuloma model (Misme-Aucouturier *et al.* 2017). However, so far it was not possible to study the interaction of *C. glabrata* with mononuclear cells on a longer time scale in isolation, as *C. glabrata* replicates profusely inside standard *ex vivo* and *in vitro* macrophage models and usually overgrows the macrophages within two to three days (Seider *et al.* 2011). Such models, therefore, seem unlikely to reflect the normal *in vivo* interaction of yeasts and macrophages, especially in respect to potentially quiescent subpopulations.

Here, we used novel models of at least week-long *C. glabrata*-macrophage interactions, which allow us to investigate the fungal genes and processes required for intramacrophagal persistence. We probed a large-scale mutant library (Schwarzmüller *et al.* 2014) and obtained *C. glabrata* transcriptomes during this long-term interaction. Our analysis shows that, among others, stress adaptation factors linked to yeast quiescence and a tight regulation of energy homeostasis and of the cell wall structure is critical for fungal persistence. Furthermore, our data show persistence of intracellular *C. glabrata* cells despite continuous treatment with common antifungal agents. Surprisingly, we also found that *C. glabrata* cells show a transcriptional pattern indicative for a mating response during their residence inside macrophages.

Results

The *C. glabrata*-macrophage persistence model

Our previous studies showed that *C. glabrata* is associated with mononuclear cells *in vivo*, raising the question whether macrophages might serve as the site of persistence during infection. We, therefore, decided to establish an *in vitro* model that enables us to study the long-term interaction between the fungus and macrophages. After several adjustments to a previous system (Seider *et al.* 2011), our final model uses human monocyte-derived macrophages in RPMI medium supplemented with 10% active human serum and a strict medium exchange regime which includes a washing step after 3 h of yeast-macrophage co-incubation to remove non-phagocytosed cells (for details see method section). We chose seven days of co-incubation as our last assay time point, but longer persistence periods are possible with this setting. Macrophage cell viability over all seven days was confirmed by propidium iodide staining protocols (Fig. 1). In the rare event of yeast overgrowth the affected well was discarded when microscopic inspection revealed extracellular *C. glabrata* cells. These cut-offs were set very strict for cfu-based

assays, while we allow some escaping yeasts in pool experiments where hyper-fit strains may otherwise be accidentally discarded (Fig. 2). In contrast to previously published data on macrophage-*C. glabrata* interaction, determination of cfu counts in our model showed a significant drop between 3 and 24 hours of co-incubation followed by a macrophage donor-dependent, further, much slower decline (Fig. 3A). Overall, we obtained a largely stable population of about 3.1 % (0.7 - 7.6 %) of the original phagocytosed inoculum which survived inside the human macrophages for at least seven days.

Addition of caspofungin or amphotericin B at MIC_{100} after six hours of co-incubation led only to a moderate (29-35 %) additional decrease in intracellular cfus over the course of one day, indicating that the fungi are somewhat protected inside the macrophages. After seven days of constant antimycotic treatment, the cfus dropped significantly to about 4.1 % (caspofungin) or 8.9 % (amphotericin B) of the non-treated control, and increasing the caspofungin concentration fivefold did not further enhance intracellular killing (Fig. 3B). These numbers are roughly comparable to survival levels of persister cells under *in vitro* antimycotic treatment (LaFleur, Kumamoto, and Lewis 2006; Al-Dhaheri and Douglas 2008; Bojsen *et al.* 2016; Wuyts, Van Dijck, and Holtappels 2018), although the underlying phenotypes might be not directly comparable given the differences of the treatment strategies. We did not increase the amphotericin B concentration further since this directly affected the macrophages (data not shown). Intracellular *C. glabrata* persistence can therefore occur even under administration of antifungals and is therefore possibly relevant also in clinical situations.

Establishment of the Bar-Seq technique

A pooled approach allows the intramacrophagal long-term survival of many mutants to be determined at the same time (Fig. 4). We made use of a previously established large-scale, barcoded *C. glabrata* deletion mutant library [Suppl. Table 1; (Schwarzmüller *et al.* 2014)] with a modification of a previously described detection and quantification approach (Brunke *et al.* 2015). We here used amplicon sequencing (instead of microarrays) of the up- and downstream barcode sequences that flank the selection marker used for gene disruption. Our amplification primers additionally contained varying, experiment-specific 10 nt sequences at their 5´ end (Suppl. Table 2) to allow multiplexing of samples.

For our persistence experiments, mutants were distributed into 16 randomized pools with a size of 39-50 strains each. Inocula preparation aimed for the same relative amounts for all mutants. All inocula were additionally plated on YPD medium to determine the actual starting distribution of the mutants as reference for all further calculations (Fig. 4B). The samples were taken after one and seven days of co-incubation with macrophages, and the supernatant and macrophage lysate were combined and plated

on YPD for DNA isolation from colonies and barcode amplification. After sequencing, counts were normalized to the median count values for each pool as a comparison which is independent of parental strains. Since different mutants of the collection have different parental strains (Schwarzmüller *et al.* 2014), we determined how this alternative normalization approach correlates with an individual parent-referenced approach. Correlation was good to excellent with Pearson r values of 0.81 and 0.92 for one and seven days, respectively (Suppl. Fig. 1). The distribution of depleted and enriched strains follows the expected pattern: the majority shows wild type-like survival, and more mutants were depleted than enriched in comparison to the wild types (compare Fig. 5 and Suppl. Fig. 1). Accordingly, the wild types showed higher recovery than the median of the strains created in the respective background. However, the median-normalized mean recovery (recovery of both barcodes, geometric mean) was in part statistically significant different between different wild type strains (Fig. 5B; e.g. after seven days 1.21 for BC, 1.08 for H-BC and 1.63 for HLT-BC). These differences are reflected in statistically significant differences of the recovery of strains from these different wild type backgrounds (Suppl. Fig. 1). The strain background and its auxotrophies therefore seems to have an influence on the intracellular persistence of *C. glabrata* in macrophages, in contrast to what we found previously in a systemic mice infection model (Jacobsen *et al.* 2010). Therefore, we used parent-normalized values for all pools except 16, for which no direct parent strain is available (Schwarzmüller *et al.* 2014); for the latter, we employed median normalization, with cut-off accordingly adjusted (see Material and Methods, Fig. 7+8, Suppl. Fig. 2, Suppl. Tables 3+4).

Pool experiments are usually competition experiments among the tested mutants. To ensure that as few yeasts as possible share the same phagosome and influence each other, we characterized the distribution pattern of a fluorescent *C. glabrata* strain within the macrophages over the seven day time course. As expected, over time and with declining cfu counts, more and more macrophages did not contain any *C. glabrata* anymore. However, the number of yeasts per infected macrophage remained largely stable at low numbers, with the majority containing 1-2 yeasts (Fig. 6). We conclude that there should only be a limited competition or influence between cohabitating yeasts.

Identification of genes required for intracellular persistence

The number of depleted mutant strains (cut-off factors: pool 1-15 < 0.5; pool 16 < 0.7, $p<0.1$) increased between 1 and 7 days, indicating continuing selective forces at work inside the macrophages (Suppl. Table 3). Additionally, most (27/29) *C. glabrata* mutants which were depleted already after one day, showed further depletion with prolonged

incubation. To reflect this increasing depletion, we set the cut-off for 7 days depletion to a more stringent 0.35 (0.5 pool 16, p<0.1). Of the 101 mutants depleted after seven days, at day one 94 would not have been considered depleted at the 7d cut-off, and 75 not even at the less stringent cut-off of day 1, while 18 were not depleted at all (≥1.0, ≥1.2) after one day. These different numbers also indicate that some genes are permanently required in macrophage interactions and some mainly during persistence.

Finally, of all mutants that met the cut-off criterion at seven days, 30 were even strongly reduced to less than 0.15 (0.25, p<0.05; Fig. 7, Suppl. Table 3). To obtain a general impression of the underlying processes, we used GoTermFinder (Boyle *et al.* 2004) to identify enriched GO terms within this group which we then summarized using Revigo (Supek *et al.* 2011). Based on multiple testing corrected p values with a cut-off of 0.05, we found among the strongly depleted mutants GO terms pertaining to cellular component biogenesis, kinase activity, lipid binding, and to the cell wall, both to its biogenesis and the regulation of its organisation (Suppl. Table 4, Suppl. Fig. 2). For regulation of cell wall organisation, this includes (cut-off < 0.35, < 0.5) mutants of parts of the MAPK pathways (cell wall integrity pathway: Δ*bck1*, Δ*mkk1*, Δ*slt2*; general adapter: Δ*ste50*; osmosensory signalling pathway: Δ*sho1*, but interestingly not Δ*pbs2*, Δ*sko1*, Δ*msn2*, Δ*msn4*) and mutants which affect the activity of the cell wall integrity MAPK cascade (Δ*ypk2*, ΔCAGL0I07513g, Δ*stt4*, Δ*sac7*; Fig. 7). Especially interesting is Δ*ssd1*, which was the second most strongly depleted mutant in the mutant pool after seven days. The *S. cerevisiae* orthologue of the gene affects the cell wall through regulation of mRNA stability of cell wall biosynthesis effectors (Uesono, Toh-e, and Kikuchi 1997; Kaeberlein and Guarente 2002; Jansen *et al.* 2009; Kurischko, Kim, *et al.* 2011). We found four further mutants whose orthologous genes are involved in mRNA trafficking, metabolism, and translation efficiency (Δ*pop2*, ΔCAGL0L06226g, Δ*aep3*, Δ*spt4*).

At a level of < 0.35 (0.5, p<0.1) after seven days, the deleted genes potentially directly related to cell wall biosynthesis can be categorized into those involved in protein glycosylation (Δ*anp1*, Δ*mnn10*, Δv*ig9*, Δ*ktr2*, Δ*pmt2*) and those which are so far functionally uncharacterized (Δ*she10*, Δ*ecm33*). Furthermore, GO terms relating to chromatin modification can be found, including “chromosome organization” in the Revigo-summarized GO term list (Fig. 8, Suppl. Table 4). This is due to mutants for genes coding for members of histone acetyltransferase complexes like SAGA (Δ*ada2*, Δ*gcn5*, Δ*spt8*) and SAS (Δ*sas5*), but also histone deacetylase complexes like RPD3L (Δ*sin3*, Δ*pho23*, Δ*sds3*), SET3 (Δ*set3*), the Sum1p/Rfm1p/Hst1p complex (Δ*hst1*), the HDA1 complex (Δ*hda1*), and finally the histone deacetylase gene HST3. Histone methyltransferases (Δ*set2*, Δ*swd1*), the HIR complex (Δ*hir2*, Δ*hir3*) regulating histone

gene transcription, and mediator-related gene deletion mutants (Δ*anc1*, Δ*gal11a*) were similarly depleted, as was a mutant in the general chromatin remodelling Paf1 complex (Δ*rtf1*).

Mutants of four transcription factors were depleted whose regulated genes contribute to stress responses: Sfl1 as part of the cAMP-PKA pathway (see also below), Yap7 which is a transcriptional repressor of the nitric oxide oxidase (Merhej *et al.* 2015), Yrr1 which activates multi-drug resistance genes in *S. cerevisiae* (Cui *et al.* 1998; Le Crom *et al.* 2002) and Hac1 which controls transcription of genes relevant for the unfolded protein response (UPR; (Miyazaki *et al.* 2013)). Genes encoding proteins involved in metabolic pathways are generally underrepresented in our mutant collection (Schwarzmüller *et al.* 2014) but we found Δ*oaf1* (orthologue controls transcription of lipid oxidation genes; (Luo *et al.* 1996; Rottensteiner *et al.* 1997; Karpichev *et al.* 1997; Karpichev and Small 1998; Baumgartner *et al.* 1999)) depleted at day 1 (no statistical significance) and day 7 (p=0.013) while Δ*pho4* (the deleted gene is necessary for expression of phosphate-starvation genes; (Kerwin and Wykoff 2009)) was depleted specifically at day 7. Furthermore, mutants were depleted which lack transcription factors relevant for nitrogen metabolism regulation like Gln3, Ste12, and Cagl0l02585gp, as well as for ion homeostasis (Hap2, Hap3, Hap5, Imp2; but not Aft2, Sef1, Ccc1 and Fth1). Again specifically depleted at day 7, but not day 1, were mutants of members of the AMP-activated Snf1p kinase complex (Δ*snf1*, Δ*snf4*). In contrast, mutants of the cAMP-PKA signalling pathway showed a general trend towards depletion already after one day and mainly further depletion after seven days (Δ*gbp2*, Δ*pde2*, Δ*sfl1*, Δ*bcy1*, Δ*gpa2*, Δ*gpr1*). We found only three depleted mutants directly involved in metabolic pathways – one each for glycolysis (Δ*pfk1*), gluconeogenesis (ΔCAGL0H06633g = best hit in *S. cerevisiae* is *PCK1*) and the TCA and/or glyoxylate cycle (Δ*aco1*). Their time courses differed markedly: Δ*pfk1* was strongly depleted within one day and decreased no further, ΔCAGL0H06633g was not depleted after one, but clearly after seven days, and for Δ*aco1* the depletion increased over time. Nutrient depletion was also visible in the form of autophagy (enriched GO term, p-value <0.05) which includes previously mentioned genes, the t-SNARE mutant Δ*pep12*, the Atg1 kinase regulating subunit mutant Δ*atg13* and the ESCRT-III complex mutants Δ*snf7* and Δ*did4*. The most severely depleted mutant at seven days finally, Δ*slm1* and the related, also depleted mutants Δ*stt4*, Δ*sla2*, Δ*sac7*, Δ*rom2*, Δ*swf1*, Δ*mon2*, Δ*vps1*, Δ*pkh2*, Δ*ypk2* lack genes which are involved in endocytosis, actin cytoskeleton organization and/or cytokinesis.

Characteristics of long-term macrophage-*C. glabrata* interactions

To better understand the biological basis of the mutants' enrichment or depletion, we

went on to characterize the long-term model in more detail using the wild type. We started by determining the dynamics of the cytokine levels during the experiments. Our measurements showed secretion of the pro-inflammatory cytokines, IL-6, IL-8, and TNF-α by hMDMs in response to *C. glabrata* in our persistence model (Fig. 9A). IL-6 and IL-8 levels peaked after one day and steadily declined afterwards, likely being diluted by the daily media exchange. However, while there was clearly no renewed secretion of IL-6 after day one, IL-8 secretion seemed to continue at least between days one and two (Fig. 9B). In contrast, TNF-α levels similarly peaked after one day, but rapidly declined to zero after approximately three days, which suggests active removal in addition to the dilution effect (Fig. 9B). Interestingly, when we used LPS as a control, the hMDMs secreted IL-8 over the whole time course, in contrast to the *C. glabrata* infection, and IL-6 secretion stopped only after three days. TNF-α secretion was more similar and ended after one day (Suppl. Fig. 3).

We turned to transcriptional analyses to follow the long-term fate of the fungi inside the macrophages, with slight changes to the protocol to allow for sufficiently high RNA yields at the late time points. With a higher *C. glabrata* MOI and addition of caspofungin to the medium (see method section for technical details) we obtained sufficient RNA for our analyses. Caspofungin influenced intracellular survival of *C. glabrata* (Fig. 3B), which may have an unavoidable effect on the later time points of *C. glabrata* in hMDMs (1d, 2d, 4d, 7d). We sampled different time points of *C. glabrata* yeast in co-incubation with hMDMs (0 [yeast pre-infection], 0.25, 1, 2, 4, 7d) and control conditions (logarithmic growth in complex medium [YPD] and 7d incubation in different media [YPD, YNB pH6, RPMI + 10% HS]).

At a global scale, the number of differentially regulated genes was highest between the two first time points, and the difference between consecutive time points steadily declined over the course of the experiment (Suppl. Fig. 4, Suppl. Table 5), indicative of a stabilizing transcriptional equilibrium. The immediate answer of *C. glabrata* (0d vs 0.25d) towards phagocytosis comprises mainly a broad metabolic adaptation to a nutrient-poor environment (compare e.g. Suppl. Table 6; (Kaur, Ma, and Cormack 2007)): Large energy-consuming processes like all aspects of gene expression (transcription, translation, ribosomal components, RNA processing; Suppl. Table 6) are downregulated, while use of alternative carbon sources (e.g. fatty acids, certain amino acids; Suppl. Tables 6 + 7), the tricarboxylic acid cycle, and the respiratory chain are upregulated. Furthermore, genes that mediate the response to reactive oxygen species were found upregulated. In more detail, we found the following processes to determine the transcriptional pattern of *C. glabrata* persisting within macrophages:

Cell cycle arrest and pheromone response

Unsurprisingly, the core response during the long-term incubation compared to logarithmic growth included upregulation of genes annotated with the GO term “cell cycle arrest”, while genes associated with cell cycle progression were downregulated (Suppl. Table 6). For some of these processes (like DNA replication and S phase) downregulation was observed only at mid-term (1d, 2d) and the transcription resumed later (Suppl. Table 8). This suggests an entry into normal cell cycles at later time points. Surprisingly for a fungus for which mating has not been observed so far, we found several strong signs of the pheromone response developing over time within the macrophages. The mating type switch-mediating HO endonuclease homologue (as assigned in *S. cerevisiae*) was strongly upregulated within the first two days, and the orthologue of the gene for its transcriptional repressor *ASH1* (CAGL0D00462g), was downregulated (Suppl. Tables 5 + 7). Also, despite our ATCC 2001 strain being mating-type α, we observed a likely upregulation of both mating type pheromones and receptor genes. Similarly, the orthologue of a gene for an a-pheromone secretion transporter in *S. cerevisiae*, *STE6*, was expressed at permanently higher levels in hMDMs than during growth in medium, and the orthologue of *AXL1*, required for pheromone maturation, was found temporarily up-regulated. Of the MAP kinase pathway relaying the pheromone signal, we found several components to be upregulated after 7d of *C. glabrata*-hMDM co-incubation vs YPD log growth (*FUS3*, *STE5*, *STE50*, *STE11*, and *PTP3*). Furthermore, the orthologous gene for the transcriptional repressor of mating in *S. cerevisiae*, *ADF1*, is strongly downregulated early on. However, genes of effectors directly involved in mating (e.g. *FIG1*, *FUS1*, *PRM1*, *JEM1*, and *FUS2*) showed no relevant expression changes. In summary, the transcriptomic response of *C. glabrata* during long-term engulfment by hMDMs shows signs of a mating pheromone response. Notably, parts of this response were also visible, albeit to a lesser extent, during long-term medium culture.

Genes associated with transcriptional regulation

A significant part of the early *C. glabrata* answer (0d to 0.25d) to hMDM engulfment consisted of a downregulation of genes involved in gene expression (Suppl. Tables 6 + 7 + 8), which however may be explained by a transient upregulation of these processes in the inoculum compared to logarithmic growth (Suppl. Fig 5). However, individual direct comparisons, at every time point of the time series, of engulfed yeasts vs logarithmic growth also showed enrichment of the downregulation of gene expression processes (Suppl. Tables 7 + 8). This indicates that a repression of the gene expression apparatus is an ongoing process for yeasts within the phagosome and not limited to the initial change in environment. Notably, some aspects of gene expression like translation and

amino acid activation were even stronger repressed in the YNB medium 7d control condition (Suppl. Table 8), suggesting further downregulation of gene expression is possible respectively alternative ways of its detailed arrangement exist.

Regulation of cell wall associated genes

The accessibility of different cell wall components to macrophage receptors is often critical for intracellular survival of pathogens as they largely determine the immune cell's immediate response. While the initial yeast cell wall structure is determined before infection, cell wall synthesis or repair processes in long-term interactions can change the outcome and may be required to cope with the stresses inside the phagosome. We observed both stable and transient transcriptional upregulation of MAPK cascades components (cell wall integrity, HOG, pseudohyphal growth, and pheromone pathways) in phagocytosed yeast vs YPD log growth (Suppl. Tables 7 + 8), which indicates an active cell wall remodelling.

There was a general tendency for genes annotated with GO terms like “cell wall” to be upregulated mainly at later time points (4d and especially 7d) when compared to log growth, while the long-term medium control conditions showed a tendency towards downregulation of genes associated with cell wall-associated GO terms (Suppl. Table 8). Furthermore, the hMDM 7d time point showed upregulation of cell surface-associated GO terms in comparison to all other time points and conditions (Suppl. Table 8).

Metabolism and associated (transport) processes

As expected, the general metabolic situation for C. glabrata inside hMDMs was poor compared to growth in YPD: all hMDM time points as well as long-term medium controls showed marked downregulation of biosynthetic processes in general. Catabolic processes in contrast were generally upregulated. However, a detailed view discloses a more nuanced picture.

Phagocytosed yeasts (main response between 0.25d – 2d) as well as the long-term controls showed signs of an upregulation of the glycolysis/gluconeogenesis-driving 6-phosphofructo-2-kinase/fructose-2,6-bisphosphate 2-phosphatase activity in comparison to YPD log growth (e.g. increased transcript levels of orthologues of *S. cerevisiae* PFK26 and FBP26; Suppl. Tables 7 + 8). This would allow the fungus increased control over and fast switching between glycolysis and gluconeogenesis. However, only the gluconeogenesis orthologues *PCK1* (CAGL0H06633g) and *FBP1* (CAGL0H04939g) were upregulated vs YPD log growth in hMDMs at all time points and in long term controls (Suppl. Table 7), indicating that fungal gluconeogenesis takes place within the phagosome. In support of that, genes annotated with the GO terms “tricarboxylic acid cycle”, “glyoxylate cycle” and “2-methylcitrate cycle” were enriched at

all time points for hMDM phagocytosed yeast and long-term controls, while genes of the pentose phosphate shunt showed no marked regulation in hMDMs (Suppl. Table 8). Genes related to aerobic respiration were induced in all hMDM time points in comparison to logarithmic growth (Suppl. Table 8).

Mobilization of storage carbohydrates is indicated by a consistent upregulation of trehalose utilization genes at all time points in hMDMs and long-term cultures vs logarithmic growth (Suppl. Tables 7 + 8). However, late in hMDM interaction (7d) the opposite GO term, “trehalose biosynthetic process”, was also enriched among upregulated genes and two long-term conditions (Suppl. Tables 7 + 8). Among the three *C. glabrata* genes which are putatively involved in glycogen degradation (*GPH1*, *GDB1*, and *SGA1*), only the gene for the glucoamylase, *SGA1*, was consistently upregulated in hMDMs (and in the long-term controls; Suppl. Table 7). Interestingly, in *S. cerevisiae* transcription of *SGA1* is sporulation-specific (Colonna and Magee 1978; Clancy, Smith, and Magee 1982) which suggest differences in the regulation between *C. glabrata* and baker's yeast for this enzyme. However, deletion of *SGA1* had no major effect on persistence of *C. glabrata* in hMDMs (Suppl. Table 3).

Genes involved in lipid degradation were consistently upregulated in hMDMs at all time points (as well as in long-term controls) compared to log growth in YPD (Suppl. Table 8). Accordingly, GO terms indicating lipid biosynthetic processes were associated with downregulated genes, especially in the YNB and RPMI long-term control conditions and in hMDM after 1d (but less so at 7d; Suppl. Table 8).

Genes involved in autophagic processes, especially mitophagy, were enriched among the upregulated genes for all time points within macrophages and during long-term cultivations, with the latter showing the higher upregulation in direct comparison with the 7d hMDM time point (Suppl. Table 8). GO terms like “protein localization to vacuole” and “protein localization by the Cvt pathway” showed similar patterns (Suppl. Table 8) which together with the upregulation of some genes involved in “endosome” and “late endosome” (compared to YPD log growth) could represent the attempt to acquire nutrients by uptake of extracellular macromolecules and shuttling of nutrients into the vacuole (Suppl. Table 8).

In general, ion homeostasis showed no marked up- or downregulation for all hMDM time points in relation to YPD log growth. Among the long-term controls, only RPMI with serum showed a clear upregulation of genes involved in iron ion homeostasis compared to logarithmic growth (Suppl. Table 8). RPMI with serum also was the only condition where

the genes for the iron homeostasis regulator, *AFT1* (Gerwien *et al.* 2016), and for the high-affinity iron uptake transporter, *FTR1* (Sharma, Purushotham, and Kaur 2016), (Suppl. Table 7) were upregulated. In contrast, *SEF1*, encoding a regulator of iron-consumption processes (Gerwien *et al.* 2016), and *CCC1*, coding for a putative vacuolar iron importer (Sharma, Purushotham, and Kaur 2016) were consistently upregulated in hMDMs and in the long-term controls (Suppl. Table 7).

As expected, several GO terms describing the stress response against oxidative stress were upregulated in hMDMs compared to YPD log growth, especially at early time points (Suppl. Table 8). This indicates a significant antimicrobial response by the human macrophages in the form of oxidative stress.

Single mutant tests resemble the screening results

Pool experiments always bear the risk of unpredictable interactions among the tested strains. To get a better insight whether the pool mutant screening data is valid for single mutants in interaction with macrophages, we created single deletion mutants in an independent, non-auxotrophic background. Three representative genes with different phenotypes of their mutants were chosen, ranging from strong depletion at day 7 (Δ*ssd1*: mean recovery 0.01), intermediate depletion (Δ*she10*: 0.31) to minor depletion (Δ*dit2*: 0.43) compared to their triple-auxotrophic background strain (Suppl. Table 3 and Fig. 5 + 10). Despite their independent creation, the newly created strains Δ*ssd1* and Δ*she10* exhibited a nearly identical survival as their pool mutant counterparts (Fig. 10). The already minor phenotype of Δ*dit2* was however not reproducible with the newly created strain (Suppl. Fig. 6), indicating that robust, but maybe not subtle, pool phenotypes can translate into single strain behaviour. We therefore considered, in this manuscript, only mutants with a recovery (at seven days) of less than 0.35 (0.5 for pool 16) as “depleted” for the sake of our pool experiments and analysed the two mutants, Δ*ssd1* and Δ*she10*, in more detail.

To test whether *SSD1* and *SHE10* play a general role in long-term survival of *C. glabrata*, we incubated mutants lacking these genes for seven days in YNB pH 6 medium and tested survival by cfu plating. Cfu counts of the wild type declined to around 58% of the inoculum; the Δ*she10* mutants showed a similar decline, while the two Δ*ssd1* mutants showed a much more pronounced decline to less than half the wild type survival (40 % and 43 % of wild type levels, Fig. 10). Therefore, *SSD1* seems to be necessary for long-term survival of *C. glabrata*.

Transcriptional responses of *C. glabrata* Δ*she10*

The gene *SHE10* is not characterized yet in *C. glabrata*, while its *S. cerevisiae*

orthologue is known to encode a protein involved in the assembly of the outer spore wall, with a likely function in the assembly of the dityrosine layer (Lin *et al.* 2013). To unveil the function of *C. glabrata* She10, we performed microarray analyses of the Δ*she10* mutant both during logarithmic growth and after seven days in YPD, reflecting the controls we used for the hMDM persistence experiment. The Δ*she10* mutant did not show any marked differences in overall gene regulation during YPD log growth compared to the wild type, consistent with either a redundant or negligible role of She10 under optimal growth conditions (Suppl. Table 9). Only during long-term incubation in YPD, the wild type and the Δ*she10* mutant show differences in their transcriptional profiles (Suppl. Table 9). GO terms of upregulated genes in the Δ*she10* mutant generally relate to transport (Suppl. Tables 10 + 11), while downregulated genes show patterns of a general reduction of gene expression and endoplasmic reticulum (ER) function (e.g. "(protein O-linked) glycosylation" and "ergosterol biosynthetic process"; Suppl. Table 11). This might indicate that She10 plays a role in ER organization. Such a role would fit with the deletion mutant data of the hMDM persistence model, as strains lacking genes with roles in ER functions (protein glycosylation, unfolded protein response) and in the downstream secretory pathway were frequently detected in this screen.

Discussion

With this work we addressed the question whether *C. glabrata* can persist within macrophages as a possible lifestyle in the host? Furthermore we questioned whether such a lifestyle would affect antimycotic treatment of *C. glabrata*, which, consequently, would have implications for the clinical situation. Most importantly, we aimed to unravel the characteristics of such a long-term interaction and to identify fungal factors which are critical for intracellular persistence. To do so, we established an in vitro model of intracellular *C. glabrata* persistence.

Establishment of a long-term *C. glabrata*-macrophage interaction model

The possibility that *C. glabrata* can replicate and reside within macrophages for several days during infection has been considered for long (Otto and Howard 1976; Kaur, Ma, and Cormack 2007; Roetzer *et al.* 2010; Seider *et al.* 2011; Kasper, Seider, and Hube 2015). There are, however, currently no models available that can imitate such long term host-pathogen interactions for in-depth investigations . Here, we established the first model (to our knowledge) to investigate intracellular persistence of *C. glabrata* within human monocyte-derived macrophages (hMDMs). With our *in vivo*-like experimental parameters, like the presence of human serum, our model strikes a balance between hindering extracellular yeast overgrowth via evasion or escape from macrophages and

obtaining sufficiently high cfu numbers for downstream experiments. With the exception of the transcriptional analysis, which required high numbers of yeasts, it was not necessary to employ any antimycotic treatment to remove extracellular yeasts. In this "standard *C. g.* – hMDM persistence model", yeast cfus decline rapidly during the first day, which is followed for the next days (up to a week) by a macrophage donor-dependent progress ending either in stable cfu counts or a further decline (Fig. 3A). Superficially, this seems to contradict previous publications describing the high potential of *C. glabrata* to survive and replicate within the phagosome of macrophages in vitro (Otto and Howard 1976; Kaur, Ma, and Cormack 2007; Seider *et al.* 2011; Kasper, Seider, and Hube 2015). We suggest that the conditions in our model allow the human macrophages to more efficiently control or kill phagocytosed yeasts than previous models (as indicated by the initial steep decline in cfu). *C. glabrata* then probably continues to replicate inside macrophages at a low rate, likely more comparable to the *in vivo* situation, leading to a mostly steady equilibrium of replication and killing. It is noteworthy that the generally non-pathogenic baker´s yeast *Saccharomyces cerevisiae* is not able to replicate inside macrophages even in "classical" *in vitro* models (Seider *et al.* 2011), while *C. albicans* is able to kill macrophages by hyphal outgrowth within hours (de Brabander *et al.* 1980; Westman *et al.* 2018). Clearly, *C. glabrata* differs from both these related fungi in its interaction with human macrophages, and future studies may reveal which host factors are critical to control the switch between intracellular *C. glabrata* persistence and replication.

Influence of antimicrobial treatment on *C. glabrata*-macrophage long-term interaction

With this persistence model available, we tested the influence of antimycotic administration of clinically relevant antimycotics after intracellular *C. glabrata* ingestion, which may affect persistence in a clinical situation. We observed additional killing of intramacrophagal yeasts by antimycotics after seven days. This is in accordance with previous data on non-persisting yeasts where such combined macrophage-antimycotic action was observed at earlier time-points (Baltch *et al.* 2005; Bopp *et al.* 2006; Baltch *et al.* 2008) although these previous models allowed intra- and extramacrophagal proliferation. Both antimycotics used in this study (caspofungin and amphotericin B) failed, however, to completely eradicate intracellular *C. glabrata*. This provides evidence that intracellular persistence of *C. glabrata* within macrophages is possible despite antifungal treatment and therefore might be of relevance in a clinical treatment scenario.

Genes and processes needed for persistence of *C. glabrata* in human MDM´s

The potential clinical relevance of a *C. glabrata* persistent state within macrophages

motivated us to study this long-term interaction in more detail. Our data supported the prevalent notion of the phagosome as a nutrient-limited and stressful environment (Kaur, Ma, and Cormack 2007; Roetzer *et al.* 2010; Rai *et al.* 2012; Kasper, Seider, and Hube 2015). We found biosynthesis and the transcriptional and translational machineries to be generally downregulated, which indicates a cell cycle arrest. This matched the mutant screen findings that important energy homeostasis regulators show early or late-stage depletion after phagocytosis.

Unsurprisingly, the *C. glabrata* transcriptome within hMDMs showed signs of a classical response to oxidative stress, and also disposal of damaged organelle parts: in agreement with a previous study, (Roetzer *et al.*, 2010), autophagy of mitochondria was a strongly enriched functional category, likely due to damage by ROS formation in the respiratory chain. The amplitude of the response towards exogenous oxidative stress declined over time which indicates that either the generation of intraphagosomal ROS was not kept up at full level and/or that *C. glabrata* adapted sufficiently to be protected without further up-regulation.

C. glabrata´s *cell wall in the long-term interaction with macrophages*

The cell wall plays a central role in host-fungus interactions and can influence the immunological reaction of phagocytes (Gow, Latge, and Munro 2017; Hünniger and Kurzai 2019) while it is itself under severe attack inside the phagosome, which requires efficient cell wall repair responses. The approaches used by us limit the analysis of this aspect somewhat: we had to use a cell wall-affecting antimycotic in our transcriptome experiment, and the cytokine response of macrophages in the pool experiments reflect the response to a mixture of strains. Nevertheless, in accordance with previous studies (Kaur, Ma, and Cormack 2007; Rasheed, Battu, and Kaur 2018) we found that *C. glabrata* initiates and needs active cell wall remodelling in response to macrophage internalization. This includes transcriptional upregulation of gene associated with cell wall integrity, cell wall-regulating MAP kinase pathways, and the redirection of cellular resources towards cell wall repair and biosynthesis. Furthermore, severely depleted mutants in hMDM persistence included mutants lacking genes encoding proteins of the cell wall integrity pathway (Bck1, Mkk1, Slt2). Interestingly, this was not the case for genes coding for proteins of the cell integrity-controlling calcineurin pathway (*CNA1*, *CNB1*, *RCN1*, *CRZ1*; Suppl. Table 3). In summary, specific cell wall repair processes are required for persistence of *C. glabrata* in macrophages.

Where does the energy come from in the phagosome?

C. glabrata reacts to the nutrient limitation within the phagosome by a mobilization of energy storages, e.g. through upregulation of autophagy (shown to be important previously by (Roetzer *et al.* 2010; Rai *et al.* 2015; Chew *et al.* 2019)), carbohydrate and lipid utilization as well as of certain amino acid degradation pathways (Suppl. Table 8). Glucose production is also indicated by activation of the glyoxylate and 2-methylcitrate pathways, regulation of gluconeogenesis and glycolysis flux rates via fructose-2,6-bisphosphate levels as well as high expression of specific gluconeogenic genes (Kaur, Ma, and Cormack 2007; Rai *et al.* 2012). Interestingly, together with the phenotype of the Δ*pfk1* mutant, this would mean that two contrasting metabolic pathways are important for intraphagosomal yeast survival, glycolysis (*PFK1*, mutant depleted from early time points on) and gluconeogenesis (*PCK1*, mutant depleted at late time points). The differences of their depletion kinetics may be a hint to differing contributions to survival – e.g., while glucose availability within the phagosome is thought to be limited for fungal pathogens (Sprenger *et al.* 2018), glycolysis could be important to quickly mobilize energy from the active glycogen and trehalose utilization pathways to withstand suddenly occurring stresses. Alternatively, *PFK1* may be required for the return from an induced quiescent state inside the macrophages (Laporte *et al.* 2011). Gluconeogenesis could be needed (in later stages) to maintain a constant pool of sugar skeletons for cell wall repair or synthesis and/or for the NADPH-regenerating oxidative pentose phosphate pathway. The importance of gluconeogenesis for engulfed *C. glabrata* yeasts has also been suggested by earlier transcriptomic findings (Kaur, Ma, and Cormack 2007). While the deletion of the upregulated malate dehydrogenase gene *MDH2* led to no marked phenotype (Suppl. Table 3) despite its function in gluconeogenesis of *S. cerevisiae* (Gibson and McAlister-Henn 2003), both *C. glabrata* and *S. cerevisiae* encode three malate dehydrogenases with potential functional redundancies. In summary, the results show a reliance of *C. glabrata* on gluconeogenesis in macrophage persistence.

In agreement with previous studies (Kaur, Ma, and Cormack 2007; Rai *et al.* 2012), *C. glabrata* genes involved in β-oxidation were upregulated in direct response to macrophage engulfment, and we here show that that these genes remain upregulated also during long-term interaction. A deletion mutant of *OAF1*, whose orthologous gene in *S. cerevisiae* is a transcriptional activator of β-oxidation and peroxisome genes, was found depleted after 7d in hMDM persistence and might therefore be an important regulator in this context. In addition to fatty acids, β-oxidation can enable the use of acetate, and interestingly *C. glabrata* strongly induces genes coding for putative acetate transporters and one of its two putative Acetyl-CoA synthetases. Based on our data, it is not possible to tell which carbon source (acetate or fatty acids) is used, and whether it is

derived from internal sources or the phagosome. We did detect an up-regulation of genes annotated with the GO terms “lipase activity” and “phospholipase activity”, but our available mutants and transcriptional data did not provide clear evidence that *C. glabrata* feeds on exogenous lipids within the phagosome. One problem may be functional redundancy: for example, a *C. glabrata* phospholipase double mutant (Δ*plb1*Δ*plb2*) is known to persist less within abscesses in a murine model of intra-abdominal candidiasis while single deletion mutants showed wild type like behaviour (Cheng *et al.* 2014). Our single deletion mutants of such genes showed no marked phenotype (Suppl. Table 3), but our data shows that future investigations into the role of (phospho)lipases may prove to be very fruitful.

Finally, engulfed yeast cells do not completely shut down the flux through nitrogen-containing metabolic pathways: While our transcriptional data proves again that gene expression is immediately restricted after uptake by macrophages (Lorenz, Bender, and Fink 2004; Kaur, Ma, and Cormack 2007), *C. glabrata* seems to maintain constant low-level translation during persistence in hMDMs.

Iron metabolism

Contrary to the expectation of the phagosome being actively depleted of iron, we did not find any direct signs of iron restriction with our hMDM persistence model. Neither was the high-affinity iron uptake significantly regulated, nor did we observe a phenotype for deletion mutants of the vacuolar iron im- and exporter genes *CCC1* and *FTH1* (Gerwien *et al.* 2016). However, deletion of *HAP2*, *HAP3*, *HAP5* and *FET3* led to a marked depletion in the hMDM mutant screen within seven days (Fig. 7, Suppl. Table 3). Hap2, Hap3 and Hap5 are part of the CCAAT-binding factor complex which is active under iron replete conditions (Thiébaut *et al.* 2017), and Fet3 putatively encodes a copper ferroxidase involved in high-affinity iron uptake (Sharma, Purushotham, and Kaur 2016). However, such a counter-intuitive lack of an iron starvation response by *C. glabrata* has recently been observed in a human blood infection model (P. Kämmer *et al.*, mBio, accepted), where other *Candida* species exhibited a strong transcriptional signal of iron restriction. It may therefore represent a unique strategy of *C. glabrata* during host interactions.

Does C. glabrata *enter a quiescent state during persistence in hMDMs?*

The conditions *C. glabrata* faces within the phagosome like nutrient limitation and oxidative stress are well known to initiate cellular quiescence in other environments. In addition, the yeast´s reaction encompassing e.g. autophagy, alternative carbon source utilization, cell cycle arrest, decreased translation and putatively enhanced aerobic respiration, resembles processes frequently described to be associated to quiescence

(for a review see (Valcourt *et al.* 2012; Sagot and Laporte 2019)). Furthermore, a number of the deletion mutants identified within our screen is involved in the establishment, maintenance or exit from quiescence like e.g. mutants of the cAMP-PKA pathway, the Snf1 kinase pathway, the cell wall integrity pathway, Ssd1, the Rpd3 complex (Toda *et al.* 1985; Thompson-Jaeger *et al.* 1991; Herman 2002; Gray *et al.* 2004; De Virgilio 2012; McKnight *et al.* 2015; Miles and Breeden 2017; Miles *et al.* 2019). The same is likely true for some of the other chromatin modifying factors we identified, given the central roles of chromatin silencing for quiescence establishment and (most likely) of Acetyl-CoA levels for the decision to enter quiescence (Kuang, Ji, and Boeke 2018); and finally potentially Pfk1 (Laporte *et al.* 2011). However, the concept of quiescence encompasses a broad diversity of cellular states and their realizations also depend on the actual trigger for quiescence (Sagot and Laporte 2019). Although quiescence is thought to convey in general enhanced stress resistance (Valcourt *et al.* 2012), not all of these states might be compatible with survival within a macrophages phagosome, since a minimum of reaction ability might be required to counter the macrophage stressors. We would suggest that the main *C. glabrata* population in our hMDM persistence model cycles between quiescence and cell division since we expect that *C. glabrata* actually does have access to exogenous nutrient supply, although in a limited amount which slows down the yeast´s growth rate, but nevertheless should allow constant growth. This assumption is supported by previous *C. glabrata*-macrophage models where *C. glabrata* replicates rapidly within the phagosome (Otto and Howard 1976; Kaur, Ma, and Cormack 2007; Roetzer *et al.* 2010; Seider *et al.* 2011), an observation which cannot be solely explained by reliance on internal energy storages. Furthermore, our transcriptome data supports this view since we found (1) that S-phase regulating and DNA replication genes were initially strongly repressed (1d), but converge towards the levels reached at logarithmic growth conditions at the later time points (7d) and (2) that the shutdown of central cellular processes like (aspects of) translation can be much more pronounced or realized in a different manner under different conditions, like within the YNB 7d control. Regarding quiescence, there are some interesting questions remaining: (1) to what extent is the re-induction of the yeasts cell cycle dependent on the macrophage status and the amount of stress exerted by it over time? It is noteworthy that the levels of proinflammatory cytokines which may promote a more effective antifungal macrophage response constantly decline within our model and that this correlates with re-induction of the yeasts' cell cycle. (2) Does the surviving *C. glabrata* population under antimycotic treatment within macrophages represent the equivalent of a “persister population” under antimycotic treatment without macrophages? This would mean that these cells are in a more pronounced quiescent state, and they may possess typical characteristics like an

altered cell membrane composition and a strengthened cell wall. In general, it is assumed that successful antimycotic treatment in the clinic relies on the effect of the antifungal therapy in combination with the ability of the patient's immune system to eradicate fungal persister cells (Lewis 2010; Bojsen, Regenberg, and Folkesson 2017). In summary, while the intracellular *C. glabrata* population clearly adopts quiescence characteristics, the surviving mechanisms of the persistent yeast cell population in our model especially under antimycotic treatment requires further investigations, as well as the conditions which must be fulfilled that such an intracellular state can be established.

C. glabrata *initiates a transcriptional mating response inside macrophages*

One unusual finding was that long-term incubation, especially within hMDMs, seems to trigger a mating-like transcriptional response in *C. glabrata*. There is a precedent in a distantly related fungus: For *Cryptococcus neoformans* a transcriptional mating response is triggered after 24 h in the phagosome (Fan *et al.* 2005). Induction of mating genes could therefore represent a conserved response of fungal pathogens to prolonged exposure to macrophage phagosomes. In general, the induction of mating is induced in some yeast species by nutrient limitation and / or stress (Bernstein and Johns 1989; Mochizuki and Yamamoto 1992; Miyata *et al.* 1997; Davey 1998; Dumitru *et al.* 2007; Huang *et al.* 2009; Alby and Bennett 2009; Barsoum, Rajaei, and Åström 2011), the situation present in phagosomes. A *C. glabrata* clade analysis suggests that it is able to mate (Carreté *et al.* 2018) despite a lack of direct observation, and it can be assumed that *C. glabrata*, like other yeast species, links the decision to mate to a non-beneficial environment. However, deletion mutants of parts of the mating pathway or its associated effectors were mainly unchanged in survival, with the exception of Δ*ste12* and Δ*ste50*, both of which also take part in other signalling pathways. For the moment, whether mating type switching (or even mating) happens within phagosomes remains elusive – and if yes, it is unclear whether it provides any advantage or constitutes an "accidental" reaction to the environment. While intraphagosomal mating of the descendants would not increase genetic diversity, one or the other mating type, or a hypothetical diploid, may still be intrinsically more resistant to the stress inside the phagosome.

SHE10 *is necessary for long-term persistence of* C. glabrata *in hMDMs and likely functions in the ER*

SHE10 was of interest to us since the deletion mutants showed a medium-level depletion in macrophages. In *S. cerevisiae*, the orthologous gene product and its paralog *OSW7* were shown to be involved in the assembly of the dityrosine layer, a part of the outer spore wall (Lin *et al.* 2013). As such, it had potential connections to the mating program and the resistance properties of the cell envelope. A large-scale localization study in

S. cerevisiae found She10 and Osw7 in the ER (Yofe *et al.* 2016), and an in silico study suggested that *S. cerevisiae* She10 carries a GPI anchor (De Groot, Hellingwerf, and Klis 2003). In *C. glabrata*, She10 and Osw7 are both present despite *C. glabrata´s* tendency to eliminate redundant genes (Brunke and Hube 2013), and both were identified within a membrane-enriched proteome sample (Pais *et al.* 2016), but not in the secretome (Rasheed, Kumar, and Kaur 2020). The *C. glabrata* protein is also predicted to have an N-terminal signal peptide for ER localization (Suppl. Fig. 7). Our transcriptome analysis of a Δ*she10* mutant showed only few differences to the wild type during long-term incubation in YPD, mostly related to the ER stress response. Our attempts to detect signs of a (spore-independent) dityrosine layer deposition were inconclusive (data not shown). The precise function and basis for the protective effect of She10 inside macrophage phagosomes therefore remains elusive. Based on our data we however suggest that *Cg*She10 (and possibly *Cg*Osw7) might play a function within the secretory pathway; e.g. in control of protein localization or quality of protein glycosylation. A similar role is also possible for its *S. cerevisiae* counterpart, the precise function of which is also still unclear.

SSD1 *is necessary for short- and long-term survival in response to multiple stressors*

The deletion of *SSD1* had a striking effect on survival in macrophages, which was confirmed by an independently constructed mutant in a different background. In contrast to *SHE10*, *SSD1* is well-characterized in *S. cerevisiae*: It encodes an mRNA-binding protein which, in dependency of its phosphorylation state, can act as translational repressor or mediator of polarized mRNA localization (Uesono, Toh-e, and Kikuchi 1997; Shepard *et al.* 2003; Hogan *et al.* 2008; Jansen *et al.* 2009; Kurischko, Kim, *et al.* 2011; Kurischko, Kuravi, *et al.* 2011; Wanless, Lin, and Weiss 2014). It is therefore involved in a broad variety of functions like regulation of cell wall integrity, transcription, cellular aging, transition into quiescence, and protein homeostasis (Stettler *et al.* 1993; Kaeberlein *et al.* 2004; Reinke *et al.* 2004; Jansen *et al.* 2009; Mir, Fiedler, and Cashikar 2009; Li *et al.* 2009; Kurischko, Kim, *et al.* 2011; Li *et al.* 2013; Miles *et al.* 2019). Ssd1 has a preference for a specific subset of mRNAs, including cell wall protein-encoding mRNAs (Hogan *et al.* 2008; Jansen *et al.* 2009). At least one of them is delivered by Ssd1 to sites of polarized growth for subsequent translation, which is enabled by Cbk1-mediated inhibition of Ssd1´s repressor function (Kurischko, Kim, *et al.* 2011). Upon stress or on entry into the stationary phase which is accompanied by release of Ssd1 from Cbk1-mediated inhibition, Ssd1 delivers the mRNAs instead to accumulating P-bodies where they are either stored or degraded (Holmes *et al.* 2004; Brengues, Teixeira, and Parker 2005; Jansen *et al.* 2009; Kurischko, Kim, *et al.* 2011). Ssd1 can also affect the stability of non-Ssd1 bound mRNAs (Jansen *et al.* 2009; Li *et al.* 2009). Thereby,

Ssd1 controls when and where cell wall growth and remodelling takes place, but also mediates global gene expression (Stettler *et al.* 1993; Hogan *et al.* 2008; Jansen *et al.* 2009; Li *et al.* 2009; Kurischko, Kim, *et al.* 2011). This central place in cell wall integrity is certainly linked to its role in conferring resistance against host-derived antimicrobial peptides in *C. albicans* (Gank *et al.* 2008; Jung *et al.* 2013).

Based on our data and the role of Ssd1 in *S. cerevisiae*, we suggest that *C. glabrata* Ssd1 plays a role in the transition to quiescence after uptake by macrophages. The recruitment and degradation of mRNA coding for growth processes is most likely a central step in adapting to the phagosome environment. In fact our data shows a fast decrease in mRNAs coding for components of the ribosome – a process which is among the targets for Ssd1 in baker's yeast (Li *et al.* 2009). In accordance with this hypothesis, transcription of *SSD1* was upregulated in hMDMs and during long-term stationary phase, compared to log growth (Fig. 10). Finally, a *C. g.* Δ*ssd1* strain was also found depleted in our previous pool experiments in systemically infected mice and in a fruit fly model (Brunke *et al.* 2015). In conclusion, Ssd1 seems to play a similar central role in *C. glabrata* as described in *S. cerevisiae* in conferring stress resistance, and especially so for the long-term persistence in macrophages and in vivo.

Material and Methods

Ethics statement

Blood was obtained from healthy human volunteers with written informed consent according to the declaration of Helsinki. The blood donation protocol and use of blood for this study were approved by the Jena institutional ethics committee (Ethik-Kommission des Universitätsklinikums Jena, Permission No 2207–01/08).

Yeast strains and growth conditions

If not stated otherwise, *C. glabrata* strains were routinely streaked on YPD (1% yeast extract, 2% peptone, 2% glucose, pH 7) agar and incubated one day at 37 °C (*C. albicans* SC5314 two days at 30 °C). Yeast colonies on plates were stored at 4 °C for up to one month. Yeast cultures were routinely grown overnight in YPD (1% yeast extract, 2% peptone, 2% glucose, pH ≈ 7) at 37 °C (*C. glabrata*) or 30 °C (*C. albicans*) with shaking (180 rpm). For an overview of *C. glabrata* strains used within this study, see Suppl. Tables 1 + 12.

For long-term incubation (7d) under carbon source limitation, overnight cultures of *C. glabrata* strains were pelleted, washed twice with sterile dH_2O (centrifugation 1 min 5,000 g), adjusted to 10^6 yeast cells/mL in YNB pH 6 in a total volume of 50 mL, and incubated for seven days at 37°C with shaking (180 rpm). Inoculum and seven day

samples were diluted to appropriate concentrations and plated for subsequent cfu counting (4 technical replicates per time point and mutant).

Lysis of *C. glabrata* infected macrophages for yeast plating (24 well plate)

After removal of supernatant and optionally two further washing steps for removal and separate plating of extracellular yeast, macrophages were lysed by addition of either 0.5% Triton-X-100 (100 µL per well) or 0.05% Triton-X-100 (1 mL per well) and incubated 15 min with light shaking (≤ 30 rpm). Then, an additional volume of dH_2O or PBS was added, the well content mixed with a pipette and transferred to a falcon or Eppendorf tube. Optionally, each well was washed twice and the washing fluid was added to the lysate to obtain a total count. Appropriate dilutions were plated onto YPD agar plates, incubated for 24 hours at 37°C and optionally stored until examination or further processing at 4°C.

***C. glabrata*-macrophage persistence model**

Differentiation of human monocytes into human monocyte-derived macrophages (hMDMs)

Preparation of hMDMs was performed as described before (Sprenger *et al.* 2020) based on selection of monocytes by magnetic automated cell sorting of CD14 positive monocytes and a differentiation period of seven days. Adherent hMDMs were detached with 50 mM EDTA in PBS and seeded in RPMI supplemented with 2 mM glutamine + 10% fetal bovine serum (FBS, Gibco) + 50 ng/mL M-CSF (ImmunoTools) (if not stated otherwise: 1.5×10^5 MDMs per well in a 24 well plate) and incubated overnight. Incubation of hMDMs was always performed at 37°C and 5% CO_2. Before infection with *C. glabrata*, the previous medium was removed, hMDMs were washed once with PBS, and RPMI + 10% human serum (from AB male donors; sterile-filtered, Bio&Sell) was added.

Mutant pool experiments

Barcoded *C. glabrata* strains from YPD agar were used to inoculate 500 µL YPD in 2 mL safe-lock Eppendorf tubes per culture. These were incubated for at least 17 hours at 37°C with shaking (180 rpm). Pools of *C. glabrata* mutants were prepared by mixing individual cultures in a one-to-one ratio based on OD_{600} measurements and stored on ice until use (see Suppl. Table 1 for mutant pool compositions). The *C. glabrata* pools were pelleted, washed twice with PBS (centrifugation 5 min 4,248 g) and finally resuspended in 5 mL PBS. The pools were adjusted with RPMI to 1.05×10^7 yeast cells/mL. An appropriate dilution was used for plating the inocolum onto YPD agar (seven plates of 2,000 cfus each per pool).

hMDMs were infected with *C. glabrata* mutant pools (MOI 7, 100 µL yeast solution) and

incubated 3h before extracellular yeasts were removed by washing twice with sterile PBS, after which 1 mL fresh medium was added. From wells intended for seven days co-incubation, 0.5 mL of supernatant was removed after one day and 1 mL fresh medium was added (total volume 1.5 mL). On each following day, 0.5 mL was replaced with fresh medium. All wells were constantly checked for appearance of yeast microcolonies by naked eye. Before macrophage lysis and yeast plating, each well was systematically checked for extracellular yeasts with an inverse microscope, and only wells that met the cut-off criteria (compare Fig. 2) were used for plating.

For plating after one and seven days of co-incubation, the supernatant was discarded and macrophage lysates were used. The yeast concentration was adjusted to obtain seven plates with ≈2,000 colonies each by stepwise dilution. For the seven days' time-point, six wells were prepared per pool and per biological replicate. The intact wells (i.e. no microcolonies) were used for plating, aiming again for ≈2,000 colonies per plate. Colony counts were determined with an automated colony counter (protoCOL 3, Synbiosis) to ensure sufficiently high numbers to cover all individual mutants. Yeast colonies from all YPD agar plates that had not substantially more than the expected 2,000 colonies were scraped, dissolved in PBS and pooled per pool for DNA isolation (Brunke *et al.* 2015).

Single mutant tests

For the preparation of yeast inocula, overnight cultures of *C. glabrata* strains were pelleted, washed twice with sterile dH_2O (centrifugation 1 min 5,000 g) and adjusted to 1.5×10^6 yeasts/mL with sterile dH_2O and briefly stored at room temperature if required. The single mutant test procedure deviated from the mutant pool only in its MOI of 1 (100 µl suspension) and an additional plating at three hours. The inoculum solution was diluted as independent quadruplicate samples. For the time points, four individual wells of infected hMDMs were plated individually. After three hours, the pooled supernatant and PBS used for washing were plated in addition to the lysate. At one and seven days, the supernatant was removed without washing, and the hMDMs lysed and plated. Cfu counts on YPD agar plates were determined manually.

Cytokine measurements

Samples were treated as during the single mutant test. The supernatants of two wells per biological replicate were gently mixed, precipitates removed by centrifugation (10 min 10.000 g), and stored in aliquots at -20°C until use. Medium without supplements served as negative control, and LPS (at 100 ng/mL) and *C. albicans* SC5314 (MOI 1, up to one day) were used as positive controls. Quantification of cytokines was performed by Enzyme-linked Immunosorbent Assay according to the manufacturer's instructions

(Ready-SET-Go! ELISA; Thermo Fisher Scientific).

Transcriptome analysis

For transcriptomes, 4.2×10^6 or 9.8×10^6 hMDMs were seeded in 75 cm^2 or 175 cm^2 cell culture flasks (Greiner), respectively, and incubated for two days. *C. glabrata* ATCC2001 overnight cultures were pelleted, washed twice with dH_2O (centrifugation 5 min 4,248 g), dissolved in RPMI (storage on ice from this point on), and adjusted to 5×10^8 yeast cells/mL with RPMI. An aliquot of the adjusted yeast solution stored on ice was taken as "time point zero". hMDMs were infected after media exchange, but with an MOI of 20 and incubated for three hours before extracellular yeasts were removed by washing twice with sterile PBS, and 9 mL (75 cm^2) or 20 mL (175 cm^2) fresh media was added. Caspofungin was added after six hours and added to keep a (theoretical) level of 5 µg/mL. For prolonged co-incubation, another 9 mL (75 cm^2) or 20 mL (175 cm^2) fresh medium was added after one day. The same volume was replaced daily with fresh medium. Samples were taken after 6 hours and one, two, four and seven days.

For media transcriptomes, *C. glabrata* overnight cultures were pelleted, washed twice with dH_2O (centrifugation 5 min 4,248 g), and adjusted to OD_{600} = 0.1 in YPD or RPMI + 10% human serum or to OD_{600} = 1 in YNB pH 6. YPD and YNB pH 6 cultures were incubated at 37°C with shaking (180 rpm) in Erlenmeyer flasks. RPMI + 10% human serum cultures remained stationary in 175 cm^2 cell culture flasks at 37°C with 5% CO_2. Samples were taken during log-growth phase in YPD (OD_{600} = 2-4) and after seven days of incubation for all media.

RNA was isolated using a modified freeze-thaw protocol (Lüttich, Brunke, and Hube 2012). hMDMs were first lysed in AE buffer + 10% SDS to remove human DNA and RNA by centrifugation (2 min, 12,000 g, 4°C). The yeast pellet(s) was frozen in liquid nitrogen. β-mercaptoethanol was used at a final concentration of ≈5% in AE buffer for yeast resuspension. Cy5-labeled cRNA (Cy5 CTP; GE Healthcare) was generated using the QuickAmp Labeling Kit (Agilent). Samples were co-hybridized with a common Cy3-labeled reference (RNA from mid-log phase grown *C. glabrata* ATCC2001) on Agilent arrays (8-by-15K format), scanned in a GenePix 4200AL with GenePix Pro 6.1 (Auto PMT, pixel size 5 µm) and analysed with GeneSpring 14.8 (Agilent) and Revigo (Supek *et al.* 2011).

C. glabrata mutant generation

The barcoded reference strains H-BC (ATCC2001 Δ*his3* (REF)) and BC (ATCC2001 (REF)) as well as the strains for the single mutant tests (ATCC2001 Δ*ssd1*, ATCC2001 Δ*dit2*, ATCC2001 Δ*she10*) were generated using the TEF1P-NAT1-TEF1T marker cassette originating from pJK863 (Shen, Guo, and Köhler 2005) used in the previous

study for construction of mutants in the ATCC2001 Δ*his3* Δ*leu2* Δ*trp1* background [compare Suppl. Table 3 in reference] (Schwarzmüller *et al.* 2014). All reference (REF) strains contain individual barcodes. For detailed information on strain construction, see Suppl. Method 1.

Pool experiments: barcode amplification, next generation sequencing and data analysis

PCR and PCR fragment purification

Amplicons of ≈150 bp containing up and down barcodes were generated from isolated gDNA with Phusion HighFidelity DNA polymerase (NEB) (detailed program in Suppl. Method 2). The primers added 10 bp of experiment-specific sequence on each side (Fig. 4, Suppl. Fig. 8) to allow multiplexing (see Suppl. Table 2 for primer sequences). The same primer pairs were used for replicates and samples for direct comparisons to ensure identical amplification efficiencies. Pool 16 mutants required a different primer set due to their alternative NAT1 cassette (Schwarzmüller *et al.* 2014). PCR fragments were purified using the QIAquick PCR purification Kit (Qiagen, Cat. No 28106) and their concentration determined with a Nanodrop^{R} ND-1000 spectrophotometer (PEQLAB). The purified amplicons were pooled at 150 ng each, these libraries again purified and quality assured by Nanodrop measurement and gel electrophoresis.

Sequencing

The libraries were paired-end sequenced on an Illumina sequencing platform (GATC). Amplicon sequences were sorted by their experiment- and mutant-specific barcodes using a local BLAST search against the expected barcode regions. Data were normalized as described in the text and Suppl. Table 3 (see description). Cut-offs for definition of mutant depletion were set slightly different in dependency of the normalization method (parent or median) used. If not stated otherwise, cut-off and corresponding p-values refer always to the fulfilment of the criteria by at least one barcode. Mean recovery values represent combined recovery values of Up and Down barcodes (geometric mean calculation).

Life cell imaging experiments

hMDMs were prepared as described above and 0.8×10^5 hMDM cells were seeded into 8 well µ-slides (ibidi, Cat. No. 80826) in a final volume of 395 µL per well. A *C. glabrata* ATCC2001 or ATCC2001 yeGFP overnight culture was pelleted, washed twice with sterile PBS (centrifugation 1 min 5,000 g), and adjusted to 2.2×10^7 yeast cells/mL in RPMI. Each well was infected with 25 µL of this solution (MOI 7) and incubated together

with uninfected controls at 37°C and 5% CO2 for seven days with media exchange: at three hours, the wells were washed twice with PBS and supplemented with 300 µl RPMI + 10% human serum, then daily exchange of 200 µl medium. Fluorescence micrographs were obtained with an Zeiss AXIO Observer.Z1 (Carl Zeiss Microscopy) under cell culture atmospheric conditions. Viability was ensured by adding 1 µL propidium iodide (1 mg/mL) before obtaining micrographs.

Statistics

Experiments were performed in biological replicates from independent samples ($n \geq 3$) unless stated otherwise. All experiments were performed unblinded. Data points in graphs represent either arithmetic or geometric means (see individual graphs) ± the standard deviations. Data were analysed using GraphPad Prism 7 (GraphPad Software, Inc., La Jolla), Excel 2010, GeneSpring GX (v14.8; Agilent Technologies, Inc., Santa Clara, CA), and Revigo (Supek *et al.* 2011). Where applicable, samples were tested for significance ($P < 0.05$ unless stated otherwise) using a two-sided t test, and GO-term enrichment was determined by using the Fisher exact test.

Acknowledgements

We thank Fabrice Hille, Ankido Gustin, Leon Cyranka, André Bordinassi Medina, Lucas Unger, Maximilian Arlt, Nadja Jablonowski, Stephanie Wisgott, Daniela Schulz, Dorothee Eckhardt, Volha Skrahina, Franziska Gerwien, Osama Elshafee, Annika König, Lydia Kasper, Philipp Kämmer, and Sofía Lewin for help with the *C. glabrata* hMDM persistence assays. We thank Philipp Kämmer, Karolin Mielke and Fabrice Hille for help with construction of *C. glabrata* strains, Mark Gresnigt for preparation and donation of LPS and Lydia Kasper, Katja Seider, Ilse D. Jacobsen, and Silke Machata for fruitful discussions.

References

Al-Dhaheri, R. S., and L. J. Douglas. 2008. 'Absence of amphotericin B-tolerant persister cells in biofilms of some Candida species', *Antimicrob Agents Chemother*, **52**: 1884-7.

Alby, K., and R. J. Bennett. 2009. 'Stress-induced phenotypic switching in Candida albicans', *Mol Biol Cell*, **20**: 3178-91.

Alexander, B. D., M. D. Johnson, C. D. Pfeiffer, C. Jiménez-Ortigosa, J. Catania, R. Booker, M. Castanheira, S. A. Messer, D. S. Perlin, and M. A. Pfaller. 2013. 'Increasing echinocandin resistance in Candida glabrata: clinical failure correlates with presence of FKS mutations and elevated minimum inhibitory concentrations', *Clin Infect Dis*, **56**: 1724-32.

Arendrup, M., T. Horn, and N. Frimodt-Møller. 2002. 'In vivo pathogenicity of eight medically relevant Candida species in an animal model', *Infection*, **30**: 286-91.

Aybay, C., and T. Imir. 1996. 'Tumor necrosis factor (TNF) induction from

monocyte/macrophages by Candida species', *Immunobiology*, **196**: 363-74.

Baltch, A. L., L. H. Bopp, R. P. Smith, W. J. Ritz, C. J. Carlyn, and P. B. Michelsen. 2005. 'Effects of voriconazole, granulocyte-macrophage colony-stimulating factor, and interferon gamma on intracellular fluconazole-resistant Candida glabrata and Candida krusei in human monocyte-derived macrophages', *Diagn Microbiol Infect Dis*, **52**: 299-304.

Baltch, A. L., L. H. Bopp, R. P. Smith, W. J. Ritz, and P. B. Michelsen. 2008. 'Anticandidal effects of voriconazole and caspofungin, singly and in combination, against Candida glabrata, extracellularly and intracellularly in granulocyte-macrophage colony stimulating factor (GM-CSF)-activated human monocytes', *J Antimicrob Chemother*, **62**: 1285-90.

Barsoum, E., N. Rajaei, and S. U. Åström. 2011. 'RAS/cyclic AMP and transcription factor Msn2 regulate mating and mating-type switching in the yeast Kluyveromyces lactis', *Eukaryot Cell*, **10**: 1545-52.

Baumgartner, U., B. Hamilton, M. Piskacek, H. Ruis, and H. Rottensteiner. 1999. 'Functional analysis of the Zn(2)Cys(6) transcription factors Oaf1p and Pip2p. Different roles in fatty acid induction of beta-oxidation in Saccharomyces cerevisiae', *J Biol Chem*, **274**: 22208-16.

Berman, J., and D. J. Krysan. 2020. 'Drug resistance and tolerance in fungi', *Nat Rev Microbiol.*, **18**: 319–331

Bernstein, C., and V. Johns. 1989. 'Sexual reproduction as a response to H2O2 damage in Schizosaccharomyces pombe', *J Bacteriol*, **171**: 1893-7.

Bojsen, R., B. Regenberg, and A. Folkesson. 2014. 'Saccharomyces cerevisiae biofilm tolerance towards systemic antifungals depends on growth phase', *BMC Microbiol*, **14**: 305.

Bojsen, R., B. Regenberg, and A. Folkesson. 2017. 'Persistence and drug tolerance in pathogenic yeast', *Curr Genet*, **63**: 19-22.

Bojsen, R., B. Regenberg, D. Gresham, and A. Folkesson. 2016. 'A common mechanism involving the TORC1 pathway can lead to amphotericin B-persistence in biofilm and planktonic Saccharomyces cerevisiae populations', *Sci Rep*, **6**: 21874.

Bopp, L. H., A. L. Baltch, W. J. Ritz, P. B. Michelsen, and R. P. Smith. 2006. 'Antifungal effect of voriconazole on intracellular Candida glabrata, Candida krusei and Candida parapsilosis in human monocyte-derived macrophages', *J Med Microbiol*, **55**: 865-70.

Boyle, E. I., S. Weng, J. Gollub, H. Jin, D. Botstein, J. M. Cherry, and G. Sherlock. 2004. 'GO::TermFinder--open source software for accessing Gene Ontology information and finding significantly enriched Gene Ontology terms associated with a list of genes', *Bioinformatics*, **20**: 3710-5.

Brengues, M., D. Teixeira, and R. Parker. 2005. 'Movement of eukaryotic mRNAs between polysomes and cytoplasmic processing bodies', *Science*, **310**: 486-9.

Brieland, J., D. Essig, C. Jackson, D. Frank, D. Loebenberg, F. Menzel, B. Arnold, B. DiDomenico, and R. Hare. 2001. 'Comparison of pathogenesis and host immune responses to Candida glabrata and Candida albicans in systemically infected immunocompetent mice', *Infect Immun*, **69**: 5046-55.

Brunke, S., and B. Hube. 2013. 'Two unlike cousins: Candida albicans and C. glabrata infection strategies', *Cell Microbiol*, **15**: 701-8.

Brunke, S., J. Quintin, L. Kasper, I. D. Jacobsen, M. E. Richter, E. Hiller, T. Schwarzmüller, C. d'Enfert, K. Kuchler, S. Rupp, B. Hube, and D. Ferrandon. 2015. 'Of mice, flies--and men? Comparing fungal infection models for large-scale screening efforts', *Dis Model Mech*, **8**: 473-86.

Butler, G., M. D. Rasmussen, M. F. Lin, M. A. Santos, S. Sakthikumar, C. A. Munro, E. Rheinbay, M. Grabherr, A. Forche, J. L. Reedy, I. Agrafioti, M. B. Arnaud, S. Bates, A. J. Brown, S. Brunke, M. C. Costanzo, D. A. Fitzpatrick, P. W. de Groot, D. Harris, L. L. Hoyer, B. Hube, F. M. Klis, C. Kodira, N. Lennard, M. E. Logue, R. Martin, A. M. Neiman, E. Nikolaou, M. A. Quail, J. Quinn, M. C. Santos, F. F. Schmitzberger, G. Sherlock, P. Shah, K. A. Silverstein, M. S. Skrzypek, D. Soll, R. Staggs, I. Stansfield, M. P. Stumpf, P. E. Sudbery, T. Srikantha, Q. Zeng, J. Berman, M. Berriman, J. Heitman, N. A. Gow, M. C. Lorenz, B. W. Birren, M. Kellis, and C. A. Cuomo. 2009. 'Evolution of pathogenicity and sexual reproduction in eight Candida genomes', *Nature*, **459**: 657-62.

Carreté, L., E. Ksiezopolska, C. Pegueroles, E. Gómez-Molero, E. Saus, S. Iraola-Guzmán, D. Loska, O. Bader, C. Fairhead, and T. Gabaldón. 2018. 'Patterns of Genomic Variation in the Opportunistic Pathogen Candida glabrata Suggest the Existence of Mating and a Secondary Association with Humans', *Curr Biol*, **28**: 15-27 e7.

Cheng, S., C. J. Clancy, D. J. Hartman, B. Hao, and M. H. Nguyen. 2014. 'Candida glabrata intra-abdominal candidiasis is characterized by persistence within the peritoneal cavity and abscesses', *Infect Immun*, **82**: 3015-22.

Chew, S. Y., K. L. Ho, Y. K. Cheah, T. S. Ng, D. Sandai, A. J. P. Brown, and L. T. L. Than. 2019. 'Glyoxylate cycle gene ICL1 is essential for the metabolic flexibility and virulence of Candida glabrata', *Sci Rep*, **9**: 2843.

Clancy, M. J., L. M. Smith, and P. T. Magee. 1982. 'Developmental regulation of a sporulation-specific enzyme activity in Saccharomyces cerevisiae', *Mol Cell Biol*, **2**: 171-8.

Colonna, W. J., and P. T. Magee. 1978. 'Glycogenolytic enzymes in sporulating yeast', *J Bacteriol*, **134**: 844-53.

Csank, C., and K. Haynes. 2000. 'Candida glabrata displays pseudohyphal growth', *FEMS Microbiol Lett*, **189**: 115-20.

Cui, Z., T. Shiraki, D. Hirata, and T. Miyakawa. 1998. 'Yeast gene YRR1, which is required for resistance to 4-nitroquinoline N-oxide, mediates transcriptional activation of the multidrug resistance transporter gene SNQ2', *Mol Microbiol*, **29**: 1307-15.

Davey, J. 1998. 'Fusion of a fission yeast', *Yeast*, **14**: 1529-66.

de Brabander, M., F. Aerts, J. van Cutsem, H. van den Bossche, and M. Borgers. 1980. 'The activity of ketoconazole in mixed cultures of leukocytes and Candida albicans', *Sabouraudia*, **18**: 197-210.

De Groot, P. W., K. J. Hellingwerf, and F. M. Klis. 2003. 'Genome-wide identification of fungal GPI proteins', *Yeast*, **20**: 781-96.

De Virgilio, C. 2012. 'The essence of yeast quiescence', *FEMS Microbiol Rev*, **36**: 306-39.

Diekema, D. J., S. A. Messer, A. B. Brueggemann, S. L. Coffman, G. V. Doern, L. A. Herwaldt, and M. A. Pfaller. 2002. 'Epidemiology of candidemia: 3-year results from the emerging infections and the epidemiology of Iowa organisms study', *J Clin Microbiol*, **40**: 1298-302.

Duggan, S., F. Essig, K. Hünniger, Z. Mokhtari, L. Bauer, T. Lehnert, S. Brandes, A. Häder, I. D. Jacobsen, R. Martin, M. T. Figge, and O. Kurzai. 2015. 'Neutrophil activation by Candida glabrata but not Candida albicans promotes fungal uptake by monocytes', *Cell Microbiol*, **17**: 1259-76.

Dujon, B., D. Sherman, G. Fischer, P. Durrens, S. Casaregola, I. Lafontaine, J. De Montigny, C. Marck, C. Neuvéglise, E. Talla, N. Goffard, L. Frangeul, M. Aigle, V. Anthouard, A. Babour, V. Barbe, S. Barnay, S. Blanchin, J. M. Beckerich, E. Beyne, C. Bleykasten, A. Boisramé, J. Boyer, L. Cattolico, F. Confanioleri, A. De Daruvar, L. Despons, E. Fabre, C. Fairhead, H. Ferry-Dumazet, A. Groppi, F. Hantraye, C. Hennequin, N. Jauniaux, P. Joyet, R. Kachouri, A. Kerrest, R. Koszul, M. Lemaire, I. Lesur, L. Ma, H. Muller, J. M. Nicaud, M. Nikolski, S. Oztas, O. Ozier-Kalogeropoulos, S. Pellenz, S. Potier, G. F. Richard, M. L. Straub, A. Suleau, D. Swennen, F. Tekaia, M. Wésolowski-Louvel, E. Westhof, B. Wirth, M. Zeniou-Meyer, I. Zivanovic, M. Bolotin-Fukuhara, A. Thierry, C. Bouchier, B. Caudron, C. Scarpelli, C. Gaillardin, J. Weissenbach, P. Wincker, and J. L. Souciet. 2004. 'Genome evolution in yeasts', *Nature*, **430**: 35-44.

Dumitru, R., D. H. Navarathna, C. P. Semighini, C. G. Elowsky, R. V. Dumitru, D. Dignard, M. Whiteway, A. L. Atkin, and K. W. Nickerson. 2007. 'In vivo and in vitro anaerobic mating in Candida albicans', *Eukaryot Cell*, **6**: 465-72.

Fan, W., P. R. Kraus, M. J. Boily, and J. Heitman. 2005. 'Cryptococcus neoformans gene expression during murine macrophage infection', *Eukaryot Cell*, **4**: 1420-33.

Farmakiotis, D., J. J. Tarrand, and D. P. Kontoyiannis. 2014. 'Drug-resistant Candida glabrata infection in cancer patients', *Emerg Infect Dis*, **20**: 1833-40.

Fidel, P. L., Jr., J. A. Vazquez, and J. D. Sobel. 1999. 'Candida glabrata: review of epidemiology, pathogenesis, and clinical disease with comparison to C. albicans', *Clin Microbiol Rev*, **12**: 80-96.

Filler, S. G., A. S. Pfunder, B. J. Spellberg, J. P. Spellberg, and J. E. Edwards, Jr. 1996. 'Candida albicans stimulates cytokine production and leukocyte adhesion molecule expression by endothelial cells', *Infect Immun*, **64**: 2609-17.

Gank, K. D., M. R. Yeaman, S. Kojima, N. Y. Yount, H. Park, J. E. Edwards, Jr., S. G. Filler, and Y. Fu. 2008. 'SSD1 is integral to host defense peptide resistance in Candida albicans', *Eukaryot Cell*, **7**: 1318-27.

Gerwien, F., A. Safyan, S. Wisgott, F. Hille, P. Kaemmer, J. Linde, S. Brunke, L. Kasper, and B. Hube. 2016. 'A Novel Hybrid Iron Regulation Network Combines Features from Pathogenic and Nonpathogenic Yeasts', *mBio*, **7** (5): e01782-16.

Gibson, N., and L. McAlister-Henn. 2003. 'Physical and genetic interactions of cytosolic malate dehydrogenase with other gluconeogenic enzymes', *J Biol Chem*, **278**: 25628-36.

Gow, N. A. R., J. P. Latge, and C. A. Munro. 2017. 'The Fungal Cell Wall: Structure, Biosynthesis, and Function', *Microbiol Spectr*, **5** (3).

Gray, J. V., G. A. Petsko, G. C. Johnston, D. Ringe, R. A. Singer, and M. Werner-Washburne. 2004. '"Sleeping beauty": quiescence in Saccharomyces cerevisiae', *Microbiol Mol Biol Rev*, **68**: 187-206.

Herman, P. K. 2002. 'Stationary phase in yeast', *Curr Opin Microbiol*, **5**: 602-7.

Hogan, D. J., D. P. Riordan, A. P. Gerber, D. Herschlag, and P. O. Brown. 2008. 'Diverse RNA-binding proteins interact with functionally related sets of RNAs, suggesting an extensive regulatory system', *PLoS Biol*, **6**: e255.

Holmes, L. E., S. G. Campbell, S. K. De Long, A. B. Sachs, and M. P. Ashe. 2004. 'Loss of translational control in yeast compromised for the major mRNA decay pathway', *Mol Cell Biol*, **24**: 2998-3010.

Huang, G., T. Srikantha, N. Sahni, S. Yi, and D. R. Soll. 2009. 'CO(2) regulates white-to-opaque switching in Candida albicans', *Curr Biol*, **19**: 330-4.

Hünniger, K., and O. Kurzai. 2019. 'Phagocytes as central players in the defence against invasive fungal infection', *Semin Cell Dev Biol*, **89**: 3-15.

Jacobsen, I. D., S. Brunke, K. Seider, T. Schwarzmüller, A. Firon, C. d'Enfert, K. Kuchler, and B. Hube. 2010. 'Candida glabrata persistence in mice does not depend on host immunosuppression and is unaffected by fungal amino acid auxotrophy', *Infect Immun*, **78**: 1066-77.

Jansen, J. M., A. G. Wanless, C. W. Seidel, and E. L. Weiss. 2009. 'Cbk1 regulation of the RNA-binding protein Ssd1 integrates cell fate with translational control', *Curr Biol*, **19**: 2114-20.

Jung, S. I., J. S. Finkel, N. V. Solis, S. Chaili, A. P. Mitchell, M. R. Yeaman, and S. G. Filler. 2013. 'Bcr1 functions downstream of Ssd1 to mediate antimicrobial peptide resistance in Candida albicans', *Eukaryot Cell*, **12**: 411-9.

Kaeberlein, M., A. A. Andalis, G. B. Liszt, G. R. Fink, and L. Guarente. 2004. 'Saccharomyces cerevisiae SSD1-V confers longevity by a Sir2p-independent mechanism', *Genetics*, **166**: 1661-72.

Kaeberlein, M., and L. Guarente. 2002. 'Saccharomyces cerevisiae MPT5 and SSD1 function in parallel pathways to promote cell wall integrity', *Genetics*, **160**: 83-95.

Karpichev, I. V., Y. Luo, R. C. Marians, and G. M. Small. 1997. 'A complex containing two transcription factors regulates peroxisome proliferation and the coordinate induction of beta-oxidation enzymes in Saccharomyces cerevisiae', *Mol Cell Biol*, **17**: 69-80.

Karpichev, I. V., and G. M. Small. 1998. 'Global regulatory functions of Oaf1p and Pip2p (Oaf2p), transcription factors that regulate genes encoding peroxisomal proteins in Saccharomyces cerevisiae', *Mol Cell Biol*, **18**: 6560-70.

Kasper, L., K. Seider, and B. Hube. 2015. 'Intracellular survival of Candida glabrata in macrophages: immune evasion and persistence', *FEMS Yeast Res*, **15**: fov042.

Kaur, R., B. Ma, and B. P. Cormack. 2007. 'A family of glycosylphosphatidylinositol-linked aspartyl proteases is required for virulence of Candida glabrata', *Proc Natl Acad Sci U S A*, **104**: 7628-33.

Kerwin, C. L., and D. D. Wykoff. 2009. 'Candida glabrata PHO4 is necessary and sufficient for Pho2-independent transcription of phosphate starvation genes', *Genetics*,

182: 471-9.

Kuang, Z., H. Ji, and J. D. Boeke. 2018. 'Stress response factors drive regrowth of quiescent cells', *Curr Genet*, **64**: 807-10.

Kurischko, C., H. K. Kim, V. K. Kuravi, J. Pratzka, and F. C. Luca. 2011. 'The yeast Cbk1 kinase regulates mRNA localization via the mRNA-binding protein Ssd1', *J Cell Biol*, **192**: 583-98.

Kurischko, C., V. K. Kuravi, C. J. Herbert, and F. C. Luca. 2011. 'Nucleocytoplasmic shuttling of Ssd1 defines the destiny of its bound mRNAs', Mol Microbiol, 81: 831-49.
Kurtzman, C. P., and C. J. Robnett. 1997. 'Identification of clinically important ascomycetous yeasts based on nucleotide divergence in the 5' end of the large-subunit (26S) ribosomal DNA gene', *J Clin Microbiol*, **35**: 1216-23.

LaFleur, M. D., C. A. Kumamoto, and K. Lewis. 2006. 'Candida albicans biofilms produce antifungal-tolerant persister cells', *Antimicrob Agents Chemother*, **50**: 3839-46.

Laporte, D., A. Lebaudy, A. Sahin, B. Pinson, J. Ceschin, B. Daignan-Fornier, and I. Sagot. 2011. 'Metabolic status rather than cell cycle signals control quiescence entry and exit', *J Cell Biol*, **192**: 949-57.

Le Crom, S., F. Devaux, P. Marc, X. Zhang, W. S. Moye-Rowley, and C. Jacq. 2002. 'New insights into the pleiotropic drug resistance network from genome-wide characterization of the YRR1 transcription factor regulation system', *Mol Cell Biol*, **22**: 2642-9.

Lewis, K. 2010. 'Persister cells', *Annu Rev Microbiol*, **64**: 357-72.

Li, L., and A. Dongari-Bagtzoglou. 2007. 'Oral epithelium-Candida glabrata interactions in vitro', *Oral Microbiol Immunol*, **22**: 182-7.

Li, L., Y. Lu, L. X. Qin, Z. Bar-Joseph, M. Werner-Washburne, and L. L. Breeden. 2009. 'Budding yeast SSD1-V regulates transcript levels of many longevity genes and extends chronological life span in purified quiescent cells', *Mol Biol Cell*, **20**: 3851-64.

Li, L., S. Miles, Z. Melville, A. Prasad, G. Bradley, and L. L. Breeden. 2013. 'Key events during the transition from rapid growth to quiescence in budding yeast require posttranscriptional regulators', *Mol Biol Cell*, **24**: 3697-709.

Li, L., S. Redding, and A. Dongari-Bagtzoglou. 2007. 'Candida glabrata: an emerging oral opportunistic pathogen', *J Dent Res*, **86**: 204-15.

Lin, C. P., C. Kim, S. O. Smith, and A. M. Neiman. 2013. 'A highly redundant gene network controls assembly of the outer spore wall in S. cerevisiae', *PLoS Genet*, **9**: e1003700.

Lorenz, M. C., J. A. Bender, and G. R. Fink. 2004. 'Transcriptional response of Candida albicans upon internalization by macrophages', *Eukaryot Cell*, **3**: 1076-87.

Luo, Y., I. V. Karpichev, R. A. Kohanski, and G. M. Small. 1996. 'Purification, identification, and properties of a Saccharomyces cerevisiae oleate-activated upstream activating sequence-binding protein that is involved in the activation of POX1', *J Biol Chem*, **271**: 12068-75.

Lüttich, A., S. Brunke, and B. Hube. 2012. 'Isolation and amplification of fungal RNA for

microarray analysis from host samples', *Methods Mol Biol*, **845**: 411-21.

McCarty, T. P., and P. G. Pappas. 2016. 'Invasive Candidiasis', *Infect Dis Clin North Am*, **30**: 103-24.

McKnight, J. N., J. W. Boerma, L. L. Breeden, and T. Tsukiyama. 2015. 'Global Promoter Targeting of a Conserved Lysine Deacetylase for Transcriptional Shutoff during Quiescence Entry', *Mol Cell*, **59**: 732-43.

Merhej, J., T. Delaveau, J. Guitard, B. Palancade, C. Hennequin, M. Garcia, G. Lelandais, and F. Devaux. 2015. 'Yap7 is a transcriptional repressor of nitric oxide oxidase in yeasts, which arose from neofunctionalization after whole genome duplication', *Mol Microbiol*, **96**: 951-72.

Miles, S., and L. Breeden. 2017. 'A common strategy for initiating the transition from proliferation to quiescence', *Curr Genet*, **63**: 179-86.

Miles, S., L. H. Li, Z. Melville, and L. L. Breeden. 2019. 'Ssd1 and the cell wall integrity pathway promote entry, maintenance, and recovery from quiescence in budding yeast', *Mol Biol Cell*, **30**: 2205-17.

Mir, S. S., D. Fiedler, and A. G. Cashikar. 2009. 'Ssd1 is required for thermotolerance and Hsp104-mediated protein disaggregation in Saccharomyces cerevisiae', *Mol Cell Biol*, **29**: 187-200.

Misme-Aucouturier, B., M. Albassier, N. Alvarez-Rueda, and P. Le Pape. 2017. 'Specific Human and Candida Cellular Interactions Lead to Controlled or Persistent Infection Outcomes during Granuloma-Like Formation', *Infect Immun*, **85**.

Miyata, M., H. Doi, H. Miyata, and B. F. Johnson. 1997. 'Sexual co-flocculation by heterothallic cells of the fission yeast Schizosaccharomyces pombe modulated by medium constituents', *Antonie Van Leeuwenhoek*, **71**: 207-15.

Miyazaki, T., H. Nakayama, Y. Nagayoshi, H. Kakeya, and S. Kohno. 2013. 'Dissection of Ire1 functions reveals stress response mechanisms uniquely evolved in Candida glabrata', *PLoS Pathog*, **9**: e1003160.

Mochizuki, N., and M. Yamamoto. 1992. 'Reduction in the intracellular cAMP level triggers initiation of sexual development in fission yeast', *Mol Gen Genet*, **233**: 17-24.

Otto, V., and D. H. Howard. 1976. 'Further studies on the intracellular behavior of Torulopsis glabrata', *Infect Immun*, **14**: 433-8.

Pais, P., C. Costa, C. Pires, K. Shimizu, H. Chibana, and M. C. Teixeira. 2016. 'Membrane Proteome-Wide Response to the Antifungal Drug Clotrimazole in Candida glabrata: Role of the Transcription Factor CgPdr1 and the Drug:H+ Antiporters CgTpo1_1 and CgTpo1_2', *Mol Cell Proteomics*, **15**: 57-72.

Perlroth, J., B. Choi, and B. Spellberg. 2007. 'Nosocomial fungal infections: epidemiology, diagnosis, and treatment', *Med Mycol*, **45**: 321-46.

Pfaller, M. A., M. Castanheira, S. R. Lockhart, A. M. Ahlquist, S. A. Messer, and R. N. Jones. 2012. 'Frequency of decreased susceptibility and resistance to echinocandins among fluconazole-resistant bloodstream isolates of Candida glabrata', *J Clin Microbiol*, **50**: 1199-203.

Pfaller, M. A., G. J. Moet, S. A. Messer, R. N. Jones, and M. Castanheira. 2011.

'Geographic variations in species distribution and echinocandin and azole antifungal resistance rates among Candida bloodstream infection isolates: report from the SENTRY Antimicrobial Surveillance Program (2008 to 2009)', *J Clin Microbiol*, **49**: 396-9.

Rai, M. N., S. Balusu, N. Gorityala, L. Dandu, and R. Kaur. 2012. 'Functional genomic analysis of Candida glabrata-macrophage interaction: role of chromatin remodeling in virulence', *PLoS Pathog*, **8**: e1002863.

Rai, M. N., V. Sharma, S. Balusu, and R. Kaur. 2015. 'An essential role for phosphatidylinositol 3-kinase in the inhibition of phagosomal maturation, intracellular survival and virulence in Candida glabrata', *Cell Microbiol*, **17**: 269-87.

Rasheed, M., A. Battu, and R. Kaur. 2018. 'Aspartyl proteases in Candida glabrata are required for suppression of the host innate immune response', *J Biol Chem*, **293**: 6410-33.

Rasheed, M., N. Kumar, and R. Kaur. 2020. 'Global Secretome Characterization of the Pathogenic Yeast Candida glabrata', *J Proteome Res*, **19**: 49-63.

Reinke, A., S. Anderson, J. M. McCaffery, J. Yates, 3rd, S. Aronova, S. Chu, S. Fairclough, C. Iverson, K. P. Wedaman, and T. Powers. 2004. 'TOR complex 1 includes a novel component, Tco89p (YPL180w), and cooperates with Ssd1p to maintain cellular integrity in Saccharomyces cerevisiae', *J Biol Chem*, **279**: 14752-62.

Roetzer, A., N. Gratz, P. Kovarik, and C. Schüller. 2010. 'Autophagy supports Candida glabrata survival during phagocytosis', *Cell Microbiol*, **12**: 199-216.

Rottensteiner, H., A. J. Kal, B. Hamilton, H. Ruis, and H. F. Tabak. 1997. 'A heterodimer of the Zn2Cys6 transcription factors Pip2p and Oaf1p controls induction of genes encoding peroxisomal proteins in Saccharomyces cerevisiae', *Eur J Biochem*, **247**: 776-83.

Sagot, I., and D. Laporte. 2019. 'The cell biology of quiescent yeast - a diversity of individual scenarios', *J Cell Sci*, **132**.

Schaller, M., R. Mailhammer, G. Grassl, C. A. Sander, B. Hube, and H. C. Korting. 2002. 'Infection of human oral epithelia with Candida species induces cytokine expression correlated to the degree of virulence', *J Invest Dermatol*, **118**: 652-7.

Schwarzmüller, T., B. Ma, E. Hiller, F. Istel, M. Tscherner, S. Brunke, L. Ames, A. Firon, B. Green, V. Cabral, M. Marcet-Houben, I. D. Jacobsen, J. Quintin, K. Seider, I. Frohner, W. Glaser, H. Jungwirth, S. Bachellier-Bassi, M. Chauvel, U. Zeidler, D. Ferrandon, T. Gabaldón, B. Hube, C. d'Enfert, S. Rupp, B. Cormack, K. Haynes, and K. Kuchler. 2014. 'Systematic phenotyping of a large-scale Candida glabrata deletion collection reveals novel antifungal tolerance genes', *PLoS Pathog*, **10**: e1004211.

Seider, K., S. Brunke, L. Schild, N. Jablonowski, D. Wilson, O. Majer, D. Barz, A. Haas, K. Kuchler, M. Schaller, and B. Hube. 2011. 'The facultative intracellular pathogen Candida glabrata subverts macrophage cytokine production and phagolysosome maturation', *J Immunol*, **187**: 3072-86.

Sharma, V., R. Purushotham, and R. Kaur. 2016. 'The Phosphoinositide 3-Kinase Regulates Retrograde Trafficking of the Iron Permease CgFtr1 and Iron Homeostasis in Candida glabrata', *J Biol Chem*, **291**: 24715-34.

Shen, J., W. Guo, and J. R. Köhler. 2005. 'CaNAT1, a heterologous dominant selectable

marker for transformation of Candida albicans and other pathogenic Candida species', *Infect Immun*, **73**: 1239-42.

Shepard, K. A., A. P. Gerber, A. Jambhekar, P. A. Takizawa, P. O. Brown, D. Herschlag, J. L. DeRisi, and R. D. Vale. 2003. 'Widespread cytoplasmic mRNA transport in yeast: identification of 22 bud-localized transcripts using DNA microarray analysis', *Proc Natl Acad Sci U S A*, **100**: 11429-34.

Sprenger, M., T. S. Hartung, S. Allert, S. Wisgott, M. J. Niemiec, K. Graf, I. D. Jacobsen, L. Kasper, and B. Hube. 2020. 'Fungal biotin homeostasis is essential for immune evasion after macrophage phagocytosis and virulence', *Cell Microbiol*, **22**: e13197.

Sprenger, M., L. Kasper, M. Hensel, and B. Hube. 2018. 'Metabolic adaptation of intracellular bacteria and fungi to macrophages', *Int J Med Microbiol*, **308**: 215-27.

Stettler, S., N. Chiannilkulchai, S. Hermann-Le Denmat, D. Lalo, F. Lacroute, A. Sentenac, and P. Thuriaux. 1993. 'A general suppressor of RNA polymerase I, II and III mutations in Saccharomyces cerevisiae', *Mol Gen Genet*, **239**: 169-76.

Sudbery, P. E. 2011. 'Growth of Candida albicans hyphae', *Nat Rev Microbiol*, **9**: 737-48.

Supek, F., M. Bošnjak, N. Škunca, and T. Šmuc. 2011. 'REVIGO summarizes and visualizes long lists of gene ontology terms', *PLoS One*, **6**: e21800.

Thiébaut, A., T. Delaveau, M. Benchouaia, J. Boeri, M. Garcia, G. Lelandais, and F. Devaux. 2017. 'The CCAAT-Binding Complex Controls Respiratory Gene Expression and Iron Homeostasis in Candida Glabrata', *Sci Rep*, **7**: 3531.

Thompson-Jaeger, S., J. François, J. P. Gaughran, and K. Tatchell. 1991. 'Deletion of SNF1 affects the nutrient response of yeast and resembles mutations which activate the adenylate cyclase pathway', *Genetics*, **129**: 697-706.

Toda, T., I. Uno, T. Ishikawa, S. Powers, T. Kataoka, D. Broek, S. Cameron, J. Broach, K. Matsumoto, and M. Wigler. 1985. 'In yeast, RAS proteins are controlling elements of adenylate cyclase', *Cell*, **40**: 27-36.

Uesono, Y., A. Toh-e, and Y. Kikuchi. 1997. 'Ssd1p of Saccharomyces cerevisiae associates with RNA', J Biol Chem, 272: 16103-9.
Valcourt, J. R., J. M. Lemons, E. M. Haley, M. Kojima, O. O. Demuren, and H. A. Coller. 2012. 'Staying alive: metabolic adaptations to quiescence', *Cell Cycle*, **11**: 1680-96.

Vandeputte, P., G. Tronchin, T. Bergès, C. Hennequin, D. Chabasse, and J. P. Bouchara. 2007. 'Reduced susceptibility to polyenes associated with a missense mutation in the ERG6 gene in a clinical isolate of Candida glabrata with pseudohyphal growth', *Antimicrob Agents Chemother*, **51**: 982-90.

Vandeputte, P., G. Tronchin, G. Larcher, E. Ernoult, T. Bergès, D. Chabasse, and J. P. Bouchara. 2008. 'A nonsense mutation in the ERG6 gene leads to reduced susceptibility to polyenes in a clinical isolate of Candida glabrata', *Antimicrob Agents Chemother*, **52**: 3701-9.

Wanless, A. G., Y. Lin, and E. L. Weiss. 2014. 'Cell morphogenesis proteins are translationally controlled through UTRs by the Ndr/LATS target Ssd1', *PLoS One*, **9**: e85212.

Weinberger, M., L. Leibovici, S. Perez, Z. Samra, I. Ostfeld, I. Levi, E. Bash, D. Turner,

A. Goldschmied-Reouven, G. Regev-Yochay, S. D. Pitlik, and N. Keller. 2005. 'Characteristics of candidaemia with Candida-albicans compared with non-albicans Candida species and predictors of mortality', *J Hosp Infect*, **61**: 146-54.

Westman, J., G. Moran, S. Mogavero, B. Hube, and S. Grinstein. 2018. 'Candida albicans Hyphal Expansion Causes Phagosomal Membrane Damage and Luminal Alkalinization', *mBio*, **9**.

Wuyts, J., P. Van Dijck, and M. Holtappels. 2018. 'Fungal persister cells: The basis for recalcitrant infections?', *PLoS Pathog*, **14**: e1007301.

Yofe, I., U. Weill, M. Meurer, S. Chuartzman, E. Zalckvar, O. Goldman, S. Ben-Dor, C. Schütze, N. Wiedemann, M. Knop, A. Khmelinskii, and M. Schuldiner. 2016. 'One library to make them all: streamlining the creation of yeast libraries via a SWAp-Tag strategy', *Nat Methods*, **13**: 371-78.

Figures and figure legends

Fig. 1

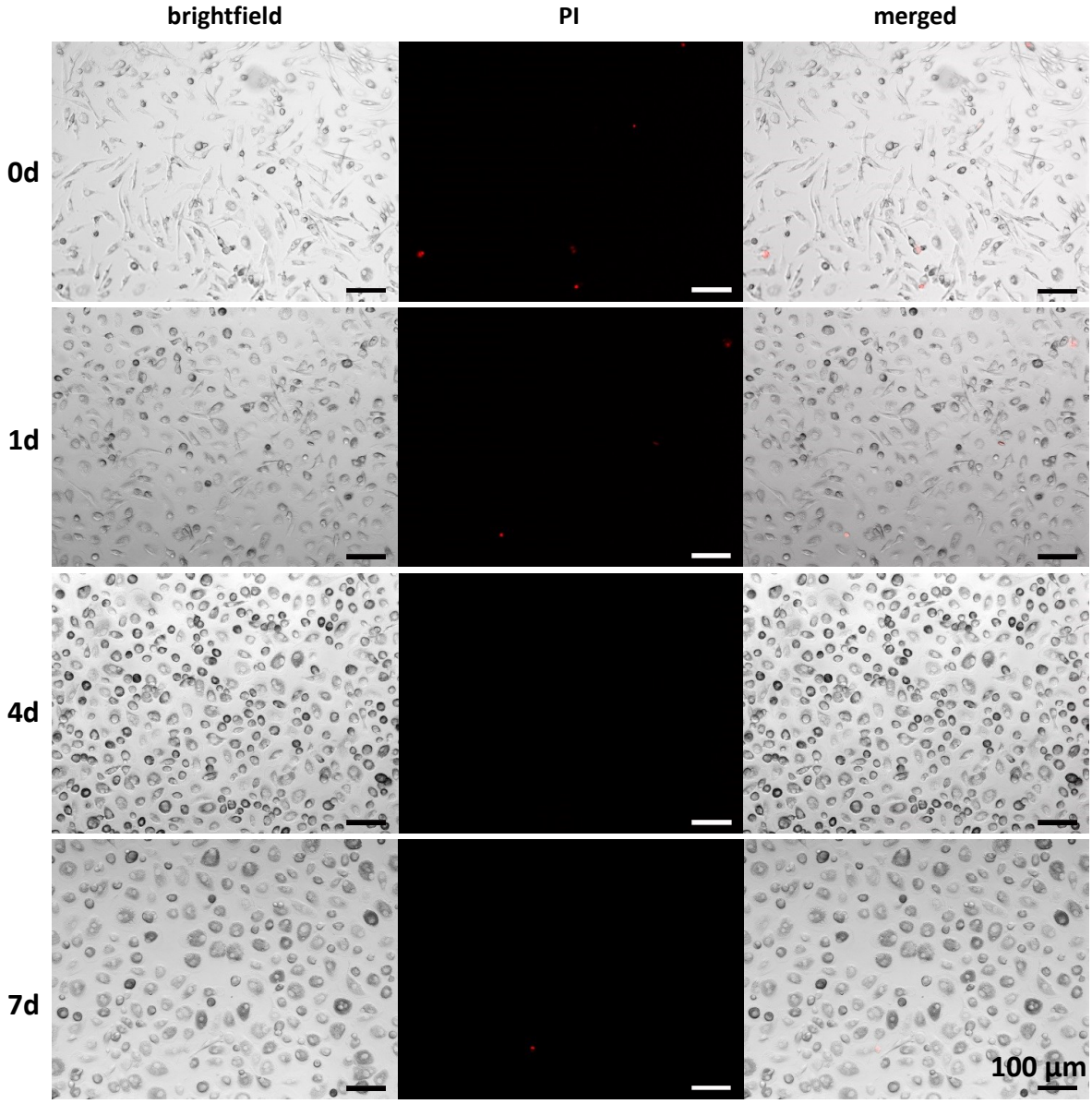

Fig. 1 PI staining of *C. glabrata*-infected hMDMs at indicated time points.

Fig. 2

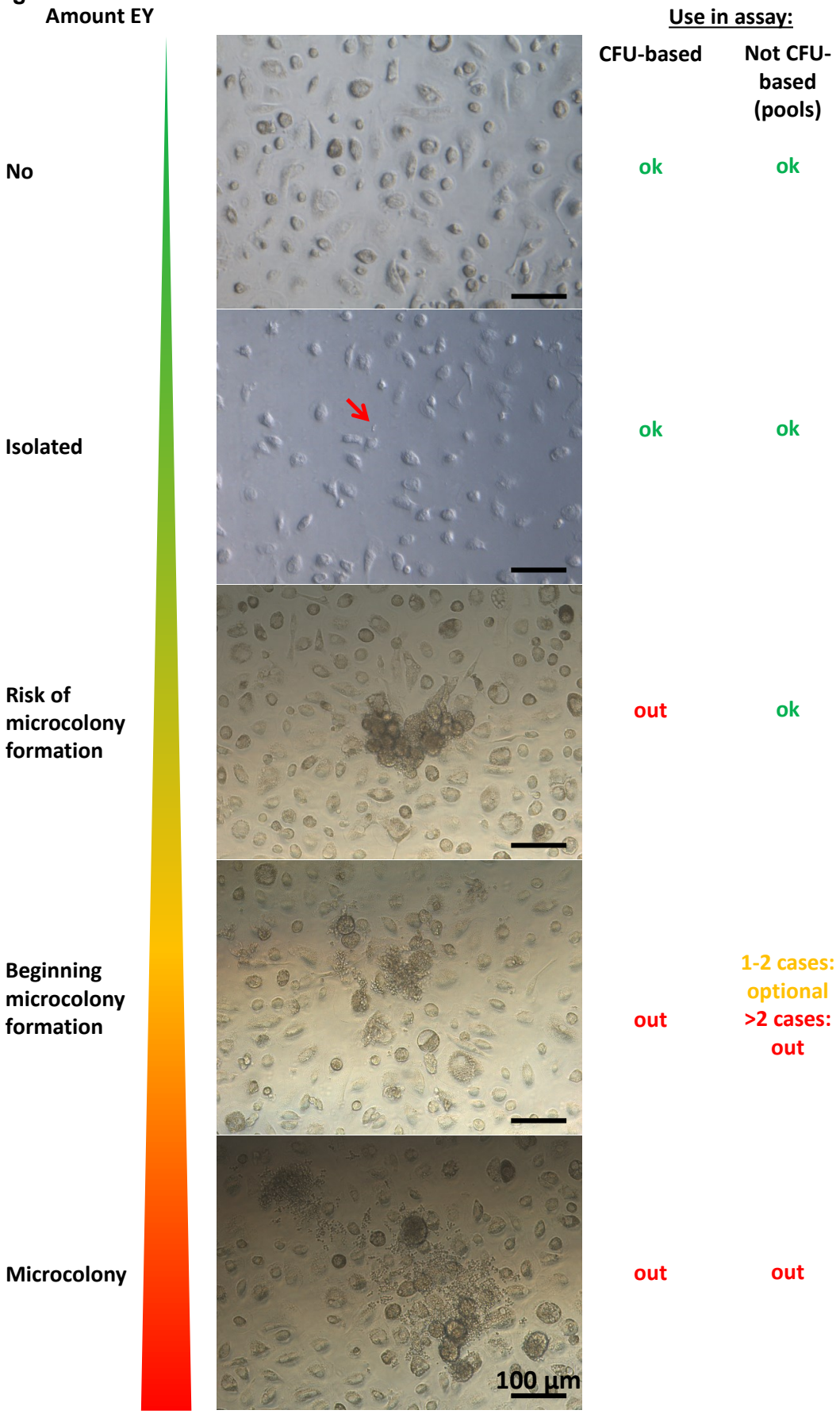

Fig. 2 Cut-off criteria for disposal of individual wells depending on the type of assay. EY = extracellular yeast.

Fig. 3

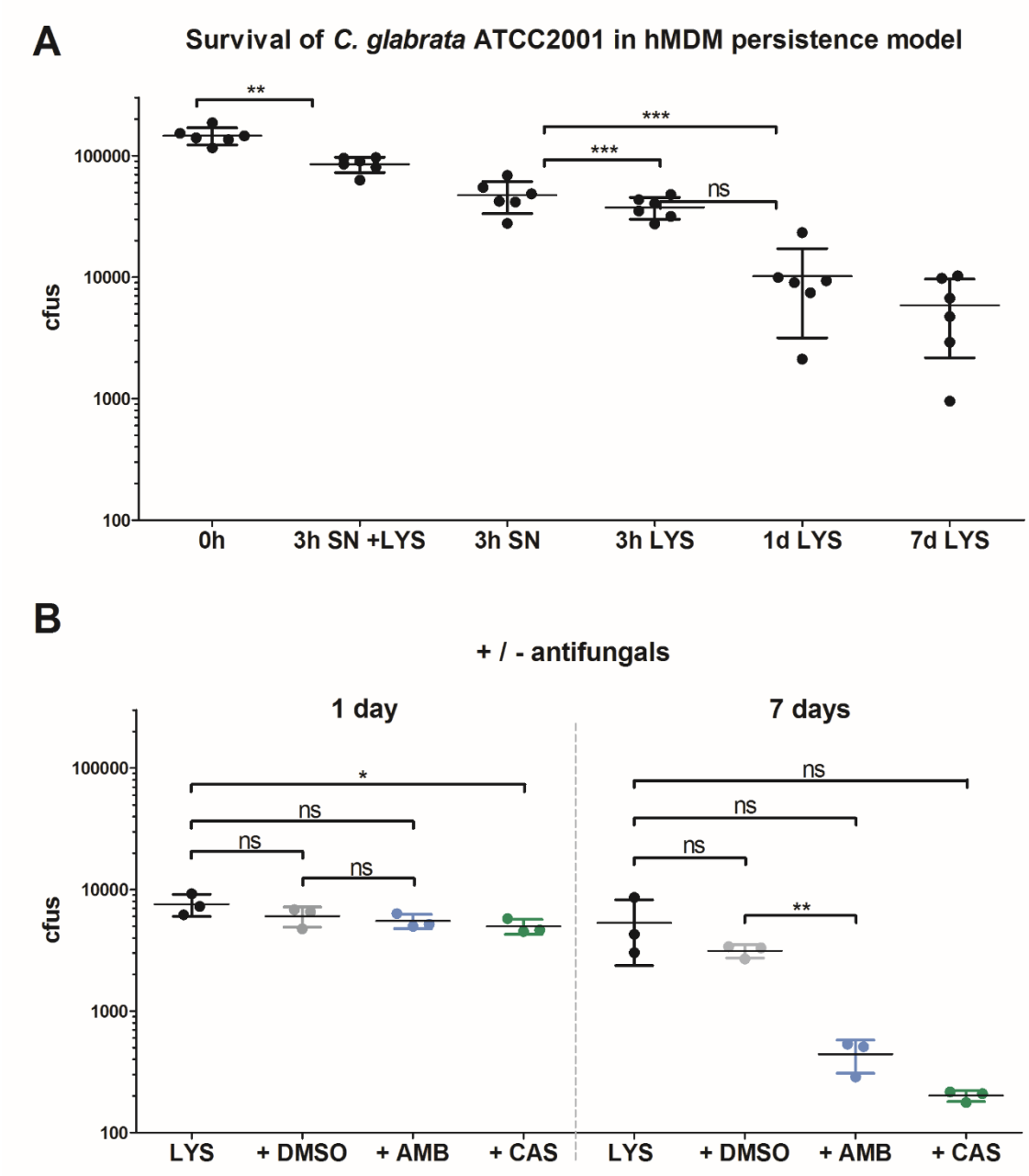

Fig. 3 (A) *C. glabrata* ATCC2001 cfu development during persistence in hMDMs starting at MOI 1. Significant decreases in numbers are seen between zero and three hours ($p = 0.0017$) for the whole sample between three and 24 hours ($p = 0.0002$) for intracellular yeasts (LYS). Mean ± standard deviation of 6 biological replicates (dots); two-tailed, paired Student´s t-test; ns > 0.05 (non-significant), * = 0.01 - 0.05, ** = 0.001 - 0.01, *** < 0.001. (B) Same as in (A), but with addition of 1 µg/mL AMB, 4 µg/mL CAS or DMSO control (for AMB) from 6h after infection. SN, supernatant; LYS, lysate.

Fig. 4

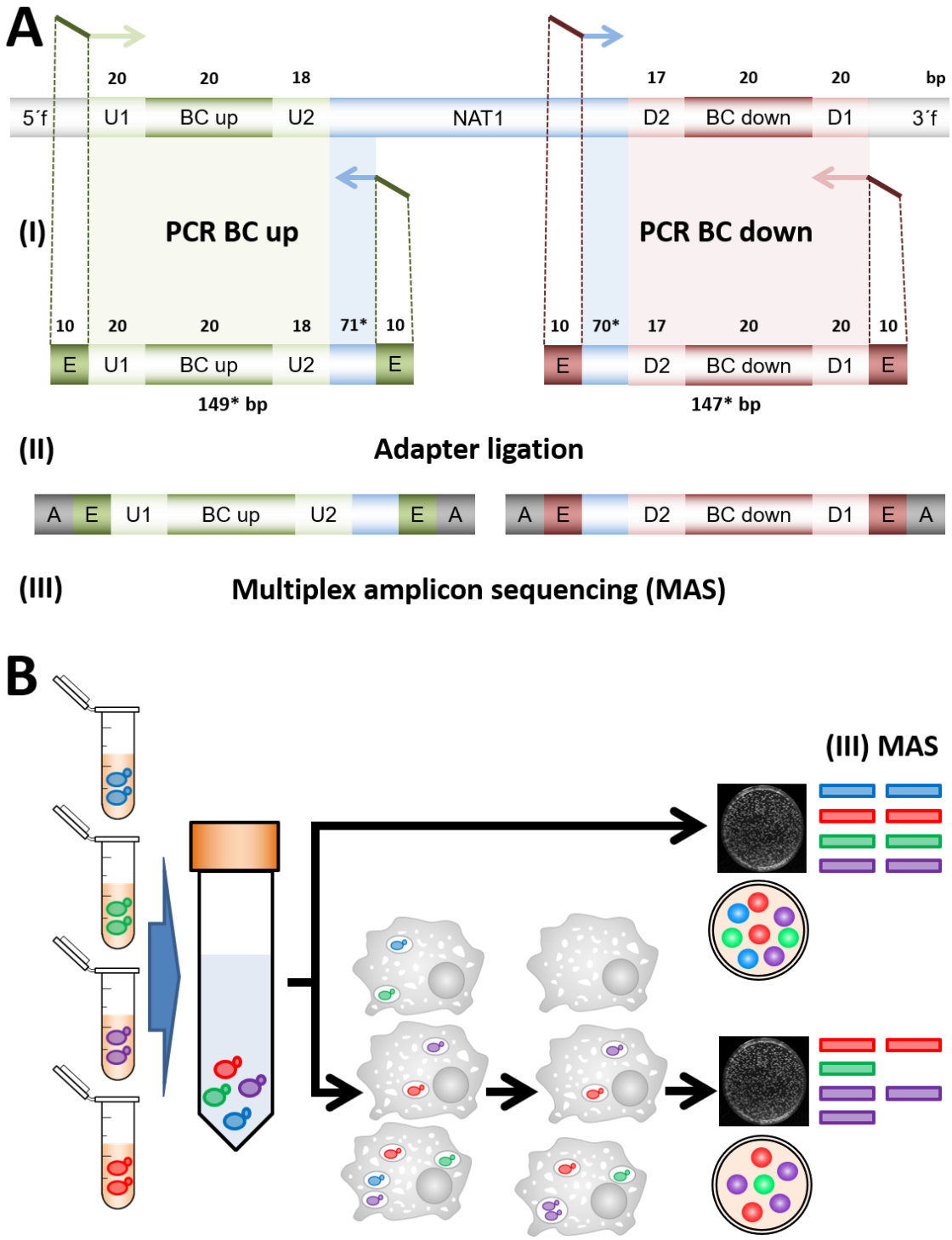

Fig. 4 Design for screening of a *C. glabrata* mutant library by barcode sequencing. (A) All library mutants contain a NAT1 cassette flanked by barcode (BC) sequences which are unique within each pool. Barcodes can be PCR-amplified by the constant regions U1 and D1. (*) The use of three different types of NAT1 cassettes in the mutant library (Schwarzmüller *et al.* 2014) makes the use of a further primer set necessary, with slightly different amplicon sizes. The majority of mutants contain the NAT1 cassette shown here (see Suppl. Fig. 8 for more information on the cassettes). The primers also add a 10 nt

experiment-specific tag (E) at both ends to allow multiplexing of experiments in libraries. (B) Schematic overview of a typical pool experiment with barcoded mutants. For the hMDM pool screening, individually grown *C. glabrata* mutants were mixed into pools for hMDM infection at a one-to-one ratio. The inoculum and lysates taken at day one and seven were plated. The colonies were used for DNA isolation, followed by barcode amplification and sequencing. The barcode sequence counts were normalized to the inoculum samples.

Fig. 5

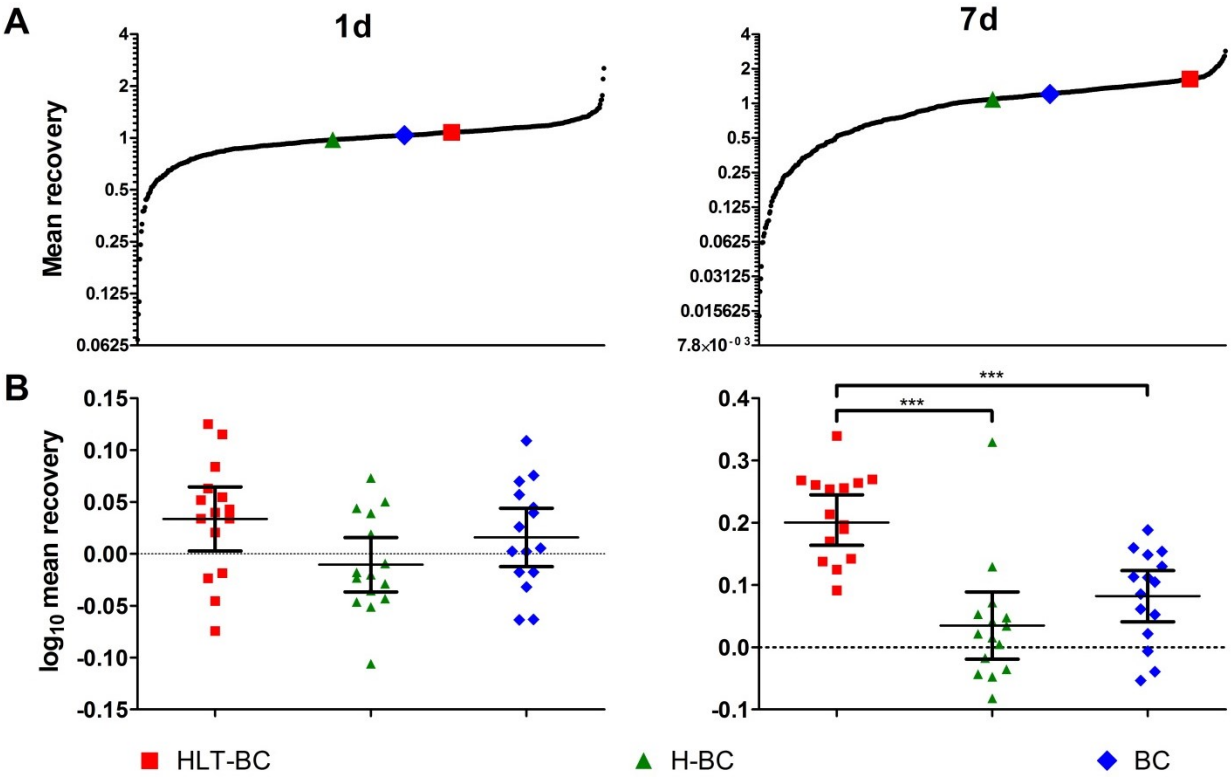

Fig. 5 (A) Distribution of mean recovery scores throughout the whole mutant library in the *C. glabrata*-hMDM persistence model. Values were normalized to their pool sample median and corrected by the strain's inoculum counts. The three wild types are indicated by coloured symbols; the vast majority of mutants were depleted compared to the wild types, especially at day seven. (B) Distribution of the wild type enrichment within each individual pool. Values were normalized to their pool sample median and corrected by the wild type's inoculum counts. Bars depict the geometric mean + 95% confidence interval; dots represent the geometric mean of 3 biological replicates of the wild type within a pool. Two-tailed, paired Student´s t-test; non-significant p-values (> 0.05) are not depicted, * = 0.01 - 0.05, ** = 0.001 - 0.01, *** < 0.001.

Fig. 6

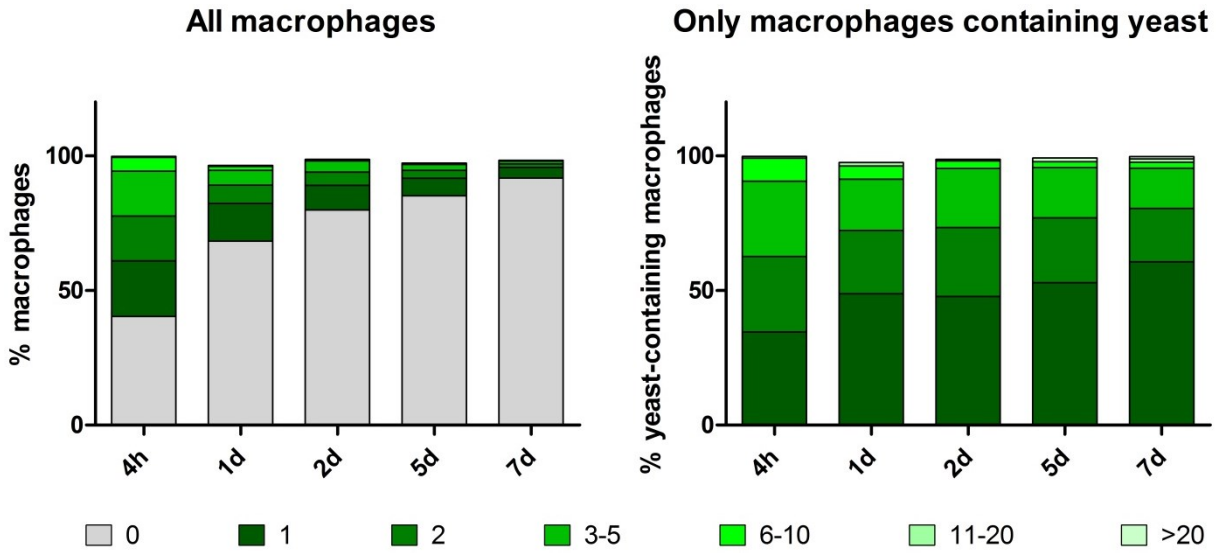

Fig. 6 Distribution of *C. glabrata* yeasts inside macrophages. Yeasts were constitutively expressing yeGFP and were quantified in all macrophages (left) or only macrophages which had taken up at least one yeast (right). The amount of macrophages containing no yeast(s) steadily increased over time, but the distribution of yeast numbers in hosting macrophages remained mostly constant. This suggests that the killing capacity of macrophages is not impaired by high yeast burdens. Macrophages were randomly chosen and intracellular yeasts identified by their green fluorescence. Counting continued until at least 150 yeast-containing macrophages were detected. Geometric means for 2 biological replicates are shown.

Fig. 7

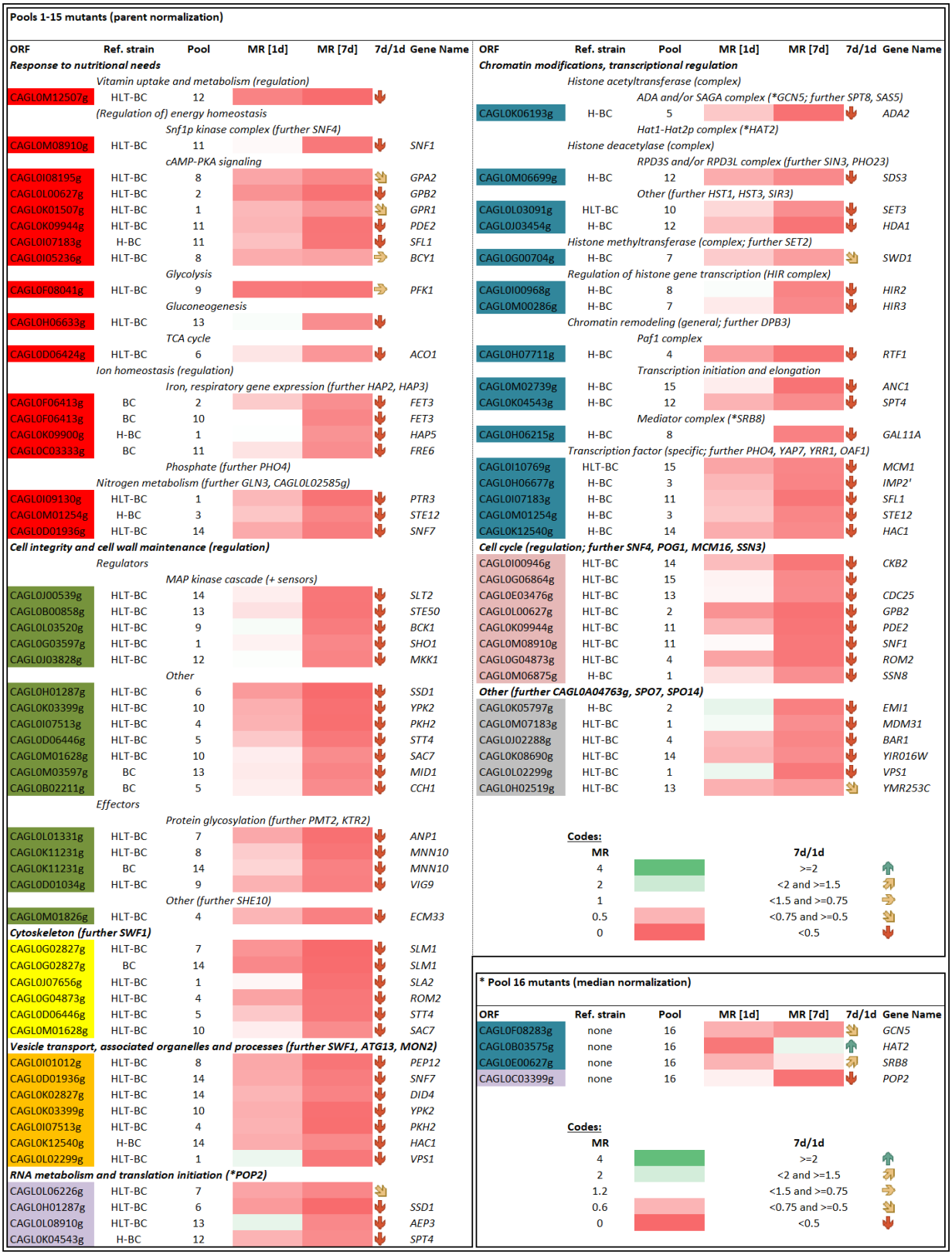

Fig. 7 A selection of *C. glabrata* mutants depleted during long-term interaction with human macrophages, using the stringent cut-off levels of 0.5 (1d) and 0.25 (7d) for pools 1-15 and 0.7/0.35 for pool 16 (to be met by at least one barcode, p<0.01). Additional genes in the categories that met the standard cut-offs (e.g. used in Fig. 8) are listed as

"further". The corresponding wild types are indicated as "ref. strain", and the normalization method are shown with different scales. The change between days one and seven of co-incubation is indicated by arrows ("7d/1d"). "Gene names" are taken from *Candida* genome database gene symbols for *C. glabrata* or, if lacking, of the *S. cerevisiae* homolog. MR = mean recovery.

Fig. 8

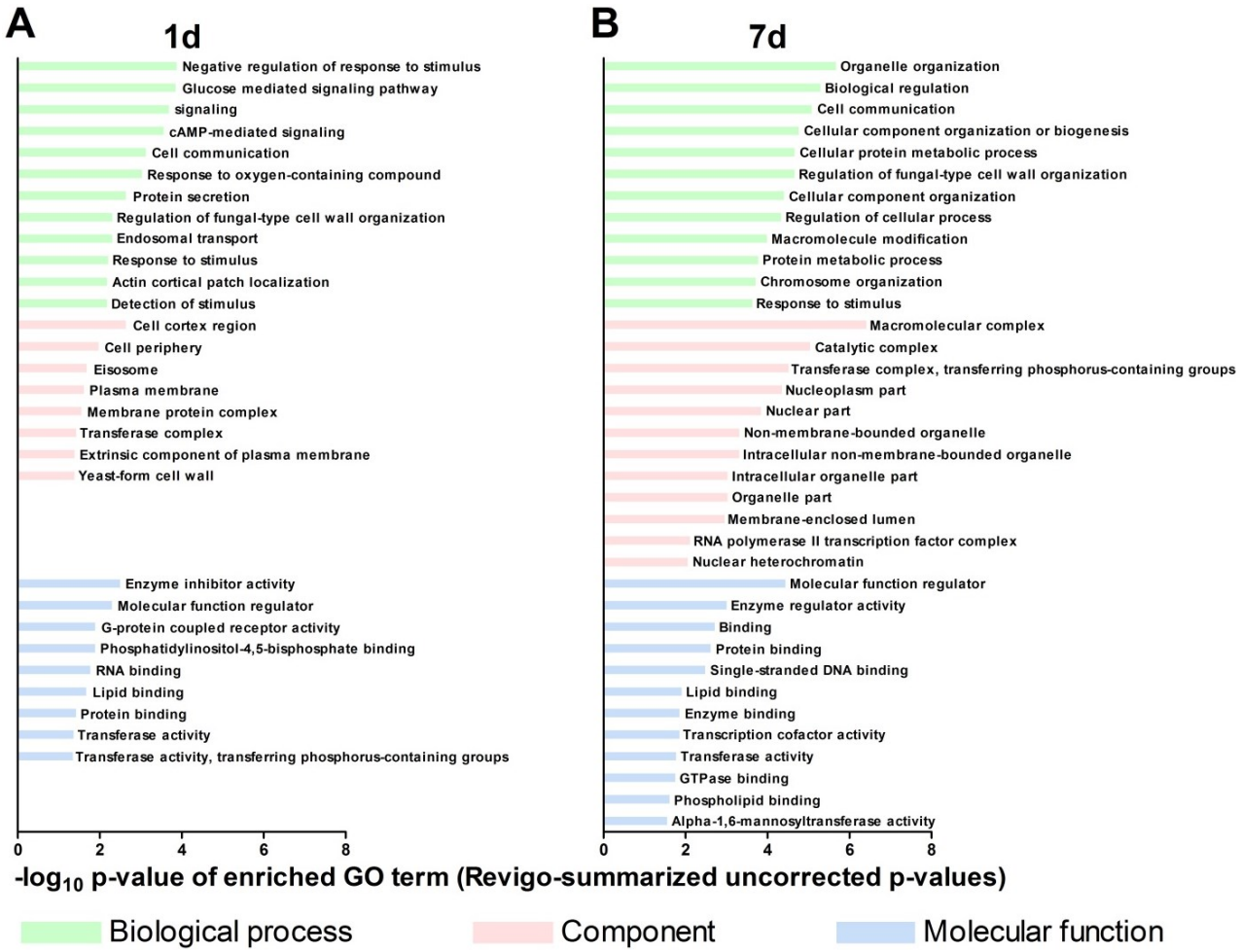

Fig. 8 GO term enrichment of genes depleted below (A) a parent normalized recovery of 0.5 (for at least one barcode, p<0.1; pools 1-15) respectively a median-normalized recovery of 0.7 (for at least one barcode, p<0.1; pool 16) after one day or (B) a parent normalized recovery of 0.35 (for at least one barcode, p<0.1; pools 1-15) respectively a median-normalized recovery of 0.5 (for at least one barcode, p<0.1; pool 16) after seven days. The GO terms (with p < 0.05) were summarized by Revigo and the most enriched for each domain shown (for more information see Suppl. Table 4).

Fig. 9

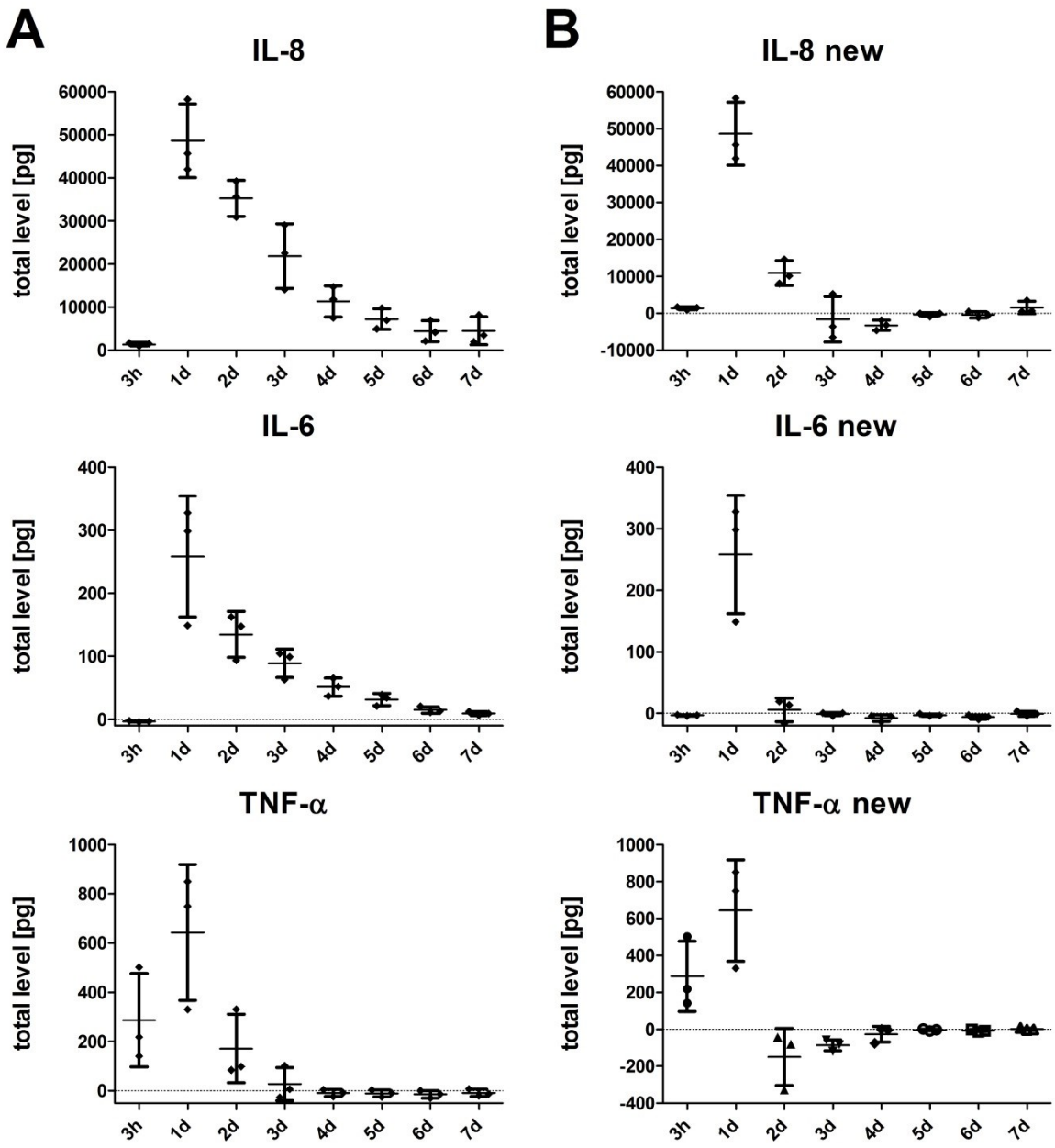

Fig. 9 Cytokine secretion patterns of hMDMs in response to the wild type strain *C. glabrata* ATCC2001 (MOI 1) in the *C. glabrata*-hMDM persistence model. Note that cytokine levels are influenced by the media exchange strategy used (3h: total exchange, addition of 1 mL medium; 1d: removal of 0.5 mL supernatant and addition of 1 mL medium; on each following day: removal of 0.5 mL supernatant and addition of 0.5 mL medium; see Methods). (A) Total cytokine levels calculated from measured cytokine supernatant concentrations. (B) Calculated amount of newly secreted cytokines in between the indicated time point and the previous time point. Negative values might indicate cytokine degradation or removal.

Fig. 10

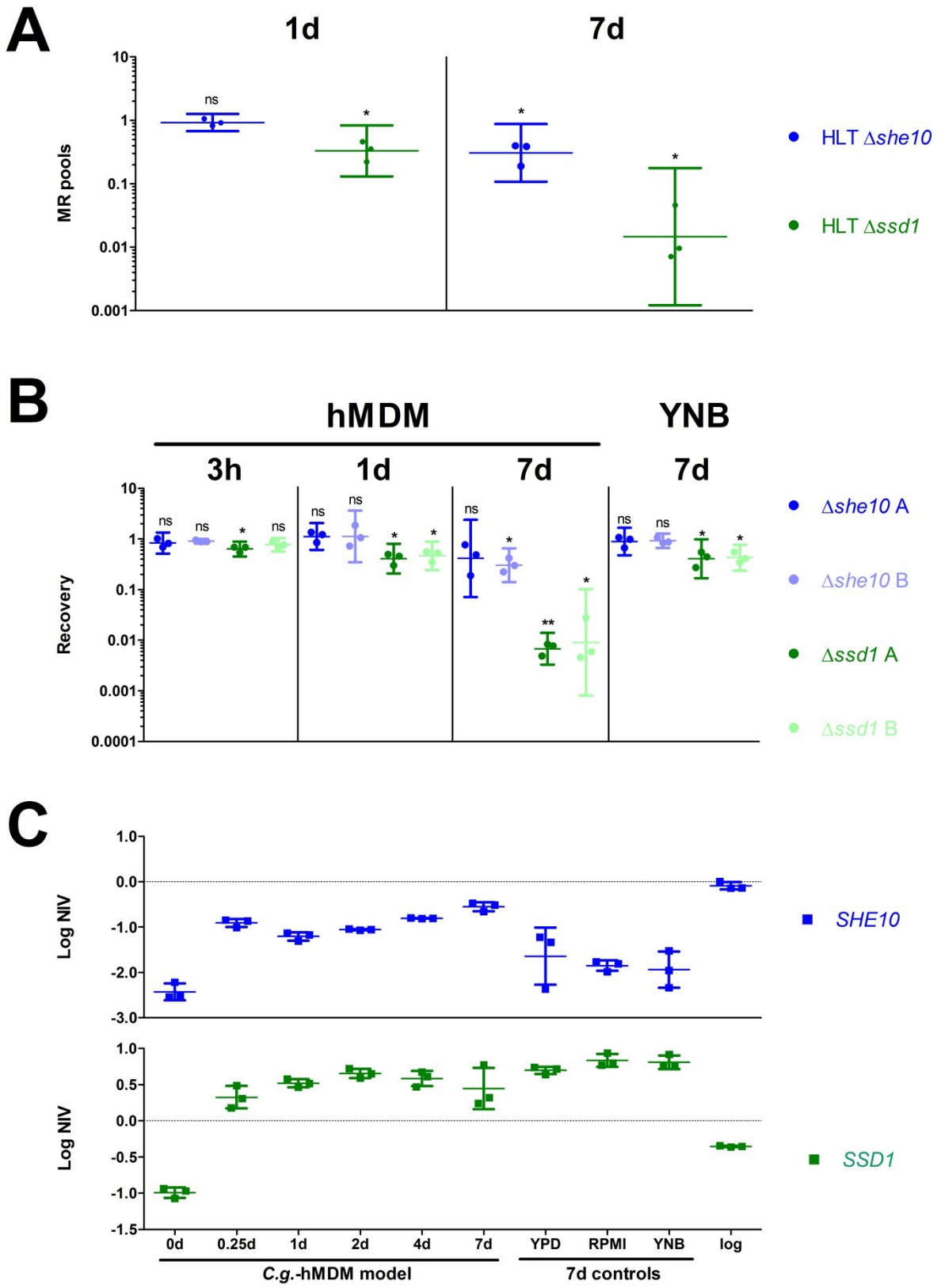

Fig. 10 Summary of test results regarding *C. glabrata SHE10* and *SSD1* genes. A) Mean recovery (MR) results of *C. glabrata* ATCC2001 HLT Δ*ssd1* and *C. glabrata* ATCC2001

HLT Δ*she10* in hMDMs normalized by their reference strain in the mutant pool screening approach. B) Inoculum- and reference strain-normalized recovery of cfus from mutants tested singly in the hMDM persistence model or incubated for 7d in YNB pH6. 3h, supernatant and lysate (uptake process); 1d and 7d, lysate only (persistence stage). Three biological replicates with four technical replicates each. A), B) Bars depict geometric means + 95% confidence interval; dots represent the geometric mean of technical replicates (B) respectively Up and Down barcode (A) for individual biological replicates. Two-tailed, one sample t-test against 0 of log-transformed values; * $p < 0.05$, ** $p < 0.01$, *** $p < 0.001$. C) *SHE10* and *SSD1* transcript levels (log_2FC) relative to YPD logarithmic growth (log) during long-term interaction with hMDMs and in control conditions. Log NIV = log normalized intensity values.

Supplement

Supplemental figures and legends

Suppl. Fig. 1

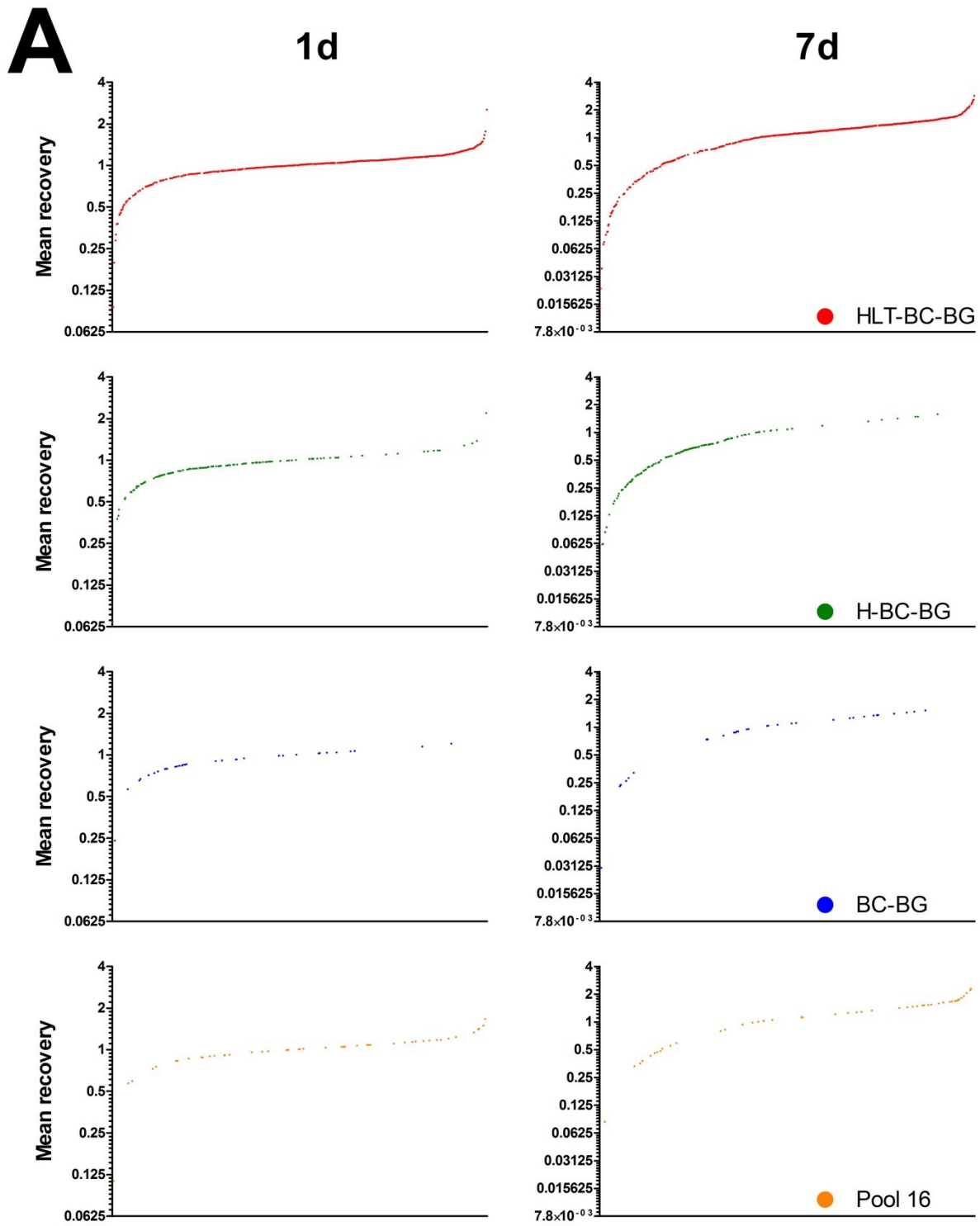

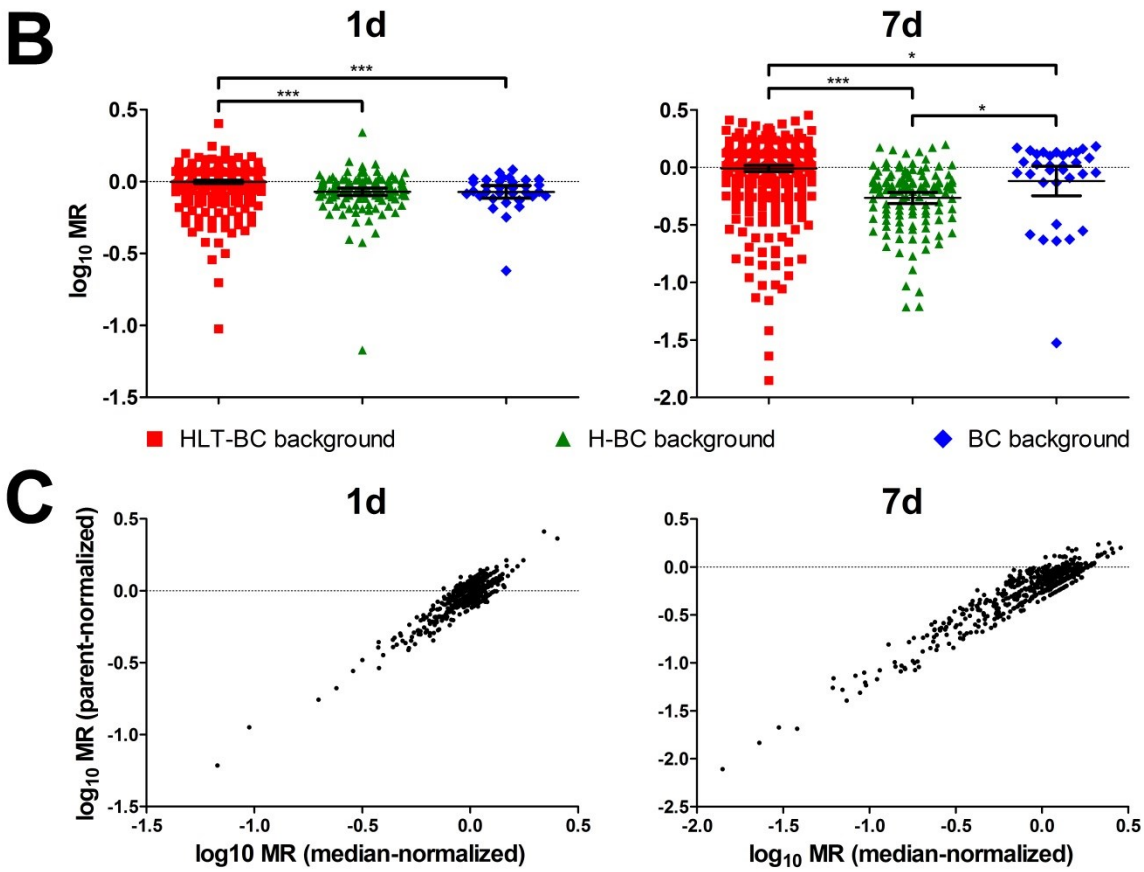

Suppl. Fig. 1 (A) Distribution of mean recovery (MR) scores throughout mutants of either HLT-BC, H-BC, BC background (BG) or from pool 16 from the mutant library in the *C. glabrata*-hMDM persistence model. Values were normalized to their pool sample median and corrected by the strain's inoculum counts. The mutant background partially influenced the distribution pattern. (B) Distribution of $\log_{10}$ MR in dependency of mutant background. Significant differences in mean recovery between reference strains (Fig. 5) are reflected by significant differences between distributions of mutants with different backgrounds. Values were normalized to their pool sample median and corrected by the strains inoculum counts. Bars depict the geometric mean + 95% confidence interval; dots represent the geometric mean of 3 biological replicates for each mutant. Two-tailed, paired Student´s t-test; * $p < 0.05$, ** $p < 0.01$, *** $p < 0.001$. (C) Correlation of enrichment values calculated by different normalization approaches (parent or median normalization). Correlation was good to excellent indicated by Pearson r values ranging from 0.9061 (95% confidence interval 0.8906 to 0.9195, two tailed $p<0.0001$) at day one to 0.9435 (95% confidence interval 0.9340 to 0.9517, two tailed $p<0.0001$) at day seven.

Suppl. Fig. 2

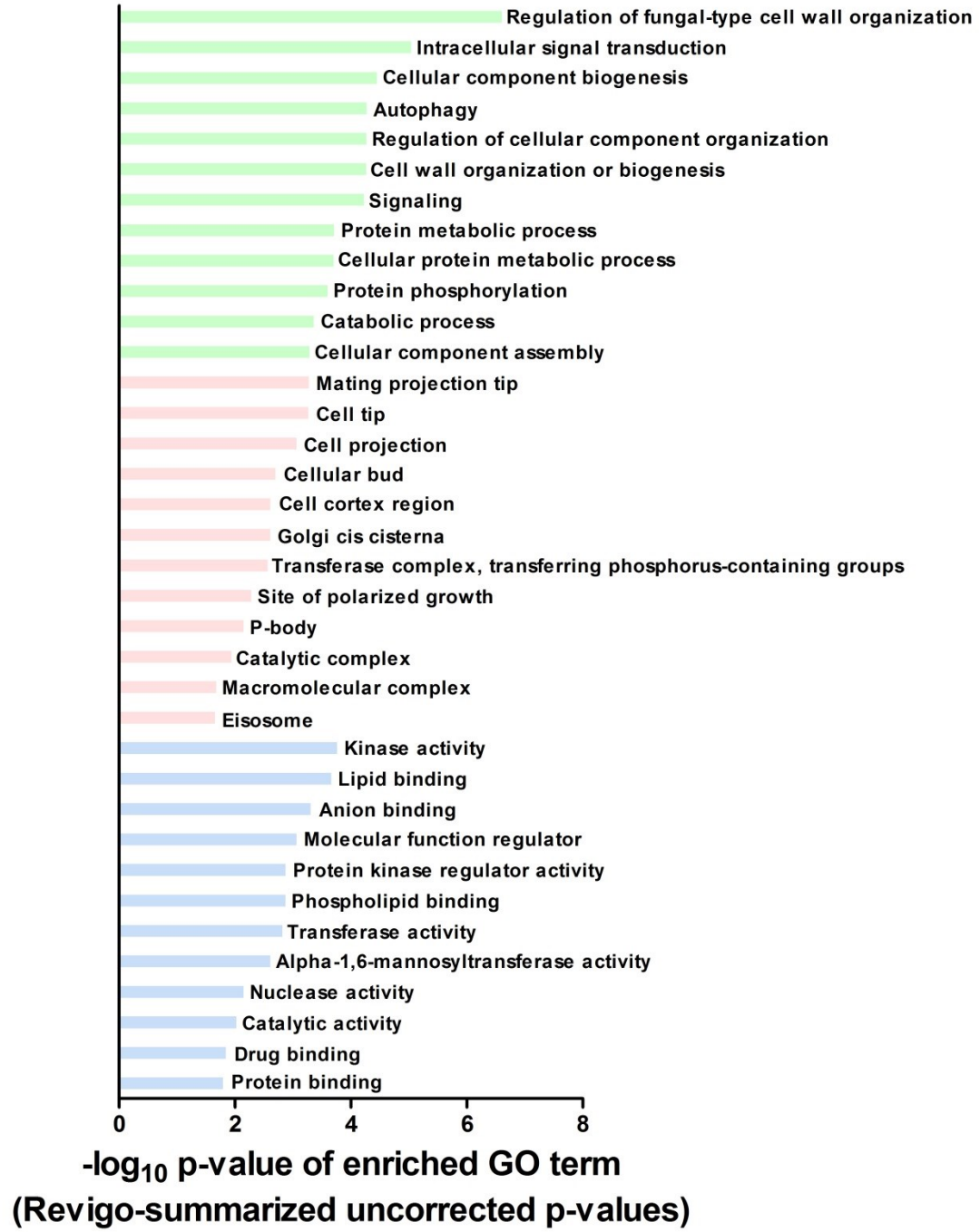

Suppl. Fig. 2 GO term enrichment of genes depleted below a parent-normalized recovery of 0.15 (for at least one barcode, p<0.1; pools 1-15) or a median-normalized recovery of 0.25 (for at least one barcode, p<0.1; pool 16) after seven days. Enriched GO terms were further analysed based on uncorrected p-values (cut-off $p < 0.05$) using Revigo. The top 12 Revigo-summarized GO terms per functional category (biological process, component, molecular function) are shown here (for more information see Suppl. Table 4).

Suppl. Fig. 3

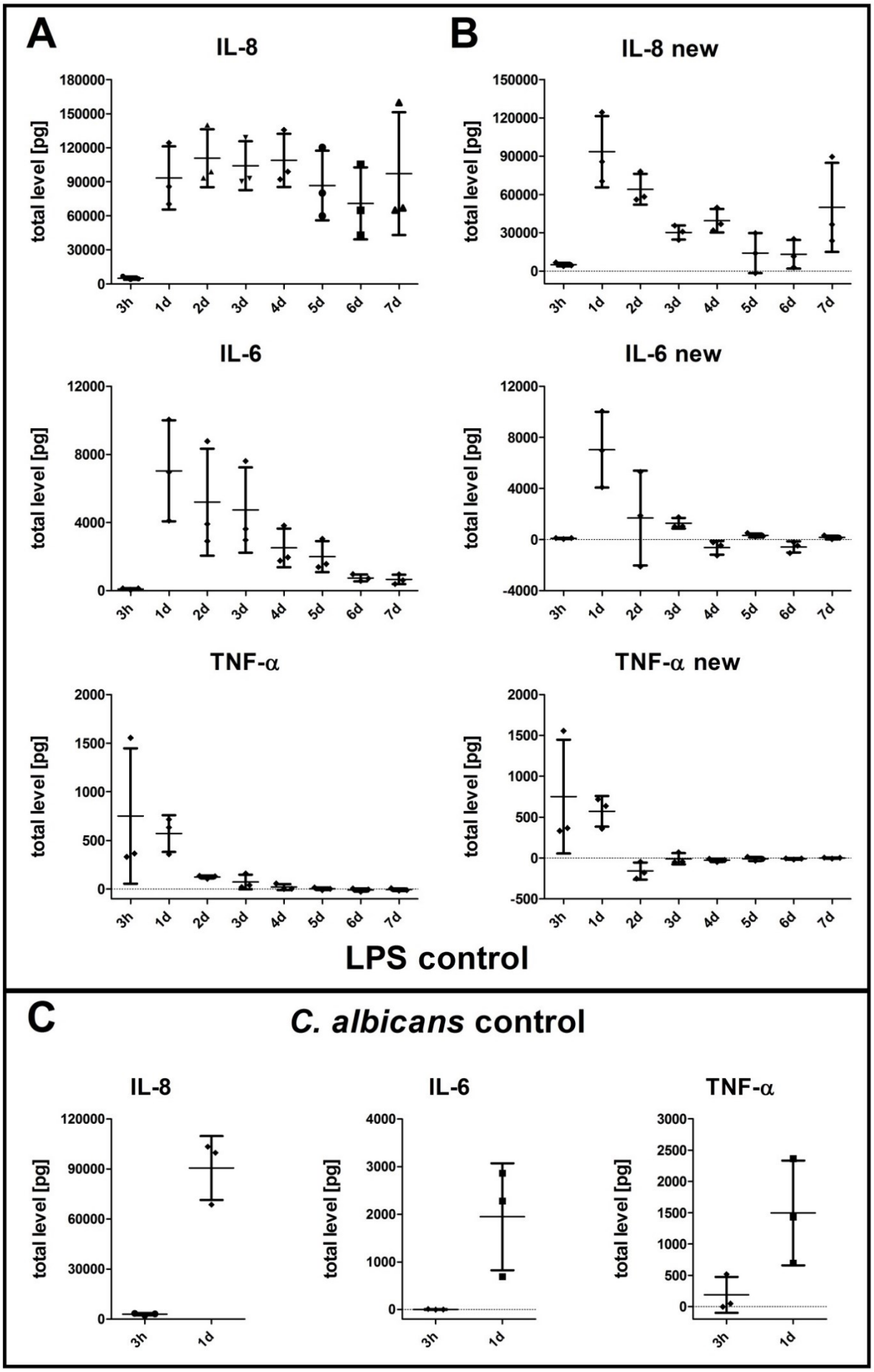
A
IL-8
B
IL-8 new
IL-6
IL-6 new
TNF-α
TNF-α new
total level [pg]
3h
1d
2d
3d
4d
5d
6d
7d
LPS control
C
C. albicans control
IL-8
IL-6
TNF-α

Suppl. Fig. 3 Cytokine secretion patterns of hMDMs in response to LPS (A, B) or *C. albicans* SC5314 (MOI 1, C) in the *C. glabrata*-hMDM persistence model. Note that cytokine levels are influenced by the media exchange strategy used (3h: total exchange, addition of 1 mL medium; 1d: removal of 0.5 mL supernatant and addition of 1 mL medium; on each following day: removal of 0.5 mL supernatant and addition of 0.5 mL medium). (A, C) Total cytokine levels calculated from measured cytokine supernatant concentrations. (B) Calculated amount of newly secreted cytokines since the previous time point. Negative values might indicate cytokine degradation or removal.

Suppl. Fig. 4

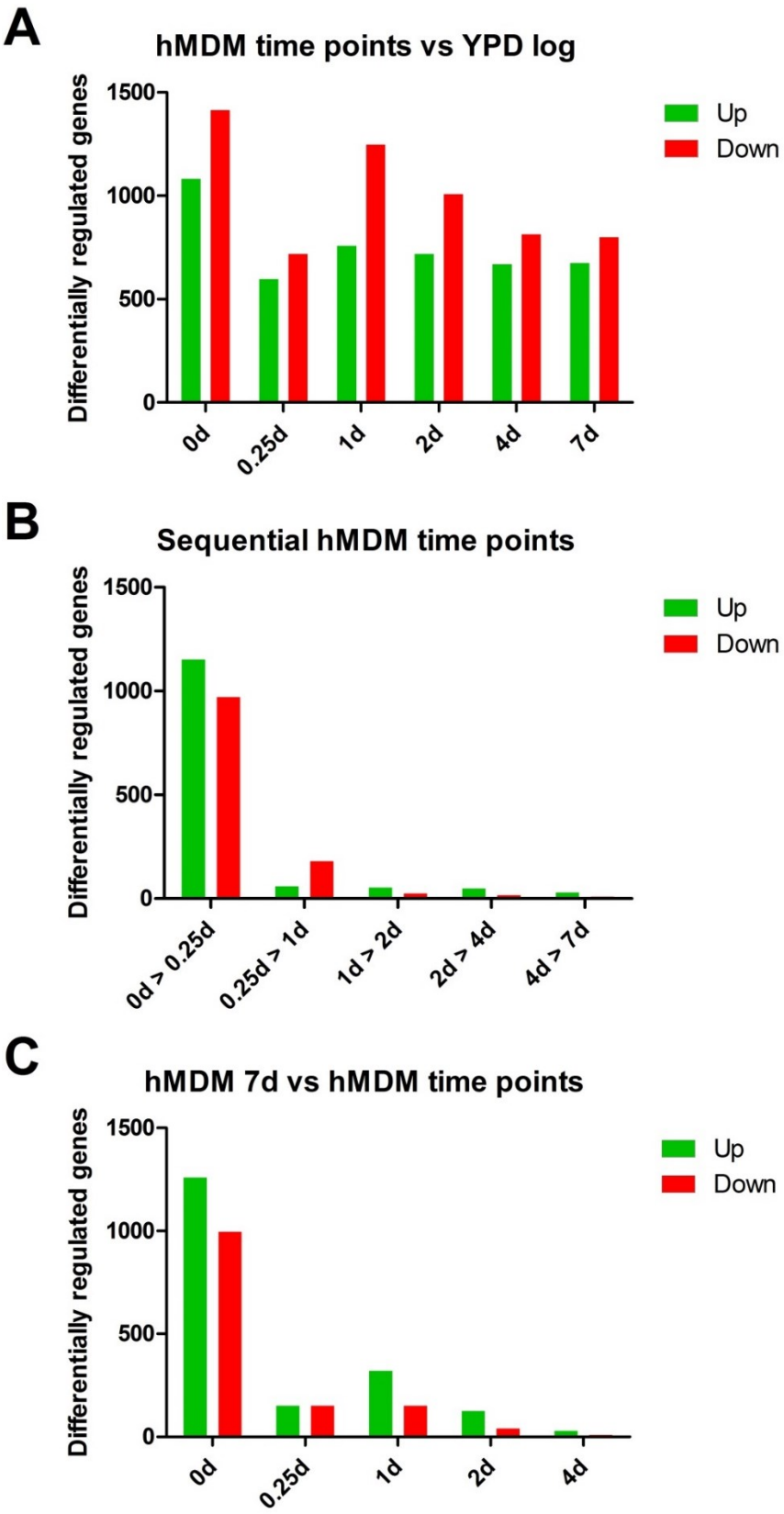

Suppl. Fig. 4 Number of at least twofold ($p<0.1$) up- or down-regulated genes (A) between individual hMDM time points and YPD logarithmic growth, (B) between sequential hMDM time points, and (C) between the hMDM 7d time point and individual hMDM time points.

Suppl. Fig. 5

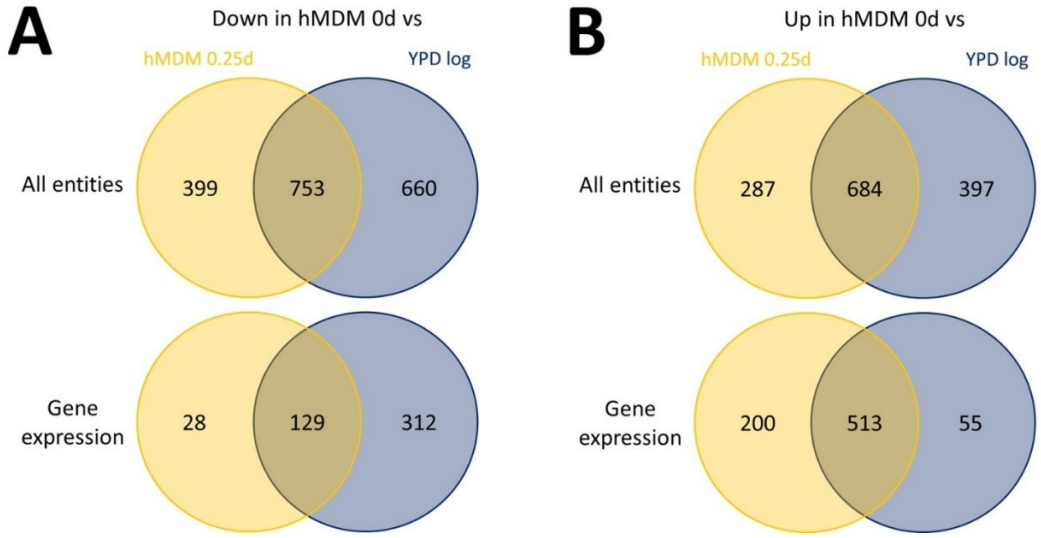

Suppl. Fig. 5 Overlap of at least twofold ($p<0.1$) differentially regulated genes. "All entities" represents all 5205 *C. glabrata* ORFs represented on the microarray, while "Gene expression" represents all 2182 *C. glabrata* ORFs involved in this process (manually curated based on gene expression (associated) GO terms, Suppl. Table 7, lines 93-2324). (A) Downregulated and (B) upregulated genes in hMDMs 0d compared to hMDM 0.25d or logarithmic growth in YPD.

Suppl. Fig. 6

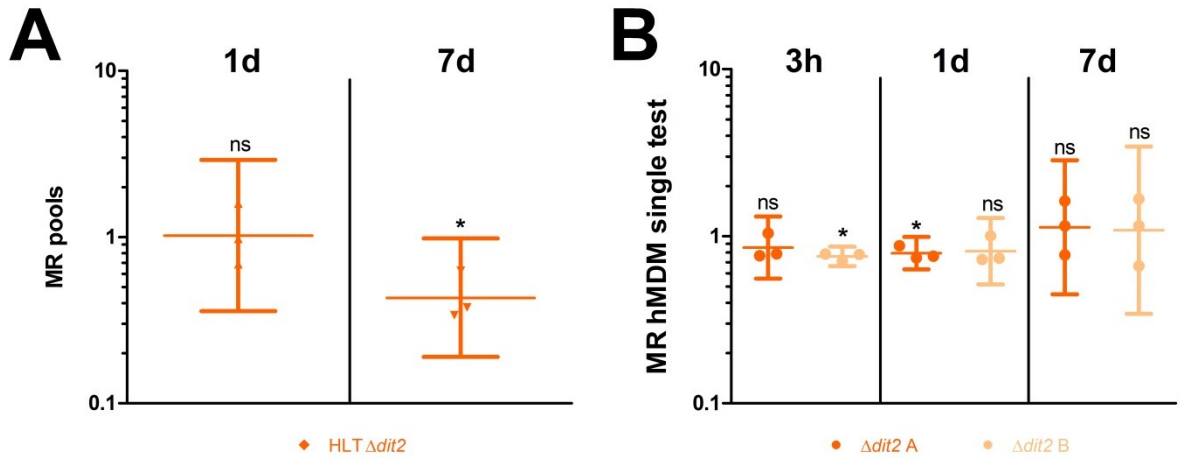

Suppl. Fig. 6 The subtle *C. glabrata* Δ*dit2* pool phenotype does not translate into a robust phenotype in a single mutant test in the hMDM persistence model. A) Mean recovery (MR) results of *C. glabrata* ATCC2001 HLT Δ*dit2* in hMDMs normalized by its reference strain in the mutant pool screening approach. B) Inoculum- and reference strain-normalized recovery of cfus from *C. glabrata* ATCC2001 Δ*dit2* clones tested singly in the hMDM persistence model. 3h, supernatant and lysate (uptake process); 1d and 7d, lysate only (persistence stage). Three biological replicates with four technical replicates each. A), B) Bars depict geometric means + 95% confidence interval; dots

represent the geometric mean of technical replicates (B) respectively Up and Down barcode (A) for individual biological replicates. Two-tailed, one sample t-test against 0 of log-transformed values; * p < 0.05, ** p < 0.01, *** p < 0.001.

Suppl. Fig. 7

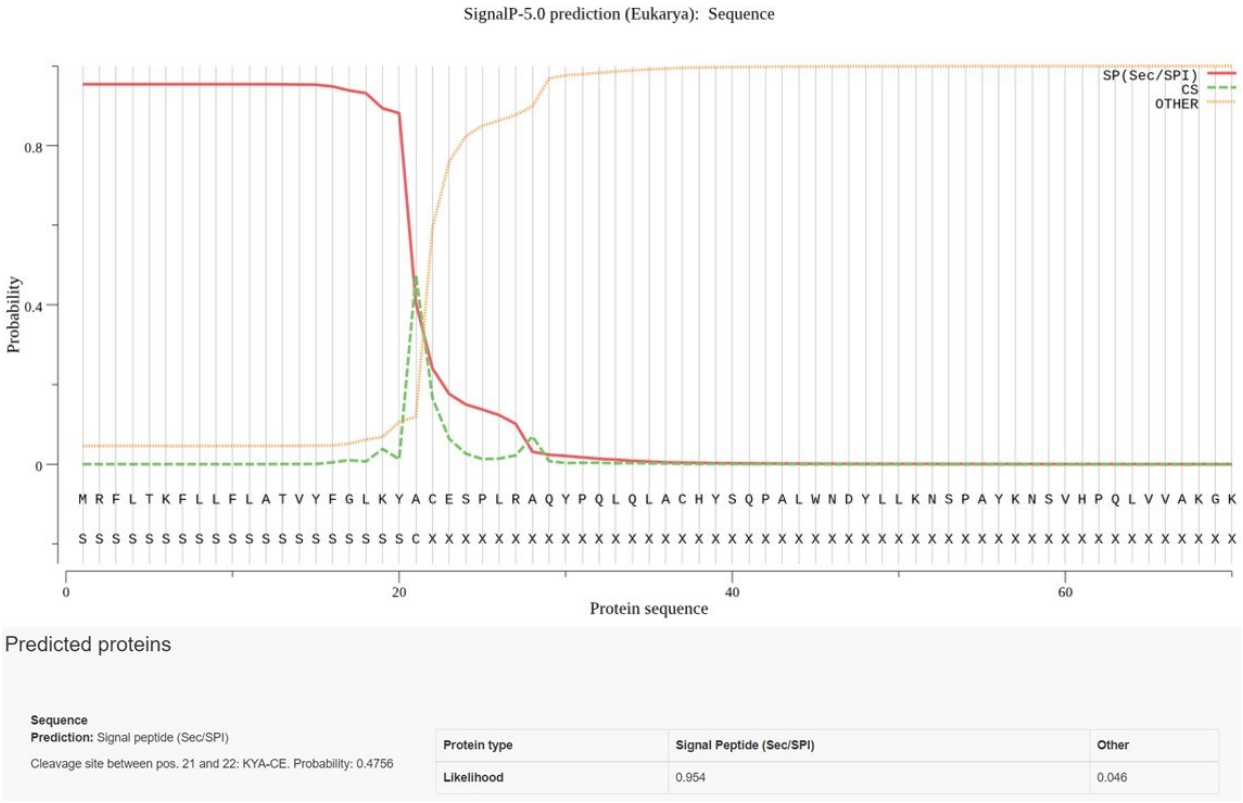

Suppl. Fig. 7 *CgSHE10* signal peptide prediction. Analysis was done using SignalP 5.0 (Almagro Armenteros *et al.* 2019) and similar results were obtained by using Phobius (Käll, Krogh, and Sonnhammer 2004) and Philius 3.0 (Reynolds *et al.* 2008) (not shown).

Suppl. Fig. 8

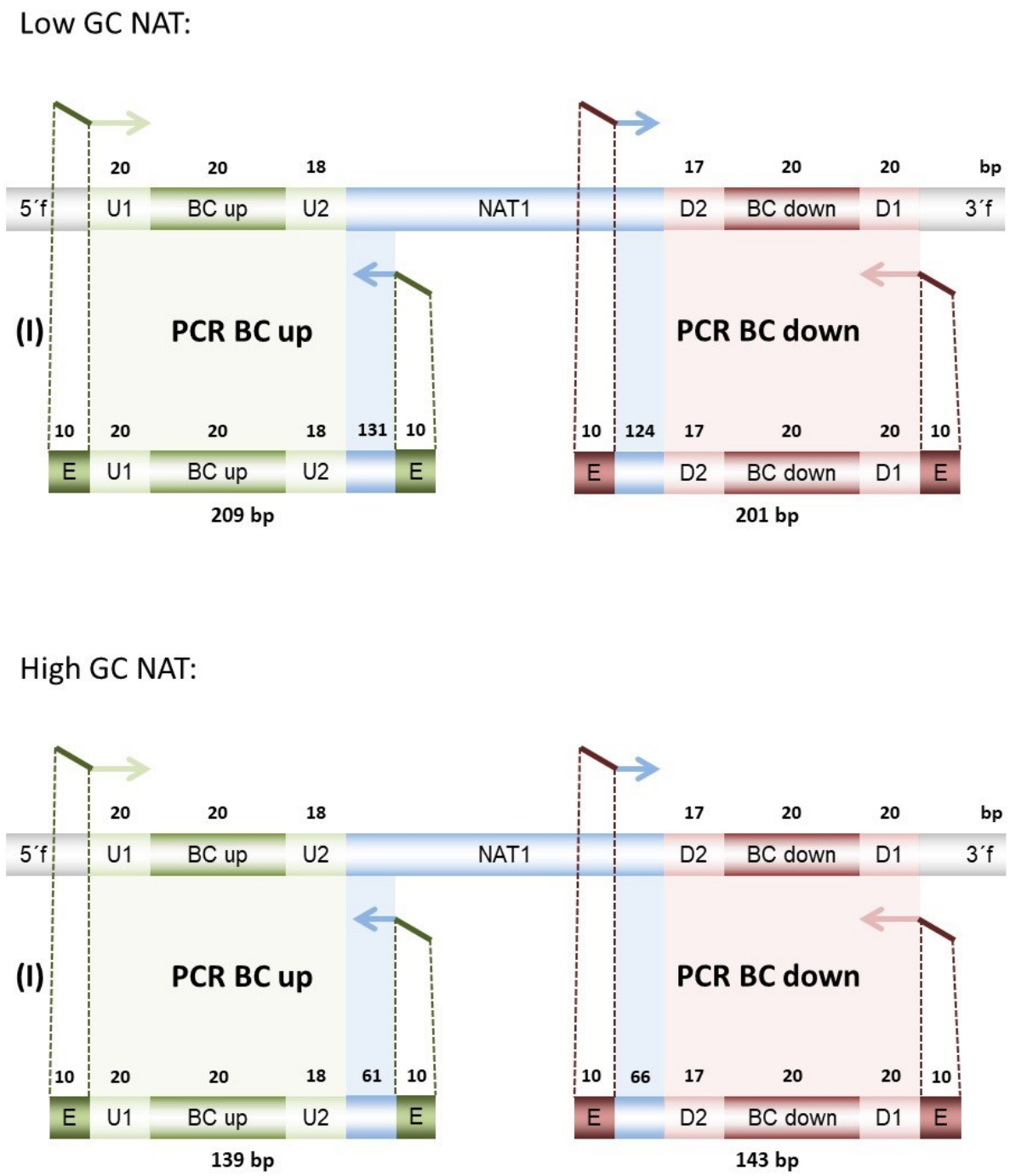

Suppl. Fig. 8 Schematic internal arrangement of "Low GC NAT" and "High GC NAT" cloning cassettes, which were used in (Schwarzmüller *et al.* 2014) in addition to the TEF1P-NAT1-TEF1T cassette (based on pJK863) used in Fig. 4. Arrows indicate primer binding sites for barcode amplification. Note that while all three NAT1 cassettes contain identical U1, U2, D1 and D2 sequences, the NAT1 cassettes and the amplicon sizes differ. For mutants containing the "High GC NAT" cassette, barcode amplification requires a different set of primers (Suppl. Table 2), and therefore, all these mutants were combined in the separate pool 16 (Suppl. Table 1).

Supplemental tables

Suppl. Table 1

C. glabrata mutant pools composition for Bar-Seq analysis originating mainly from (Schwarzmüller *et al.* 2014) and some from (Seider *et al.* 2014; Gerwien *et al.* 2016; Gerwien *et al.* 2017; Kasper *et al.* 2014). Reference strains are always included in pools 1-15, while no reference strain is available for pool 16. Mutants which according to a NGS test run and subsequent Sanger sequencing did not contain the expected barcodes (Schwarzmüller *et al.* 2014) were corrected to the found barcodes (marked in green; applies to 15 mutants). In case we cannot exclude that these mistakes are linked to a false ORF annotation, ORFs are marked in red (12 out of in total 661 strains).

Suppl. Table 2

Primers used for amplification of barcodes.

Suppl. Table 3

C. glabrata-hMDM Bar-Seq mutant analysis: Inoculum and reference strain-normalized mean recovery values after one or seven days incubation in the *C. glabrata*-hMDM persistence model for all *C. glabrata* mutants quantified by Bar-Seq.

Suppl. Table 4

C. glabrata-hMDM Bar-Seq mutant analysis: GO term enrichment of genes depleted below a recovery of 0.5 (pool 16: 0.7; $p<0.1$) after one day (sheet “1d”) or of 0.15 (0.25; sheet “7d_low recovery”; $p<0.05$) or 0.35 (0.5; “7d_intermediate-low recovery”; $p<0.1$) after seven days for at least one barcode. Revigo-summarized GO terms based on uncorrected p-values (cut-off $p < 0.05$) are preceded by “R”.

Suppl. Table 5

Microarray-derived transcriptomes of the *C. glabrata* ATCC2001-hMDM experiment and (long-term) controls. This file includes a list of genes twofold up- or downregulated between the indicated conditions (see “overview” sheet; asymptotic p-value computation, no multiple testing correction of p-values). Reflecting the experimental design, paired t-tests were used for comparisons between hMDM time points, while unpaired t-tests were used for all other comparisons. Statistical significance threshold for inclusion $p < 0.1$, all comparison in direction condition 1 to condition 2. Relative transcript levels were calculated with GeneSpring 14.8 (Agilent).

Suppl. Table 6

GO term analyses of the gene lists in Suppl. Table 5. GO term analyses performed in GeneSpring 14.8 (Agilent) using the GO term annotation of the Candida Genome

Database (Skrzypek *et al.* 2017).

Suppl. Table 7

Microarray-derived transcriptomes of the *C. glabrata* ATCC2001-hMDM experiment and (long-term) controls. This file includes gene expression patterns in relation to YPD log growth respectively the 7d time point in hMDMs. Specific processes can be found in sheet “specific process_YPD log ref”. Compare the following lines to find the desired processes:

Process	**Lines**
Selected pheromone / mating (-associated) genes (list manually curated)	5-89
Gene expression (-associated) processes	93-2324
Cell wall integrity (CWI) and CWI controlling pathways	2328-2423
Glycolysis + gluconeogenesis	2426-2468
Trehalose metabolism	2472-2485
Glycogen metabolism	2488-2510
Iron metabolism	2513-2552
Induced amino acid catabolism and uptake paths	2556-2583
Lipid catabolism and uptake	2587-2655

C. g. gene names in brackets were individually added, mostly based on “best hit” annotations in *S. c.* by the Candida Genome Database (Skrzypek *et al.* 2017), and do not represent official annotations.

Suppl. Table 8

Microarray-derived transcriptomes of the *C. glabrata* ATCC2001-hMDM experiment and (long-term) controls. This file includes enrichment patterns of selected GO terms in twofold up- or downregulated ($p<0.1$) genes in relation to YPD log growth respectively the 7d time point in hMDMs. Compare the following lines to find the desired processes:

Process	**Lines**
Gene expression	6-40
(MAP kinase) signaling	44-53
Cell surface / cell wall	57-63
Cell surface / plasma membrane	67-75
Carbohydrate metabolism (i. a. glycolysis, gluconeogenesis, citrate cycle, glyoxylate cycle, 2-methylcitrate cycle, pentose phosphate shunt, trehalose metabolism, glycogen metabolism)	79-162

Process	Lines
Lipid metabolism	166-240
Mitochondria, respiration	244-255
Autophagy	259-275
Vacuole, vacuolar transport, endocytosis	279-302
Iron homeostasis	306-324
Oxidative stress response	328-349
Nitrogen metabolism > amino acid metabolism	353-450
Cell cycle, DNA replication	454-647

Suppl. Table 9

ATCC2001 Δ*she10* vs wild type ATCC2001 microarray analysis. Number of differentially regulated genes (ATCC2001 Δ*she10* vs wild type ATCC2001) in dependency of growth phase and mathematical calculation method.

Condition	Regulation	2fold regulation	Volcano-Plot (2fold regulation, p<0.1)
YPD log growth	Up	6	2
	Down	20	12
YPD 7d	Up	495	27
	Down	336	25

Suppl. Table 10

ATCC2001 Δ*she10* vs wild type ATCC2001 microarray analysis. This file includes a summary of genes twofold up- or downregulated between the indicated strains and conditions (see “overview” sheet; without p-value computation or with asymptotic p-value computation, no multiple testing correction of p-values, paired t-test, p < 0.1). Relative transcript levels were calculated with GeneSpring 14.8 (Agilent).

Suppl. Table 11

GO term analyses of the gene lists (without p-value computation) in Suppl. Table 10. GO term analyses performed in GeneSpring 14.8 (Agilent) using the GO term annotation of the Candida Genome Database (Skrzypek *et al.* 2017) and GO terms for 7d incubation in YPD (uncorrected p-value < 0.05) were summarized using Revigo (Supek *et al.* 2011). *SHE10* (CAGL0I04092g) was removed from regulated gene lists prior to GO term analysis.

Suppl. Table 12

Lists of wild type strains, mutants (except for pool mutants listed in Suppl. Table 1), oligonucleotides and plasmids used within this study. Apart from being constructed within

this study, strains originate from (Schwarzmüller *et al.* 2014), oligonucleotides originate from (Schwarzmüller *et al.* 2014; Gerwien *et al.* 2016; Sprenger *et al.* 2020) and plasmids originate from (Schwarzmüller *et al.* 2014; Sprenger *et al.* 2020).

Supplemental Methods

Suppl. Method 1: *C. glabrata* mutant generation details

Strain name: ATCC2001 (REF)
Abbreviation: BC
Genotype: ATCC2001 Δ*trp1*::*TRP1-TEF1p-NAT1-TEF1t*

The TEF1P-NAT1-TEF1T cassette originating from pJK863 (Shen, Guo, and Köhler 2005) used in the previous study for construction of mutants in the ATCC2001 Δ*his3* Δ*leu2* Δ*trp1* background [compare Suppl. Table 3 in reference] (Schwarzmüller *et al.* 2014) was PCR amplified from the U1 to the D1 sequence using appropriate primers by in parallel integrating new barcode sequences (in between of U1 and U2 respectively D1 and D2) and at both ends appropriate overlapping end regions with the ends of a Xma I-linearized p*TRP1* plasmid (Sprenger *et al.* 2020) for In-Fusion®HD Cloning Kit (Clontech, Cat. No. #639649)-based cloning of the PCR product into the Xma I-linearized plasmid p*TRP1*. The construct was PCR amplified from successful cloned plasmids and transformed into *C. g.* ATCC2001 Δ*trp1* (Karl Kuchler, unpublished) by using a modified heat-shock based method (heat shock for 15 min at 44°C; (Walther and Wendland 2003)). Mutants were selected on YPD agar plates containing 200 µg/mL Nurseothricin and further checked for prototrophic growth on SD agar.

Strain name: ATCC2001 Δ*his3* (REF)
Abbreviation: H-BC
Genotype: ATCC2001 *HIS3*::*TEF1p-NAT1-TEF1t*

As above, the TEF1P-NAT1-TEF1T cassette was PCR amplified from the U1 to the D1 sequence using appropriate primer by in parallel integrating new unique barcode sequences (in between of U1 and U2 respectively D1 and D2). Additionally, > 500 bp flanking regions of the *HIS3* gene were PCR amplified with primers that added an overlapping sequence with a Xba I-linearized pUC19 on one and a U1 respectively D1 overlapping sequence on the other side. The resultant PCR fragments were fused together and integrated into the Xba I-linearized vector pUC19 using the In-Fusion®HD Cloning Kit (Clontech, Cat. No. #639649). The resultant plasmid pUC19 Δ*his3-NAT1* was

linearized with Xmn I and transformed into *C. glabrata* ATCC2001. Mutants were selected on YPD agar plates containing 200 µg/mL Nurseothricin and further checked for growth inability on synthetic defined medium (SD) agar.

Strain names: ATCC2001 Δ*ssd1* (A / B)
ATCC2001 Δ*dit2* (A / B)
ATCC2001 Δ*she10* (A / B)

Genotypes: ATCC2001 *SSD1*::*TEF1p-NAT1-TEF1t*
ATCC2001 *DIT2*::*TEF1p-NAT1-TEF1t*
ATCC2001 *SHE10*::*TEF1p-NAT1-TEF1t*

All mutants that were investigated in detail were constructed again in the ATCC2001 background. The deletion cassettes from the mutant library clones (Schwarzmüller *et al.* 2014) were amplified together with > 500 bp flanking regions and used for transformation. Mutants were selected on YPD agar plates containing 250 µg/mL Nurseothricin and validated by PCR, Southern Blot and Sanger sequencing of the barcodes.

Suppl. Method 2: PCR programs for PCR amplification of barcodes from mutant pools

PCR program 1: Used for amplification of Up-barcodes from pool 1-15. HF buffer was used for amplification.

Step		Temperature [°C]	Time
1x	Initial Denaturation	98	30 s
10x	Denaturation	98	10 s
	Annealing	60	10 s
	Elongation	72	5 s
18x	Denaturation	98	10 s
	Annealing	68	10 s
	Elongation	72	5 s
1x	Final Elongation	72	5 min
1x	Hold	10	∞

PCR program 2: Used for amplification of Down-barcodes from pool 1-15. HF buffer was used for amplification.

Step		Temperature [°C]	Time
1x	Initial Denaturation	98	30 s
10x	Denaturation	98	10 s
	Annealing	65	10 s
	Elongation	72	5 s
18x	Denaturation	98	10 s
	Annealing	72	10 s
	Elongation	72	5 s
1x	Final Elongation	72	5 min
1x	Hold	10	∞

PCR program 3: Used for amplification of Up- and Down-barcodes from pool 16. GC buffer was used for amplification.

Step		Temperature [°C]	Time
1x	Initial Denaturation	98	30 s
10x	Denaturation	98	10 s
	Annealing	65	10 s
	Elongation	72	5 s
18x	Denaturation	98	10 s
	Annealing	72	10 s
	Elongation	72	5 s
1x	Final Elongation	72	10 min
1x	Hold	10	∞

Suppl. References

Almagro Armenteros, J. J., K. D. Tsirigos, C. K. Sønderby, T. N. Petersen, O. Winther, S. Brunak, G. von Heijne, and H. Nielsen. 2019. 'SignalP 5.0 improves signal peptide predictions using deep neural networks', *Nat Biotechnol*, **37**: 420-23.

Gerwien, F., A. Safyan, S. Wisgott, S. Brunke, L. Kasper, and B. Hube. 2017. 'The Fungal Pathogen Candida glabrata Does Not Depend on Surface Ferric Reductases for Iron Acquisition', *Front Microbiol*, **8**: 1055.

Gerwien, F., A. Safyan, S. Wisgott, F. Hille, P. Kaemmer, J. Linde, S. Brunke, L. Kasper, and B. Hube. 2016. 'A Novel Hybrid Iron Regulation Network Combines Features from Pathogenic and Nonpathogenic Yeasts', *mBio*, **7**.

Käll, L., A. Krogh, and E. L. Sonnhammer. 2004. 'A combined transmembrane topology and signal peptide prediction method', *J Mol Biol*, **338**: 1027-36.

Kasper, L., K. Seider, F. Gerwien, S. Allert, S. Brunke, T. Schwarzmüller, L. Ames, C. Zubiria-Barrera, M. K. Mansour, U. Becken, D. Barz, J. M. Vyas, N. Reiling, A. Haas, K. Haynes, K. Kuchler, and B. Hube. 2014. 'Identification of Candida glabrata genes involved in pH modulation and modification of the phagosomal environment in macrophages', *PLoS One*, **9**: e96015.

Reynolds, S. M., L. Käll, M. E. Riffle, J. A. Bilmes, and W. S. Noble. 2008. 'Transmembrane topology and signal peptide prediction using dynamic bayesian networks', *PLoS Comput Biol*, **4**: e1000213.

Schwarzmüller, T., B. Ma, E. Hiller, F. Istel, M. Tscherner, S. Brunke, L. Ames, A. Firon, B. Green, V. Cabral, M. Marcet-Houben, I. D. Jacobsen, J. Quintin, K. Seider, I. Frohner, W. Glaser, H. Jungwirth, S. Bachellier-Bassi, M. Chauvel, U. Zeidler, D. Ferrandon, T. Gabaldón, B. Hube, C. d'Enfert, S. Rupp, B. Cormack, K. Haynes, and K. Kuchler. 2014. 'Systematic phenotyping of a large-scale Candida glabrata deletion collection reveals novel antifungal tolerance genes', *PLoS Pathog*, **10**: e1004211.

Seider, K., F. Gerwien, L. Kasper, S. Allert, S. Brunke, N. Jablonowski, T. Schwarzmüller, D. Barz, S. Rupp, K. Kuchler, and B. Hube. 2014. 'Immune evasion, stress resistance, and efficient nutrient acquisition are crucial for intracellular survival of Candida glabrata within macrophages', *Eukaryot Cell*, **13**: 170-83.

Shen, J., W. Guo, and J. R. Köhler. 2005. 'CaNAT1, a heterologous dominant selectable marker for transformation of Candida albicans and other pathogenic Candida species', *Infect Immun*, **73**: 1239-42.

Skrzypek, M. S., J. Binkley, G. Binkley, S. R. Miyasato, M. Simison, and G. Sherlock.

2017. 'The Candida Genome Database (CGD): incorporation of Assembly 22, systematic identifiers and visualization of high throughput sequencing data', *Nucleic Acids Res*, **45**: D592-D96.

Sprenger, M., T. S. Hartung, S. Allert, S. Wisgott, M. J. Niemiec, K. Graf, I. D. Jacobsen, L. Kasper, and B. Hube. 2020. 'Fungal biotin homeostasis is essential for immune evasion after macrophage phagocytosis and virulence', *Cell Microbiol*, **22**: e13197.

Supek, F., M. Bošnjak, N. Škunca, and T. Šmuc. 2011. 'REVIGO summarizes and visualizes long lists of gene ontology terms', *PLoS One*, **6**: e21800.

Walther, A., and J. Wendland. 2003. 'An improved transformation protocol for the human fungal pathogen Candida albicans', *Curr Genet*, **42**: 339-43.

Complete supplemental material for this article is included in the enclosed **CD ROM (folder: CgMDM persistence)**. Suppl. Tables 1-8 and 10-12 are Excel files and were therefore not included in the printed version.

2.4 Manuscript IV

The involvement of the *Candida glabrata* trehalase enzymes in stress resistance and gut colonization

Mieke Van Ende, Bea Timmermans, Giel Vanreppelen, Sofía Siscar-Lewin, Daniel Fischer, Stefanie Wijnants, Celia Lobo Romero, Saleh Yazdani, Ona Rogiers, Liesbeth Demuyser, Griet Van Zeebroeck, Yuke Cen, Karl Kuchler, Sascha Brunke, Patrick Van Dijck

Submitted to *PLoS Pathogens*

Summary:
Trehalose is a disaccharide with a well-established double role as a storage and protector molecule in fungi: while its cleavage provides two glucose molecules for support of (re-)growth, the molecule itself stabilizes membranes as well as proteins and hinders denatured protein aggregation; due to these properties, it protects cells against e.g. thermal, oxidative, and antifungal stress. Accordingly, it typically accumulates either in response to or in expectation of stress and in absence of nutrients. However, since trehalose “freezes” membranes and proteins, it also hampers refolding by chaperones after the immediate stress ends. Therefore, a fast breakdown of trehalose is critical to start regrowth after stress relief. *C. glabrata* is assumed to possess three trehalase enzymes: the acid trehalase Ath1 and two putative cytoplasmic neutral trehalases, Nth1 and Nth2. In this study, we confirm previous findings that Ath1 acts on extracellular trehalose. In agreement with a putative role in stress recovery, Nth1 was found to be important for resistance against oxidative stress. While all single deletion mutants of trehalase encoding genes individually showed a persistence defect in human monocyte-derived macrophages, only a triple deletion mutant showed lowered colonisation in a murine gut colonisation model and a somewhat decreased ability to cause clinical symptoms in a systemic murine infection model. In summary, this study provides new insights into the role of trehalose metabolism in fungal stress resistance and pathogenicity mechanisms.

Own Contribution:
Daniel Fischer had developed the model used in parts in this work, took part in planning and supervision of the *C. glabrata* survival/persistence tests in macrophages, generated and evaluated the transcriptome data of *C. glabrata* in human MDMs, and proof-read the manuscript.

Estimated authors' contributions:

Mieke Van Ende	30%
Bea Timmermans	30%
Giel Vanreppelen	7%
Sofía Siscar-Lewin	5%
Daniel Fischer	3%
Stefanie Wijnants	2%
Celia Lobo Romero	2%
Saleh Yazdani	2%
Ona Rogiers	2%
Liesbeth Demuyser	2%
Griet Van Zeebroeck	2%
Yuke Cen	2%
Karl Kuchler	2%
Sascha Brunke	2%
Patrick Van Dijck	7%

Prof. Bernhard Hube

The involvement of the *Candida glabrata* trehalase enzymes in stress resistance and gut colonization

Authors

Mieke Van Ende ¶, Bea Timmermans ¶, Giel Vanreppelen, Sofía Siscar-Lewin, Daniel Fischer, Stefanie Wijnants, Celia Lobo Romero, Saleh Yazdani, Ona Rogiers, Liesbeth Demuyser, Griet Van Zeebroeck, Yuke Cen, Karl Kuchler, Sascha Brunke, Patrick Van Dijck

¶ These authors contributed equally to this work.

Abstract

Candida glabrata is an opportunistic human fungal pathogen and is frequently present in the human microbiome. It has a high relative resistance to environmental stresses and several antifungal drugs. An important component involved in microbial stress tolerance is trehalose. In this work, we characterized the three *C. glabrata* trehalase enzymes Ath1, Nth1 and Nth2. Single, double and triple deletion strains were constructed and characterized both *in vitro* and *in vivo* to determine the role of these enzymes in virulence. Ath1 was found to be located in the periplasm and was essential for growth on trehalose as only carbon source, while Nth1 on the other hand was important for oxidative stress resistance, an observation which was confirmed by the lower survival rate of the *NTH1* deletion strain in human macrophages. No significant phenotype was observed for Nth2. The triple deletion strain was unable to establish a stable colonization of the gastrointestinal (GI) tract in mice. Furthermore, this strain had an attenuated virulence upon systemic infection in mice.

Author Summary

Candida glabrata is a fungus causing both superficial as well as life-threatening infections in humans. Most vulnerable are intensive care unit patients, elderly or transplant recipients due to an impaired immune system. At present, only few antifungal drug classes are available to treat these infections and resistance against these drugs is rising. Therefore, there is an urgency for the development of new antifungal drugs. This work focused on the investigation of a biological pathway used by *C. glabrata* to deal with stressors encountered in the human body: the trehalose metabolism. We characterized different enzymes involved in this pathway and discovered that removing three enzymes at the same time causes a decrease in virulence. This study provides new insights in the stress resistance of *C. glabrata* and opens up future possibilities to discover new antifungal drugs to tackle the fungus.

Introduction

Annually, invasive fungal infections cause 1.5 million deaths [1, 2]. *Candida* species are among the most frequently isolated human fungi, with a mortality rate of up to 50% [1, 3, 4]. Of all *Candida* spp., *Candida albicans* is isolated most frequently [5]. However, the introduction of fluconazole as the first line antifungal used in the clinic caused a decrease in the number of *C. albicans* infections and introduced an increase in infections caused by inherently more fluconazole tolerant species, such as *Candida glabrata* [5-8]. *C. glabrata* bloodstream infections are associated with high mortality rates and therefore, this fungus is becoming a major threat in hospitals [9, 10]. The most important virulence factors of *C. glabrata* are its capacity to grow very rapidly at 37°C, adherence to various substrates and subsequent biofilm formation, its ability to intrinsically tolerate certain antifungal drugs, and its rapid adaptation to stresses [11-13]. In the human body, environmental stresses are ubiquitous, such as nutrient limitation and stress imposed by the host immune response. This activates the *C. glabrata* general stress response, which includes the induction of genes encoding enzymes involved in trehalose metabolism [14]. Trehalose is a non-reducing glucose disaccharide with a double role in fungi. It serves as a storage carbon source but is also crucial as a stress protectant molecule by stabilizing proteins and membranes, thereby causing resistance to antifungal drugs, oxidative stress and heat stress [15-21]. The trehalose biosynthesis pathway is defined by two main enzymes: trehalose-6-phosphate synthase (Tps1) and trehalose-6-phosphate phosphatase (Tps2). Tps1 converts uridine diphosphate (UDP)-glucose and glucose-6-phosphate into trehalose-6-phosphate (T6P) and UDP, after which Tps2 hydrolyzes T6P into trehalose and free phosphate (Fig S1). Trehalose as well as the enzymes linked to its biosynthesis have been described to be involved in virulence and pathogenesis, with functions in infection, biofilm formation, etc. [21-28]. Despite their absence in the human body and their long-known role in virulence, still no Tps1 or Tps2 inhibitor has been discovered and brought to clinical trials or to the clinic. As trehalose accumulates under stress conditions and thereby ‘freezes’ proteins and membranes, a fast hydrolysis of trehalose upon relief of stress is essential to resume growth in *Saccharomyces cerevisiae* [29, 30]. This hydrolysis is mediated by trehalase enzymes. Fungal species generally have two trehalase enzymes: a neutral and an acid trehalase enzyme. In the yeast model organism *S. cerevisiae*, the neutral trehalase enzyme *Sc*Nth1 is regulated by cAMP-dependent phosphorylation and ensures endogenous trehalose metabolization [31-33]. It requires divalent cations (Ca2+ and Mn2+) and has a pH optimum of 7 [34, 35]. This neutral trehalase shows higher activity during exponential growth on fermentable carbon sources and is located in the cytoplasm of the cells [36]. On the other hand, fungal acid trehalase enzymes contain either a

transmembrane domain or a signal peptide and are therefore located on the outside of the fungal cell; in the cell membrane, periplasm or cell wall [37-39]. The extracellular localization ensures hydrolysis of external trehalose [39-41]. In *S. cerevisiae*, the acid trehalase enzyme is also present in the vacuole [37, 38]. The acid trehalase enzyme has an optimal pH of 4.5 and is not regulated by cAMP, phosphorylation or divalent cations [36].

Based on sequence homology with the *S. cerevisiae* trehalase enzymes, the *C. glabrata* genome encodes three trehalase enzymes: Ath1, Nth1 and Nth2. *C. glabrata* very rapidly hydrolyzes extracellular trehalose, a feature which is used in the clinic to diagnose *C. glabrata* infections in a quick and cost-effective way [42-48]. Recently, Ath1 (CAGL0K05137g) was found to be responsible for this extracellular trehalose fermentation [41]. The Ath1 orthologues in *C. albicans* (*CaATC1*) and *C. parapsilosis* (*CpATC1*) were found to be involved in virulence and stress resistance. The *CaATC1* and *CpATC1* deletion strains showed both an increased thermotolerance and an increased resistance towards oxidative stress [49-51]. Whereas these results would suggest an increase in virulence, this was not observed using a systemic mouse model, where these deletion strains showed a reduced virulence [49, 51]. The *C. glabrata* neutral trehalases, Nth1 (CAGL0M10439g) and Nth2 (CAGL0C04323g) are considered to be cytosolic trehalases responsible for the hydrolysis of intracellular trehalose. In *C. albicans*, deletion of the neutral trehalase *CaNTC1* does not affect virulence in a mouse model of systemic infection [52].

Based on the importance of the trehalose metabolism for virulence in other pathogenic fungi and the observation that *C. glabrata* consumes extracellular trehalose very rapidly, we aimed to characterize the *C. glabrata* trehalase enzymes [49-51]. Therefore, we constructed the single, double and triple trehalase deletion strains. To our knowledge, there are no prior publications in which a mutant lacking all three trehalase enzymes in a pathogenic yeast strain is characterized. To characterize the trehalases and to investigate the role of trehalose breakdown in virulence, *in vitro* growth of the deletion strains was first assessed on different relevant fermentable carbon sources. We confirm the data of Zilli, Lopes [41], where it was shown that the acid trehalase Ath1 is required for utilization of exogenous trehalose. Moreover, we show that this enzyme is present in the periplasm. Hence, we hypothesized that the Ath1 enzyme could play a role in colonization of the human gut. To test this, we infected the gastrointestinal tract of mice with the different *C. glabrata* trehalase deletion strains and followed the colonization over time. In contrast to our expectation, the *ath1*Δ mutant showed a wild type phenotype, whereas the triple deletion strain was unable to form a stable colonization of the GI tract. Next, we assessed the role of the trehalases in the stress response. In contrast to the

situation in *C. albicans* and *C. parapsilosis* [50, 53], we show that *C. glabrata* Nth1 is involved in the oxidative stress response. As *C. glabrata* has the capability to survive and replicate in immune cells, the trehalase mutant strains were tested for survival in human macrophages. After four days, the single deletion strains and the triple deletion strain showed a reduced survival in the macrophages compared to the wild type. Finally, we also tested the single trehalase deletions and the triple deletion strain for virulence in a mouse model of systemic infection. A small, yet significant increase in mortality rate was observed for the *nth1*Δ strain whereas the mice infected with the triple deletion strain appeared healthier. Together, these results indicate that the trehalase enzymes could be a good target for the development of new antifungal drugs. However, targeting only one of the enzymes is expected to be insufficient or not effective. Targeting all three trehalase enzymes with a competitive inhibitor could be more profitable.

Results

C. glabrata *trehalase enzymes are phylogenetically closely related to* S. cerevisiae *trehalase enzymes*

Despite what its name suggests, *C. glabrata* is more related to species within the *Saccharomycetaceae* clade than to species within the *Candida* clade [54, 55]. Therefore, we used the *S. cerevisiae* trehalase protein sequences in a BLASTP search to identify the *C. glabrata* trehalase enzymes. In this manuscript, genes/proteins of other species than *C. glabrata* are indicated with a prefix. For the neutral trehalases *Sc*Nth1 (YDR001C) and *Sc*Nth2 (YBR001C), the *C. glabrata* Nth1 (CAGL0M10439g) and Nth2 (CAGL0C04323g) were identified as closest orthologs respectively. These proteins are highly conserved to their *S. cerevisiae* orthologs, as reflected by the high percentage of amino acid identity (80% for Nth1 and 68% for Nth2). As is the case for *S. cerevisiae*, Nth1 and Nth2 are highly similar with one another (71% amino acid identity), indicating that these enzymes are most probably the result of the whole genome duplication event [56]. NTH1 encodes for a polypeptide of 769 amino acids with a molecular mass of 87.4 kDa, while NTH2 encodes for a polypeptide of 750 amino acids with a molecular mass of 86.5 kDa. Both Nth1 and Nth2 amino acid sequences contain neither a transmembrane domain nor a signal sequence [57, 58]. Alignment of Nth1 with *Ca*Nth1 (CR_00560W_A) shows 58% amino acid identity, reflecting the more distant phylogenetic relationship between *C. glabrata* and *C. albicans*.

For the acid trehalase *Sc*Ath1 (YPR026W), Ath1 (CAGL0K05137g) was found as an ortholog in *C. glabrata*, sharing 67% amino acid identity. *ATH1* encodes for a polypeptide of 1212 amino acids and 136.5 kDa. In contrast, alignment of Ath1 with *Ca*Atc1 (C1_06940C_A) showed only 41% amino acid identity. In other organisms, Ath1 was

often found on the extracellular side of the cells [37, 39, 40, 51, 59, 60]. Hence, the PROTTER and the SignalP4.1 algorithms were used to predict a possible transmembrane domain or a signal sequence [57, 58]. No signal peptide was found, but Ath1 is predicted to contain one transmembrane (TM) domain at the N-terminus (between positions 83 and 103). The orthologous N-terminus and TM domain of *Sc*Ath1 confers the extracellular localization, suggesting identical extracellular localization for Ath1 in *C. glabrata* [37].

To represent the evolutionary relationship, we constructed a phylogenetic tree of the different fungal trehalase enzymes and also included the human trehalase enzyme (Fig 1). Two main clusters can be distinguished: the neutral trehalases and the acid trehalases. The *C. glabrata* neutral trehalases Nth1 and Nth2 are closely related to *S. cerevisiae Sc*Nth1 and *Sc*Nth2 respectively. The acid trehalase Ath1 is most related to *Sc*Ath1. Again, this is not unexpected as these species share a close evolutionary relationship [54, 55].

Disruption of the C. glabrata *trehalase encoding genes*

ATH1, *NTH1* and *NTH2* were deleted by the introduction of a deletion cassette consisting of 100 base-pare upstream and downstream homologous sequences of the trehalase open reading frames flanking a nourseothricin N-acetyl transferase (NAT) cassette mediating resistance towards nourseothricin between flippase recognition target (FRT) sites (Fig S2). After insertion and selection on nourseothricin, transformants were checked by PCR using primers outside the region of homologous recombination. For correct deletion strains, the NAT cassette was subsequently removed by the introduction of a plasmid for expression of a flippase. Removal of the cassette was verified by PCR using the outside primers. In this way, the three deletion cassettes could be reused for the construction of both the double and triple deletion strains. Finally, we constructed three independent mutants for the single, double and triple deletion strains which were verified by sequencing.

Ath1 is required for growth on trehalose as a carbon source

As a first step of the in vitro characterization of the constructed mutants, we tested the growth of the strains in minimal medium supplemented with glucose or trehalose, two carbon sources that *C. glabrata* is able to ferment [61]. All strains grew to the same extent on glucose in both solid and liquid medium (Figs 2A-B). When trehalose was used as external carbon source, the growth of all strains lacking *ATH1* had a growth defect in both liquid and solid medium (Figs 2A and 2C). These results indicate that Ath1 is responsible for the hydrolysis of exogenous trehalose, which led to two hypotheses: either *C. glabrata* transports extracellular trehalose to the inside of the cell by a trehalose

transporter and Ath1 hydrolyzes the disaccharide intracellularly, or Ath1 is present at the extracellular side of the cells and hydrolyzes trehalose in the surrounding medium after which glucose is taken up by the glucose transporters. In *S. cerevisiae*, extracellular trehalose is transported by the high-affinity sugar transporter *Sc*Agt1 [62]. Therefore, a BLASTP search was performed using *Sc*Agt1, however no orthologs could be identified in *C. glabrata*. Hence, we measured the concentration of trehalose in the medium over time during the growth on trehalose. We postulated that if Ath1 does indeed hydrolyze trehalose intracellularly after uptake by transporters, a strain deleted for *ATH1* would still show reducing extracellular trehalose levels over time. Yet, for the strains with a deletion of *ATH1*, the trehalose in the medium remained constant (Fig 2D). In contrast, the strains with wild type *ATH1* could still hydrolyze the extracellular trehalose, which is reflected by a drop of trehalose in the medium (Fig 2D). Additionally, coinciding with this decrease in trehalose, a small increase of glucose in the medium was observed, confirming extracellular hydrolysis of trehalose in two glucose molecules (Fig 2E). Taken together, these results suggest that Ath1 hydrolyses extracellular trehalose and thus indicate that Ath1 is present at the cell surface or is secreted. Therefore, we determined its localization by tagging Ath1 endogenously with a fluorescent protein, mCherry. When *C. glabrata* was grown in glucose-containing medium to the exponential phase, no fluorescence was detected. However, when trehalose was used as a carbon source, a signal on the border and in the vacuole of the cells was observed (Fig 3A and data not shown). Next, we investigated whether Ath1 is anchored in the plasma membrane as Ath1 contains one predicted TM domain. Therefore, we generated protoplasts of cells grown in glucose or trehalose containing medium and measured the trehalase activity. The basal activity of the cells grown on glucose is very low and is not affected by protoplast formation. When grown on trehalose, the high trehalase activity observed in untreated cells, dropped dramatically in protoplasts (Fig 3B). In addition, the fluorescent signal observed on the outside of untreated cells, was no longer visible in protoplasts (Fig 3A). These results indicate that Ath1 is not anchored to the cell membrane but is rather present in the periplasmic space or in the cell wall.

The triple deletion strain is unable to stably colonize the gut

As humans cannot produce trehalose, its presence in the gut originates from ingested food or from microorganisms as a result of production or release after microbial death. As Ath1 is required for growth on extracellular trehalose, we hypothesized that this enzyme could give *C. glabrata* cells a competitive advantage over other micro-organisms. To test this hypothesis, we verified whether the deletion strain was able to colonize the gut over a longer period of time in a mouse model. To achieve *Candida* colonization in the gut, mice are frequently treated with antibiotics [63, 64]. As we want

to assess the competition with these other micro-organisms, a pilot experiment was performed in non-treated mice and mice which received ampicillin in their drinking water (1 mg/ml) infecting them via oral gavage with wild type *C. glabrata* (Fig S3). Despite the higher colonization in mice receiving ampicillin, we also obtained a stable colonization in mice where microbial perturbation was not induced (Fig S3). Because of the higher relevance of the latter model, we continued the experiments in untreated mice and tested the trehalase single deletion strains and the triple deletion strain (Fig 4). Similar to the pilot experiment, a stable colonization was obtained for the wild type strain (Fig 4A). The main habitat of *Candida* in the GI tract was in the cecum, which had a log (CFU/g) of around 3 (Fig 4B). The single deletion strains showed a similar colonization as the wild type strain (Fig 4A). The triple deletion strain was not able to establish a stable colonization of the GI-tract, as over 66% of the mice cleared the *C. glabrata* administered at day 21. This trend is clearly reflected in the right panel of Fig 4A. Logically, the average colonization of the cecum of mice which were orally infected with the triple deletion strain was significantly lower, as over 66% of the mice showed no colonies (Fig 4B).

Nth1 is involved in regulation of in vitro oxidative stress resistance and survival in human macrophages.

Inside the human body, fungal pathogens are continuously exposed to different types of environmental stresses [65]. As trehalose is a disaccharide important for stress resistance, we assessed the growth phenotype of the trehalase deletion strains upon stress treatment. Therefore, cells were grown in the presence of different relevant stresses: oxidative stress (H_2O_2), salt stress (NaCl) and cell wall stress (Calcofluor White, CFW). Deletion of *ATH1* and/or *NTH2* did not affect the growth in the presence of these stressors, while strains lacking *NTH1* were more sensitive towards oxidative stress (Fig 5 and Fig S4). The disruption of *NTH1* did not affect growth in the presence of salt nor cell wall stress (Fig S4).

One of *C. glabrata's* virulence traits is its ability to survive and replicate inside human macrophages [66-69]. This survival demands for a high stress resistance as the yeast cells encounter a change in pH, nutrient limitation and oxidative stress within the macrophages [70, 71]. As a difference in oxidative stress resistance was observed for the *nth1*Δ strains, their survival in macrophages was investigated. We used microarrays to obtain the transcriptional response of *C. glabrata* cells to incubation with a macrophage like-murine RAW cell line (Fischer, in preparation). These data showed that in comparison to growth in complex medium, the expression level of the acid trehalase gene *ATH1* was overall very high, slightly dropped during the first hour and went up again (Fig S5A). Furthermore, the expression of *NTH1* and *NTH2* increased within the first

hour of incubation, with the transcript level especially of *NTH2* remaining very high at all later timepoints inside the macrophage-like cells (Fig S5A). We therefore also tested if the deletion of the trehalase enzymes could influence the survival in human macrophages, especially at later timepoints, when trehalose utilization may play an important role. To this end, we infected human monocyte-derived macrophages with the different *C. glabrata* strains at a multiplicity of infection (MOI) of 1:1 for a long-term co-incubation. At different timepoints (3 hours, 1 day and 4 days), the macrophages were lysed and the *C. glabrata* cells were used for transcript determination by microarrays and plated for CFU counting to determine survival (Fig S5B and 6A-D). To ensure the difference in survival was due to killing by macrophages and not to altered uptake or escape and extracellular growth of the *Candida* cells, we measured the uptake rate and ensured that our samples did not contain extracellular *C. glabrata*. The uptake by the immune cells was nearly identical for all trains, with a somewhat increased uptake of *nth2*Δ (Fig 6A). After 3 hours, more *nth1*Δ than wild type yeasts were re-isolated (not statistically significant), while the *nth2*Δ and the triple deletion mutant were found to be slightly reduced in surviving numbers. These small differences were gone after one day of incubation, with the strains adapting to long-term survival (Fig 6C). After 4 days of incubation, all single deletion strains and the triple deletion strain showed a significantly decreased survival (down to 44% for *ath1*Δ, 65% for *nth1*Δ, 35% for *nth2*Δ and 64% for *ath1*Δ *nth1*Δ *nth2*Δ) compared to the wild type strain (Fig 6D). The requirement for these genes in human macrophages was reflected by the continuously increased transcript levels as determined in parallel by microarray experiments (Fig S5B).

Trehalase is involved in in vivo C. glabrata *virulence during a systemic infection*

In order to investigate whether the trehalase enzymes are involved in *C. glabrata* virulence in a systemic infection, mice were infected intravenously with the different deletion strains. Experimental infection of immunocompetent mice with *C. glabrata* generally does not cause mortality [72]. We confirmed this in a pilot experiment during which we determined the optimal concentration of the immunosuppressant dexamethasone (Fig S6). 75 mg/kg dexamethasone was chosen to be given to the mice at day -3, 0, 7 and 14. For each deletion strain, at least 8 mice were included in the experiment (Fig 7). The mice infected with the *nth1*Δ strain appeared ill more rapidly and died earlier compared to the wild type (p-value of 0.0184 in log-rank test). The mice infected with the triple deletion strain showed no significant difference in survival compared to mice infected with the wild type strain (p-value 0.0873 in log-rank test), although they did appear healthier, comparable to the PBS control mice. It should be noted that two mice of the PBS control group died, which is most probably due to the immunosuppression of the mice and the duration of the experiment. The other mice of

the PBS control group showed a healthy appearance throughout the experiment.

Discussion

This work focused on the characterization of the different *C. glabrata* trehalase enzymes and their role in virulence. Comparison with the *S. cerevisiae* trehalase enzymes resulted in the identification of three trehalase enzymes in *C. glabrata*: Ath1, Nth1 and Nth2. When comparing the *C. glabrata* trehalase enzymes to those present in other pathogenic and non-pathogenic fungi two clusters can be distinguished: a cluster of neutral trehalase enzymes and a cluster of acid trehalase enzymes. Both types of these proteins have a different structure: the neutral trehalases contain one large domain for trehalase activity containing the active site and binding site for the substrate, next to a small calcium binding domain. The acid trehalase contains one predicted transmembrane domain and two domains for trehalase activity [73].

Single and multiple deletions of the encoding genes were constructed and functionally characterized. We showed that Ath1 is important for the rapid hydrolysis of extracellular trehalose, a phenotype on which the rapid identification of *C. glabrata* in the hospital is based [42-48]. In different organisms, the acid trehalase enzyme is present on the outside of the cells in order to hydrolyze exogenous trehalose [37, 39, 40, 51, 59, 60]. Our microscopy data, where Ath1 was tagged to a fluorophore, showed that Ath1 is present both on the outside of the cells as well as in the vacuole. Furthermore, high acid trehalase activity was measured in complete cells, which was lost upon preparation of protoplasts. At the same time, the fluorescent signal of the labeled Ath1 at the outside of the cells is lost. This shows that Ath1 is localized in the periplasmic space, similar to the situation in *S. cerevisiae* [37]. We hypothesize that this localization helps the cells to quickly hydrolyze extracellular trehalose to glucose, which is then taken up by the glucose transporters in the plasma membrane [74]. Zilli, *et al.* showed that Ath1 is also secreted to the outside of the cells and is released into the medium [41]. As the activity of Ath1 is very high, we hypothesized that *C. glabrata* cells would have a competitive advantage over other microbes in those conditions where there is trehalose present, such as in the gut. In humans, *Candida* is present in the gastrointestinal tract as part of the normal microbiota [75], hence we hypothesized that Ath1 might play a relevant role in the colonization of *C. glabrata* at this body site. This appeared not to be the case, as in our experiments, the *ath1*Δ strain showed a wild type phenotype in the mouse model of GI colonization. Interestingly, additional deletion of *NTH1* and *NTH2* resulted in a clear drop in GI colonization. This indicates that trehalase activity is indeed important to achieve persistent colonization, however, any of the enzymes could to contribute to this. In *C. albicans* and in *C. parapsilosis*, the acid trehalase Atc1 is a stress-responsive

protein and is important for in vitro stress resistance. Moreover, mice infected intravenously with *C. albicans* or *C. parapsilosis* cells lacking their acid trehalase enzyme show an increased survival, suggesting a role for *ATC1* in virulence [49, 51, 53]. None of these phenotypes are observed for the acid trehalase of *C. glabrata*. However, after 4 days of infection in macrophages, Ath1 seemed to play a role in the survival of *C. glabrata* cells. We hypothesize that through binding to trehalose as a stress protectant, many proteins are cycled to the vacuole for autophagy [68]. As such, it is likely that Ath1 is present in the vacuole which allows trehalose hydrolysis in the vacuole, as is the case in *S. cerevisiae* [37], providing energy to the cells. These data confirm that the function of Ath1 is different from its orthologous enzymes in other *Candida* species, explaining why the specific trehalose test is used to diagnose *C. glabrata*.

Similar to *S. cerevisiae*, *C. glabrata* Nth1 is important for stress tolerance, specifically towards oxidative stress, which is encountered inside immune cells. Deletion of *NTH1* indeed results in a lower survival upon engulfment by macrophages. We hypothesize that the reason for this is the lower tolerance towards oxidative stress for this deletion strain. The role of Nth2 remains unclear. Under in vitro conditions, the *NTH2* gene is rapidly upregulated inside macrophages and its deletion results in a lower survival under these conditions. Its higher expression in macrophages resembles the higher *ScNTH2* expression during the onset of stationary phase growth [76]. This suggests that the cells encounter conditions in the macrophages similar to the ones they encounter when reaching stationary phase. The decreased survival of the mutant strain after 4 days remains to be investigated.

The *ath1*Δ *nth1*Δ *nth2*Δ strain did not show detectable trehalase activity in any growth phases, indicating that these three genes are all the trehalase enzymes present in *C. glabrata*. In general, the triple deletion strain showed results consistent with the single deletion strains. The triple deletion strain showed a decreased survival on hydrogen peroxide and in human macrophages after 4 days of inoculation. Additionally, the triple deletion strain was unable to use trehalose as a carbon source, as is also the case for the *ATH1* deletion strains.

Based on our animal experiments, we can conclude that none of the single enzymes alone constitutes an interesting antifungal drug target, however a combined inactivation of these enzymes is of interest as the triple deletion showed a decreased survival in human macrophages and was fully cleared from the murine GI tract. Additionally, the mice infected intravenously with the triple deletion strain appeared more fit compared to the wild type control. As they share trehalose as a substrate, variants of trehalose may cause inhibition of all three enzymes. As far as the single targets are concerned, inactivation of Ath1 may already be interesting, as this enzyme is required for cells to

grow on trehalose and its deletion results in a decrease in survival inside macrophages. *C. glabrata* infections are frequent in immunocompromised patients, where the endogenous *C. glabrata* can disseminate from the GI tract to cause invasive infection [77]. These results seem promising and therefore, we propose that a drug targeting all three trehalases could have a positive effect on the outcome of a *C. glabrata* infection. As all enzymes have the same substrate, the search for a competitive inhibitor seems the most straight-forward. Structural analogues of trehalose can act as a competitive inhibitor of trehalase [78]. Validamycin A, a well-known trehalase inhibitor, is already used in food crops to prevent fungal infections [79]. This compound showed to have weak antifungal activity against *C. albicans* whereas a strong effect was observed against *A. flavus* [80, 81]. Based on this work, we propose to test different structural analogues of trehalose for their antifungal activity against *C. glabrata*.

Even though humans cannot synthesize trehalose, their genome encodes for one trehalase. The human trehalase enzyme can be found in the intestines and kidneys but also in the urinary tract, where it is used as a marker for renal tubular damage [82, 83]. The human enzyme clusters together with the fungal neutral trehalases (Fig 1). It shows only 27% amino acid identity to both Nth1 and Nth2 of *C. glabrata*, but the amino acids involved in the substrate binding and the active site are conserved (supplementary data). However, a deficiency of the human trehalase is rare and causes diarrhoea due to an intolerance to trehalose enriched food, such as mushrooms [84]. This should be taken into account when looking for competitive inhibitors of the *C. glabrata* trehalase enzymes.

Materials and methods

Construction of phylogenetic tree

To create the trehalase phylogenetic tree, protein sequences were retrieved from the Candida Genome Database (CGD), Saccharomyces Genome Database (SGD), Aspergillus Genome Database (AspGD), UniProt and PomBase [85-89]. In CLC Main Workbench, protein sequences were aligned and the phylogenetic tree was constructed using the unweighted pair method with arithmetic mean (UPGMA) and the Kimura Protein as a protein distance measure [90].

Yeast strains, plasmids, primers and media

The yeast strains, plasmids and primers used in this study are listed in Supplementary Table 1. Yeast cells were grown in either YP (1% yeast extract, 2% bacteriological peptone), synthetic complete (SC) medium (1.7 g/L Difco yeast nitrogen base without amino acids and without ammonium sulphate, 0.79 g/L complete supplement mixture

[CSM; MP Biomedicals], 5 g/L ammonium sulphate), YNB (1.7 g/L Difco yeast nitrogen base without amino acids and without ammonium sulphate, 20 mg/L tryptophan, 20 mg/L histidine, 30 mg/L leucine, 5 g/L ammonium sulphate) or RPMI 1640 medium. These media were supplemented with glucose or trehalose as indicated in the experiment. For solid media, 15 g/L Difco agar granulated was added.

Construction of plasmids

For expression of the flippase enzyme, the nourseothricin cassette of vector pLS9 was replaced by the hygromycin marker resulting in pLS10. The hygromycin marker was amplified using primers C6240 and C6241 from plasmid pgRNA-uni-hph (p58) and subsequently ligated into the NotI digested pLS9. Colonies were checked using primers 7883 and B3220 and verified by sequencing. For localization experiments, the trehalase enzymes were fused to mCherry. Therefore, open reading frames (ORFs) were amplified using primers D84 and D1728 (*ATH1*), D88 and D89 (*NTH1*) or D92 and D93 (*NTH2*) from wild type genomic DNA. The terminators were amplified using primers D86 and D87 (*ATH1*), D90 and D91 (*NTH1*) or D94 and D95 (*NTH2*) from wild type genomic DNA. The corresponding ORF and terminator fragments were inserted in BamHI and XhoI digested pYC56 vector using NEBuilder (New England Biolabs), resulting in the expression vectors pBM13 (*ATH1*), pBM14 (*NTH1*) and pBM15 (*NTH2*). Correct insertion of the ORF fragments was checked using primers C2950 and A9050, insertion of terminator fragments was checked using primers B1222 and A2047. To construct the NTH1 reintegrant, plasmid pBM16 was constructed by insertion of the *NTH1* promoter plus ORF and terminator in vector pYC48. The promoter and ORF were amplified from gDNA using primers D1549 and D1550, the terminator using primers D90 and D91. The products were inserted using NEBuilder (New England Biolabs) into BamHI and KpnI restricted pYC48 respectively. Insertion of the fragments was checked by PCR using primers B4165 and 9064 for promoter plus ORF and primers 9064 and A2047 for insertion of the terminator. The resulting vector was verified by sequencing.

Construction of C. glabrata *strains*

The trehalase deletion strains were constructed in the ATCC2001 *his3*Δ *trp1*Δ *leu2*Δ background [91]. The wild type strain was transformed by electroporation with the deletion cassette (a nourseothricin cassette flanked by FRT sites and a 100 bp region flanking the targeted gene). The deletion cassettes were PCR amplified from the pYC44 plasmid using primers C6315 and C6316 (*ATH1*), C6317 and C6318 (*NTH1*) or C6319 and C6320 (*NTH2*). Cells were plated on YPD agar medium supplemented with 200 µg/mL nourseothricin. Transformants were checked for insertion of the deletion cassette by PCR using control primers C3177 and C3178 (*ATH1*), C3183 and C3184 (*NTH1*) or

C3161 and B3162 (*NTH2*). Correct strains were subsequently transformed with plasmid pLS10 to induce expression of the flippase enzyme (300 µg/ml hygromycin selection). Removal of the nourseothricin cassettes of the transformants was checked by PCR using primers C3177 and C8497 (*ATH1*), C3183 and C3835 (*NTH1*) or C3161 and B2011 (*NTH2*). The pLS10 plasmid was lost by growth on non-selective YPD medium and checked by replating on YPD supplemented with 300 µg/mL hygromycin. The trehalase double and triple mutants were constructed similarly, by transformation of the nourseothricin deletion cassettes mentioned above in the single or double deletion strains respectively, followed by removal of the selective marker by expression of pLS10. Endogenously tagged trehalase strains were constructed by electroporation of the wild type strain with EciI digested plasmid pBM13 (*ATH1*-mCherry), pBM14 (*NTH1*-mCherry) or pBM15 (*NTH2*-mCherry). The resulting transformants were checked using primers C9381 (*ATH1*), C9385 (*NTH1*) or C9388 (*NTH2*) and A9050 (mCherry). The *NTH1* reintegrant strain was constructed by insertion of a cassette consisting of the *NTH1* promoter and ORF, nourseothricin cassette and *NTH1* terminator. Therefore, vector pBM16 was digested with SacII and EciI and the product was transformed into strain BM2 (*nth1*Δ). Correct insertion of the cassette in the genome was checked by PCR using primers B3274 and C4415 (upstream) or 9065 and C8895 (downstream), resulting in strain *Cg*BM8.

Growth phenotype

Growth of the strains was followed in time both in liquid and on solid YNB medium over time. Overnight cultures of the different strains were washed three times with sterile milli-Q water and subsequently diluted to an OD_{600} of 0.1. For growth assays in liquid medium, cells were grown in 50 mL YNB containing either 10 mM of glucose or 10 mM of trehalose as the carbon source. The cells were grown at 37°C with continuous shaking at 200 rpm for 72 hours during which the OD_{600} was monitored. For growth assays on solid medium, a tenfold dilution series of the cultures was spotted on YNB plates containing 5 mM of glucose or 5 mM of trehalose. To investigate the stress response, the cells were spotted on YNB plates supplemented with 100 mM glucose, containing either 6 mM H_2O_2, 1.5 M NaCl or 0.4 mg/mL CFW. The plates were incubated at 37°C for 72 hours during which growth was assessed.

Protoplast preparation

Overnight cultures of the different strains were made in YPD medium. Subsequently, the cultures were grown until mid-exponential phase in YPD (100 mM glucose) or YPT (100 mM trehalose). The cells were collected and washed twice, after which they were incubated for 15 to 45 minutes in the protoplasting solution (600 mM KCl, 800 mM

Sorbitol, 41.7 mM K_2HPO_4, 8.3 mM KH_2PO_4, 4.8 units/mL Zymolase, 9.65 mM β-mercaptoethanol) until the OD_{600} dropped. The cells were collected and washed twice with cold protoplasting buffer (166.8 mM K_2HPO_4, 33.2 mM KH_2PO_4, 800 mM Sorbitol), after which trehalase activity was determined as described below.

Determination of trehalase activity

Trehalase activity was determined as described in Pernambuco, 1996 [92]. In short, crude extracts were incubated with 50 µL of acid trehalose buffer (50 mM trehalose, 200 mM sodium citrate, 2 mM EDTA, pH 4.5). After 30 minutes of incubation at 30°C, the reaction was terminated by boiling for 5 minutes at 90°C. The glucose liberated was determined by the glucose oxidase–peroxidase method. Protein levels were determined by the Lowry method. Trehalase specific activity is expressed as nmol of glucose released per min and mg of protein.

Determination of extracellular compounds

Extracellular glucose and trehalose concentrations during growth were analyzed by the Shimadzu HPLC system using an Agilent 87H column at 0.7 mL/min and a RID-20A detector (Shimadzu).

Fluorescence microscopy

We used a FluoView FV1000 confocal microscope (Olympus IX81) and its software for localization of Ath1. We visualized mCherry with a 559-nm laser and BA575-675 emission filter. A 60x UPlanSApo (numerical aperture [NA], 1.35) objective lens was used.

Expression analysis

Short term analysis in murine cell line macrophages (RAW264.7)

5 X 10^6 RAW264.7 cells (murine macrophage cell line) were seeded in 14 mL DMEM + 10% FBS (PAA laboratories) into 100 mm diameter cell culture petri dishes (TPP, Techno Plastic Products) and incubated for two days with a medium exchange after one day. A *C. glabrata* ATCC2001 overnight culture was pelleted, taken up in DMEM + 100 µg/mL Ampicillin + 100 µg/mL Kanamycin and cell counts were determined. 10^8 *C. glabrata* yeast cells were added per petri dish and infected petri dishes were stored immediately for 30 min on ice for synchronization of phagocytosis. After 30 min, non-adhered yeast were washed away twice with PBS after which 14 mL DMEM + 100 µg/mL Ampicillin + 100 µg/mL Kanamycin was added and co-incubation at 37°C and 5% CO_2 was started. Samples were taken after 0 (directly from ice), 10, 30, 60, 180 and 360 min: non-phagocytosed yeast were washed away twice with PBS and macrophages were lysed

with AE buffer + 1% SDS. Centrifugation (2 min 12.000 g) was used for separation of the fungal cell pellet from macrophagal DNA and RNA. The fungal cell pellet was frozen in liquid nitrogen.

Long term analysis in human monocyte-derived macrophages (hMDMs)

Method details are described in Fischer *et al.* (in preparation). Briefly, hMDM monolayers in RPMI + 10% HS were infected in cell culture flasks (Greiner) with *C. glabrata* ATCC2001 at an MOI of 20 and non-phagocytosed yeasts were washed away with PBS twice after 3 hours of co-incubation. Caspofungin was added after 6 hours of co-incubation and further held constant on a level of 5 µg/mL to hinder extramacrophagal yeast growth. Medium was in part exchanged daily. Samples were taken after 0,25, 1, 2, and 4 days widely similar as above (but with AE + 10% SDS).

RNA isolation, labelling and microarray analysis

Fungal RNA was isolated using a modified freeze-thaw protocol [93]. Optionally, β-mercaptoethanol was used at a final concentration of ≈ 5% in AE buffer for yeast resuspension. The QuickAmp Labelling Kit (Agilent) was used to generate Cy5-labeled cRNA (Cy5 CTP; GE Healthcare). Cy5-labeled samples were co-hybridized with a Cy3-labeled reference (RNA isolated from *C. glabrata* ATCC2001 grown to mid-log phase) on 8-by-15K format arrays (Agilent) and scanned either in Agilent´s High Resolution C Scanner with Scan Control (Agilent) or in a GenePix 4200AL with GenePix Pro 6.1 (Auto PMT, pixel size 5 µm). Microarray data were analysed using GeneSpring 14.8 (Agilent).

Fungal killing by human macrophages

Differentiation of human monocytes into human monocyte-derived macrophages

Preparation of human monocyte-derived macrophages (hMDMs) was done as described previously [94]. Briefly, monocytes were selected from buffy coats by magnetic automated cell sorting of CD14 positive monocytes, seeded in 175 cm^2 cell culture flasks (Greiner) and differentiated over a time period of seven days. At day 7, hMDMs were detached, and 1.5 x 10^5 cells/well were seeded for infection in a 24-well plate in RPMI + 10% FBS (Gibco). The day after, the medium was exchanged to RPMI + 10% human serum (HS; from AB male donors; sterile-filtered, Bio&Sell) with an intermediate PBS washing step.

Macrophage infection with *C. glabrata*

For the preparation of yeast inocula, overnight cultures of *C. glabrata* strains were pelleted, washed twice with PBS and adjusted to 1.5 x 10^6 cells/mL. The macrophages were infected with 1.5 x 10^5 C. glabrata cells (multiplicity of infection (MOI) 1:1). Three

hours after infection, the non-phagocyted cells were washed away and plated to check for phagocytosis efficiency and 1 mL of fresh RPMI + 10% HS was added per well. At this same time point, also the lysate was plated for the 3 hour timepoint. At one and four days, the supernatant was removed without washing, and the hMDMs lysed and plated. From wells intended for four days co-incubation, 0.5 mL of supernatant was removed after one day and 1 mL fresh medium was added (total volume 1.5 mL). On each following day, 0.5 mL was replaced with fresh medium. All wells were constantly checked for appearance of yeast microcolonies by naked eye. Before macrophage lysis and yeast plating, each well was systematically checked for extracellular yeasts with an inverse microscope, and only wells that met the cut-off criteria were used for plating. CFU counts on YPD agar plates were determined manually.

In vivo *mouse model of systemic infection*

The virulence of the different strains was assessed in an *in vivo* mouse model of systemic infection in female BALB/c mice (8 weeks old). The mice were housed in groups of four in filter-top cages in a dedicated animal room where temperature, light and humidity were regulated. The animals received a standard ad libitum diet and water. At day -3, all mice were immunosuppressed with 75 mg/kg dexamethasone (Fagron) through intraperitoneal injection. After this, the animals received the same amount of immunosuppression on day 0 and from then on, every seven days. On day 0, the mice were injected intravenously via the lateral tail vein with 5 x 10^7 *C. glabrata* cells in 200 µL PBS. After this, the infected mice were monitored daily and when they reached humane endpoints, they were euthanized by cervical dislocation under anaesthesia. The survival assay was terminated at day 18 after infection.

In vivo *mouse model of gastrointestinal colonization*

The gut colonization capacity of the different strains was determined in an *in vivo* mouse model of gastrointestinal colonization in female c57BL6/J mice (8 weeks old). The mice were housed in groups of four in filter-top cages in a dedicated animal room where temperature, light and humidity were regulated. The animals received a standard ad libitum diet and water. At day 0, the mice received 10^8 C. glabrata cells via oral gavage. From this day on, stool samples from each mouse were collected during 21 days at the timepoints indicated and plated on CHROMagar™ for CFU counting. The GI colonization is expressed as log(CFU/gram of stool). The gastrointestinal colonization model was terminated at day 21 after gavage. The animals were sacrificed by cervical dislocation under anaesthesia and duodenum, ileum, cecum, proximal colon, distal colon, tongue and kidneys were plated for CFU counting on CHROMagar™.

Ethical statement

Animals were maintained in accordance with the KU Leuven animal care guidelines and all animal experiments were approved by the Ethical Committee for Animal Experimentation of the KU Leuven (project numbers P061/2019 and P010/2020).
Human blood was obtained from healthy human volunteers with written informed consent according to the declaration of Helsinki. The blood donation protocol and use of blood for this study were approved by the Jena institutional ethics committee (Ethik-Kommission des Universitätsklinikums Jena, Permission No 2207–01/08).

Acknowledgements

M.V.E. and B.T. prepared the manuscript and performed the experiments. S.W. performed the mouse macrophage experiments in the lab of K.K. We thank the labs of K.K. and B.H. for the collaborations on the macrophage experiments. We thank Alejandro De Las Peñas and Irene Castaño for kindly sending us plasmids. We acknowledge Nico Vangoethem for assistance in preparation of the figures. All authors contributed to discussion of the results.

References

1. Brown GD, Denning DW, Gow NA, Levitz SM, Netea MG, White TC. Hidden killers: human fungal infections. *Sci Transl Med.* 2012;**4**(165):165rv13. Epub 2012/12/21. doi: 10.1126/scitranslmed.3004404. PubMed PMID: 23253612.

2. des Champs-Bro B, Leroy-Cotteau A, Mazingue F, Pasquier F, François N, Corm S, *et al.* Invasive fungal infections: epidemiology and analysis of antifungal prescriptions in onco-haematology. *J Clin Pharm Ther*. 2011;**36**(2):152-60. Epub 2011/03/04. doi: 10.1111/j.1365-2710.2010.01166.x. PubMed PMID: 21366643.

3. Falagas ME, Apostolou KE, Pappas VD. Attributable mortality of candidemia: a systematic review of matched cohort and case-control studies. *Eur J Clin Microbiol Infect Dis*. 2006;**25**(7):419-25. Epub 2006/06/15. doi: 10.1007/s10096-006-0159-2. PubMed PMID: 16773391.

4. Kang CI, Kim SH, Park WB, Lee KD, Kim HB, Kim EC, *et al.* Bloodstream infections caused by antibiotic-resistant gram-negative bacilli: risk factors for mortality and impact of inappropriate initial antimicrobial therapy on outcome. *Antimicrob Agents Chemother.* 2005;**49**(2):760-6. Epub 2005/01/28. doi: 10.1128/AAC.49.2.760-766.2005. PubMed PMID: 15673761; PubMed Central PMCID: PMCPMC547233.

5. ECDC. Incidence and attributable mortality of healthcare-associated infections in intensive care units in Europe, 2008-2012. Stockholm: *ECDC*. 2018.

6. Diekema D, Arbefeville S, Boyken L, Kroeger J, Pfaller M. The changing epidemiology of healthcare-associated candidemia over three decades. *Diagn Microbiol Infect Dis.* 2012;**73**(1):45-8. Epub 2012/05/15. doi: 10.1016/j.diagmicrobio.2012.02.001. PubMed PMID: 22578938.

7. Pfaller MA, Andes DR, Diekema DJ, Horn DL, Reboli AC, Rotstein C, *et al.* Epidemiology and outcomes of invasive candidiasis due to non-albicans species of

Candida in 2,496 patients: data from the Prospective Antifungal Therapy (PATH) registry 2004-2008. *PLoS One*. 2014;**9**(7):e101510. Epub 2014/07/06. doi: 10.1371/journal.pone.0101510. PubMed PMID: 24991967; PubMed Central PMCID: PMCPMC4081561.

8. Pfaller MA, Diekema DJ, Rinaldi MG, Barnes R, Hu B, Veselov AV, *et al.* Results from the ARTEMIS DISK Global Antifungal Surveillance Study: a 6.5-year analysis of susceptibilities of Candida and other yeast species to fluconazole and voriconazole by standardized disk diffusion testing. *J Clin Microbiol*. 2005;**43**(12):5848-59. Epub 2005/12/08. doi: 10.1128/JCM.43.12.5848-5859.2005. PubMed PMID: 16333066; PubMed Central PMCID: PMCPMC1317207.

9. Malani A, Hmoud J, Chiu L, Carver PL, Bielaczyc A, Kauffman CA. Candida glabrata fungemia: experience in a tertiary care center. *Clin Infect Dis*. 2005;**41**(7):975-81. Epub 2005/09/06. doi: 10.1086/432939. PubMed PMID: 16142662.

10. Panackal AA, Gribskov JL, Staab JF, Kirby KA, Rinaldi M, Marr KA. Clinical significance of azole antifungal drug cross-resistance in Candida glabrata. *J Clin Microbiol.* 2006;**44**(5):1740-3. Epub 2006/05/05. doi: 10.1128/JCM.44.5.1740-1743.2006. PubMed PMID: 16672401; PubMed Central PMCID: PMCPMC1479212.

11. Miyazaki T, Kohno S. ER stress response mechanisms in the pathogenic yeast Candida glabrata and their roles in virulence. *Virulence*. 2014;**5**(2):365-70. Epub 2013/12/18. doi: 10.4161/viru.27373. PubMed PMID: 24335436; PubMed Central PMCID: PMCPMC3956515.

12. Timmermans B, De Las Peñas A, Castaño I, Van Dijck P. Adhesins in Candida glabrata. *J Fungi (Basel)*. 2018;**4**(2). Epub 2018/05/23. doi: 10.3390/jof4020060. PubMed PMID: 29783771; PubMed Central PMCID: PMCPMC6023314.

13. Roetzer A, Gabaldón T, Schüller C. From Saccharomyces cerevisiae to Candida glabrata in a few easy steps: important adaptations for an opportunistic pathogen. *FEMS Microbiol Lett*. 2011;**314**(1):1-9. Epub 2010/09/18. doi: 10.1111/j.1574-6968.2010.02102.x. PubMed PMID: 20846362; PubMed Central PMCID: PMCPMC3015064.

14. Ishchuk OP, Ahmad KM, Koruza K, Bojanovič K, Sprenger M, Kasper L, *et al.* RNAi as a Tool to Study Virulence in the Pathogenic Yeast Candida glabrata. *Front Microbiol*. 2019;**10**:1679. Epub 2019/08/10. doi: 10.3389/fmicb.2019.01679. PubMed PMID: 31396189; PubMed Central PMCID: PMCPMC6667738.

15. Alvarez-Peral FJ, Zaragoza O, Pedreno Y, Argüelles JC. Protective role of trehalose during severe oxidative stress caused by hydrogen peroxide and the adaptive oxidative stress response in Candida albicans. *Microbiology*. 2002;**148**(Pt 8):2599-606. Epub 2002/08/15. doi: 10.1099/00221287-148-8-2599. PubMed PMID: 12177354.

16. Argüelles JC. Why can't vertebrates synthesize trehalose? *J Mol Evol*. 2014;**79**(3-4):111-6. Epub 2014/09/19. doi: 10.1007/s00239-014-9645-9. PubMed PMID: 25230776.

17. Eleutherio EC, Araujo PS, Panek AD. Protective role of trehalose during heat stress in Saccharomyces cerevisiae. *Cryobiology*. 1993;**30**(6):591-6. Epub 1993/12/01. doi: 10.1006/cryo.1993.1061. PubMed PMID: 8306706.

18. Elliott B, Haltiwanger RS, Futcher B. Synergy between trehalose and Hsp104 for thermotolerance in Saccharomyces cerevisiae. *Genetics*. 1996;**144**(3):923-33. Epub 1996/11/01. PubMed PMID: 8913738; PubMed Central PMCID: PMCPMC1207632.

19. González-Párraga P, Sánchez-Fresneda R, Zaragoza O, Argüelles JC. Amphotericin B induces trehalose synthesis and simultaneously activates an antioxidant enzymatic response in Candida albicans. *Biochim Biophys Acta*. 2011;**1810**(8):777-83. Epub 2011/05/17. doi: 10.1016/j.bbagen.2011.04.012. PubMed PMID: 21570449.

20. Lillie SH, Pringle JR. Reserve carbohydrate metabolism in Saccharomyces cerevisiae: responses to nutrient limitation. *J Bacteriol*. 1980;**143**(3):1384-94. Epub 1980/09/01. PubMed PMID: 6997270; PubMed Central PMCID: PMCPMC294518.

21. Tournu H, Fiori A, Van Dijck P. Relevance of trehalose in pathogenicity: some general rules, yet many exceptions. *PLoS Pathog*. 2013;**9**(8):e1003447. Epub 2013/08/24. doi: 10.1371/journal.ppat.1003447. PubMed PMID: 23966851; PubMed Central PMCID: PMCPMC3744402.

22. Argüelles JC, Rodriguez T, Alvarez-Peral FJ. Trehalose hydrolysis is not required for human serum-induced dimorphic transition in Candida albicans: evidence from a tps1/tps1 mutant deficient in trehalose synthesis. *Res Microbiol*. 1999;**150**(8):521-9. Epub 1999/11/30. doi: 10.1016/s0923-2508(99)00105-9. PubMed PMID: 10577485.

23. Fillinger S, Chaveroche MK, van Dijck P, de Vries R, Ruijter G, Thevelein J, *et al.* Trehalose is required for the acquisition of tolerance to a variety of stresses in the filamentous fungus Aspergillus nidulans. *Microbiology*. 2001;**147**(Pt 7):1851-62. Epub 2001/06/29. doi: 10.1099/00221287-147-7-1851. PubMed PMID: 11429462.

24. Ngamskulrungroj P, Himmelreich U, Breger JA, Wilson C, Chayakulkeeree M, Krockenberger MB, *et al.* The trehalose synthesis pathway is an integral part of the virulence composite for Cryptococcus gattii. *Infect Immun*. 2009;**77**(10):4584-96. Epub 2009/08/05. doi: 10.1128/IAI.00565-09. PubMed PMID: 19651856; PubMed Central PMCID: PMCPMC2747965.

25. Petzold EW, Himmelreich U, Mylonakis E, Rude T, Toffaletti D, Cox GM, *et al.* Characterization and regulation of the trehalose synthesis pathway and its importance in the pathogenicity of Cryptococcus neoformans. *Infect Immun*. 2006;**74**(10):5877-87. Epub 2006/09/22. doi: 10.1128/IAI.00624-06. PubMed PMID: 16988267; PubMed Central PMCID: PMCPMC1594924.

26. Van Dijck P, De Rop L, Szlufcik K, Van Ael E, Thevelein JM. Disruption of the Candida albicans TPS2 gene encoding trehalose-6-phosphate phosphatase decreases infectivity without affecting hypha formation. *Infect Immun*. 2002;**70**(4):1772-82. Epub 2002/03/16. doi: 10.1128/iai.70.4.1772-1782.2002. PubMed PMID: 11895938; PubMed Central PMCID: PMCPMC127825.

27. Zaragoza O, Blazquez MA, Gancedo C. Disruption of the Candida albicans TPS1 gene encoding trehalose-6-phosphate synthase impairs formation of hyphae and decreases infectivity. *J Bacteriol*. 1998;**180**(15):3809-15. Epub 1998/07/31. PubMed PMID: 9683476; PubMed Central PMCID: PMCPMC107363.

28. Zhu Z, Wang H, Shang Q, Jiang Y, Cao Y, Chai Y. Time course analysis of Candida albicans metabolites during biofilm development. *J Proteome Res*. 2013;**12**(6):2375-85. Epub 2012/07/28. doi: 10.1021/pr300447k. PubMed PMID: 22834926.

29. Singer MA, Lindquist S. Multiple effects of trehalose on protein folding in vitro and in vivo. *Mol Cell*. 1998;**1**(5):639-48. Epub 1998/07/14. doi: 10.1016/s1097-2765(00)80064-7. PubMed PMID: 9660948.

30. Wera S, De Schrijver E, Geyskens I, Nwaka S, Thevelein JM. Opposite roles of trehalase activity in heat-shock recovery and heat-shock survival in Saccharomyces cerevisiae. *Biochem J*. 1999;**343** Pt 3:621-6. Epub 1999/10/21. PubMed PMID: 10527941; PubMed Central PMCID: PMCPMC1220594.

31. van der Plaat JB. Cyclic 3',5'-adenosine monophosphate stimulates trehalose degradation in baker's yeast. *Biochem Biophys Res Commun*. 1974;**56**(3):580-7. Epub 1974/02/04. doi: 10.1016/0006-291x(74)90643-3. PubMed PMID: 4363744.

32. van Solingen P, van der Plaat JB. Partial purification of the protein system controlling the breakdown of trehalose in baker's yeast. *Biochem Biophys Res Commun*. 1975;**62**(3):553-60. Epub 1975/02/03. doi: 10.1016/0006-291x(75)90434-9. PubMed PMID: 235257.

33. Schepers W, Van Zeebroeck G, Pinkse M, Verhaert P, Thevelein JM. In vivo phosphorylation of Ser21 and Ser83 during nutrient-induced activation of the yeast protein kinase A (PKA) target trehalase. *J Biol Chem*. 2012;**287**(53):44130-42. Epub 2012/11/17. doi: 10.1074/jbc.M112.421503. PubMed PMID: 23155055; PubMed Central PMCID: PMCPMC3531729.

34. Londesborough J, Varimo K. Characterization of two trehalases in baker's yeast. *Biochem J*. 1984;**219**(2):511-8. Epub 1984/04/15. doi: 10.1042/bj2190511. PubMed PMID: 6430270; PubMed Central PMCID: PMCPMC1153508.

35. Thevelein JM. Regulation of trehalose mobilization in fungi. *Microbiol Rev*. 1984;**48**(1):42-59. Epub 1984/03/01. PubMed PMID: 6325857; PubMed Central PMCID: PMCPMC373002.

36. Sánchez-Fresneda R, González-Párraga P, Esteban O, Laforet L, Valentín E, Argüelles JC. On the biochemical classification of yeast trehalases: Candida albicans contains two enzymes with mixed features of neutral and acid trehalase activities. *Biochem Biophys Res Commun*. 2009;**383**(1):98-102. Epub 2009/04/02. doi: 10.1016/j.bbrc.2009.03.134. PubMed PMID: 19336219.

37. He S, Bystricky K, Leon S, François JM, Parrou JL. The Saccharomyces cerevisiae vacuolar acid trehalase is targeted at the cell surface for its physiological function. *FEBS J*. 2009;**276**(19):5432-46. Epub 2009/08/26. doi: 10.1111/j.1742-4658.2009.07227.x. PubMed PMID: 19703229.

38. Parrou JL, Jules M, Beltran G, François J. Acid trehalase in yeasts and filamentous fungi: localization, regulation and physiological function. *FEMS Yeast Res*. 2005;**5**(6-7):503-11. Epub 2005/03/23. doi: 10.1016/j.femsyr.2005.01.002. PubMed PMID: 15780651.

39. Pedreño Y, Maicas S, Argüelles JC, Sentandreu R, Valentín E. The ATC1 gene encodes a cell wall-linked acid trehalase required for growth on trehalose in Candida albicans. *J Biol Chem*. 2004;**279**(39):40852-60. Epub 2004/07/15. doi: 10.1074/jbc.M400216200. PubMed PMID: 15252058.

40. Nwaka S, Mechler B, Holzer H. Deletion of the ATH1 gene in Saccharomyces cerevisiae prevents growth on trehalose. *FEBS Lett*. 1996;**386**(2-3):235-8. Epub 1996/05/20. doi: 10.1016/0014-5793(96)00450-4. PubMed PMID: 8647289.

41. Zilli DM, Lopes RG, Alves SL, Jr., Barros LM, Miletti LC, Stambuk BU. Secretion of the acid trehalase encoded by the CgATH1 gene allows trehalose fermentation by Candida glabrata. *Microbiol Res*. 2015;**179**:12-9. Epub 2015/09/29. doi: 10.1016/j.micres.2015.06.008. PubMed PMID: 26411890.

42. Fenn JP, Billetdeaux E, Segal H, Skodack-Jones L, Padilla PE, Bale M, *et al.* Comparison of four methodologies for rapid and cost-effective identification of Candida glabrata. *J Clin Microbiol*. 1999;**37**(10):3387-9. Epub 1999/09/17. PubMed PMID: 10488214; PubMed Central PMCID: PMCPMC85577.

43. Fraser M, Borman AM, Johnson EM. Evaluation of the commercial rapid trehalose test (GLABRATA RTT) for the point of isolation identification of Candida glabrata isolates in primary cultures. *Mycopathologia*. 2012;173(4):259-64. Epub 2012/01/12. doi: 10.1007/s11046-011-9508-5. PubMed PMID: 22234529.

44. Freydiere AM, Robert R, Ploton C, Marot-Leblond A, Monerau F, Vandenesch F. Rapid identification of Candida glabrata with a new commercial test, GLABRATA RTT. *J Clin Microbiol*. 2003;**41**(8):3861-3. Epub 2003/08/09. doi: 10.1128/jcm.41.8.3861-3863.2003. PubMed PMID: 12904403; PubMed Central PMCID: PMCPMC179766.

45. Land G, Burke J, Shelby C, Rhodes J, Collett J, Bennett I, *et al.* Screening protocol for Torulopsis (Candida) glabrata. *J Clin Microbiol*. 1996;**34**(9):2300-3. Epub 1996/09/01. PubMed PMID: 8862605; PubMed Central PMCID: PMCPMC229238.

46. Lopez J, Dalle F, Mantelin P, Moiroux P, Nierlich AC, Pacot A, *et al.* Rapid identification of Candida glabrata based on trehalose and sucrose assimilation using Rosco diagnostic tablets. *J Clin Microbiol*. 2001;**39**(3):1172-4. Epub 2001/03/07. doi: 10.1128/JCM.39.3.1172-1174.2001. PubMed PMID: 11230452; PubMed Central PMCID: PMCPMC87898.

47. Murray CK, Beckius ML, Green JA, Hospenthal DR. Use of chromogenic medium in the isolation of yeasts from clinical specimens. *J Med Microbiol*. 2005;**54**(Pt 10):981-5. Epub 2005/09/15. doi: 10.1099/jmm.0.45942-0. PubMed PMID: 16157554.

48. Willinger B, Wein S, Hirschl AM, Rotter ML, Manafi M. Comparison of a new commercial test, GLABRATA RTT, with a dipstick test for rapid identification of Candida glabrata. *J Clin Microbiol*. 2005;**43**(1):499-501. Epub 2005/01/07. doi: 10.1128/JCM.43.1.499-501.2005. PubMed PMID: 15635027; PubMed Central PMCID: PMCPMC540123.

49. Pedreño Y, González-Párraga P, Martínez-Esparza M, Sentandreu R, Valentín E, Argüelles JC. Disruption of the Candida albicans ATC1 gene encoding a cell-linked acid trehalase decreases hypha formation and infectivity without affecting resistance to oxidative stress. *Microbiology*. 2007;**153**(Pt 5):1372-81. Epub 2007/04/28. doi: 10.1099/mic.0.2006/003921-0. PubMed PMID: 17464051.

50. Sánchez-Fresneda R, Guirao-Abad JP, Martinez-Esparza M, Maicas S, Valentín E, Argüelles JC. Homozygous deletion of ATC1 and NTC1 genes in Candida parapsilosis abolishes trehalase activity and affects cell growth, sugar metabolism, stress resistance, infectivity and biofilm formation. *Fungal Genet Biol*. 2015;**85**:45-57. Epub 2015/11/04. doi: 10.1016/j.fgb.2015.10.007. PubMed PMID: 26529381.

51. Sánchez-Fresneda R, Martínez-Esparza M, Maicas S, Argüelles JC, Valentín E. In Candida parapsilosis the ATC1 gene encodes for an acid trehalase involved in trehalose hydrolysis, stress resistance and virulence. *PLoS One*. 2014;**9**(6):e99113. Epub 2014/06/13. doi: 10.1371/journal.pone.0099113. PubMed PMID: 24922533; PubMed Central PMCID: PMCPMC4055668.

52. Eck R, Bergmann C, Ziegelbauer K, Schönfeld W, Künkel W. A neutral trehalase gene from Candida albicans: molecular cloning, characterization and disruption. *Microbiology*. 1997;**143**(Pt12):3747-56. Epub 1998/01/09. doi: 10.1099/00221287-143-

12-3747. PubMed PMID: 9421900.

53. Pedreño Y, González-Párraga P, Conesa S, Martínez-Esparza M, Aguinaga A, Hernández JA, *et al.* The cellular resistance against oxidative stress (H2O2) is independent of neutral trehalase (Ntc1p) activity in Candida albicans. *FEMS Yeast Res*. 2006;**6**(1):57-62. Epub 2006/01/21. doi: 10.1111/j.1567-1364.2005.00025.x. PubMed PMID: 16423071.

54. Gabaldón T, Carreté L. The birth of a deadly yeast: tracing the evolutionary emergence of virulence traits in Candida glabrata. *FEMS Yeast Res*. 2016;**16**(2):fov110. Epub 2015/12/20. doi: 10.1093/femsyr/fov110. PubMed PMID: 26684722; PubMed Central PMCID: PMCPMC5815135.

55. Gabaldón T, Martin T, Marcet-Houben M, Durrens P, Bolotin-Fukuhara M, Lespinet O, *et al.* Comparative genomics of emerging pathogens in the Candida glabrata clade. *BMC Genomics*. 2013;**14**:623. Epub 2013/09/17. doi: 10.1186/1471-2164-14-623. PubMed PMID: 24034898; PubMed Central PMCID: PMCPMC3847288.

56. Wolfe KH, Shields DC. Molecular evidence for an ancient duplication of the entire yeast genome. *Nature*. 1997;**387**(6634):708-13. Epub 1997/06/12. doi: 10.1038/42711. PubMed PMID: 9192896.

57. Nielsen H. Predicting Secretory Proteins with SignalP. *Methods Mol Biol*. 2017;**1611**:59-73. Epub 2017/04/30. doi: 10.1007/978-1-4939-7015-5_6. PubMed PMID: 28451972.

58. Omasits U, Ahrens CH, Müller S, Wollscheid B. Protter: interactive protein feature visualization and integration with experimental proteomic data. *Bioinformatics*. 2014;**30**(6):884-6. Epub 2013/10/29. doi: 10.1093/bioinformatics/btt607. PubMed PMID: 24162465.

59. Jules M, Guillou V, François J, Parrou JL. Two distinct pathways for trehalose assimilation in the yeast Saccharomyces cerevisiae. *Appl Environ Microbiol*. 2004;**70**(5):2771-8. Epub 2004/05/07. doi: 10.1128/aem.70.5.2771-2778.2004. PubMed PMID: 15128531; PubMed Central PMCID: PMCPMC404389.

60. Lucio AK, Polizeli ML, Jorge JA, Terenzi HF. Stimulation of hyphal growth in anaerobic cultures of Mucor rouxii by extracellular trehalose. Relevance of cell wall-bound activity of acid trehalase for trehalose utilization. *FEMS Microbiol Lett*. 2000;**182**(1):9-13. Epub 1999/12/29. doi: 10.1111/j.1574-6968.2000.tb08865.x. PubMed PMID: 10612723.

61. Rodrigues CF, Silva S, Henriques M. Candida glabrata: a review of its features and resistance. *Eur J Clin Microbiol Infect Dis*. 2014;**33**(5):673-88. Epub 2013/11/20. doi: 10.1007/s10096-013-2009-3. PubMed PMID: 24249283.

62. Han EK, Cotty F, Sottas C, Jiang H, Michels CA. Characterization of AGT1 encoding a general alpha-glucoside transporter from Saccharomyces. *Mol Microbiol*. 1995;**17**(6):1093-107. Epub 1995/09/01. doi: 10.1111/j.1365-2958.1995.mmi_17061093.x. PubMed PMID: 8594329.

63. Healey KR, Nagasaki Y, Zimmerman M, Kordalewska M, Park S, Zhao Y, *et al.* The Gastrointestinal Tract Is a Major Source of Echinocandin Drug Resistance in a Murine Model of Candida glabrata Colonization and Systemic Dissemination. *Antimicrob Agents Chemother*. 2017;**61**(12). Epub 2017/10/04. doi: 10.1128/AAC.01412-17. PubMed PMID: 28971865; PubMed Central PMCID: PMCPMC5700336.

64. Mason KL, Erb Downward JR, Mason KD, Falkowski NR, Eaton KA, Kao JY, *et al.* Candida albicans and bacterial microbiota interactions in the cecum during recolonization following broad-spectrum antibiotic therapy. *Infect Immun*. 2012;**80**(10):3371-80. Epub 2012/07/11. doi: 10.1128/IAI.00449-12. PubMed PMID: 22778094; PubMed Central PMCID: PMCPMC3457555.

65. Brown AJ, Budge S, Kaloriti D, Tillmann A, Jacobsen MD, Yin Z, *et al.* Stress adaptation in a pathogenic fungus. *J Exp Biol*. 2014;**217**(Pt 1):144-55. Epub 2013/12/20. doi: 10.1242/jeb.088930. PubMed PMID: 24353214; PubMed Central PMCID: PMCPMC3867497.

66. Kaur R, Ma B, Cormack BP. A family of glycosylphosphatidylinositol-linked aspartyl proteases is required for virulence of Candida glabrata. *Proc Natl Acad Sci U S A*. 2007;**104**(18):7628-33. Epub 2007/04/26. doi: 10.1073/pnas.0611195104. PubMed PMID: 17456602; PubMed Central PMCID: PMCPMC1863504.

67. Otto V, Howard DH. Further studies on the intracellular behavior of Torulopsis glabrata. *Infect Immun*. 1976;**14**(2):433-8. Epub 1976/08/01. PubMed PMID: 987021; PubMed Central PMCID: PMCPMC420903.

68. Roetzer A, Gratz N, Kovarik P, Schüller C. Autophagy supports Candida glabrata survival during phagocytosis. *Cell Microbiol*. 2010;**12**(2):199-216. Epub 2009/10/09. doi: 10.1111/j.1462-5822.2009.01391.x. PubMed PMID: 19811500; PubMed Central PMCID: PMCPMC2816358.

69. Seider K, Brunke S, Schild L, Jablonowski N, Wilson D, Majer O, *et al.* The facultative intracellular pathogen Candida glabrata subverts macrophage cytokine production and phagolysosome maturation. *J Immunol*. 2011;**187**(6):3072-86. Epub 2011/08/19. doi: 10.4049/jimmunol.1003730. PubMed PMID: 21849684.

70. Haas A. The phagosome: compartment with a license to kill. *Traffic*. 2007;**8**(4):311-30. Epub 2007/02/06. doi: 10.1111/j.1600-0854.2006.00531.x. PubMed PMID: 17274798.

71. Vieira OV, Botelho RJ, Grinstein S. Phagosome maturation: aging gracefully. *Biochem J*. 2002;**366**(Pt 3):689-704. Epub 2002/06/14. doi: 10.1042/BJ20020691. PubMed PMID: 12061891; PubMed Central PMCID: PMCPMC1222826.

72. Jacobsen ID, Brunke S, Seider K, Schwarzmüller T, Firon A, d'Enfért C, *et al.* Candida glabrata persistence in mice does not depend on host immunosuppression and is unaffected by fungal amino acid auxotrophy. *Infect Immun*. 2010;**78**(3):1066-77. Epub 2009/12/17. doi: 10.1128/IAI.01244-09. PubMed PMID: 20008535; PubMed Central PMCID: PMCPMC2825948.

73. The Pfam protein families database in 2019 [Internet]. 2019.

74. Van Ende M, Wijnants S, Van Dijck P. Sugar Sensing and Signaling in Candida albicans and Candida glabrata. *Front Microbiol*. 2019;**10**:99. Epub 2019/02/15. doi: 10.3389/fmicb.2019.00099. PubMed PMID: 30761119; PubMed Central PMCID: PMCPMC6363656.

75. Underhill DM, Iliev ID. The mycobiota: interactions between commensal fungi and the host immune system. *Nat Rev Immunol*. 2014;**14**(6):405-16. Epub 2014/05/24. doi: 10.1038/nri3684. PubMed PMID: 24854590; PubMed Central PMCID: PMCPMC4332855.

76. Nwaka S, Kopp M, Holzer H. Expression and function of the trehalase genes NTH1 and YBR0106 in Saccharomyces cerevisiae. *J Biol Chem*. 1995;**270**(17):10193-8. Epub 1995/04/28. doi: 10.1074/jbc.270.17.10193. PubMed PMID: 7730323.

77. Charlet R, Pruvost Y, Tumba G, Istel F, Poulain D, Kuchler K, *et al.* Remodeling of the Candida glabrata cell wall in the gastrointestinal tract affects the gut microbiota and the immune response. *Sci Rep*. 2018;**8**(1):3316. Epub 2018/02/22. doi: 10.1038/s41598-018-21422-w. PubMed PMID: 29463799; PubMed Central PMCID: PMCPMC5820338.

78. El Nemr A, El Ashry el SH. Potential trehalase inhibitors: syntheses of trehazolin and its analogues. *Adv Carbohydr Chem Biochem*. 2011;**65**:45-114. Epub 2011/07/19. doi: 10.1016/B978-0-12-385520-6.00003-0. PubMed PMID: 21763511.

79. Asano N, Yamaguchi T, Kameda Y, Matsui K. Effect of validamycins on glycohydrolases of Rhizoctonia solani. *J Antibiot (Tokyo)*. 1987;**40**(4):526-32. Epub 1987/04/01. doi: 10.7164/antibiotics.40.526. PubMed PMID: 3583921.

80. Guirao-Abad JP, Sánchez-Fresneda R, Valentín E, Martinez-Esparza M, Argüelles JC. Analysis of validamycin as a potential antifungal compound against Candida albicans. *Int Microbiol*. 2013;**16**(4):217-25. Epub 2014/08/12. doi: 10.2436/20.1501.01.197. PubMed PMID: 25102722.

81. Plabutong N, Ekronarongchai S, Niwetbowornchai N, Edwards SW, Virakul S, Chiewchengchol D, *et al.* The Inhibitory Effect of Validamycin A on Aspergillus flavus. *Int J Microbiol*. 2020;**2020**:3972415. Epub 2020/07/18. doi: 10.1155/2020/3972415. PubMed PMID: 32676114; PubMed Central PMCID: PMCPMC7336217 publication of this article.

82. Ishihara R, Taketani S, Sasai-Takedatsu M, Kino M, Tokunaga R, Kobayashi Y. Molecular cloning, sequencing and expression of cDNA encoding human trehalase. *Gene*. 1997;**202**(1-2):69-74. Epub 1998/01/14. doi: 10.1016/s0378-1119(97)00455-1. PubMed PMID: 9427547.

83. Sacktor B. Trehalase and the transport of glucose in the mammalian kidney and intestine. *Proc Natl Acad Sci U S A*. 1968;**60**(3):1007-14. Epub 1968/07/01. doi: 10.1073/pnas.60.3.1007. PubMed PMID: 5243919; PubMed Central PMCID: PMCPMC225153.

84. Bergoz R. Trehalose malabsorption causing intolerance to mushrooms. Report of a probable case. *Gastroenterology*. 1971;**60**(5):909-12. Epub 1971/05/01. PubMed PMID: 5104075.

85. Skrzypek MS BJ, Binkley G, Miyasato SR, Simison M, Sherlock G.); . The Candida Genome Database (CGD): incorporation of Assembly 22, systematic identifiers and visualization of high throughput sequencing data. *Nucleic Acids Res* **45** 2017;(D1):D592-D6.

86. Cerqueira GC AM, Inglis DO, Skrzypek MS, Binkley G, Simison M, Miyasato SR, Binkley J, Orvis J, Shah P, Wymore F, Sherlock G, Wortman JR. The Aspergillus Genome Database: multispecies curation and incorporation of RNA-Seq data to improve structural gene annotations. *Nucleic Acids Res* 2014;**42**: D705-10.

87. Consortium TU. UniProt: a worldwide hub of protein knowledge. *Nucleic Acids Res*. 2019;**47**:D506-15.

88. Cherry JM HE, Amundsen C, Balakrishnan R, Binkley G, Chan ET, Christie KR,

Costanzo MC, Dwight SS, Engel SR, Fisk DG, Hirschman JE, Hitz BC, Karra K, Krieger CJ, Miyasato SR, Nash RS, Park J, Skrzypek MS, Simison M, Weng S, Wong ED Saccharomyces Genome Database: the genomics resource of budding yeast. . *Nucleic Acids Res* 2012;Jan;**40**((Database issue)):D700-5.

89. Lock A RK, Harris MA, Hayles J, Oliver SG, Bähler J; Wood V. PomBase 2018: user-driven reimplementation of the fission yeast database provides rapid and intuitive access to diverse, interconnected information. *Nucleic Acids Res* 2018;Oct 13((Database issue)).

90. Qiagen. CLC Main Workbench.

91. Schwarzmüller T, Ma B, Hiller E, Istel F, Tscherner M, Brunke S, *et al.* Systematic phenotyping of a large-scale Candida glabrata deletion collection reveals novel antifungal tolerance genes. *PLoS Pathog*. 2014;**10**(6):e1004211. Epub 2014/06/20. doi: 10.1371/journal.ppat.1004211. PubMed PMID: 24945925; PubMed Central PMCID: PMCPMC4063973.

92. Pernambuco MB, Winderickx J, Crauwels M, Griffioen G, Mager WH, Thevelein JM. Glucose-triggered signalling in Saccharomyces cerevisiae: different requirements for sugar phosphorylation between cells grown on glucose and those grown on non-fermentable carbon sources. *Microbiology*. 1996;**142** (Pt 7):1775-82. Epub 1996/07/01. doi: 10.1099/13500872-142-7-1775. PubMed PMID: 8757741.

93. Lüttich A, Brunke S, Hube B. Isolation and amplification of fungal RNA for microarray analysis from host samples. *Methods Mol Biol*. 2012;**845**:411-21. Epub 2012/02/14. doi: 10.1007/978-1-61779-539-8_28. PubMed PMID: 22328391.

94. Sprenger M, Hartung TS, Allert S, Wisgott S, Niemiec MJ, Graf K, *et al.* Fungal biotin homeostasis is essential for immune evasion after macrophage phagocytosis and virulence. *Cell Microbiol*. 2020;**22**(7):e13197. Epub 2020/02/23. doi: 10.1111/cmi.13197. PubMed PMID: 32083801.

Figures and figure legends

Fig. 1

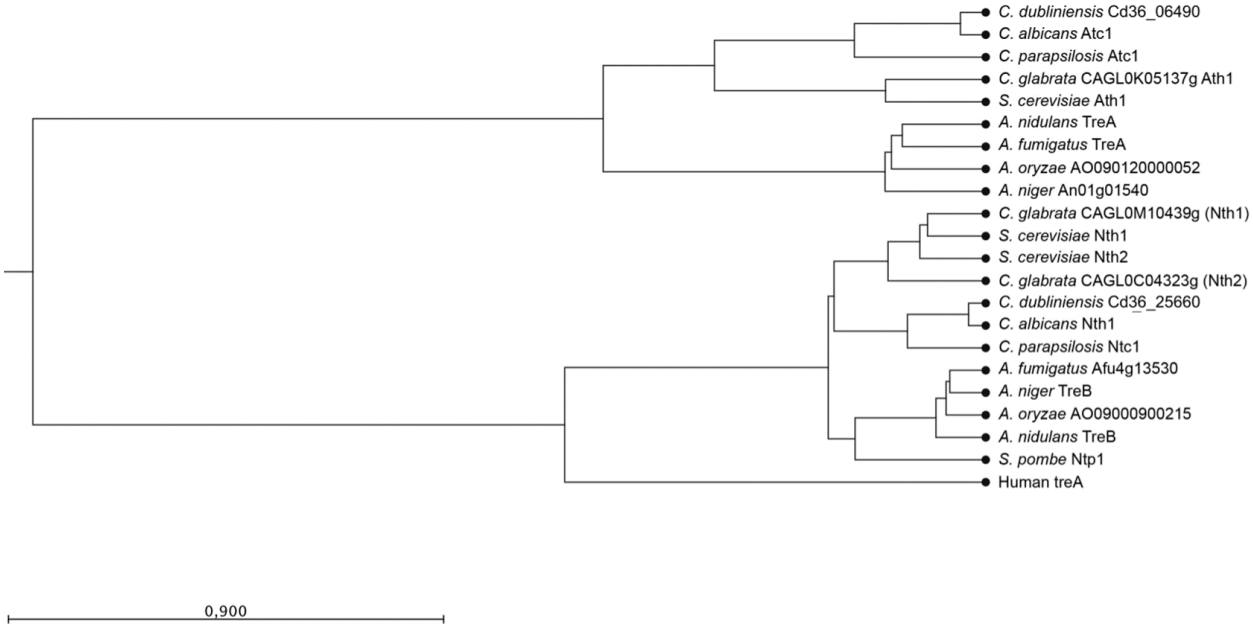

Fig. 1: **Phylogenetic tree of fungal trehalases**. Two main clusters can be distinguished: the neutral trehalases and the acid trehalases. The human trehalase enzyme was included and is present in the cluster of neutral trehalase enzymes. Protein sequences were aligned and the phylogenetic tree was constructed using the unweighted pair method with arithmetic mean (UPGMA) and the Kimura Protein as a protein distance measure.

Fig. 2

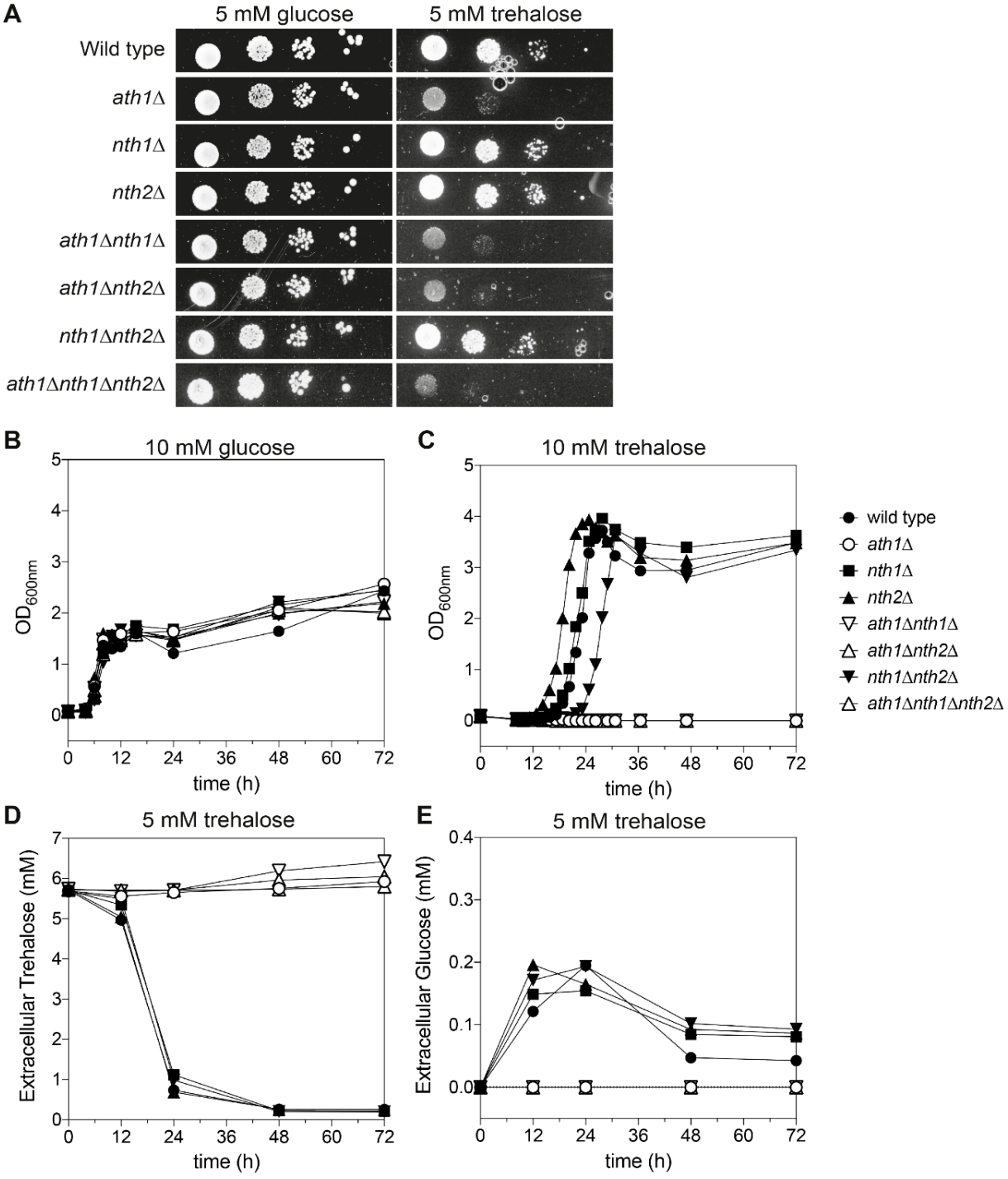

Fig. 2: **Growth of the different trehalase deletion strains**. Cells were grown on YNB solid (A) and in liquid (B-E) medium containing glucose (A-B) or trehalose (A, C-E) as a fermentable carbon source. During growth in YNB trehalose, we also measured the trehalose and glucose concentrations in the medium over time (D-E, respectively). The experiments were performed at least twice and average results of three independent transformants are shown.

Fig. 3

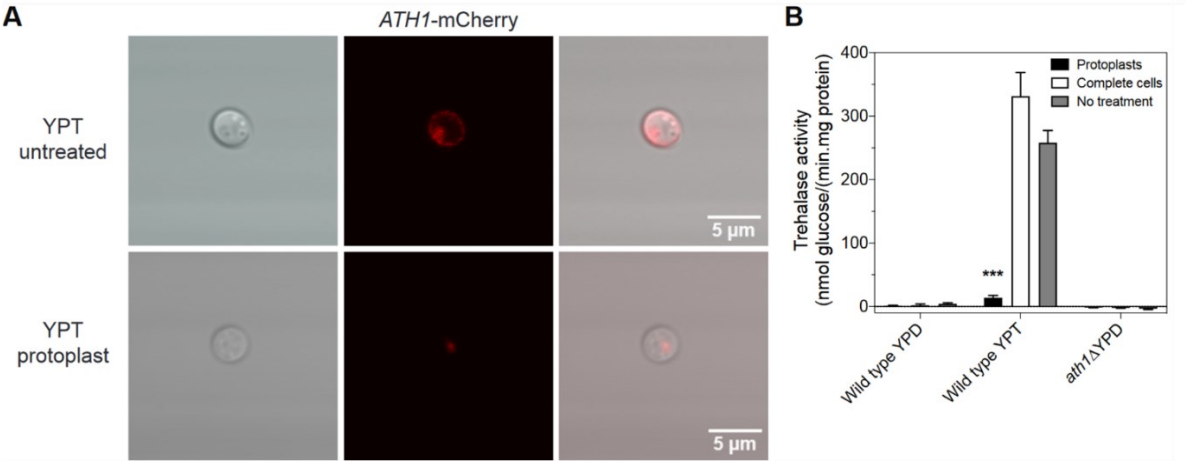

Fig. 3: **Ath1 is present in the periplasm and is responsible for high trehalase activity when cells are grown in presence of trehalose**. Imaging of Ath1-mCherry cells taken with a Fluoview 1000 confocal microscope (A). Cells were grown in presence of trehalose to exponential phase after which protoplasts were made. The upper panel of A shows complete cells, the lower panel shows protoplasts of Ath1-mCherry. The trehalase activity was measured in complete cells, protoplasts and cells with no treatment after growth on YPD or YPT (B). Average trehalase activity of at least two experiments is shown with the standard error of the mean (SEM). Statistical Kruskal-Wallis test was used with Dunn's correction for comparing treated and untreated conditions for each strain (*, P ≤ 0,05; **, P ≤ 0,01; *** P ≤ 0,001 and ****, P ≤ 0,0001).

Fig. 4

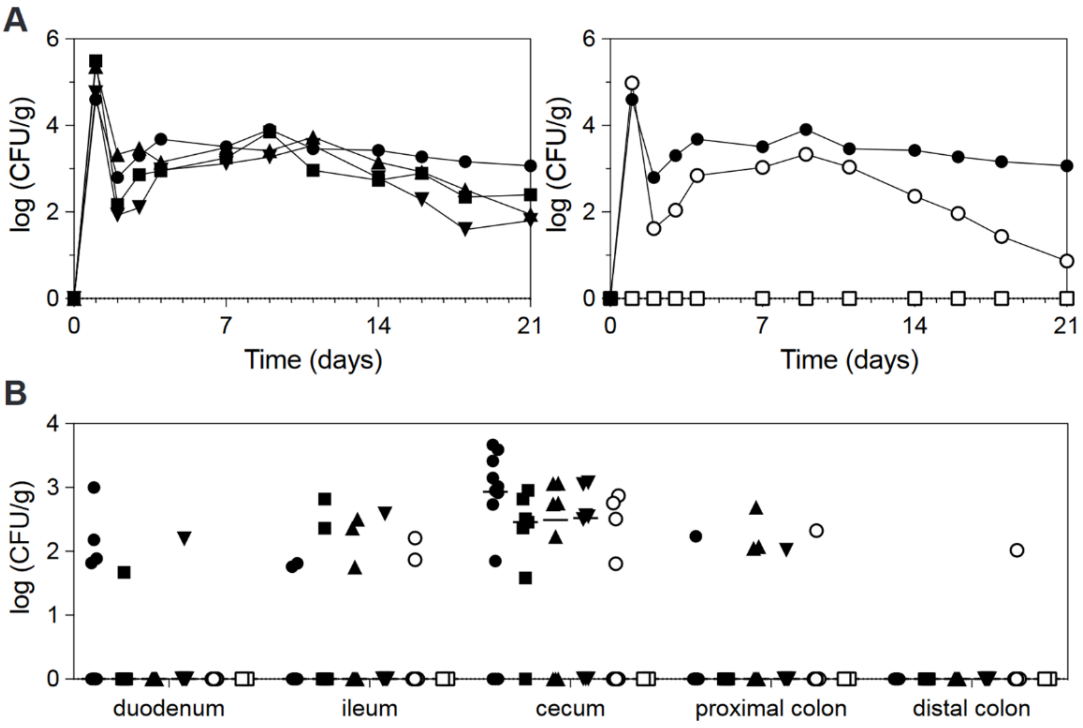

Fig. 4: Colonization in the GI tract is not maintained in the triple trehalase deletion strain. At day 0, mice are orally infected with 10^8 *C. glabrata* cells (gavage). Wild type (●), *ath1*Δ (○), *nth1*Δ (■), *nth2*Δ (▲) and *ath1*Δ*nth1*Δ*nth2*Δ (△) or PBS as a control (□) were tested. At the indicated days a stool sample was collected from each mouse and plated for CFU counting, during 21 days (A). Upon termination of the experiment, mice were sacrificed and different tissues were collected to plate for CFU counting (B). All data are expressed in Log10 values.

Fig. 5

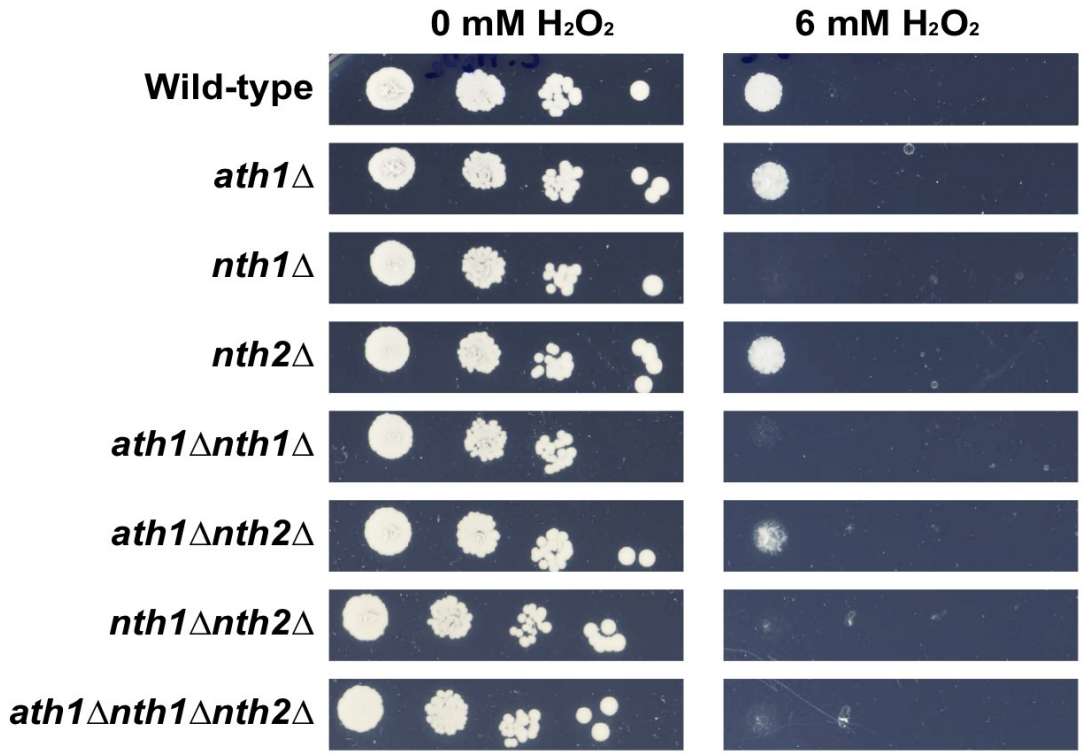

Fig. 5: **Oxidative stress resistance of different trehalase mutant strains**. The different strains were grown overnight in SC 100 mM glucose. After 3 washing steps, cells were spotted on YNB plus 100 mM glucose agar plates containing 6 mM of H_2O_2 and grown at 37°C for 72 hours.

Fig. 6

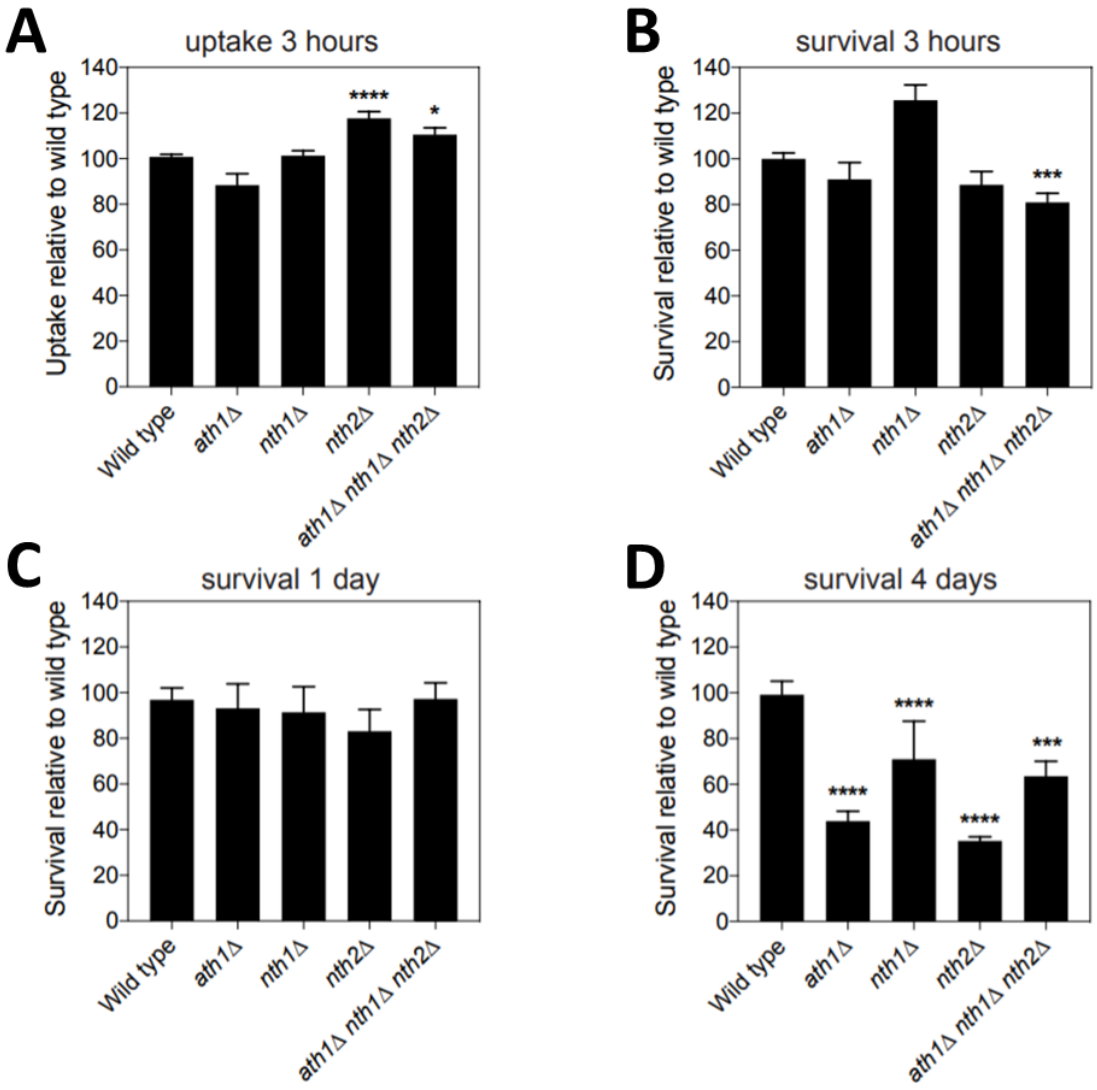

Fig. 6: ***Candida glabrata*** **trehalase survival inside macrophages**. Differentiated human macrophages were infected with the indicated *C. glabrata* strain at multiplicity of infection (MOI) 1:1, after which the cells were plated for CFU counting at the indicated days (B-D). Additionally, at 3 hours post infection, also the uptake of each strain was counted (A). Average survival relative to the wild type strain is shown with SEM of minimal three experiments, statistical Kruskal-Wallis test was performed with Dunn's correction (*, P ≤ 0,05; **, P ≤ 0,01; *** P ≤ 0,001 and ****, P ≤ 0,0001), comparing the survival of all strains to wild type.

Fig. 7

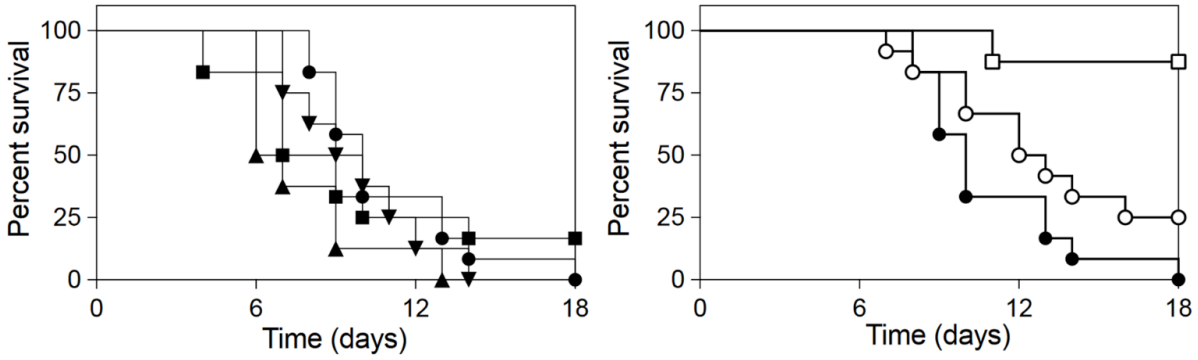

Fig. 7: Mice survival after systemic infection. Mice were immunosuppressed with 75 mg/kg dexamethasone and received 5 . 10^7 *C. glabrata* cells via injection in the lateral tail vain. Wild type (●), *ath1*Δ (○), *nth1*Δ (■), *nth2*Δ (▲) and *ath1*Δ*nth1*Δ*nth2*Δ (△) or PBS as a control (□) were tested. The mice were monitored two times per day for 18 days. When they reached humane endpoints, they were sacrificed. Statistical analysis by the use of a log-rank test was performed comparing the deletion strains to the wild type (*, P ≤ 0,05; **, P ≤ 0,01; *** P ≤ 0,001 and ****, P ≤ 0,0001).

Supplement

Supplemental figures and legends

Fig. S1

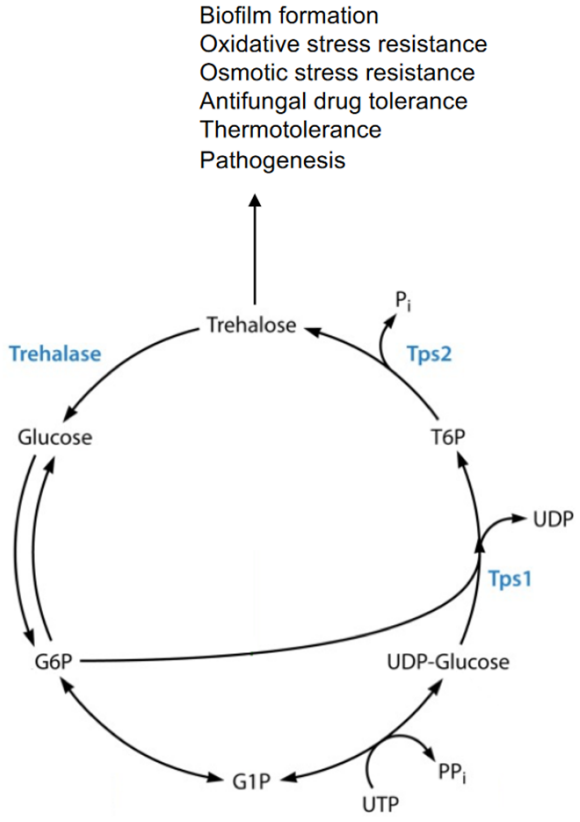

Fig. S1: **Overview of the fungal trehalose metabolism**. Trehalose is synthesized in two steps: Trehalose-6-phosphate (T6P) synthase (Tps1) forms T6P, after which it is converted into trehalose by T6P phosphatase (Tps2). Breakdown of trehalose into two glucose molecules is mediated by the trehalase enzymes. Apart from being a carbon source, trehalose also plays an important role in the stress resistance of fungal cells.

Fig. S2

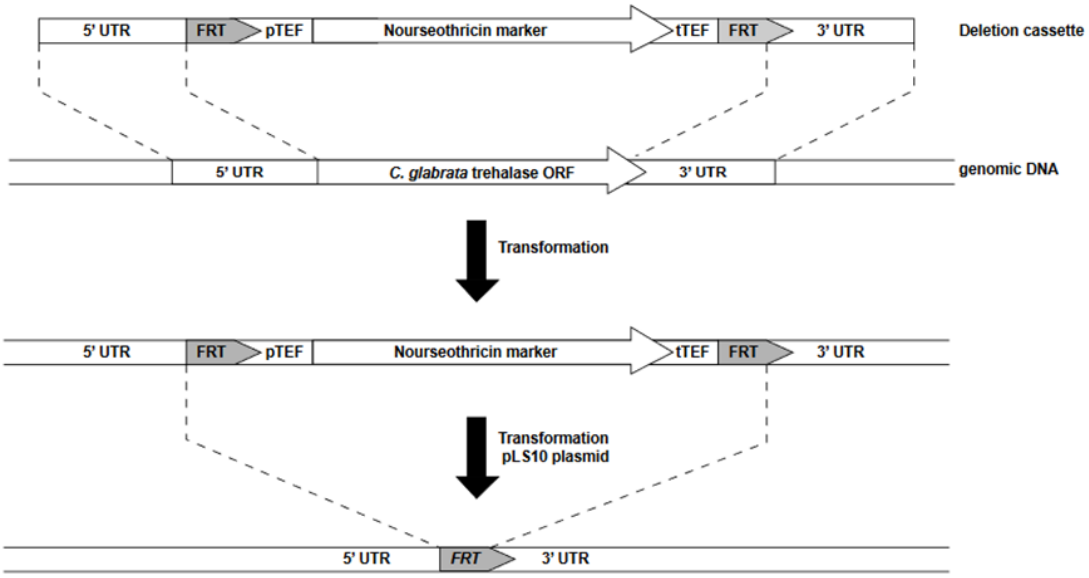

Fig. S2: **Overview of construction of the *C. glabrata* trehalase deletion mutants**. The deletion cassette was constructed by PCR amplification of the nourseothricin cassette flanked by FRT sites and 100 base pair sequences up- and downstream of the targeted gene. After correct insertion in the genome, the nourseothricin cassette was removed by introduction of the pLS10 vector which expresses a flippase enzyme. After removal of the nourseothricin cassette, the deletion cassette for the other trehalase enzymes could be introduced again to construct the double and triple deletion strains.

Fig. S3

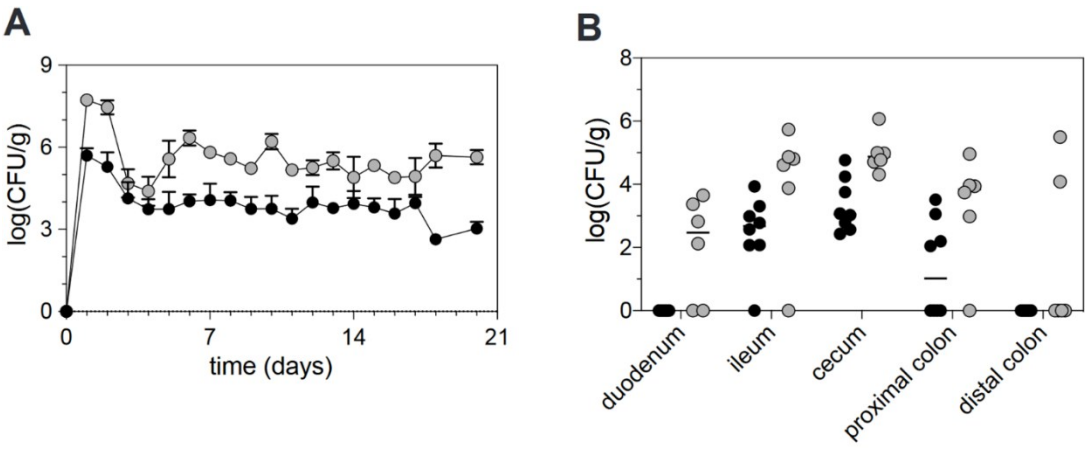

Fig. S3: Optimization of the *Candida glabrata* GI colonization murine model. Mice

received either normal water (black ●) or ampicillin (1mg/ml) (grey ●) in their drinking water from four days before gavage. At day 0, mice were orally infected with 10^8 *C. glabrata* cells (gavage). At the indicated days a stool sample was collected of each mice and plated for CFU counting, during 21 days (A). Upon termination of the experiment, mice were sacrificed using cervical dislocation under anesthesia and different tissues were collected to plate for CFU counting (B).

Fig. S4

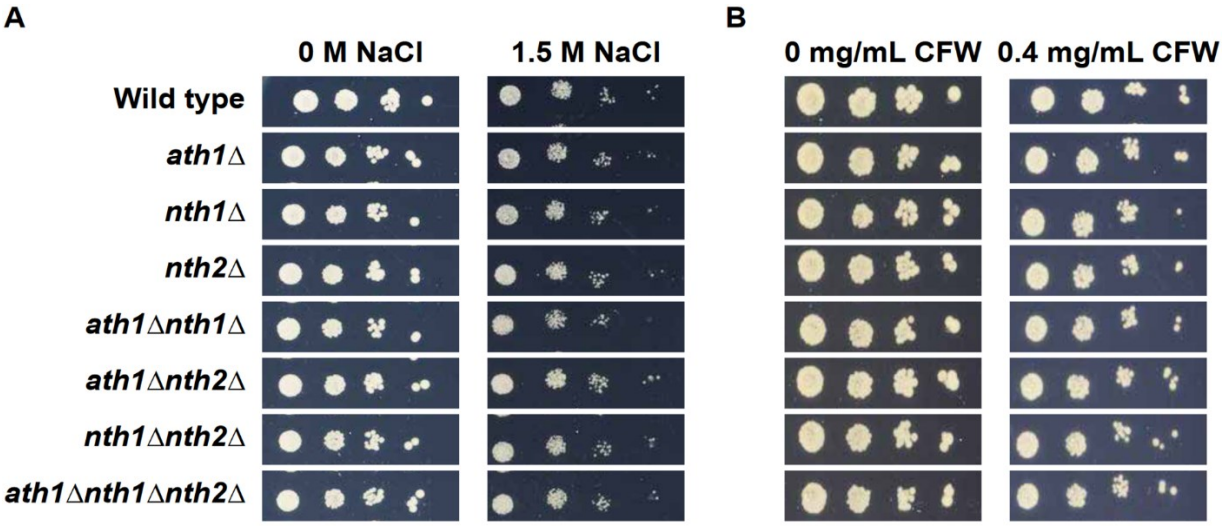

Fig. S4: **Salt stress and cell wall stress resistance of different trehalase mutant strains**. The different strains were grown overnight in SC 100 mM glucose. After 3 washing steps, cells were spotted on YNB plus 100 mM glucose agar plates with or without 1.5 M NaCl or 0.4 mg/mL CFW and grown at 37°C for 72 hours.

Fig. S5

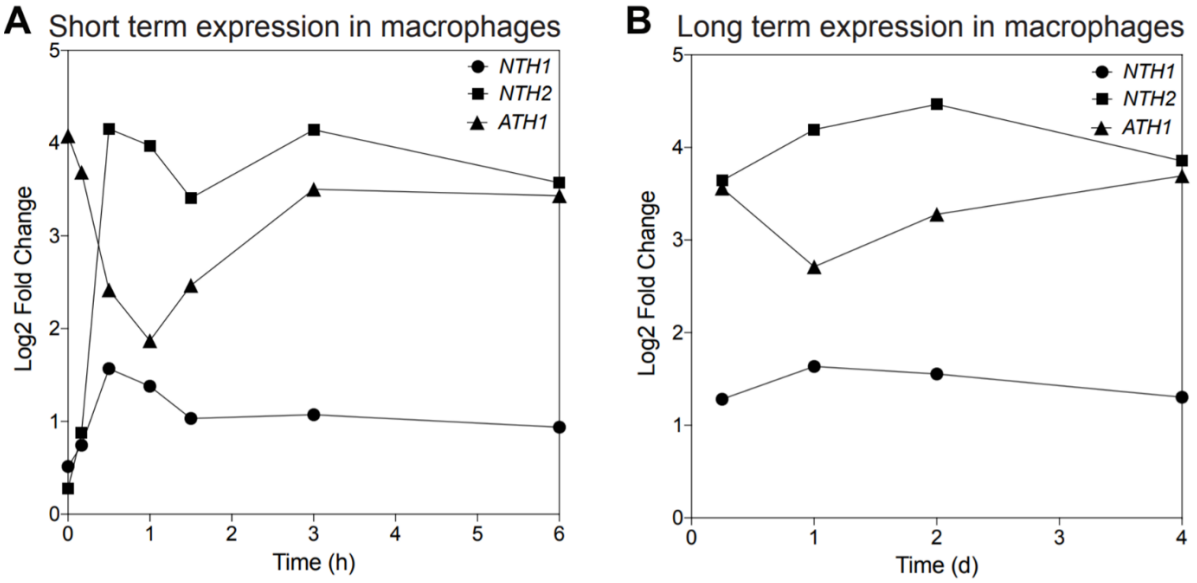

Fig. S5 *Candida glabrata* trehalase gene expression inside macrophages. Murine macrophage-like RAW264.7 cells (A) or human monocyte-derived macrophages (B) were infected with *C. glabrata* wild type cells after which gene expression of the fungal cells was determined at different time points. (A, B) Average gene expression of three experiments is shown relative to the condition of exponential growth in YPD for each strain individually (Fold Change, FC).

Fig. S6

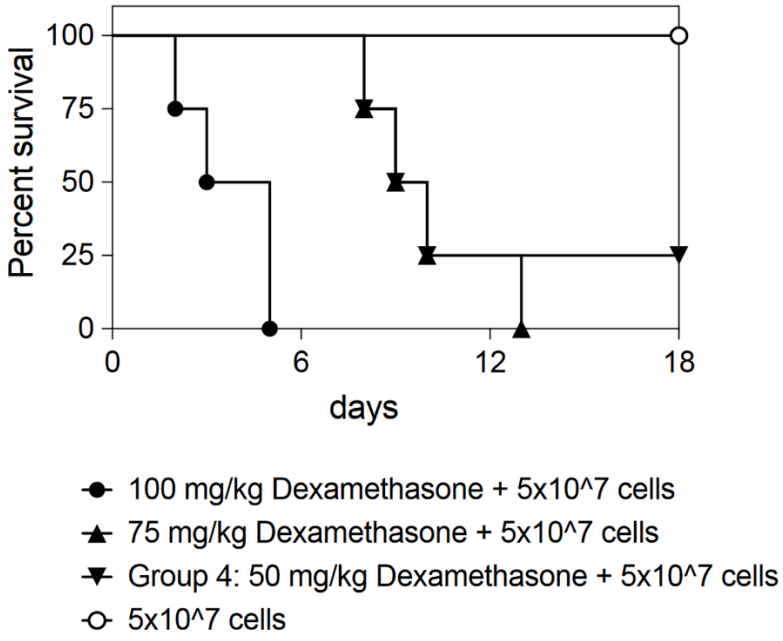

Fig. S6: Optimization of *Candida glabrata* systemic infection murine model. Mice were immunosuppressed with different concentrations of dexamethasone (0 mg/kg; 50 mg/kg; 75 mg/kg; 100 mg/kg) and received no or 5 . 10^7 cells of the indicated *C. glabrata* strain via injection in the lateral tail vain. The mice were monitored two times per day for 18 days. When they reached humane endpoints, they were sacrificed. Statistical analysis by the use of a log-rank test was performed comparing the deletion strains to the wild type (*, P ≤ 0,05; **, P ≤ 0,01; *** P ≤ 0,001 and ****, P ≤ 0,0001).

Supplementary Data – Alignment of neutral trehalases and human trehalase

Using Swiss model, residues of the active site or involved in substrate binding were searched for all species of the phylogenetic tree (Waterhouse *et al.*, 2018). These residues were reported for *S. cerevisiae*, *S. pombe* and *A. nidulans* neutral trehalases. For alignment, we also included *C. glabrata* and the human trehalase enzyme. The amino acid sequences were aligned using Clustal O. Residues of the active site are highlighted in blue, amino acids conferring substrate binding are highlighted in purple.

Supplemental tables

Supplementary Table 1: Strains, plasmids and primers

Supplemental references

Waterhouse, A., Bertoni, M., Bienert, S., Studer, G., Tauriello, G., Gumienny, R., Heer, F.T., de Beer, T.A.P., Rempfer, C., Bordoli, L., *et al.* (2018). SWISS-MODEL: homology modelling of protein structures and complexes. *Nucleic Acids Res* **46**, W296-W303.

Complete supplemental material for this article is included in the enclosed **CD ROM (folder: Trehalases)**. Suppl. Tables 1 is an Excel file and was therefore not included in the printed version.

3 Discussion

3.1 Jagaricin´s mode of action and application possibilities

A central aspect of this study was to investigate pathogenic interactions of fungi, with a long-term benefit in the clinical setting in mind. In terms of fungal pathogens, it has become widely acknowledged within the last years or decades that new antifungal drugs are desperately needed. Therefore, screening a broad range of potential producers for possible candidates, ideally with new lead structures, and further evaluation of their mode of action as well as their application potential is necessary.

Manuscript I shows that the antifungal action of one of these potential new structures, jagaricin is based on membrane disturbance. This involves formation of large unspecific lesions or pores within susceptible target species. Such a mode of action makes the impact critically dependent on the membrane composition and properties of the target species. Conversely, modifications of jagaricin`s structure will most likely allow to change the spectrum of membrane types with which it can interact. By these means the species specificity can potentially be changed to make it suitable for treatment of humans against pathogenic fungi. Manuscript I discusses how jagaricin might exert its species specificity and how this can be potentially optimized for human treatment. As an alternative, use of jagaricin or certain derivatives in agriculture might also be promising. We furthermore propose that *Janthinobacteria* might be useful as biocontrol species, especially if they harbour jagaricin-related biosynthetic clusters. Interestingly, in addition to *Janthinobacterium agaricidamnosum*, a second *Janthinobacteria* species was recently identified which harbours a jagaricin-related cluster (Clark *et al.* 2019). This might fuel further research into jagaricin and related compounds and their application possibilities.

3.2 Implications on further studies of secondary metabolism of (fungal) interactions

The mode of action of jagaricin does not seem to be atypical for virulence factors of mushroom-infecting bacteria, since other bacterial virulence factors from such interactions (WLIP, tolaasin) also exhibit membrane activity (Cho and Kim 2003; Coraiola *et al.* 2006). Although the number of examples is quite low, this could be a common theme: membrane lysis is likely to be a successful strategy for a bacterium to convert the comparatively soft fungal tissue of e.g. a champignon cap into a nutritious medium for the bacterium. However, while it is believed that typical fungal species used for mushroom cultivation have only little means of defence at their disposal against infecting bacteria or other pathogens (Soler-Rivas *et al.* 1999; Savoie and Largeteau 2004; Largeteau and Savoie 2010; Berendsen *et al.* 2013) – which points to a different strategy

to circumvent or deal with mushroom fruiting body infections of these fungi in nature – other fungal species are well known to produce a plethora of molecules to defend their mycelia (Fleming 1929; Netzker *et al.* 2018) as well as their fruiting bodies (Lübken *et al.* 2004; De Silva *et al.* 2013; Sandargo *et al.* 2019) against attacking bacteria. Importantly, secondary metabolite clusters which mostly produce these compounds are often silent under standard laboratory conditions, while they might become activated in confrontation with an interaction partner (Netzker *et al.* 2018). In addition, most mushroom fruiting body-forming basidio- and ascomycota (especially mycorrhizal fungi) are hard to cultivate (Sandargo *et al.* 2019), which may have limited the identification of secondary metabolites from these species or restricted to those which are (constitutively) produced in sufficient amounts for detection during fruiting body formation. Therefore, we propose that further studies of pathogenic bacteria-mushroom interactions, e.g. based on MALDI-Imaging similar to the original identification of jagaricin (Graupner *et al.* 2012), might be a promising avenue despite the technical challenges, since frequently both interaction partners are capable of producing putatively interesting compounds.

3.3 Establishment of the first long-term yeast-macrophage interaction model

Apart from studies on direct treatment options by novel antifungals, studying the interaction of human fungal pathogens with the host can improve our understanding of the infection process, which in turn can be used to fine-tune treatment strategies. In manuscript III, we focused on the interaction of the human fungal pathogen *C. glabrata* with macrophages, the immune cells which are believed to play a central role in the interplay of *C. glabrata* and its host (Brieland *et al.* 2001; Kaur, Ma, and Cormack 2007; Jacobsen *et al.* 2010; Seider *et al.* 2011; Cheng *et al.* 2014; Duggan *et al.* 2015). Importantly, *C. glabrata* is known to be able to persist for weeks in immunocompetent and immunocompromised mice (Brieland *et al.* 2001; Jacobsen *et al.* 2010; Cheng *et al.* 2014), while current macrophage-*C. glabrata* interaction models are only able to follow this interaction for a maximum of roughly two to three days. The endpoint of these models is dictated by yeast overgrowth due to intracellular and later, after macrophage lysis, extracellular yeast replication. We propose that the outcome of these “classical models” reflects the real *in vivo* interaction only in part. We expect that yeast-macrophage interactions rather lead to very different outcomes, ranging from yeast killing via yeast persistence to low or even robust intracellular yeast replication. Classical models reflect the initial interaction – yeast engulfment, phagosome maturation, the oxidative burst and killing of a part of the infecting *C. glabrata* population – and the very late events of intracellular yeast replication followed by bursting of the macrophages. However, they

cannot simulate the intermediate and important process of intracellular yeast persistence. The rate of these events in an infection situation likely strongly varies in dependence of the host's immune status and the properties of the infecting *C. glabrata* strain(s), as well as any antifungal treatment.

Importantly, a successful therapy relies on the complete eradication of fungal persister cells by the host (Lewis 2010; Bojsen, Regenberg, and Folkesson 2017). In manuscript III we have shown that neither treatment with the fungicidal drug amphotericin B nor with caspofungin (which is fungicidal only against growing yeast cells, otherwise fungistatic (Bojsen, Regenberg, and Folkesson 2014)) is sufficient to completely eradicate *C. glabrata* which exist within macrophages. This strongly suggests that in a clinical situation macrophages may provide a niche to persist during antimycotic treatment. Therefore, our *C. glabrata*-macrophage persistence model enables us – for the first time – to mimic this possibly clinically relevant part of the *C. glabrata*-host interaction. In light of the general finding that murine models are not always suited for the investigation of (intracellular) pathogens (Ellner 1990; Haas 1998; McMurray 2001; Nauseef 2001; Kusner 2005; Coers, Starnbach, and Howard 2009) and systemic murine *C. glabrata* infection models can explain *C. glabrata* virulence only in part (Brieland *et al.* 2001; Jacobsen *et al.* 2010; Cheng *et al.* 2014), the model becomes even more relevant. Scientific advances rely on the ability of the model to mirror the situation under investigation truthfully. Hence, our model closes a previous investigation gap and should allow us to better understand the dynamics of yeast-host interaction, hopefully enabling improved clinical treatment in future.

3.4 *C. glabrata* relies on induction of quiescence for long-term intramacrophagal survival

In manuscript III and manuscript IV this new model was put to a test, and we were able to obtain new insight into the long-term interaction of macrophage-internalized *C. glabrata*. In manuscript III, we have shown that macrophages are, in general, able to efficiently restrict growth of phagocytosed *C. glabrata* yeasts even during prolonged incubation. This was e.g. indicated by stable and even declining CFU levels, a transcriptional downregulation of the gene expression machinery and a low recovery for deletion mutants of genes which encode factors important for entry into and maintenance of quiescent cell states. In support of this, deletion mutants of some of these factors were already lost within one day in macrophages (e.g. cAMP-PKA pathway, Ssd1, Pfk1), while others were depleted mainly during later time points (Snf1 kinase pathway, cell wall integrity pathway) ((Broach 1991; Thompson-Jaeger *et al.* 1991; Herman 2002; Gray *et al.* 2004; Laporte *et al.* 2011; De Virgilio 2012; Miles *et al.* 2019) and manuscript III). This means that the macrophages phagosome of our model remains a stressful environment

for *C. glabrata*. Many obligate or facultative intracellular pathogens which use macrophages as a niche seem to modify the phagosome extensively (e.g. *Mycobacterium tuberculosis*, *Histoplasma capsulatum*; (Garfoot and Rappleye 2016; BoseDasgupta and Pieters 2018; Huang, Nazarova, and Russell 2019) or escape into the cytosol (e.g. *Francisella tularensis*, *Listeria monocytogenes*; (Ramond *et al.* 2012; Ireton, Rigano, and Dowd 2014)). *C. glabrata* is able to modify phagolysosome maturation and acidification (Seider *et al.* 2011) which seems to enable the survival of an appreciable part of the phagocytosed population. The adaptation strategy of *C. glabrata* towards macrophages involving slow-down of the cell cycle and/or induction of quiescence therefore likely benefits its pathobiology. It would be interesting to see whether induction of quiescence prior to macrophage infection would be beneficial for *C. glabrata* intracellular survival or whether instead the initial macrophage oxidative burst requires counteractivity by *C. glabrata*. In addition, yeasts are known to modify their cell wall before entering quiescence (Lesage and Bussey 2006), potentially changing immune recognition (Sherrington *et al.* 2017). The outcome might therefore depend also on the conditions used for quiescence induction.

3.5 Implications of an intracellular quiescent yeast state for treatment of *C. glabrata* infections

Maintenance of stressful conditions within its persistence niche might even be a part of the explanation why *C. glabrata* infections are often hard to treat and *C. glabrata* frequently acquires resistance towards azoles and echinocandins (Pfaller 2012; Alexander *et al.* 2013; Perlin, Rautemaa-Richardson, and Alastruey-Izquierdo 2017). Stressful conditions are known to induce cross resistance towards a second stressor (Estruch 2000; Berry and Gasch 2008; Semchyshyn *et al.* 2011; Guan *et al.* 2012; Semchyshyn 2014), like antifungals. In addition, the slow growth and quiescence can trigger tolerance mechanisms in *C. glabrata*, making azole treatment ineffective to eradicate such a population. Notably, this hypothesis seems to contradict previous studies showing that azole treatment is able to (transiently) reduce *C. glabrata* CFUs in macrophage models (Baltch *et al.* 2005; Bopp *et al.* 2006; Baltch *et al.* 2008). However, these studies seem to have used mainly the fast intracellular replication model of *C. glabrata*, which lacks the growth-restricted phase we suggest to be important. We refrained from testing the effect of azole treatment since reliable data on azole resistance is difficult to obtain in our *C. glabrata*-hMDM persistence model, as the medium contains cholesterol, which *C. glabrata* is known to use as a substitute for the azole target, ergosterol (Nakayama *et al.* 2007).

Apart from tolerance, induction of quiescence (e.g. in stationary phase yeasts or a biofilm

grown to full density) can enable a small part of a fungal population (typically less than 1 %) to survive high doses of fungicidal antimycotics like amphotericin B (Bojsen, Regenberg, and Folkesson 2014; Bojsen *et al.* 2016; Wuyts, Van Dijck, and Holtappels 2018). Amphotericin B persistence within biofilms has been ascribed to decreased plasma membrane ergosterol levels (Mukherjee *et al.* 2003; Khot *et al.* 2006), sequestration of polyene molecules by the extracellular matrix (Nett *et al.* 2007; Nett *et al.* 2010; Martins *et al.* 2012), and a subpopulation of persister cells (LaFleur, Kumamoto, and Lewis 2006). In addition, the persister phenotype is thought to explain persistence of planktonic cells grown to the stationary phase (Bojsen, Regenberg, and Folkesson 2014; Bojsen *et al.* 2016), but some confusion exists in the literature whether the cell phenotype described in these studies should be regarded as “true” persister phenotype since Bojsen and colleagues used lower-than-usual amphotericin B concentrations in their studies (Wuyts, Van Dijck, and Holtappels 2018). In general, the ability of persister cells to survive amphotericin B treatment is thought to rely on cellular quiescence and alterations of the plasma membrane composition, especially on decreased ergosterol levels (Khot *et al.* 2006; LaFleur, Kumamoto, and Lewis 2006; Bojsen *et al.* 2016). The rate of persister cell formation under quiescence-inducing conditions is positively correlated with previous inhibition of protein biosynthesis (rapamycin treatment) or with deletion of TORC1 pathway components which regulates protein biosynthesis (Bojsen *et al.* 2016). Therefore, downregulation of protein biosynthesis seems to be one pre-requisite for persister cell formation. The transcriptomic analysis in manuscript III indicates that this criterion is probably fulfilled for intramacrophagal *C. glabrata* yeast in our hMDM model. This correlated with the finding that amphotericin B treatment was not able to fully eradicate *C. glabrata* from hMDMs despite continuous treatment over seven days. It was however not possible for us to increase the antimycotic concentration further, due to cytotoxicity of amphotericin B desoxycholate (manuscript III). Future studies could investigate *C. glabrata* persistence in hMDMs under treatment with less cytotoxic lipid-based amphotericin B formulations, especially those which are preferentially taken up by the mononuclear phagocyte system in the human host (like e.g. amphotericin B Lipid Complex (Hamill 2013)). The finding that caspofungin was unable to fully eradicate intramacrophagal *C. glabrata* is likely to hold true for higher drug concentrations, and the importance of this result for clinical treatment strategies warrants further evaluation.

Importantly, continued antimycotic treatment has been shown to lead to accumulation of high-persister (hip) *C. albicans* strains in cancer patients with long-term oral *Candida* carriage (Lafleur, Qi, and Lewis 2010). Since amphotericin B-resistant isolates are normally rather rare (Pfaller 2012; Perlin, Rautemaa-Richardson, and Alastruey-

Izquierdo 2017), repopulation by persister cells provides a plausible hypothesis for recurrence of the infection under amphotericin B treatment (Lafleur, Qi, and Lewis 2010; Lewis 2010). In manuscript II we reviewed the current knowledge of evolutionary trajectories of fungal pathogens in the host and in evolution experiments performed in infection models. Importantly, these evolutionary landscapes depend on the fungal pathogen and their typical mode of infection. The ability of the pathogen to persist during an initial antimycotic treatment within a niche will determine its ability to cause a recurrent infection. This might be a part of the explanation for why *C. glabrata*, despite its less pronounced virulence capacities compared to *C. albicans*, is harder to treat: it likely enters quiescent states within the host at a higher frequency. In comparison, the situation is fundamentally different for other fungal pathogens like *C. neoformans*: this fungus often causes a primary infection in childhood which is often not treated with antifungals and is then either cleared by the immune system or enters into dormancy within granulomas encapsulated by the immune system (Coelho, Bocca, and Casadevall 2014) – and a quiescent state is known from *in vivo* models which could represent this dormant state (Alanio *et al.* 2015). Reactivation from dormancy might then happen if the host gets immunocompromised. Therefore, the adaptations of *C. neoformans* differ strongly from e.g. *C. albicans*, since its infecting population has a different, host-driven evolutionary history. Finally, the evolutionary landscapes are also determined by the host, especially for opportunistic pathogens: specifically the immune status determines the niches available (or not) for the fungus to develop persistence.

Identification of potential pathogen-specific niches and the potential obstacles that the infecting pathogen has to face - especially under antimycotic treatment - are therefore fundamental to understand fungal disease and to find new approaches for specific counteraction. It may be worthwhile therefore to repeat previous *in vitro* studies of persistence-defective mutants (e.g. (Bojsen *et al.* 2016)) with our *C. glabrata*-hMDM model and systemic animal infection models. These studies should ideally involve an evolutionary process within this persistence niche (e.g. by including repeated cycles of infection; (Forche *et al.* 2009; Lüttich *et al.* 2013)). This should allow us on the one hand to identify factors needed for persistence under clinically relevant conditions and on the other hand to find factors which drive evolution towards higher persistence.

3.6 Excursion: Expected fungal adaption paths by treatment with jagaricin-related antifungals

Which kind of fungal evolutionary “adaptation path” would we expect for a jagaricin-

related compound? Since jagaricin acts fungicidal and targets the plasma membrane as we have shown in manuscript I, the most likely way to acquire resistance would be to alter membrane composition and/or properties. Cell membrane properties are typically well adjusted to the needs of the species, accordingly changing them will likely result in severe fitness defects within the natural environment of this species. Appropriately our jagaricin susceptibility mutant screen in manuscript I found stable growth in presence of jagaricin only with inositol polyphosphate phosphatase deletion mutants of *C. albicans* (Δ*inp51*) and *C. glabrata* (Δ*inp53*). Deletion of *C. albicans INP51* is known to lead to cell wall defects and attenuated virulence (Badrane *et al.* 2008). Notably, we infrequently observed a late-onset growth by otherwise susceptible fungal strains at toxic jagaricin concentrations (see method section in manuscript I). If one assumes that this late onset growth results from (partial) jagaricin natural inactivation over time, this suggests the existence of jagaricin-tolerating persister cells which are able to outlast jagaricin treatment, similar to the situation with amphotericin B. However, this would need to be proven directly by testing the killing activity of jagaricin against quiescent yeast cells. If our hypothesis is right, we would expect that the fungal adaption path for jagaricin-related compounds would follow the principles for polyenes: while development of resistance is unlikely due to accompanied severe fitness drawbacks in the host, formation of persister cells is a more probable scenario.

3.7 *C. glabrata´s* intracellular quiescent state in human macrophages

Based on the hypothesis that persister cells which survive (fungicidal) antimycotic treatment are quiescent, we would expect that most of the genes which were identified in manuscript III as crucial for intracellular persistence in macrophages should be equally important if we add antimycotics to the *C. glabrata*-hMDM persistence model. This hypothesis is mainly based on the finding that a fair proportion of these genes is known to be involved in entry and maintenance of quiescence, at least in related species like *S. cerevisiae*. In the following, some interesting aspects of *C. glabrata* (quiescent) states within macrophages will be discussed that were identified by the work described in manuscript III and manuscript IV.

3.7.1 *What might be the benefits of a* C. glabrata *transcriptional mating response in macrophages?*

Apart from inferences by a clade analysis, no evidence exists for a *C. glabrata* mating cycle (Carreté *et al.* 2018). Therefore, maybe the most curious finding in manuscript III was that phagocytosed *C. glabrata* yeasts show all transcriptional hallmarks of a mating response. In general, this hints towards a link of *C. glabrata´s* decision to mate to non-beneficial, maybe quiescence-inducing conditions as found in the phagosome. A

connection of mating to non-beneficial conditions has been described in some other yeast species (Bernstein and Johns 1989; Mochizuki and Yamamoto 1992; Miyata *et al.* 1997; Davey 1998; Dumitru *et al.* 2007; Huang *et al.* 2009; Alby and Bennett 2009; Booth, Tuch, and Johnson 2010; Barsoum, Rajaei, and Åström 2011), and the reason for this link could be a mainly haploid lifestyle which requires mating prior to sporulation to form stress-resistant, long-lasting spores (Booth, Tuch, and Johnson 2010; Barsoum, Rajaei, and Åström 2011). It remains unclear whether initiation of the mating program can be beneficial for *C. glabrata* in interaction with macrophages, and whether it is a specific macrophage-induced response.

However, there are possible implications for clinical treatment strategies. It is unlikely that mating within macrophages provides any significant advantage through recombination, since individual phagosomes normally contain only a clonal yeast population from the same phagocytosed progenitor. However, a mating type switch and the induction of the mating signalling cascades and transcriptional regulons, will enhance the diversity of *C. glabrata's* cellular stages, and thereby will diversify the *C. glabrata* population in the host. This could have effects on e.g. the time point of yeast outbreak from macrophages, potentially delaying it. A reduced rate of escaping yeast might help to keep the immune reaction low and tip it into a tolerance state, aiding pathogen persistence in the host. Furthermore, diversification of clonal populations into subpopulations with different properties is a well-known strategy of yeasts to enhance the chance of survival under suddenly changing conditions (Thattai and van Oudenaarden 2004; Acar, Mettetal, and van Oudenaarden 2008; Lohse and Johnson 2009; Gaál, Pitchford, and Wood 2010; Holland *et al.* 2014). In a clinical situation, this could be e.g. an enhanced pro-inflammatory response within the host or antimycotic treatment. Finally, although quite speculative, we cannot definitely exclude that *C. glabrata* yeasts pass through a whole mating and sporulation cycle in infected patients. Although we have no direct evidence from our hMDM persistence model so far (e.g. detection of spores), it could well be that an essential trigger present *in vivo* is simply missing within our model. The resulting spores might play a role e.g. as long-lasting survivors in latent infections. Importantly, if mating happens mainly within clonal populations, these mating events would evade detection by genetic clade analyses. The seemingly out-of-place mating response of *C. glabrata* may therefore have clinical relevance, which warrants further research into this unexpected finding.

3.7.2 The nutritional situation within C. glabrata *containing phagosomes*

C. glabrata yeasts likely exist in two growth modes – „strict quiescence“ and “cycling between growth and storage build-up” – in macrophages. While further studies are

needed to better define the proportions of these states (e.g. non-transferable FITC labelling to visualize mother and daughter cells (Seider *et al.* 2011)), the main factor for yeast mode determination is likely the intracellular nutrient availability in the phagosome. The data in manuscript III did not reveal any limitation of specific nutrients apart from the non-availability of preferred carbon sources. However, *C. glabrata* cfus in the hMDM persistence model were either stable or constantly declining in the intracellular persistence stage. Since non-dividing yeasts do not require high amounts of nutrients, the general growth reduction may mask any specific limitation in the transcriptomes. Since nutrient restriction is generally thought to play a role in phagosomes, a prestarvation of yeast, as previously done for biotin (Sprenger *et al.* 2020), could deplete any storage and thereby uncover specific nutrient limitations. Additionally, modifying the persistence model in a way that it allows resumption of intracellular growth (after an initial stage of yeast quiescence) could allow the identification of nutrient requirements which are critical for the growth phase.

3.7.3 The role of energy storage for intracellular persistence in macrophages

Next to glycogen, trehalose is a central storage molecule for non-growing yeast states. When nutrients become limited, yeast cells arrest the cell cycle and stop cell division after a limited number of further divisions (Lillie and Pringle 1980; Herman 2002; Gray *et al.* 2004; Argüello-Miranda *et al.* 2018; Sagot and Laporte 2019). In this phase, they use the remaining nutrients to build up their energy storages, i.e. in the form of trehalose (Lillie and Pringle 1980; Gray *et al.* 2004; Eleutherio *et al.* 2015; Sagot and Laporte 2019). These storages are then slowly used during quiescence to maintain cellular viability (Lillie and Pringle 1980; Gray *et al.* 2004; Samokhvalov, Ignatov, and Kondrashova 2004; Sagot and Laporte 2019). When nutrients become available again, trehalose storages are rapidly mobilized to support yeast regrowth (Shi *et al.* 2010; Kyryakov *et al.* 2012; Laporte *et al.* 2017). However, this situation differs if nutrient supply is limited, but constant like e.g. in a chemostat adjusted to unfavourable conditions. Here, energy storages can be constantly build up until they exceed a critical point which allows re-entry into a limited number of cell divisions. When the storages are used up, this start-stop cycle starts over again (Küenzi and Fiechter 1972; Porro *et al.* 1988; Silljé *et al.* 1997; Beuse *et al.* 1998; Paalman *et al.* 2003; Tu *et al.* 2005; Robertson *et al.* 2008). Similar to the exit from quiescence, trehalose storages are rapidly mobilized at the G1/S transition to support yeast regrowth which includes support of anabolic processes (Ewald *et al.* 2016; Zhao *et al.* 2016). Both scenarios are able to explain the persistence defect of trehalase mutants in the hMDM persistence model (manuscript IV), depending on the growth mode of intramacrophagal *C. glabrata* yeast. Importantly, it could also provide an explanation why we found a macrophage persistence defect for deletion strains (Δ*ath1*,

Δ*nth1*, Δ*nth2*) of all three individual trehalases, as their activity might be required for different cell cycle- or growth mode-specific tasks. This assumption is supported by the finding that all trehalases were continuously transcriptionally upregulated in the hMDM persistence model (Suppl. Table 7, manuscript III). In addition, the acid trehalase *Cg*Ath1 has been shown to act on extracellular and probably vacuolar trehalose ((Zilli *et al.* 2015) and manuscript IV), while one or both of the putative neutral trehalases *Cg*Nth1 and *Cg*Nth2 likely act on cytoplasmic trehalose storages: in *S. cerevisiae*, only *Sc*Nth1 has been found to exert neutral trehalose activity, while *Sc*Nth2 has only been shown to be required for thermotolerance, but does not influence intracellular trehalose levels (van der Plaat 1974; van Solingen and van der Plaat 1975; Kopp, Muller, and Holzer 1993; Nwaka, Kopp, and Holzer 1995). While the origin of cytosolic trehalose is provided by the fungal trehalose biosynthetic enzymes Tps1 and Tps2 (Bell *et al.* 1992; De Virgilio *et al.* 1993), the origin of the extracellular / vacuolar trehalose on which *Cg*Ath1 acts on is less clear: humans do not synthesize trehalose (Elbein 1974; Elbein *et al.* 2003; Edavana *et al.* 2004), which leaves a fungal origin as the last explanation in the hMDM persistence model. In *S. cerevisiae*, fungal trehalose has been shown to be transported outside into the periplasmic space in response to stress (da Costa Morato Nery *et al.* 2008; Magalhães *et al.* 2018), which might provide a plausible hypothesis for the situation of *C. glabrata* in the phagosome. Future investigations with these and further independent mutant strains may shed more light on the specific roles of the *C. glabrata* trehalases in the phagosome (manuscript IV).

Apart from being a storage molecule, trehalose is a well-known stress protectant: It can stabilize proteins and membranes and thereby mediates resistance e.g. against heat, oxidative, and antifungal drug stress (Lillie and Pringle 1980; Eleutherio, Araujo, and Panek 1993; Elliott, Haltiwanger, and Futcher 1996; Alvarez-Peral *et al.* 2002; González-Párraga *et al.* 2011; Tournu, Fiori, and Van Dijck 2013; Argüelles 2014; Eleutherio *et al.* 2015). Presence on both sides of the membrane is needed for full stress resistance e.g. against thermal or oxidative stress (Crowe, Crowe, and Chapman 1984; Mansure *et al.* 1994; da Costa Morato Nery *et al.* 2008; Eleutherio *et al.* 2015; Magalhães *et al.* 2018). However, its degradation after stress relief is also needed to release proteins from their stabilized form. Otherwise, damaged proteins cannot be eliminated, which eventually can lead to cell death (Singer and Lindquist 1998; Wera *et al.* 1999). In accordance with this, *Cg*Nth1 was found to be necessary for oxidative stress resistance in manuscript IV. Localization of the trehalose which needs to be degraded by specific localized trehalase enzymes therefore might also explain the requirement for all three trehalases for intramacrophagal persistence. In summary, a functional trehalose metabolism –

biosynthesis and degradation – seems to be important for yeast quiescence and *C. glabrata* persistence in macrophages. Its potential role in *C. glabrata* latent infections therefore warrants further assessment.

3.7.4 The role of phosphate metabolism for intracellular persistence in macrophages

One particular interesting finding of manuscript III worth of further investigations was that *C. glabrata* Δ*pho4* shows a persistence defect after seven days in the *C. glabrata*-hMDM mutant screen, while it was inconspicuous at the day one (Suppl. Table 3 in manuscript III). In contrast to *S. cerevisiae*, Pho4 in *C. glabrata* and other fungal pathogens like *C. albicans* and *C. neoformans* is not restricted to regulation of phosphate metabolism, but adopts further roles, mainly in stress adaptation via polyphosphate (Kerwin and Wykoff 2009; Ikeh *et al.* 2016; He, Zhou, and O'Shea 2017; Ikeh, Ahmed, and Quinn 2017; Lev *et al.* 2017; Lev and Djordjevic 2018). However, deletion of one of Pho4's central targets, the high-affinity phosphate transporter Pho84, led to no effect within this screen (Suppl. Table 3 in manuscript III) despite pronounced transcriptional induction of this gene and other phosphate uptake-related genes like *GIT1* (Suppl. Table 7 in manuscript III) indicating an attempt of *C. glabrata* to increase phosphate uptake within the phagosome. In a broader view, phosphate metabolism and its regulation have been linked to virulence of *C. neoformans* and *C. albicans* (Ikeh *et al.* 2016; Lev *et al.* 2017). Phosphate acquisition is specifically critical within the alkaline environment of blood and therefore for dissemination: *C. neoformans* quickly mobilizes its polyphosphate storages in blood, as most of its phosphate transporters rely on H^+/P_i symport, which doesn´t work in the alkaline environment. Further, it depends on Pho4 activity to express the Na^+/P_i symporter Pho89 (Martinez and Persson 1998; Toh-e *et al.* 2015; Lev *et al.* 2017). Interestingly, *C. glabrata* does not possess a Pho89 transporter orthologue (Kerwin and Wykoff 2009), which raises the question how (or if) *C. glabrata* is able to take up phosphate under alkaline conditions like in human blood.

Numerous functions have been assigned to polyphosphate in diverse organisms, among them an essential role in quiescence of bacteria (Rao and Kornberg 1996; Rao, Gómez-García, and Kornberg 2009; Albi and Serrano 2016; Ikeh *et al.* 2016; Jiménez *et al.* 2017; Racki *et al.* 2017). In diverse yeast species, polyphosphate has been linked to oxidative and cationic stress tolerance (Reddi *et al.* 2009; Hothorn *et al.* 2009; Gray and Jakob 2015; Ikeh *et al.* 2016; Trilisenko *et al.* 2019) as well as cell cycle progression and genome stability: polyphosphate is used as source of phosphate supply during DNA synthesis, which helps to maintain constant free phosphate levels during this phosphate-consuming process and thereby to reduce mistakes of the replication machinery (Bru *et*

al. 2016). Further studies should therefore investigate the role of phosphate metabolism in general - and, more specific, polyphosphate - in yeast quiescence and *C. glabrata´s* pathobiology.

3.8 The macrophage´s perspective

Manuscripts III and IV focused mainly on the yeast side. This is due to the nature of our models: while the *C. glabrata*-hMDM persistence model should reflect the yeast side of the interaction quite well (as discussed above), many interaction partners which determine the behaviour of the macrophage in the host are missing within our model – basically the “non-macrophage” rest of the host. Nevertheless, the model could be refined and employed to investigate some general principles of macrophage biology: Do macrophages show different behaviour in the long term in dependence on whether they still contain intracellular persisting yeasts or succeeded to kill off all of them? If yes, how stable is this “yeast-specific fighting state” or can it be overwritten by exogenous signals, e.g. by changes in the cytokine environment? How important is the cytokine environment for the macrophages ability to keep up pressure on yeasts within the phagosome, as observed within our model? Which exogenous signals might trigger the switch between intracellular yeast persistence and intracellular replication? These questions can potentially be answered in the future with a refined *C. glabrata*-hMDM persistence model or variations thereof.

3.9 Conclusion and outlook

This work investigated effects of antifungals and long-term macrophage exposure on *Candida* species, their mode of action and the fungal response. On one side, the antifungal mode of action of jagaricin was elucidated, a substance which was identified as a virulence factor of mushroom-infecting bacteria, and possible applications were investigated. On the other side, – to our best knowledge – the first persistence model for a human pathogenic fungus in primary human macrophages was established, which allows the study of interactions with high relevance for infections. First insights include the observations that antimycotic treatment is not necessarily sufficient to eradicate intracellular *C. glabrata* from macrophages. Such an observation was only possible due to this new model, which supports its relevance for the study of host persistence niches. Genes which are needed to support entry into, maintenance of, and exit from yeast cell quiescence were found to be depleted in a mutant screening approach, complemented by an exhaustive transcriptome analysis. Together, these data showed that the conditions within the phagosome remain stressful for *C. glabrata* over the whole week-long time course. As such, the new model provided important indications why clinical treatment of *C. glabrata* can so often be difficult and what factors determine the

evolutionary path of fungal pathogens in a clinical situation.

In summary, this work used two complementary approaches to obtain knowledge about the fungal interactome which can be leveraged for future treatment: the study of molecular effectors with the potential for drug development and the study of the disease-causing mechanisms of fungal pathogens. Together, these findings will hopefully help to improve the currently often lacking antifungal treatment strategies.

4 References

Acar, M., J. T. Mettetal, and A. van Oudenaarden. 2008. 'Stochastic switching as a survival strategy in fluctuating environments', *Nat Genet*, **40**: 471-5.

Alanio, A., F. Vernel-Pauillac, A. Sturny-Leclère, and F. Dromer. 2015. 'Cryptococcus neoformans host adaptation: toward biological evidence of dormancy', *mBio*, **6**.

Albi, T., and A. Serrano. 2016. 'Inorganic polyphosphate in the microbial world. Emerging roles for a multifaceted biopolymer', *World J Microbiol Biotechnol*, **32**: 27.

Alby, K., and R. J. Bennett. 2009. 'Stress-induced phenotypic switching in Candida albicans', *Mol Biol Cell*, **20**: 3178-91.

Alexander, B. D., M. D. Johnson, C. D. Pfeiffer, C. Jiménez-Ortigosa, J. Catania, R. Booker, M. Castanheira, S. A. Messer, D. S. Perlin, and M. A. Pfaller. 2013. 'Increasing echinocandin resistance in Candida glabrata: clinical failure correlates with presence of FKS mutations and elevated minimum inhibitory concentrations', *Clin Infect Dis*, **56**: 1724-32.

Allen, C., S. Büttner, A. D. Aragon, J. A. Thomas, O. Meirelles, J. E. Jaetao, D. Benn, S. W. Ruby, M. Veenhuis, F. Madeo, and M. Werner-Washburne. 2006. 'Isolation of quiescent and nonquiescent cells from yeast stationary-phase cultures', *J Cell Biol*, 174: 89-100.

Allert, S., T. M. Förster, C. M. Svensson, J. P. Richardson, T. Pawlik, B. Hebecker, S. Rudolphi, M. Juraschitz, M. Schaller, M. Blagojevic, J. Morschhäuser, M. T. Figge, I. D. Jacobsen, J. R. Naglik, L. Kasper, S. Mogavero, and B. Hube. 2018. 'Candida albicans-Induced Epithelial Damage Mediates Translocation through Intestinal Barriers', *mBio*, **9**.

Alvarez-Peral, F. J., O. Zaragoza, Y. Pedreno, and J. C. Argüelles. 2002. 'Protective role of trehalose during severe oxidative stress caused by hydrogen peroxide and the adaptive oxidative stress response in Candida albicans', *Microbiology (Reading)*, **148**: 2599-606.

Alvarez-Rueda, N., M. Albassier, S. Allain, F. Deknuydt, F. Altare, and P. Le Pape. 2012. 'First human model of in vitro Candida albicans persistence within granuloma for the reliable study of host-fungi interactions', *PLoS One*, **7**: e40185.

Arendrup, M. C., and T. F. Patterson. 2017. 'Multidrug-Resistant Candida: Epidemiology, Molecular Mechanisms, and Treatment', J Infect Dis, 216: S445-S51.
Argüelles, J. C. 2014. 'Why can't vertebrates synthesize trehalose?', *J Mol Evol*, 79: 111-6.

Argüello-Miranda, O., Y. Liu, N. E. Wood, P. Kositangool, and A. Doncic. 2018. 'Integration of Multiple Metabolic Signals Determines Cell Fate Prior to Commitment', *Mol Cell*, 71: 733-44 e11.

Badrane, H., M. H. Nguyen, S. Cheng, V. Kumar, H. Derendorf, K. A. Iczkowski, and C. J. Clancy. 2008. 'The Candida albicans phosphatase Inp51p interacts with the EH domain protein Irs4p, regulates phosphatidylinositol-4,5-bisphosphate levels and influences hyphal formation, the cell integrity pathway and virulence', *Microbiology*, 154: 3296-308.

Baltch, A. L., L. H. Bopp, R. P. Smith, W. J. Ritz, C. J. Carlyn, and P. B. Michelsen. 2005. 'Effects of voriconazole, granulocyte-macrophage colony-stimulating factor, and

interferon gamma on intracellular fluconazole-resistant Candida glabrata and Candida krusei in human monocyte-derived macrophages', *Diagn Microbiol Infect Dis*, 52: 299-304.

Baltch, A. L., L. H. Bopp, R. P. Smith, W. J. Ritz, and P. B. Michelsen. 2008. 'Anticandidal effects of voriconazole and caspofungin, singly and in combination, against Candida glabrata, extracellularly and intracellularly in granulocyte-macrophage colony stimulating factor (GM-CSF)-activated human monocytes', *J Antimicrob Chemother*, 62: 1285-90.

Barsoum, E., N. Rajaei, and S. U. Åström. 2011. 'RAS/cyclic AMP and transcription factor Msn2 regulate mating and mating-type switching in the yeast Kluyveromyces lactis', *Eukaryot Cell*, **10**: 1545-52.

Bell, W., P. Klaassen, M. Ohnacker, T. Boller, M. Herweijer, P. Schoppink, P. Van der Zee, and A. Wiemken. 1992. 'Characterization of the 56-kDa subunit of yeast trehalose-6-phosphate synthase and cloning of its gene reveal its identity with the product of CIF1, a regulator of carbon catabolite inactivation', *Eur J Biochem*, **209**: 951-9.

Bennett, R. J., and A. D. Johnson. 2003. 'Completion of a parasexual cycle in Candida albicans by induced chromosome loss in tetraploid strains', *EMBO J*, **22**: 2505-15.

Berendsen, R. L., N. Schrier, S. I. Kalkhove, L. G. Lugones, J. J. Baars, C. Zijlstra, M. de Weerdt, H. A. Wösten, and P. A. Bakker. 2013. 'Absence of induced resistance in Agaricus bisporus against Lecanicillium fungicola', *Antonie Van Leeuwenhoek*, **103**: 539-50.

Berman, J., and D. J. Krysan. 2020. 'Drug resistance and tolerance in fungi', *Nat Rev Microbiol.*, **18**: 319–331

Bernstein, C., and V. Johns. 1989. 'Sexual reproduction as a response to H2O2 damage in Schizosaccharomyces pombe', *J Bacteriol*, **171**: 1893-7.

Berry, D. B., and A. P. Gasch. 2008. 'Stress-activated genomic expression changes serve a preparative role for impending stress in yeast', *Mol Biol Cell*, **19**: 4580-7.

Beuse, M., R. Bartling, A. Kopmann, H. Diekmann, and M. Thoma. 1998. 'Effect of the dilution rate on the mode of oscillation in continuous cultures of Saccharomyces cerevisiae', *J Biotechnol*, **61**: 15-31.

Bliska, J. B., and A. Casadevall. 2009. 'Intracellular pathogenic bacteria and fungi--a case of convergent evolution?', *Nat Rev Microbiol*, **7**: 165-71.

Boer, V. M., C. A. Crutchfield, P. H. Bradley, D. Botstein, and J. D. Rabinowitz. 2010. 'Growth-limiting intracellular metabolites in yeast growing under diverse nutrient limitations', *Mol Biol Cell*, **21**: 198-211.

Bojsen, R., B. Regenberg, and A. Folkesson. 2014. 'Saccharomyces cerevisiae biofilm tolerance towards systemic antifungals depends on growth phase', *BMC Microbiol*, **14**: 305.

Bojsen, R., B. Regenberg, and A. Folkesson. 2017. 'Persistence and drug tolerance in pathogenic yeast', *Curr Genet*, **63**: 19-22.

Bojsen, R., B. Regenberg, D. Gresham, and A. Folkesson. 2016. 'A common mechanism involving the TORC1 pathway can lead to amphotericin B-persistence in biofilm and planktonic Saccharomyces cerevisiae populations', *Sci Rep*, **6**: 21874.

Booth, L. N., B. B. Tuch, and A. D. Johnson. 2010. 'Intercalation of a new tier of transcription regulation into an ancient circuit', *Nature*, **468**: 959-63.

Bopp, L. H., A. L. Baltch, W. J. Ritz, P. B. Michelsen, and R. P. Smith. 2006. 'Antifungal effect of voriconazole on intracellular Candida glabrata, Candida krusei and Candida parapsilosis in human monocyte-derived macrophages', *J Med Microbiol*, **55**: 865-70.

Borg-von Zepelin, M., S. Beggah, K. Boggian, D. Sanglard, and M. Monod. 1998. 'The expression of the secreted aspartyl proteinases Sap4 to Sap6 from Candida albicans in murine macrophages', *Mol Microbiol*, **28**: 543-54.

BoseDasgupta, S., and J. Pieters. 2018. 'Macrophage-microbe interaction: lessons learned from the pathogen Mycobacterium tuberculosis', *Semin Immunopathol*, **40**: 577-91.

Boucherie, H. 1985. 'Protein synthesis during transition and stationary phases under glucose limitation in Saccharomyces cerevisiae', *J Bacteriol*, **161**: 385-92.

Brakhage, A. A. 2013. 'Regulation of fungal secondary metabolism', *Nat Rev Microbiol*, **11**: 21-32.

Brieland, J., D. Essig, C. Jackson, D. Frank, D. Loebenberg, F. Menzel, B. Arnold, B. DiDomenico, and R. Hare. 2001. 'Comparison of pathogenesis and host immune responses to Candida glabrata and Candida albicans in systemically infected immunocompetent mice', *Infect Immun*, **69**: 5046-55.

Brinkmann, V., U. Reichard, C. Goosmann, B. Fauler, Y. Uhlemann, D. S. Weiss, Y. Weinrauch, and A. Zychlinsky. 2004. 'Neutrophil extracellular traps kill bacteria', *Science*, **303**: 1532-5.

Broach, J. R. 1991. 'RAS genes in Saccharomyces cerevisiae: signal transduction in search of a pathway', *Trends Genet*, **7**: 28-33.

Brown, G. D., D. W. Denning, N. A. Gow, S. M. Levitz, M. G. Netea, and T. C. White. 2012. 'Hidden killers: human fungal infections', *Sci Transl Med*, **4**: 165rv13.

Bru, S., J. M. Martínez-Laínez, S. Hernández-Ortega, E. Quandt, J. Torres-Torronteras, R. Martí, D. Canadell, J. Ariño, S. Sharma, J. Jiménez, and J. Clotet. 2016. 'Polyphosphate is involved in cell cycle progression and genomic stability in Saccharomyces cerevisiae', *Mol Microbiol*, **101**: 367-80.

Brunke, S., and B. Hube. 2013. 'Two unlike cousins: Candida albicans and C. glabrata infection strategies', *Cell Microbiol*, **15**: 701-8.

Butler, G., M. D. Rasmussen, M. F. Lin, M. A. Santos, S. Sakthikumar, C. A. Munro, E. Rheinbay, M. Grabherr, A. Forche, J. L. Reedy, I. Agrafioti, M. B. Arnaud, S. Bates, A. J. Brown, S. Brunke, M. C. Costanzo, D. A. Fitzpatrick, P. W. de Groot, D. Harris, L. L. Hoyer, B. Hube, F. M. Klis, C. Kodira, N. Lennard, M. E. Logue, R. Martin, A. M. Neiman, E. Nikolaou, M. A. Quail, J. Quinn, M. C. Santos, F. F. Schmitzberger, G. Sherlock, P. Shah, K. A. Silverstein, M. S. Skrzypek, D. Soll, R. Staggs, I. Stansfield, M. P. Stumpf, P. E. Sudbery, T. Srikantha, Q. Zeng, J. Berman, M. Berriman, J. Heitman, N. A. Gow, M. C. Lorenz, B. W. Birren, M. Kellis, and C. A. Cuomo. 2009. 'Evolution of pathogenicity and sexual reproduction in eight Candida genomes', *Nature*, **459**: 657-62.

Carreté, L., E. Ksiezopolska, C. Pegueroles, E. Gómez-Molero, E. Saus, S. Iraola-Guzmán, D. Loska, O. Bader, C. Fairhead, and T. Gabaldón. 2018. 'Patterns of Genomic

Variation in the Opportunistic Pathogen Candida glabrata Suggest the Existence of Mating and a Secondary Association with Humans', *Curr Biol*, **28**: 15-27 e7.

Casadevall, A. 2008. 'Evolution of intracellular pathogens', *Annu Rev Microbiol*, **62**: 19-33.

Casadevall, A., D. P. Kontoyiannis, and V. Robert. 2019. 'On the Emergence of Candida auris: Climate Change, Azoles, Swamps, and Birds', *mBio*, **10**.

Cheng, S., C. J. Clancy, D. J. Hartman, B. Hao, and M. H. Nguyen. 2014. 'Candida glabrata intra-abdominal candidiasis is characterized by persistence within the peritoneal cavity and abscesses', *Infect Immun*, **82**: 3015-22.

Cho, K. H., and Y. K. Kim. 2003. 'Two types of ion channel formation of tolaasin, a Pseudomonas peptide toxin', *FEMS Microbiol Lett*, **221**: 221-6.

Chowdhary, A., C. Sharma, and J. F. Meis. 2017. 'Candida auris: A rapidly emerging cause of hospital-acquired multidrug-resistant fungal infections globally', *PLoS Pathog*, **13**: e1006290.

Clark, C. E., M. G. Banyas, S. E. Noell, and D. A. Essig. 2019. 'Draft Genome Sequence of Janthinobacterium sp. Strain PC23-8, Isolated from a Freshwater Stream Impacted by Acid Mine Drainage', *Microbiol Resour Announc*, **8**.

Coelho, C., A. L. Bocca, and A. Casadevall. 2014. 'The intracellular life of Cryptococcus neoformans', *Annu Rev Pathol*, **9**: 219-38.

Coers, J., M. N. Starnbach, and J. C. Howard. 2009. 'Modeling infectious disease in mice: co-adaptation and the role of host-specific IFNgamma responses', *PLoS Pathog*, **5**: e1000333.

Coller, H. A., L. Sang, and J. M. Roberts. 2006. 'A new description of cellular quiescence', *PLoS Biol*, **4**: e83.

Coraiola, M., P. Lo Cantore, S. Lazzaroni, A. Evidente, N. S. Iacobellis, and M. Dalla Serra. 2006. 'WLIP and tolaasin I, lipodepsipeptides from Pseudomonas reactans and Pseudomonas tolaasii, permeabilise model membranes', *Biochim Biophys Acta*, **1758**: 1713-22.

Cowen, L. E., and S. Lindquist. 2005. 'Hsp90 potentiates the rapid evolution of new traits: drug resistance in diverse fungi', *Science*, **309**: 2185-9.

Cowen, L. E., D. Sanglard, S. J. Howard, P. D. Rogers, and D. S. Perlin. 2014. 'Mechanisms of Antifungal Drug Resistance', *Cold Spring Harb Perspect Med*, **5**: a019752.

Crowe, J. H., L. M. Crowe, and D. Chapman. 1984. 'Preservation of membranes in anhydrobiotic organisms: the role of trehalose', *Science*, **223**: 701-3.

Csank, C., and K. Haynes. 2000. 'Candida glabrata displays pseudohyphal growth', *FEMS Microbiol Lett*, **189**: 115-20.

da Costa Morato Nery, D., C. G. da Silva, D. Mariani, P. N. Fernandes, M. D. Pereira, A. D. Panek, and E. C. Eleutherio. 2008. 'The role of trehalose and its transporter in protection against reactive oxygen species', *Biochim Biophys Acta*, **1780**: 1408-11.

Davey, J. 1998. 'Fusion of a fission yeast', *Yeast*, **14**: 1529-66.

De Silva, D. D., S. Rapior, E. Sudarman, M. Stadler, J. Xu, S. A. Alias, and K. D. Hyde. 2013. 'Bioactive metabolites from macrofungi: ethnopharmacology, biological activities and chemistry', *Fungal Diversity*, **62**: 1-40.

De Virgilio, C. 2012. 'The essence of yeast quiescence', *FEMS Microbiol Rev*, **36**: 306-39.

De Virgilio, C., N. Burckert, W. Bell, P. Jeno, T. Boller, and A. Wiemken. 1993. 'Disruption of TPS2, the gene encoding the 100-kDa subunit of the trehalose-6-phosphate synthase/phosphatase complex in Saccharomyces cerevisiae, causes accumulation of trehalose-6-phosphate and loss of trehalose-6-phosphate phosphatase activity', *Eur J Biochem*, **212**: 315-23.

Denning, D. W. 2003. 'Echinocandin antifungal drugs', *Lancet*, **362**: 1142-51.

DeRisi, J. L., V. R. Iyer, and P. O. Brown. 1997. 'Exploring the metabolic and genetic control of gene expression on a genomic scale', *Science*, **278**: 680-6.

Doehlemann, G., B. Ökmen, W. Zhu, and A. Sharon. 2017. 'Plant Pathogenic Fungi', *Microbiol Spectr*, **5**.

Doster, R. S., L. M. Rogers, J. A. Gaddy, and D. M. Aronoff. 2018. 'Macrophage Extracellular Traps: A Scoping Review', *J Innate Immun*, **10**: 3-13.

Duggan, S., F. Essig, K. Hünniger, Z. Mokhtari, L. Bauer, T. Lehnert, S. Brandes, A. Häder, I. D. Jacobsen, R. Martin, M. T. Figge, and O. Kurzai. 2015. 'Neutrophil activation by Candida glabrata but not Candida albicans promotes fungal uptake by monocytes', *Cell Microbiol*, **17**: 1259-76.

Dujon, B., D. Sherman, G. Fischer, P. Durrens, S. Casaregola, I. Lafontaine, J. De Montigny, C. Marck, C. Neuvéglise, E. Talla, N. Goffard, L. Frangeul, M. Aigle, V. Anthouard, A. Babour, V. Barbe, S. Barnay, S. Blanchin, J. M. Beckerich, E. Beyne, C. Bleykasten, A. Boisramé, J. Boyer, L. Cattolico, F. Confanioleri, A. De Daruvar, L. Despons, E. Fabre, C. Fairhead, H. Ferry-Dumazet, A. Groppi, F. Hantraye, C. Hennequin, N. Jauniaux, P. Joyet, R. Kachouri, A. Kerrest, R. Koszul, M. Lemaire, I. Lesur, L. Ma, H. Muller, J. M. Nicaud, M. Nikolski, S. Oztas, O. Ozier-Kalogeropoulos, S. Pellenz, S. Potier, G. F. Richard, M. L. Straub, A. Suleau, D. Swennen, F. Tekaia, M. Wésolowski-Louvel, E. Westhof, B. Wirth, M. Zeniou-Meyer, I. Zivanovic, M. Bolotin-Fukuhara, A. Thierry, C. Bouchier, B. Caudron, C. Scarpelli, C. Gaillardin, J. Weissenbach, P. Wincker, and J. L. Souciet. 2004. 'Genome evolution in yeasts', *Nature*, **430**: 35-44.

Dumitru, R., D. H. Navarathna, C. P. Semighini, C. G. Elowsky, R. V. Dumitru, D. Dignard, M. Whiteway, A. L. Atkin, and K. W. Nickerson. 2007. 'In vivo and in vitro anaerobic mating in Candida albicans', *Eukaryot Cell*, **6**: 465-72.

Edavana, V. K., I. Pastuszak, J. D. Carroll, P. Thampi, E. C. Abraham, and A. D. Elbein. 2004. 'Cloning and expression of the trehalose-phosphate phosphatase of Mycobacterium tuberculosis: comparison to the enzyme from Mycobacterium smegmatis', *Arch Biochem Biophys*, **426**: 250-7.

Elbein, A. D. 1974. 'The metabolism of alpha,alpha-trehalose', *Adv Carbohydr Chem Biochem*, **30**: 227-56.

Elbein, A. D., Y. T. Pan, I. Pastuszak, and D. Carroll. 2003. 'New insights on trehalose: a multifunctional molecule', *Glycobiology*, **13**: 17R-27R.

Eleutherio, E. C., P. S. Araujo, and A. D. Panek. 1993. 'Protective role of trehalose during heat stress in Saccharomyces cerevisiae', *Cryobiology*, **30**: 591-6.

Eleutherio, E., A. Panek, J. F. De Mesquita, E. Trevisol, and R. Magalhães. 2015. 'Revisiting yeast trehalose metabolism', *Curr Genet*, **61**: 263-74.

Elliott, B., R. S. Haltiwanger, and B. Futcher. 1996. 'Synergy between trehalose and Hsp104 for thermotolerance in Saccharomyces cerevisiae', *Genetics*, **144**: 923-33.

Ellner, J. J. 1990. 'Sources of variability in assays of the interaction of mycobacteria with mononuclear phagocytes: of mice and men', *Res Microbiol*, **141**: 237-40.

Erwig, L. P., and N. A. Gow. 2016. 'Interactions of fungal pathogens with phagocytes', *Nat Rev Microbiol*, **14**: 163-76.

Estruch, F. 2000. 'Stress-controlled transcription factors, stress-induced genes and stress tolerance in budding yeast', *FEMS Microbiol Rev*, **24**: 469-86.

Ewald, J. C., A. Kuehne, N. Zamboni, and J. M. Skotheim. 2016. 'The Yeast Cyclin-Dependent Kinase Routes Carbon Fluxes to Fuel Cell Cycle Progression', *Mol Cell*, **62**: 532-45.

Flannagan, R. S., B. Heit, and D. E. Heinrichs. 2015. 'Antimicrobial Mechanisms of Macrophages and the Immune Evasion Strategies of Staphylococcus aureus', *Pathogens*, **4**: 826-68.

Fleming, A. 1929. 'On the Antibacterial Action of Cultures of a Penicillium, with Special Reference to their Use in the Isolation of B. influenzæ', *British Journal of Experimental Pathology*, **X (No. 3)**: 226-36.

Forche, A., P. T. Magee, A. Selmecki, J. Berman, and G. May. 2009. 'Evolution in Candida albicans populations during a single passage through a mouse host', *Genetics*, **182**: 799-811.

François, J., and J. L. Parrou. 2001. 'Reserve carbohydrates metabolism in the yeast Saccharomyces cerevisiae', *FEMS Microbiol Rev*, **25**: 125-45.

Fuge, E. K., E. L. Braun, and M. Werner-Washburne. 1994. 'Protein synthesis in long-term stationary-phase cultures of Saccharomyces cerevisiae', *J Bacteriol*, **176**: 5802-13.

Gaál, B., J. W. Pitchford, and A. J. Wood. 2010. 'Exact results for the evolution of stochastic switching in variable asymmetric environments', Genetics, 184: 1113-9.
Garcia-Solache, M. A., and A. Casadevall. 2010. 'Global warming will bring new fungal diseases for mammals', *mBio*, **1**.

Garfoot, A. L., and C. A. Rappleye. 2016. 'Histoplasma capsulatum surmounts obstacles to intracellular pathogenesis', *FEBS J*, **283**: 619-33.

Goldberg, A. A., S. D. Bourque, P. Kyryakov, C. Gregg, T. Boukh-Viner, A. Beach, M. T. Burstein, G. Machkalyan, V. Richard, S. Rampersad, D. Cyr, S. Milijevic, and V. I. Titorenko. 2009. 'Effect of calorie restriction on the metabolic history of chronologically aging yeast', *Exp Gerontol*, **44**: 555-71.

González-Párraga, P., R. Sánchez-Fresneda, O. Zaragoza, and J. C. Argüelles. 2011. 'Amphotericin B induces trehalose synthesis and simultaneously activates an antioxidant enzymatic response in Candida albicans', *Biochim Biophys Acta*, **1810**: 777-83.

Graupner, K., K. Scherlach, T. Bretschneider, G. Lackner, M. Roth, H. Gross, and C. Hertweck. 2012. 'Imaging mass spectrometry and genome mining reveal highly antifungal virulence factor of mushroom soft rot pathogen', *Angew Chem Int Ed Engl*, **51**: 13173-7.

Gray, J. V., G. A. Petsko, G. C. Johnston, D. Ringe, R. A. Singer, and M. Werner-Washburne. 2004. '"Sleeping beauty": quiescence in Saccharomyces cerevisiae', *Microbiol Mol Biol Rev*, **68**: 187-206.

Gray, M. J., and U. Jakob. 2015. 'Oxidative stress protection by polyphosphate--new roles for an old player', *Curr Opin Microbiol*, **24**: 1-6.

Guan, Q., S. Haroon, D. G. Bravo, J. L. Will, and A. P. Gasch. 2012. 'Cellular memory of acquired stress resistance in Saccharomyces cerevisiae', *Genetics*, **192**: 495-505.

Haas, A. 1998. 'Reprogramming the phagocytic pathway--intracellular pathogens and their vacuoles (review)', *Mol Membr Biol*, **15**: 103-21.

Haas, A. 2007. 'The phagosome: compartment with a license to kill', *Traffic*, **8**: 311-30.

Hamill, R. J. 2013. 'Amphotericin B formulations: a comparative review of efficacy and toxicity', *Drugs*, **73**: 919-34.

Hawksworth, D. L., and R. Lücking. 2017. 'Fungal Diversity Revisited: 2.2 to 3.8 Million Species', *Microbiol Spectr*, **5**.

Hawksworth, D. L., and A. Y. Rossman. 1997. 'Where are all the undescribed fungi?', *Phytopathology*, **87**: 888-91.

He, B. Z., X. Zhou, and E. K. O'Shea. 2017. 'Evolution of reduced co-activator dependence led to target expansion of a starvation response pathway', *Elife*, **6**.

Herman, P. K. 2002. 'Stationary phase in yeast', *Curr Opin Microbiol*, **5**: 602-7.

Ho, J., D. N. Wickramasinghe, S. A. Nikou, B. Hube, J. P. Richardson, and J. R. Naglik. 2020. 'Candidalysin Is a Potent Trigger of Alarmin and Antimicrobial Peptide Release in Epithelial Cells', *Cells*, **9**.

Ho, J., X. Yang, S. A. Nikou, N. Kichik, A. Donkin, N. O. Ponde, J. P. Richardson, R. L. Gratacap, L. S. Archambault, C. P. Zwirner, C. Murciano, R. Henley-Smith, S. Thavaraj, C. J. Tynan, S. L. Gaffen, B. Hube, R. T. Wheeler, D. L. Moyes, and J. R. Naglik. 2019. 'Candidalysin activates innate epithelial immune responses via epidermal growth factor receptor', *Nat Commun*, **10**: 2297.

Holland, S. L., T. Reader, P. S. Dyer, and S. V. Avery. 2014. 'Phenotypic heterogeneity is a selected trait in natural yeast populations subject to environmental stress', *Environ Microbiol*, **16**: 1729-40.

Hothorn, M., H. Neumann, E. D. Lenherr, M. Wehner, V. Rybin, P. O. Hassa, A. Uttenweiler, M. Reinhardt, A. Schmidt, J. Seiler, A. G. Ladurner, C. Herrmann, K. Scheffzek, and A. Mayer. 2009. 'Catalytic core of a membrane-associated eukaryotic polyphosphate polymerase', *Science*, **324**: 513-6.

Howard, S. J., and M. C. Arendrup. 2011. 'Acquired antifungal drug resistance in Aspergillus fumigatus: epidemiology and detection', *Med Mycol*, **49** Suppl 1: S90-5.

Hsieh, S. H., S. Brunke, and M. Brock. 2017. 'Encapsulation of Antifungals in Micelles Protects Candida albicans during Gall-Bladder Infection', *Front Microbiol*, **8**: 117.

Huang, G., T. Srikantha, N. Sahni, S. Yi, and D. R. Soll. 2009. 'CO(2) regulates white-to-opaque switching in Candida albicans', *Curr Biol*, **19**: 330-4.

Huang, L., E. V. Nazarova, and D. G. Russell. 2019. 'Mycobacterium tuberculosis: Bacterial Fitness within the Host Macrophage', *Microbiol Spectr*, **7**.

Hube, B. 2009. 'Fungal adaptation to the host environment', *Curr Opin Microbiol*, **12**: 347-9.

Hull, C. M., R. M. Raisner, and A. D. Johnson. 2000. 'Evidence for mating of the "asexual" yeast Candida albicans in a mammalian host', *Science*, **289**: 307-10.

Ikeh, M. A., S. L. Kastora, A. M. Day, C. M. Herrero-de-Dios, E. Tarrant, K. J. Waldron, A. P. Banks, J. M. Bain, D. Lydall, E. A. Veal, D. M. MacCallum, L. P. Erwig, A. J. Brown, and J. Quinn. 2016. 'Pho4 mediates phosphate acquisition in Candida albicans and is vital for stress resistance and metal homeostasis', *Mol Biol Cell*, **27**: 2784-801.

Ikeh, M., Y. Ahmed, and J. Quinn. 2017. 'Phosphate Acquisition and Virulence in Human Fungal Pathogens', *Microorganisms*, **5**.

Ipcho, S., T. Sundelin, G. Erbs, H. C. Kistler, M. A. Newman, and S. Olsson. 2016. 'Fungal Innate Immunity Induced by Bacterial Microbe-Associated Molecular Patterns (MAMPs)', *G3 (Bethesda)*, **6**: 1585-95.

Ireton, K., L. A. Rigano, and G. C. Dowd. 2014. 'Role of host GTPases in infection by Listeria monocytogenes', *Cell Microbiol*, **16**: 1311-20.

Jabra-Rizk, M. A., E. F. Kong, C. Tsui, M. H. Nguyen, C. J. Clancy, P. L. Fidel, Jr., and M. Noverr. 2016. 'Candida albicans Pathogenesis: Fitting within the Host-Microbe Damage Response Framework', *Infect Immun*, **84**: 2724-39.

Jackson, B. R., N. Chow, K. Forsberg, A. P. Litvintseva, S. R. Lockhart, R. Welsh, S. Vallabhaneni, and T. Chiller. 2019. 'On the Origins of a Species: What Might Explain the Rise of Candida auris?', *J Fungi (Basel)*, **5**.

Jacobsen, I. D., S. Brunke, K. Seider, T. Schwarzmüller, A. Firon, C. d'Enfert, K. Kuchler, and B. Hube. 2010. 'Candida glabrata persistence in mice does not depend on host immunosuppression and is unaffected by fungal amino acid auxotrophy', *Infect Immun*, **78**: 1066-77.

Jain, N. K., and I. Roy. 2009. 'Effect of trehalose on protein structure', *Protein Sci*, **18**: 24-36.

Jensen, R. H., K. M. Astvad, L. V. Silva, D. Sanglard, R. Jørgensen, K. F. Nielsen, E. G. Mathiasen, G. Doroudian, D. S. Perlin, and M. C. Arendrup. 2015. 'Stepwise emergence of azole, echinocandin and amphotericin B multidrug resistance in vivo in Candida albicans orchestrated by multiple genetic alterations', *J Antimicrob Chemother*, **70**: 2551-5.

Jiménez, J., S. Bru, M. P. Ribeiro, and J. Clotet. 2017. 'Polyphosphate: popping up from oblivion', *Curr Genet*, **63**: 15-18.

Jomori, T., Y. Hara, M. Sasaoka, K. Harada, A. Setiawan, K. Hirata, A. Kimishima, and M. Arai. 2020. 'Mycobacterium smegmatis alters the production of secondary metabolites

by marine-derived Aspergillus niger', *J Nat Med*, **74**: 76-82.

Ju, Q., and J. R. Warner. 1994. 'Ribosome synthesis during the growth cycle of Saccharomyces cerevisiae', *Yeast*, **10**: 151-7.

Kasper, L., A. König, P. A. Koenig, M. S. Gresnigt, J. Westman, R. A. Drummond, M. S. Lionakis, O. Gross, J. Ruland, J. R. Naglik, and B. Hube. 2018. 'The fungal peptide toxin Candidalysin activates the NLRP3 inflammasome and causes cytolysis in mononuclear phagocytes', *Nat Commun*, **9**: 4260.

Kasper, L., K. Seider, and B. Hube. 2015. 'Intracellular survival of Candida glabrata in macrophages: immune evasion and persistence', *FEMS Yeast Res*, **15**: fov042.

Kaur, R., B. Ma, and B. P. Cormack. 2007. 'A family of glycosylphosphatidylinositol-linked aspartyl proteases is required for virulence of Candida glabrata', *Proc Natl Acad Sci U S A*, **104**: 7628-33.

Kerwin, C. L., and D. D. Wykoff. 2009. 'Candida glabrata PHO4 is necessary and sufficient for Pho2-independent transcription of phosphate starvation genes', *Genetics*, **182**: 471-9.

Khot, P. D., P. A. Suci, R. L. Miller, R. D. Nelson, and B. J. Tyler. 2006. 'A small subpopulation of blastospores in candida albicans biofilms exhibit resistance to amphotericin B associated with differential regulation of ergosterol and beta-1,6-glucan pathway genes', *Antimicrob Agents Chemother*, **50**: 3708-16.

Klosinska, M. M., C. A. Crutchfield, P. H. Bradley, J. D. Rabinowitz, and J. R. Broach. 2011. 'Yeast cells can access distinct quiescent states', *Genes Dev*, **25**: 336-49.

Kobayashi, D. Y., and J. A. Crouch. 2009. 'Bacterial/Fungal interactions: from pathogens to mutualistic endosymbionts', *Annu Rev Phytopathol*, **47**: 63-82.

Köhler, J. R., B. Hube, R. Puccia, A. Casadevall, and J. R. Perfect. 2017. 'Fungi that Infect Humans', *Microbiol Spectr*, **5**.

König, A., B. Hube, and L. Kasper. 2020. 'The Dual Function of the Fungal Toxin Candidalysin during Candida albicans-Macrophage Interaction and Virulence', *Toxins (Basel)*, **12**.

Kopp, M., H. Muller, and H. Holzer. 1993. 'Molecular analysis of the neutral trehalase gene from Saccharomyces cerevisiae', *J Biol Chem*, **268**: 4766-74.

Krause, S. A., and J. V. Gray. 2002. 'The protein kinase C pathway is required for viability in quiescence in Saccharomyces cerevisiae', *Curr Biol*, **12**: 588-93.

Küenzi, M. T., and A. Fiechter. 1972. 'Regulation of carbohydrate composition of Saccharomyces cerevisiae under growth limitation', *Arch Mikrobiol*, **84**: 254-65.

Künzler, M. 2018. 'How fungi defend themselves against microbial competitors and animal predators', *PLoS Pathog*, **14**: e1007184.

Kurtzman, C. P., and C. J. Robnett. 1997. 'Identification of clinically important ascomycetous yeasts based on nucleotide divergence in the 5' end of the large-subunit (26S) ribosomal DNA gene', *J Clin Microbiol*, **35**: 1216-23.

Kusner, D. J. 2005. 'Mechanisms of mycobacterial persistence in tuberculosis', *Clin*

Immunol, **114**: 239-47.

Kyryakov, P., A. Beach, V. R. Richard, M. T. Burstein, A. Leonov, S. Levy, and V. I. Titorenko. 2012. 'Caloric restriction extends yeast chronological lifespan by altering a pattern of age-related changes in trehalose concentration', *Front Physiol*, **3**: 256.

Lachke, S. A., S. Joly, K. Daniels, and D. R. Soll. 2002. 'Phenotypic switching and filamentation in Candida glabrata', *Microbiology*, **148**: 2661-74.

LaFleur, M. D., C. A. Kumamoto, and K. Lewis. 2006. 'Candida albicans biofilms produce antifungal-tolerant persister cells', *Antimicrob Agents Chemother*, **50**: 3839-46.

Lafleur, M. D., Q. Qi, and K. Lewis. 2010. 'Patients with long-term oral carriage harbor high-persister mutants of Candida albicans', *Antimicrob Agents Chemother*, **54**: 39-44.

Laporte, D., L. Gouleme, L. Jimenez, I. Khemiri, and I. Sagot. 2018. 'Mitochondria reorganization upon proliferation arrest predicts individual yeast cell fate', *Elife*, **7**.

Laporte, D., L. Jimenez, L. Gouleme, and I. Sagot. 2017. 'Yeast quiescence exit swiftness is influenced by cell volume and chronological age', *Microb Cell*, **5**: 104-11.

Laporte, D., A. Lebaudy, A. Sahin, B. Pinson, J. Ceschin, B. Daignan-Fornier, and I. Sagot. 2011. 'Metabolic status rather than cell cycle signals control quiescence entry and exit', *J Cell Biol*, **192**: 949-57.

Largeteau, M. L., and J. M. Savoie. 2010. 'Microbially induced diseases of Agaricus bisporus: biochemical mechanisms and impact on commercial mushroom production', *Appl Microbiol Biotechnol*, **86**: 63-73.

Lesage, G., and H. Bussey. 2006. 'Cell wall assembly in Saccharomyces cerevisiae', *Microbiol Mol Biol Rev*, **70**: 317-43.

Lev, S., and J. T. Djordjevic. 2018. 'Why is a functional PHO pathway required by fungal pathogens to disseminate within a phosphate-rich host: A paradox explained by alkaline pH-simulated nutrient deprivation and expanded PHO pathway function', *PLoS Pathog*, **14**: e1007021.

Lev, S., K. Kaufman-Francis, D. Desmarini, P. G. Juillard, C. Li, S. A. Stifter, C. G. Feng, T. C. Sorrell, G. E. Grau, Y. S. Bahn, and J. T. Djordjevic. 2017. 'Pho4 Is Essential for Dissemination of Cryptococcus neoformans to the Host Brain by Promoting Phosphate Uptake and Growth at Alkaline pH', *mSphere*, **2**.

Levin, D. E. 2005. 'Cell wall integrity signaling in Saccharomyces cerevisiae', *Microbiol Mol Biol Rev*, **69**: 262-91.

Levin, R., S. Grinstein, and J. Canton. 2016. 'The life cycle of phagosomes: formation, maturation, and resolution', *Immunol Rev*, **273**: 156-79.

Lewis, K. 2010. 'Persister cells', *Annu Rev Microbiol*, **64**: 357-72.

Lillie, S. H., and J. R. Pringle. 1980. 'Reserve carbohydrate metabolism in Saccharomyces cerevisiae: responses to nutrient limitation', J Bacteriol, 143: 1384-94.
Lohse, M. B., and A. D. Johnson. 2009. 'White-opaque switching in Candida albicans', *Curr Opin Microbiol*, **12**: 650-4.

Lorenz, M. C., J. A. Bender, and G. R. Fink. 2004. 'Transcriptional response of Candida albicans upon internalization by macrophages', *Eukaryot Cell*, **3**: 1076-87.

Lübken, T., J. Schmidt, A. Porzel, N. Arnold, and L. Wessjohann. 2004. 'Hygrophorones A-G: fungicidal cyclopentenones from Hygrophorus species (Basidiomycetes)', *Phytochemistry*, **65**: 1061-71.

Lüttich, A., S. Brunke, B. Hube, and I. D. Jacobsen. 2013. 'Serial passaging of Candida albicans in systemic murine infection suggests that the wild type strain SC5314 is well adapted to the murine kidney', *PLoS One*, **8**: e64482.

Maarten J. Chrispeels, David E. Sadava. 2003. *Plants, Genes, and Crop Biotechnology* (**2nd Edition**) (Jones and Bartlett Publishers: 40 Tall Pine Drive, Sudbury, MA 01776, USA).

Magalhães, R. S. S., B. Popova, G. H. Braus, T. F. Outeiro, and E. C. A. Eleutherio. 2018. 'The trehalose protective mechanism during thermal stress in Saccharomyces cerevisiae: the roles of Ath1 and Agt1', *FEMS Yeast Res*, **18**.

Magee, B. B., and P. T. Magee. 2000. 'Induction of mating in Candida albicans by construction of MTLa and MTLalpha strains', *Science*, **289**: 310-3.

Mansure, J. J., A. D. Panek, L. M. Crowe, and J. H. Crowe. 1994. 'Trehalose inhibits ethanol effects on intact yeast cells and liposomes', *Biochim Biophys Acta*, **1191**: 309-16.

Martinez, P., and B. L. Persson. 1998. 'Identification, cloning and characterization of a derepressible Na+-coupled phosphate transporter in Saccharomyces cerevisiae', *Mol Gen Genet*, **258**: 628-38.

Martins, M., M. Henriques, J. L. Lopez-Ribot, and R. Oliveira. 2012. 'Addition of DNase improves the in vitro activity of antifungal drugs against Candida albicans biofilms', *Mycoses*, **55**: 80-5.

McMurray, D. N. 2001. 'Disease model: pulmonary tuberculosis', *Trends Mol Med*, **7**: 135-7.

Meena, K. R., and S. S. Kanwar. 2015. 'Lipopeptides as the antifungal and antibacterial agents: applications in food safety and therapeutics', *Biomed Res Int*, **2015**: 473050.

Miles, S., and L. Breeden. 2017. 'A common strategy for initiating the transition from proliferation to quiescence', *Curr Genet*, **63**: 179-86.

Miles, S., L. H. Li, Z. Melville, and L. L. Breeden. 2019. 'Ssd1 and the cell wall integrity pathway promote entry, maintenance, and recovery from quiescence in budding yeast', *Mol Biol Cell*, **30**: 2205-17.

Miller, M. G., and A. D. Johnson. 2002. 'White-opaque switching in Candida albicans is controlled by mating-type locus homeodomain proteins and allows efficient mating', *Cell*, **110**: 293-302.

Misme-Aucouturier, B., M. Albassier, N. Alvarez-Rueda, and P. Le Pape. 2017. 'Specific Human and Candida Cellular Interactions Lead to Controlled or Persistent Infection Outcomes during Granuloma-Like Formation', *Infect Immun*, **85**.

Misseri, G., M. Ippolito, and A. Cortegiani. 2019. 'Global warming "heating up" the ICU through Candida auris infections: the climate changes theory', *Crit Care*, **23**: 416.

Miyata, M., H. Doi, H. Miyata, and B. F. Johnson. 1997. 'Sexual co-flocculation by

heterothallic cells of the fission yeast Schizosaccharomyces pombe modulated by medium constituents', *Antonie Van Leeuwenhoek*, **71**: 207-15.

Mochizuki, N., and M. Yamamoto. 1992. 'Reduction in the intracellular cAMP level triggers initiation of sexual development in fission yeast', *Mol Gen Genet*, **233**: 17-24.

Moyes, D. L., D. Wilson, J. P. Richardson, S. Mogavero, S. X. Tang, J. Wernecke, S. Höfs, R. L. Gratacap, J. Robbins, M. Runglall, C. Murciano, M. Blagojevic, S. Thavaraj, T. M. Förster, B. Hebecker, L. Kasper, G. Vizcay, S. I. Iancu, N. Kichik, A. Häder, O. Kurzai, T. Luo, T. Krüger, O. Kniemeyer, E. Cota, O. Bader, R. T. Wheeler, T. Gutsmann, B. Hube, and J. R. Naglik. 2016. 'Candidalysin is a fungal peptide toxin critical for mucosal infection', *Nature*, **532**: 64-8.

Mukherjee, P. K., J. Chandra, D. M. Kuhn, and M. A. Ghannoum. 2003. 'Mechanism of fluconazole resistance in Candida albicans biofilms: phase-specific role of efflux pumps and membrane sterols', *Infect Immun*, **71**: 4333-40.

Muller, H., C. Hennequin, J. Gallaud, B. Dujon, and C. Fairhead. 2008. 'The asexual yeast Candida glabrata maintains distinct a and alpha haploid mating types', *Eukaryot Cell*, **7**: 848-58.

Murphy, K., P. Travers, M. Walport, L. Seidler, and I. Haußer-Silber. 2009. *Janeway Immunologie (deutsche Übersetzung)*, **7. Auflage**; (Spektrum Akademischer Verlag: Heidelberg).

Naglik, J., A. Albrecht, O. Bader, and B. Hube. 2004. 'Candida albicans proteinases and host/pathogen interactions', *Cell Microbiol*, **6**: 915-26.

Nakayama, H., K. Tanabe, M. Bard, W. Hodgson, S. Wu, D. Takemori, T. Aoyama, N. S. Kumaraswami, L. Metzler, Y. Takano, H. Chibana, and M. Niimi. 2007. 'The Candida glabrata putative sterol transporter gene CgAUS1 protects cells against azoles in the presence of serum', *J Antimicrob Chemother*, **60**: 1264-72.

Nauseef, W. M. 2001. 'The proper study of mankind', *J Clin Invest*, **107**: 401-3.

Nett, J. E., K. Crawford, K. Marchillo, and D. R. Andes. 2010. 'Role of Fks1p and matrix glucan in Candida albicans biofilm resistance to an echinocandin, pyrimidine, and polyene', *Antimicrob Agents Chemother*, **54**: 3505-8.

Nett, J., L. Lincoln, K. Marchillo, R. Massey, K. Holoyda, B. Hoff, M. VanHandel, and D. Andes. 2007. 'Putative role of beta-1,3 glucans in Candida albicans biofilm resistance', *Antimicrob Agents Chemother*, **51**: 510-20.

Netzker, T., M. Flak, M. K. Krespach, M. C. Stroe, J. Weber, V. Schroeckh, and A. A. Brakhage. 2018. 'Microbial interactions trigger the production of antibiotics', *Curr Opin Microbiol*, **45**: 117-23.

Noble, S. M., B. A. Gianetti, and J. N. Witchley. 2017. 'Candida albicans cell-type switching and functional plasticity in the mammalian host', *Nat Rev Microbiol*, **15**: 96-108.

Novohradská, S., I. Ferling, and F. Hillmann. 2017. 'Exploring Virulence Determinants of Filamentous Fungal Pathogens through Interactions with Soil Amoebae', *Front Cell Infect Microbiol*, **7**: 497.

Nwaka, S., M. Kopp, and H. Holzer. 1995. 'Expression and function of the trehalase genes NTH1 and YBR0106 in Saccharomyces cerevisiae', *J Biol Chem*, **270**: 10193-8.

Otto, V., and D. H. Howard. 1976. 'Further studies on the intracellular behavior of Torulopsis glabrata', *Infect Immun*, **14**: 433-8.

Paalman, J. W., R. Verwaal, S. H. Slofstra, A. J. Verkleij, J. Boonstra, and C. T. Verrips. 2003. 'Trehalose and glycogen accumulation is related to the duration of the G1 phase of Saccharomyces cerevisiae', *FEMS Yeast Res*, **3**: 261-8.

Palková, Z., D. Wilkinson, and L. Váchová. 2014. 'Aging and differentiation in yeast populations: elders with different properties and functions', *FEMS Yeast Res*, **14**: 96-108.

Paraje, M. G., S. G. Correa, I. Albesa, and C. E. Sotomayor. 2009. 'Lipase of Candida albicans induces activation of NADPH oxidase and L-arginine pathways on resting and activated macrophages', *Biochem Biophys Res Commun*, **390**: 263-8.

Paraje, M. G., S. G. Correa, M. S. Renna, M. Theumer, and C. E. Sotomayor. 2008. 'Candida albicans-secreted lipase induces injury and steatosis in immune and parenchymal cells', *Can J Microbiol*, **54**: 647-59.

Perlin, D. S. 2015. 'Echinocandin Resistance in Candida', *Clin Infect Dis*, **61** Suppl 6: S612-7.

Perlin, D. S., R. Rautemaa-Richardson, and A. Alastruey-Izquierdo. 2017. 'The global problem of antifungal resistance: prevalence, mechanisms, and management', *Lancet Infect Dis*, **17**: e383-e92.

Pfaller, M. A. 2012. 'Antifungal drug resistance: mechanisms, epidemiology, and consequences for treatment', *Am J Med*, **125**: S3-13.

Pfaller, M. A., M. Castanheira, S. R. Lockhart, A. M. Ahlquist, S. A. Messer, and R. N. Jones. 2012. 'Frequency of decreased susceptibility and resistance to echinocandins among fluconazole-resistant bloodstream isolates of Candida glabrata', *J Clin Microbiol*, **50**: 1199-203.

Piacenza, L., M. Trujillo, and R. Radi. 2019. 'Reactive species and pathogen antioxidant networks during phagocytosis', *J Exp Med*, **216**: 501-16.

Porro, D., E. Martegani, B. M. Ranzi, and L. Alberghina. 1988. 'Oscillations in continuous cultures of budding yeast: a segregated parameter analysis', *Biotechnol Bioeng*, **32**: 411-7.

Pradhan, G., P. Raj Abraham, R. Shrivastava, and S. Mukhopadhyay. 2019. 'Calcium Signaling Commands Phagosome Maturation Process', *Int Rev Immunol*, **38**: 57-69.

Pramer, D. 1964. 'Nematode- Trapping Fungi. An Intriguing Group of Carnivorous Plants Inhabit the Microbial World', *Science*, **144**: 382-8.

Racki, L. R., E. I. Tocheva, M. G. Dieterle, M. C. Sullivan, G. J. Jensen, and D. K. Newman. 2017. 'Polyphosphate granule biogenesis is temporally and functionally tied to cell cycle exit during starvation in Pseudomonas aeruginosa', *Proc Natl Acad Sci U S A*, **114**: E2440-E49.

Ramond, E., G. Gesbert, M. Barel, and A. Charbit. 2012. 'Proteins involved in Francisella tularensis survival and replication inside macrophages', *Future Microbiol*, **7**: 1255-68.

Rao, N. N., M. R. Gómez-García, and A. Kornberg. 2009. 'Inorganic polyphosphate:

essential for growth and survival', *Annu Rev Biochem*, **78**: 605-47.

Rao, N. N., and A. Kornberg. 1996. 'Inorganic polyphosphate supports resistance and survival of stationary-phase Escherichia coli', *J Bacteriol*, **178**: 1394-400.

Reddi, A. R., L. T. Jensen, A. Naranuntarat, L. Rosenfeld, E. Leung, R. Shah, and V. C. Culotta. 2009. 'The overlapping roles of manganese and Cu/Zn SOD in oxidative stress protection', *Free Radic Biol Med*, **46**: 154-62.

Robert, V. A., and A. Casadevall. 2009. 'Vertebrate endothermy restricts most fungi as potential pathogens', *J Infect Dis*, **200**: 1623-6.

Robertson, J. B., C. C. Stowers, E. Boczko, and C. H. Johnson. 2008. 'Real-time luminescence monitoring of cell-cycle and respiratory oscillations in yeast', *Proc Natl Acad Sci U S A*, **105**: 17988-93.

Roetzer, A., N. Gratz, P. Kovarik, and C. Schüller. 2010. 'Autophagy supports Candida glabrata survival during phagocytosis', *Cell Microbiol*, **12**: 199-216.

Sagot, I., and D. Laporte. 2019. 'The cell biology of quiescent yeast - a diversity of individual scenarios', *J Cell Sci*, **132**.

Samokhvalov, V., V. Ignatov, and M. Kondrashova. 2004. 'Reserve carbohydrates maintain the viability of Saccharomyces cerevisiae cells during chronological aging', *Mech Ageing Dev*, **125**: 229-35.

Sandargo, B., C. Chepkirui, T. Cheng, L. Chaverra-Muñoz, B. Thongbai, M. Stadler, and S. Hüttel. 2019. 'Biological and chemical diversity go hand in hand: Basidiomycota as source of new pharmaceuticals and agrochemicals', *Biotechnol Adv*, **37**: 107344.

Sasani, E., S. Khodavaisy, S. Agha Kuchak Afshari, S. Darabian, F. Aala, and S. Rezaie. 2016. 'Pseudohyphae formation in Candida glabrata due to CO2 exposure', *Curr Med Mycol*, **2**: 49-52.

Savoie, J. M., and M. L. Largeteau. 2004. 'Hydrogen peroxide concentrations detected in Agaricus bisporus sporocarps and relation with their susceptibility to the pathogen Verticillium fungicola', *FEMS Microbiol Lett*, **237**: 311-5.

Scherlach, K., G. Lackner, K. Graupner, S. Pidot, T. Bretschneider, and C. Hertweck. 2013. 'Biosynthesis and mass spectrometric imaging of tolaasin, the virulence factor of brown blotch mushroom disease', *Chembiochem*, **14**: 2439-43.

Schroeckh, V., K. Scherlach, H. W. Nützmann, E. Shelest, W. Schmidt-Heck, J. Schuemann, K. Martin, C. Hertweck, and A. A. Brakhage. 2009. 'Intimate bacterial-fungal interaction triggers biosynthesis of archetypal polyketides in Aspergillus nidulans', *Proc Natl Acad Sci U S A*, **106**: 14558-63.

Seider, K., S. Brunke, L. Schild, N. Jablonowski, D. Wilson, O. Majer, D. Barz, A. Haas, K. Kuchler, M. Schaller, and B. Hube. 2011. 'The facultative intracellular pathogen Candida glabrata subverts macrophage cytokine production and phagolysosome maturation', *J Immunol*, **187**: 3072-86.

Seider, K., F. Gerwien, L. Kasper, S. Allert, S. Brunke, N. Jablonowski, T. Schwarzmüller, D. Barz, S. Rupp, K. Kuchler, and B. Hube. 2014. 'Immune evasion, stress resistance, and efficient nutrient acquisition are crucial for intracellular survival of Candida glabrata within macrophages', *Eukaryot Cell*, **13**: 170-83.

Semchyshyn, H. M. 2014. 'Hormetic concentrations of hydrogen peroxide but not ethanol induce cross-adaptation to different stresses in budding yeast', *Int J Microbiol*, **2014**: 485792.

Semchyshyn, H. M., O. B. Abrat, J. Miedzobrodzki, Y. Inoue, and V. I. Lushchak. 2011. 'Acetate but not propionate induces oxidative stress in bakers' yeast Saccharomyces cerevisiae', *Redox Rep*, **16**: 15-23.

Sethuraman, A., N. N. Rao, and A. Kornberg. 2001. 'The endopolyphosphatase gene: essential in Saccharomyces cerevisiae', *Proc Natl Acad Sci U S A*, **98**: 8542-7.

Sherrington, S. L., E. Sorsby, N. Mahtey, P. Kumwenda, M. D. Lenardon, I. Brown, E. R. Ballou, D. M. MacCallum, and R. A. Hall. 2017. 'Adaptation of Candida albicans to environmental pH induces cell wall remodelling and enhances innate immune recognition', *PLoS Pathog*, **13**: e1006403.

Shi, L., B. M. Sutter, X. Ye, and B. P. Tu. 2010. 'Trehalose is a key determinant of the quiescent metabolic state that fuels cell cycle progression upon return to growth', *Mol Biol Cell*, **21**: 1982-90.

Silljé, H. H., E. G. ter Schure, A. J. Rommens, P. G. Huls, C. L. Woldringh, A. J. Verkleij, J. Boonstra, and C. T. Verrips. 1997. 'Effects of different carbon fluxes on G1 phase duration, cyclin expression, and reserve carbohydrate metabolism in Saccharomyces cerevisiae', *J Bacteriol*, **179**: 6560-5.

Singer, M. A., and S. Lindquist. 1998. 'Multiple effects of trehalose on protein folding in vitro and in vivo', *Mol Cell*, **1**: 639-48.

Soler-Rivas, C., S. Jolivet, N. Arpin, J. M. Olivier, and H. J. Wichers. 1999. 'Biochemical and physiological aspects of brown blotch disease of Agaricus bisporus', *FEMS Microbiol Rev*, **23**: 591-614.

Sprenger, M., T. S. Hartung, S. Allert, S. Wisgott, M. J. Niemiec, K. Graf, I. D. Jacobsen, L. Kasper, and B. Hube. 2020. 'Fungal biotin homeostasis is essential for immune evasion after macrophage phagocytosis and virulence', *Cell Microbiol*, **22**: e13197.

Sprenger, M., L. Kasper, M. Hensel, and B. Hube. 2018. 'Metabolic adaptation of intracellular bacteria and fungi to macrophages', *Int J Med Microbiol*, **308**: 215-27.

Srikantha, T., S. A. Lachke, and D. R. Soll. 2003. 'Three mating type-like loci in Candida glabrata', *Eukaryot Cell*, **2**: 328-40.

Stroe, M. C., T. Netzker, K. Scherlach, T. Krüger, C. Hertweck, V. Valiante, and A. A. Brakhage. 2020. 'Targeted induction of a silent fungal gene cluster encoding the bacteria-specific germination inhibitor fumigermin', *Elife*, **9**.

Swidergall, M., M. Khalaji, N. V. Solis, D. L. Moyes, R. A. Drummond, B. Hube, M. S. Lionakis, C. Murdoch, S. G. Filler, and J. R. Naglik. 2019. 'Candidalysin Is Required for Neutrophil Recruitment and Virulence During Systemic Candida albicans Infection', *J Infect Dis*, **220**: 1477-88.

Taff, H. T., K. F. Mitchell, J. A. Edward, and D. R. Andes. 2013. 'Mechanisms of Candida biofilm drug resistance', *Future Microbiol*, **8**: 1325-37.

Thattai, M., and A. van Oudenaarden. 2004. 'Stochastic gene expression in fluctuating environments', *Genetics*, **167**: 523-30.

Thomas, E. L., R. I. Lehrer, and R. F. Rest. 1988. 'Human neutrophil antimicrobial activity', *Rev Infect Dis*, **10** Suppl 2: S450-6.

Thompson-Jaeger, S., J. François, J. P. Gaughran, and K. Tatchell. 1991. 'Deletion of SNF1 affects the nutrient response of yeast and resembles mutations which activate the adenylate cyclase pathway', *Genetics*, **129**: 697-706.

Timár, C. I., A. M. Lőrincz, and E. Ligeti. 2013. 'Changing world of neutrophils', *Pflugers Arch*, **465**: 1521-33.

Toh-e, A., M. Ohkusu, H. M. Li, K. Shimizu, A. Takahashi-Nakaguchi, T. Gonoi, S. Kawamoto, Y. Kanesaki, H. Yoshikawa, and M. Nishizawa. 2015. 'Identification of genes involved in the phosphate metabolism in Cryptococcus neoformans', *Fungal Genet Biol*, **80**: 19-30.

Tournu, H., A. Fiori, and P. Van Dijck. 2013. 'Relevance of trehalose in pathogenicity: some general rules, yet many exceptions', *PLoS Pathog*, **9**: e1003447.

Trilisenko, L., A. Zvonarev, A. Valiakhmetov, A. A. Penin, I. A. Eliseeva, V. Ostroumov, I. V. Kulakovskiy, and T. Kulakovskaya. 2019. 'The Reduced Level of Inorganic Polyphosphate Mobilizes Antioxidant and Manganese-Resistance Systems in Saccharomyces cerevisiae', *Cells*, **8**.

Tu, B. P., A. Kudlicki, M. Rowicka, and S. L. McKnight. 2005. 'Logic of the yeast metabolic cycle: temporal compartmentalization of cellular processes', *Science*, **310**: 1152-8.

Urban, C. F., U. Reichard, V. Brinkmann, and A. Zychlinsky. 2006. 'Neutrophil extracellular traps capture and kill Candida albicans yeast and hyphal forms', *Cell Microbiol*, **8**: 668-76.

Uribe-Querol, E., and C. Rosales. 2020. 'Phagocytosis: Our Current Understanding of a Universal Biological Process', *Front Immunol*, **11**: 1066.

Valcourt, J. R., J. M. Lemons, E. M. Haley, M. Kojima, O. O. Demuren, and H. A. Coller. 2012. 'Staying alive: metabolic adaptations to quiescence', *Cell Cycle*, **11**: 1680-96.

van der Plaat, J. B. 1974. 'Cyclic 3',5'-adenosine monophosphate stimulates trehalose degradation in baker's yeast', *Biochem Biophys Res Commun*, **56**: 580-7.

van Solingen, P., and J. B. van der Plaat. 1975. 'Partial purification of the protein system controlling the breakdown of trehalose in baker's yeast', *Biochem Biophys Res Commun*, **62**: 553-60.

Vázquez-Torres, A., and E. Balish. 1997. 'Macrophages in resistance to candidiasis', *Microbiol Mol Biol Rev*, **61**: 170-92.

Verweij, P. E., E. Snelders, G. H. Kema, E. Mellado, and W. J. Melchers. 2009. 'Azole resistance in Aspergillus fumigatus: a side-effect of environmental fungicide use?', *Lancet Infect Dis*, **9**: 789-95.

Wera, S., E. De Schrijver, I. Geyskens, S. Nwaka, and J. M. Thevelein. 1999. 'Opposite roles of trehalase activity in heat-shock recovery and heat-shock survival in Saccharomyces cerevisiae', *Biochem J*, **343** Pt 3: 621-6.

Wong, S., M. A. Fares, W. Zimmermann, G. Butler, and K. H. Wolfe. 2003. 'Evidence from comparative genomics for a complete sexual cycle in the 'asexual' pathogenic yeast

Candida glabrata', *Genome Biol*, **4**: R10.

Wuyts, J., P. Van Dijck, and M. Holtappels. 2018. 'Fungal persister cells: The basis for recalcitrant infections?', *PLoS Pathog*, **14**: e1007301.

Zhao, G., Y. Chen, L. Carey, and B. Futcher. 2016. 'Cyclin-Dependent Kinase Co-Ordinates Carbohydrate Metabolism and Cell Cycle in S. cerevisiae', *Mol Cell*, **62**: 546-57.

Zhao, H., D. Shao, C. Jiang, J. Shi, Q. Li, Q. Huang, M. S. R. Rajoka, H. Yang, and M. Jin. 2017. 'Biological activity of lipopeptides from Bacillus', *Appl Microbiol Biotechnol*, **101**: 5951-60.

Zilli, D. M., R. G. Lopes, S. L. Alves, Jr., L. M. Barros, L. C. Miletti, and B. U. Stambuk. 2015. 'Secretion of the acid trehalase encoded by the CgATH1 gene allows trehalose fermentation by Candida glabrata', *Microbiol Res*, **179**: 12-9.

5 Appendix

5.1 Additional experimental procedures

5.1.1 Variations of the C. glabrata*-hMDM persistence model for different purposes*

The variations of the *C. glabrata*-hMDM persistence model are already briefly described in manuscript III. The following protocols exemplary provide detailed handling and organization advices which might be critical for the practical performance.

Variations:

Method A: Mutant pool tests

Method B: Single mutant tests (optional antimycotic administration)

Method C: Cytokine measurements

Method D: Transcriptome analysis

Method E: Life cell imaging

5.1.1.1 Materials

All or several assays

1. RPMI + 10% human serum (HS): as a compromise of standardization purposes, assay reproducibility, macrophage performance and minimalization of immune cross-reactions, commercially available sterile-filtered human serum charges from AB male blood donors (Bio&Sell) were used. Note that assay performance might differ in dependence of the serum charge used and therefore needs to be evaluated for each new serum charge. Medium was prepared directly prior use to avoid variations due to serum protein breakdown.

2. Differentiated and at least for 20 hours in the final format adhered hMDM macrophages seeded in RPMI + 10% FBS + 50 ng/ml M-CSF medium in
    a. Methods A, B, C: 24 well plates for cell culture (TPP, Cat. No. 92424;1.5 × 10^5 hMDMs/well; 1 mL medium/well)
    b. Method D: 75 cm^2 cell culture flasks (4.2 × 10^6 hMDMs/flask; 21 mL medium/flask) or 175 cm^2 cell culture flasks (9.8 × 10^6 hMDMs/flask; 49 mL medium/flask); e.g. cell culture flasks from Greiner Bio-one (TC-treated, Growth area: 75 cm^2, total volume: 250 ml, sterile; Cat. No. 658 175) or Sarstedt AG&Co. KG (TC Flask T75, Stand., Vent. Cap; Cat. No. 83.3911.002)
    c. Method E: 8 well µ-slides (ibidi; 0.8 × 10^5 hMDMs/well; 395 µL medium/well)

3. Autoclaved YPD, PBS, dH_2O and [methods A, B, D] 0.5% Triton-X-100; 0.05% Triton-X-100 for method B with antimycotic administration
4. Yeast strains streaked on YPD agar either individually in petri dishes (methods B-E) or position-coded in 96 well plate format (method A; use optionally YPD + 200 µg/mL Nurseothricin). Storage of grown cultures at 4°C, not much longer than two weeks (especially in 96 well plate format).
5. Eppendorf tubes or falcons prefilled with corresponding dilution medium for adjustment of yeast concentrations for infection and (methods A, B) for cfu plating
6. Eppendorf tube and falcon centrifuges
7. Methods A, B: pre-labelled YPD agar petri dishes (method A: mutant pool, biological and technical replicate, yeast cell concentration / dilution, time point; method B: yeast strain and/or treatment condition, biological and technical replicate, time point) filled with ~4 sterile glass beads for cfu plating
8. Inverted microscope for manual screening for extracellular yeast microcolonies and tracing of macrophage appearance
9. Biological safety cabinet (working at flame is not appropriate for cell culture work and large-scale experiments; and it might be not allowed by authorities when handling potentially harmful microorganisms)
10. Incubators for cell culture (37°C, 5% CO_2) and yeast culture (30-37°C, without and with shaking up to 180 rpm)

<u>Method A</u>

1. Colour- (for pools) + position-labelled (= position in pool) 2 mL Eppendorf tubes filled with 0.5 mL YPD and placed in the appropriate position in a 96 format Eppendorf tube holder for all mutant pools included in the respective test. Note: Continuously encoding mutants by position and pools by colour simplifies handling.
2. Single-use cuvettes filled with 990 µL PBS (one for each included mutant) for measurement of optical density (position-coded placement in pool-colour-coded cuvette boxes)
3. Spectral photometer
4. Pre-programmed table (e.g. in Excel 2010) for calculation of pool input volume for each mutant based on optical density measurement

<u>Method B</u>

1. In case of antimycotic administration: appropriate aliquoted and stored antimycotic (and respective control) stock solutions

Method C

1. Pre-labelled Eppendorf tubes and/or PCR stripes (yeast strain and/or condition, biological replicate, time point) for collection, centrifugation and aliquoting of assay supernatants
2. LPS stock solution (here: prepared and gifted by Mark Gresnigt)

Method D

1. Aliquoted caspofungin stock solutions (e.g. 5 mg/mL, diluted in PBS; store at -20°C)
2. Precooled PBS for hMDM layer washing prior to macrophage lysis
3. AE buffer + 10% SDS for macrophage lysis
4. Precooled Eppendorf tube centrifuge (4°C)
5. Several prelabelled Eppendorf tubes for centrifugation of each macrophage lysate

Method E

1. Zeiss AXIO Observer.Z1 (Carl Zeiss Microscopy) microscope or comparable microscope capable of taking fluorescence micrographs under cell culture atmospheric conditions

5.1.1.2 Experimental procedures

5.1.1.2.1 *C. glabrata* inoculum preparation

Method A

With exception of step 4, all steps should be performed under sterile working conditions in a biological safety cabinet.

Preparing pool-inoculums in this way is quite labour-intensive: consider organizing help or reducing workload (amount of tested pools / working day). Using prepared pool inoculums for several subsequent experiments is recommended.

1. Inoculate YPD o/n cultures in colour- and position -coded 2 mL Eppendorf tubes in 96 format Eppendorf tube holders from yeast cultures on solid YPD in position-coded 96 well plates
    a. Separating the tubes on two tube holders (leaving sequential rows empty) simplifies handling
    b. Sterile pipette tips can be used for inoculation (faster, but also higher risk of contamination)
    c. Possible modification: inoculate all mutants of one pool into one liquid culture. Simplifies handling at several stages, but deprives slow-growing

mutants, which might be acceptable in dependency of experimental settings. Could be partially counterbalanced by e.g. separating mutants for each pool by growth behaviour into appropriate categories, inoculating mutants of each category together (maybe time-delayed starting point of different categories) and mixing category cultures before infection.

2. Incubate yeast cultures at 37°C with shaking (180 rpm) o/n (in this study ~17h)
    a. Inoculation of several pools takes some time: for synchronisation of starting points, it makes sense to pre-inoculate cultures earlier on this day, store them at 4°C and put all cultures together into the incubator
3. Pipette 10 µL per culture in 990 µL PBS in prepared single-use cuvettes (position-coded placement in prepared and pool-colour-coded cuvette boxes)
4. Mix with stirrer and measure $OD_{600\ nm}$ with a spectral photometer; record values in pre-programmed Excel sheet and print input volume mutant culture per pool outcome
    a. We calculated from $OD_{600\ nm}$ values the amount of volume which is theoretically needed to get an optical density of 5 in a total volume of 200 µL if we would mix the original culture with water; modifications might be needed in dependency of experimental set-up
5. Pipette all calculated mutant input volumes from the original culture in their respective pool (in 50 mL falcon tube) to get an equal distribution between individual mutants
6. Fill up the total volume to 20 mL per pool with sterile PBS (equalisation of pool volumes for centrifugation)
7. Centrifuge 5 min 4248 g
8. Wash pellet twice with sterile PBS
    a. Dissolve in 10 mL PBS
    b. Centrifuge 5 min 4248 g
9. Dissolve pellet in 5 mL PBS
    a. Put solution and sequentially prepared pool culture dilutions on ice or at 4°C
10. Prepare sequential 1:10 and 1:100 pool dilutions in RPMI
    a. Pipette for each dilution step 100 µL culture of previous dilution to 900 µL RPMI
11. Use 1:100 dilution for counting with a Neubauer counting chamber
12. Adjust pools to 1.05×10^7 yeast cells/mL in RPMI and use these solutions for infection

Methods B + C

1. Inoculate yeast for each needed *C. glabrata* / *C. albicans* strain in 5 mL liquid YPD from prepared cultures on solid YPD and incubate o/n at 37°C (*C. glabrata*) or 30°C (*C. albicans*) with 180 rpm shaking
    a. *C. albicans* can serve as positive control for cytokine measurements
2. Pellet 1 mL yeast o/n culture by centrifugation (1 min at 5000 g)
3. Wash pellets twice with sterile dH_2O
    a. Dissolve in 1 mL dH_2O
    b. Centrifuge 1 min 5000 g
4. Dissolve pellet in 1 mL dH_2O
5. Prepare sequential 1:10 and 1:100 dilutions with sterile dH_2O
    a. Pipette for each dilution step 100 µL culture of previous dilution to 900 µL dH_2O
6. Use 1:100 dilution for counting with a Neubauer counting chamber
7. Adjust each strain to 1.5×10^6 yeast cells/mL in dH_2O

Method D + E

1. Inoculate yeast for each needed *C. glabrata* strain in 10 mL (method D) or 5 mL (method E) liquid YPD from prepared cultures on solid YPD and incubate o/n at 37°C with 180 rpm shaking
    a. Method E: Use a fluorescent protein-encoding *C. glabrata* strain
2. Pellet 10 mL (method D) or 1 mL (method E) yeast o/n culture by centrifugation (method D: 5 min 4248 g; method E: 1 min 5000 g)
3. Wash pellets twice with sterile dH_2O
    a. Dissolve in 10 mL (method D) or 1 mL (method E) dH_2O
    b. Centrifuge 5 min 4248 g (method D) or 1 min 5000 g (method E)
4. Dissolve pellet in 5 mL (method D) or 1 mL (method E) sterile RPMI
    a. Put solution and sequentially prepared culture dilutions on ice or at 4°C
5. Prepare sequential 1:10 and 1:100 dilutions with sterile RPMI
    a. Pipette for each dilution step 100 µL culture of previous dilution to 900 µL RPMI
6. Use 1:100 dilution for counting with a Neubauer counting chamber
7. Adjust each strain to 5×10^8 (method D) or 2.21×10^7 (method E) yeast cells/mL in RPMI

5.1.1.2.2 *C. glabrata* infection of hMDMs, coincubation

Starting materials for all methods are prepared yeast inoculums and in the final format adhered hMDM monolayers (see above)

Methods A, B and C

Prepared hMDMs are seeded in 24 well cell culture plates at a density of 1.5×10^5 hMDMs/well in a total volume of 1 mL medium/well.

Steps 2-6 and steps 9-11 are performed consecutively for each well before moving to the next well.

Pipetting steps need to be performed as careful as possible to avoid disruption of the hMDM monolayer.

We recommend using a 200 µL – 1000 µL volume range pipette for all steps (aspiration and addition of medium / washing solutions).

Aspirate medium without touching the ground with the pipette tip: by tilting the plate to an appropriate angle, it is nevertheless possible to aspirate the medium nearly completely. Avoid shear-stress by too fast aspiration.

For pipetting solutions on top of the monolayer, start to drop the solution slowly from a small height until the monolayer is completely covered with solution. You can increase the dropping rate intensity afterwards.

Recommendation: Test your pipetting technique in a test run before performing the actual experiment and check the outcome (monolayer integrity) with an inverted microscope afterwards. Perform all pipetting steps you would perform within your actual experiment. Plan your first “real” experiment in a small scale.

The infection method is time- and labour-intensive (plan 20-30 min for processing of steps 1-7 respectively steps 9-11 for each 24 well plate). If you perform the experiment alone, your maximum time for infection (and additional experiment-specific steps) is 3 hours, since you have to start to wash the wells then. Plan your experiment realistic; maybe organize help and don´t overwork yourself.

1. Note starting point for infection of the respective 24 well plate and define an infection order
2. Aspirate media from one well (24 well plate with prepared hMDMs)
3. Wash this well with 1 mL sterile PBS and discard washing-PBS
4. Add 1 mL RPMI + 10% HS per well
5. Add 100 µL yeast inoculum solution per well: pipette as much as possible evenly distributed (drop at different locations in the well)
    a. Method A: 100 µL inoculum solution equalizes with an MOI of 7
    b. Methods B + C: 100 µL inoculum solution equalizes with an MOI of 1
    c. Method C: for control wells, add instead 100 µL control solution (negative control: 100 µL dH_2O; positive control: 2 µL 50 µg/mL LPS + 98 µL dH_2O)

6. Enhance even yeast cell distribution by directly aspirating ~500 µL well supernatant and dropping it evenly at different locations in the well
    a. Perform this step twice
7. Repeat steps 2-6 for all wells of the 24 well plate which you want to infect
8. Incubate the infected hMDM-24 well plate for 3 hours at 37°C and 5% CO_2 (starting point see point 1) and continue with washing steps (9-12) for removal of non-phagocytosed yeasts afterwards
    a. Follow the same order you have used for infection during the washing steps
9. Aspirate media from one well (24 well plate with prepared hMDMs);
10. Wash this well twice with 1 mL sterile PBS and discard washing-PBS
11. Add 1 mL RPMI + 10% HS per well
    a. Method C: add 2 µL 50 µg/mL LPS (final concentration 100 ng/mL LPS) in LPS-positive control wells
12. Repeat steps 9-11 for all wells of the 24 well plate which have infected
13. Incubate the readily processed hMDM-24 well plate until 24 hours after infection at 37°C and 5% CO_2
    a. Optional: Administration of antimycotics after 6 hours of infection (method B with antimycotic)
        i. Add a small volume (< 10 µL) of antimycotic stock solution or respective control solution (e.g. DMSO) to the corresponding infected wells to reach the desired antimycotic concentration
14. Nearly before reaching the 24 hours' time point, examine each infected well for macrophage appearance and appearance of extramacrophagal yeast with an inverted microscope (documentation); where necessary, mark the well for disposal
15. Perform medium exchange 24 hours after infection (steps 16-17)
    a. From now on it is fine to perform a step for all infected wells and then to move on to the next step (instead of previous strategy)
16. Aspirate 500 µL of medium supernatant / well by pipetting from the top from each infected well (for wells which will be further incubated)
    a. "Dispose" marked wells by aspirating the total medium volume and do not further process
17. Add 1 mL RPMI + 10% HS per well (total volume: 1.5 mL per well)
    a. Optional: (method B with antimycotic) add a small volume (< 10 µL) of antimycotic stock solution or respective control solution (e.g. DMSO) to

the corresponding infected wells to reach the desired antimycotic concentration

i. In our experiments, level of antimycotics where hold theoretically constant, i.e. the amount of added antimycotic recapitulates the amount which is needed to reach the desired antimycotic concentration in the freshly added medium

b. Method C: add 2 µL 50 µg/mL LPS (final concentration 100 ng/mL LPS) in LPS-positive control wells

18. Continue incubation at 37°C and 5% CO_2 for another 24 hours
19. Repeat step 14 daily before daily medium exchange
20. Perform medium exchange daily (always after another 24 hours of incubation; steps 21-22; last medium exchange at 6 days after infection)
21. Aspirate 500 µL of medium supernatant / well by pipetting from the top from each infected well (for wells which will be further incubated)
    a. "Dispose" marked wells by aspirating the total medium volume and do not further process
22. Add 500 µL RPMI + 10% HS per well (total volume: 1.5 mL per well)
    a. Optional: (method B with antimycotic) add a small volume (< 10 µL) of antimycotic stock solution or respective control solution (e.g. DMSO) to the corresponding infected wells to reach the desired antimycotic concentration
        i. In our experiments, level of antimycotics where hold theoretically constant, i.e. the amount of added antimycotic recapitulates the amount which is needed to reach the desired antimycotic concentration in the freshly added medium
    b. Method C: add 1 µL 50 µg/mL LPS (final concentration 100 ng/mL LPS) in LPS-positive control wells
23. Continue incubation at 37°C and 5% CO_2 for another 24 hours

<u>Method D</u>

Handling is not as critical as for the other methods since caspofungin administration secures that *C. glabrata* will not start to heavily replicate in the medium. Nevertheless, macrophage monolayer integrity should be preserved as good as possible.

Method D differs from methods A-C mainly by using different cell culture container formats (cell culture flasks instead of 24 well plates): 75 cm^2 cell culture flasks (4.2×10^6 hMDMs/flask; 21 mL medium/flask; for early time points) or 175 cm^2 cell culture flasks (9.8×10^6 hMDMs/flask; 49 mL medium/flask; for later time points).

Use of serological pipettes for aspiration is recommended and partially necessary (compare step 17).

1. Aspirate media from one flask
2. Wash this flask with sterile PBS and discard washing-PBS
    a. Use 20 mL PBS for 175 cm^2 cell culture flasks and 10 mL PBS for 75 cm^2 cell culture flasks
3. Add RPMI + 10% HS
    a. Add 20 mL in 175 cm^2 cell culture flasks and 9 mL in 75 cm^2 cell culture flasks
4. Add yeast inoculum solution (MOI 20) and mix by gentle swaying the flask horizontally
    a. Add 392 µL in 175 cm^2 cell culture flasks and 168 µL in 75 cm^2 cell culture flasks
5. Repeat steps 1-4 for all flasks which you want to infect
6. Incubate the infected flasks for 3 hours at 37°C and 5% CO_2 and continue with washing steps (7-9) for removal of non-phagocytosed yeasts afterwards
7. Aspirate media from one flask
8. Wash this flask twice with sterile PBS and discard washing-PBS
    a. Use 20 mL PBS for 175 cm^2 cell culture flasks and 10 mL PBS for 75 cm^2 cell culture flasks
9. Add RPMI + 10% HS
    a. Add 20 mL in 175 cm^2 cell culture flasks and 9 mL in 75 cm^2 cell culture flasks
10. Repeat steps 7-9 for all infected flasks
11. Incubate the readily processed flask until 6 hours after infection at 37°C and 5% CO_2
12. 6 hours after infection: add caspofungin to a final concentration of 5 µg/mL
    a. 2 mg/mL caspofungin stock solution: add 50 µL mL in 175 cm^2 cell culture flasks and 22,5 µL in 75 cm^2 cell culture flasks
13. Incubate the readily processed flask until 24 hours after infection at 37°C and 5% CO_2
14. After 24 hours after infection, add additional RPMI + 10% HS and an appropriate amount of caspofungin per flask (no aspiration of “old” media; final caspofungin concentration is kept on 5 µg/mL)
    a. Add 20 mL in 175 cm^2 cell culture flasks and 9 mL in 75 cm^2 cell culture flasks

   b. 2 mg/mL caspofungin stock solution: add 50 µL mL in 175 cm^2 cell culture flasks and 22,5 µL in 75 cm^2 cell culture flasks
15. Incubate the readily processed flask until 48 hours after infection at 37°C and 5% CO_2
16. Perform the following medium exchange strategy daily starting from 48 hours after infection (always after another 24 hours of incubation; steps 17-18; last medium exchange at 6 days after infection)
17. Aspirate 9 mL (75 cm^2 flask) respectively 20 mL (175 cm^2 flask) supernatant per flask
18. Add additional RPMI + 10% HS and an appropriate amount of caspofungin per flask (final caspofungin concentration is kept on 5 µg/mL)
    a. Add 20 mL in 175 cm^2 cell culture flasks and 9 mL in 75 cm^2 cell culture flasks
    b. 2 mg/mL caspofungin stock solution: add 50 µL mL in 175 cm^2 cell culture flasks and 22,5 µL in 75 cm^2 cell culture flasks
19. Continue incubation at 37°C and 5% CO_2 for another 24 hours

Method E

The infection and incubation procedure for method E differs from methods A-C only in respect of the cell culture container used (8 well µ-slides for microscope imaging) and correspondingly in the total volumes exchanged. This results in the following protocol changes:

Steps 3 +10: Use 300 µL sterile PBS

Steps 4 + 11: Add 300 µL RPMI + 10% HS

Step 5: Add 25 µL yeast inoculum solution (MOI 7)

Step 6: Aspirate ~150 µL for mixing

Steps 16 + 21: Aspirate and discard 200 µL supernatant

Steps 17 + 22: Add 200 µL RPMI + 10% HS (total volume is kept constantly at 300 µL)

5.1.1.2.3 Generation of model-specific output

Method A

The model output is generated by plating yeast cfus for each pool from the inoculum and from hMDM lysates after different time points (one and seven day(s) of co-incubation) and measuring the shift of mutant abundance within its respective pool by using a Bar-Seq approach (see method section). For trustable quantification, this requires that yeast strains can grow individually and roughly in comparable density on YPD agar plates (maximum ~ 2000 colonies / plate and an incubation time of only 24 hours) and that enough total colonies are included for further processing to get a good mean coverage

of colonies / individual mutant (e.g. 14,000 total colonies for 50 mutants per pool results in a mean coverage of 280 colonies / mutant).

To avoid experimental failure due to extramacrophagal yeast (microcolony) growth, seven wells are infected per individual pool. One well is used for cfu plating after one day and the remaining ones for cfu plating after seven days. Optionally, hMDMs differentiated from two separate hMDM donors can be used to for parallel infection with the same pool inoculum. This avoids failure of the experiment in case the hMDMs from one blood donor show unexpected behaviour.

Since the yeast cell concentration in the lysates after seven day(s) is too low for counting with a Neubauer counting chamber, several dilution steps have to be plated after seven days (see below).

1. Inoculum plating
    a. Prepare 10^8 yeast cells/mL solution with sterile PBS from assembled pool solution
    b. Dilute sequentially in 1:10 dilution steps with sterile PBS until you reach the 10^4 yeast cells/mL dilution (always 150 µL yeast cell dilution + 1350 µL PBS)
    c. On 7 YPD agar plates: plate 200 µL from 10^4 yeast cells/mL dilution (~2000 cells/plate)
2. Lysate plating after one day of *C. glabrata*-hMDM co-incubation
    a. Aspirate and discard supernatant
    b. Add 100 µL sterile 0.5% Triton-X-100 per well
    c. Repeat a + b for all wells designated for plating after one day
    d. Incubate 15 min with gentle shaking (30 rpm, room temperature)
    e. Mix well content by pipetting several times
    f. Use 10 µL per well for yeast cell counting with a Neubauer counting chamber
    g. Add 410 µL sterile PBS per well, mix by pipetting and pipette whole well content in pre-labelled Eppendorf tube
    h. Adjust all samples to 10^4 yeast cells/mL
    i. On 7 YPD agar plates: plate 200 µL from 10^4 yeast cells/mL dilution (~2000 cells/plate)
3. Lysate plating after seven days of *C. glabrata*-hMDM co-incubation
    a. Aspirate and discard supernatant
    b. Add 100 µL sterile 0.5% Triton-X-100 per well
    c. Repeat a + b for all wells designated for plating after one day
    d. Incubate 15 min with gentle shaking (30 rpm, room temperature)

e. Mix well content by pipetting several times
f. Add 400 µL sterile PBS per well, mix by pipetting and pipette whole well content in pre-labelled 50 mL falcon tube
    i. Pool samples from the same pool + hMDM donor
g. Wash residual yeast cells out of wells with 500 µL sterile PBS and use washing PBS either directly for further dilution (if 1-3 wells remained per pool) or pipette in separate falcon tube (if 4-6 wells remained per pool)
h. In dependency of the amount of remaining wells per individual pool (those which met cut-off criteria of extramacrophagal yeast appearance for inclusion), follow the corresponding plating strategy:
    i. One remaining well
        1. Add “washing-PBS” directly to yeast cell solution (total volume 1 mL)
        2. Twice: plate 200 µL of this solution (1) on a YPD agar plate
        3. Add 1.2 mL sterile PBS to the remaining 600 µL yeast cell solution (1)
        4. Nine fold: plate 200 µL of this solution (3) on a YPD agar plate
    ii. Two remaining wells
        1. Add “washing-PBS” directly to yeast cell solution (total volume 2 mL)
        2. Seven fold: plate 200 µL of this solution (1) on a YPD agar plate
        3. Add 1.2 mL sterile PBS to the remaining 600 µL yeast cell solution (1)
        4. Nine fold: plate 200 µL of this solution (3) on a YPD agar plate
    iii. Three remaining wells
        1. Add “washing-PBS” directly to yeast cell solution (total volume 3 mL)
        2. Tenfold: plate 200 µL of this solution (1) on a YPD agar plate
        3. Prepare further yeast cell dilution: 800 µL of previous yeast cell solution (1) + 1.6 mL sterile PBS
        4. Tenfold: plate 200 µL of this solution (3) on a YPD agar plate
    iv. Four remaining wells
        1. Keep “washing-PBS” separately, combine only lysates (total volume 2 mL)
        2. Twofold: plate 200 µL of this solution (1) on a YPD agar plate
        3. Prepare further yeast cell dilution: 1.5 mL of previous yeast cell solution (1) + 1.5 mL “washing-PBS”
        4. Tenfold: plate 200 µL of this solution (3) on a YPD agar plate
        5. Prepare further yeast cell dilution: 800 µL of previous yeast cell solution (3) + 1.6 mL sterile PBS
        6. Tenfold: plate 200 µL of this solution (5) on a YPD agar plate
    v. Five remaining wells
        1. Keep “washing-PBS” separately, combine only lysates (total volume 2.5 mL)
        2. Fivefold: plate 200 µL of this solution (1) on a YPD agar plate

3. Prepare further yeast cell dilution: 1.5 mL of previous yeast cell solution (1) + 1.5 mL “washing-PBS”
4. Tenfold: plate 200 µL of this solution (3) on a YPD agar plate
5. Prepare further yeast cell dilution: 800 µL of previous yeast cell solution (3) + 1.6 mL sterile PBS
6. Tenfold: plate 200 µL of this solution (5) on a YPD agar plate

vi. Six remaining wells
1. Keep “washing-PBS” separately, combine only lysates (total volume 3 mL)
2. Sevenfold: plate 200 µL of this solution (1) on a YPD agar plate
3. Prepare further yeast cell dilution: 1.5 mL of previous yeast cell solution (1) + 1.5 mL “washing-PBS”
4. Tenfold: plate 200 µL of this solution (3) on a YPD agar plate
5. Prepare further yeast cell dilution: 800 µL of previous yeast cell solution (3) + 1.6 mL sterile PBS
6. Tenfold: plate 200 µL of this solution (5) on a YPD agar plate

Afterwards, all YPD agar plates are incubated for 24 hours at 37°C and the colony count is roughly determined with an automated colony counter (protoCOL 3, Synbiosis). For further processing see method section in manuscript III.

Method B

The output data of method B is cfus. Accordingly, at each indicated time point, yeast cell solutions need to be prepared and appropriately diluted to reach countable numbers of yeast colonies. If yeast cell concentrations cannot be determined in the original yeast cell solutions due to too low cell counts, plating of serial fivefold dilution steps can be performed.

We performed technical quadruplicates for each condition by infecting and plating 4 macrophage wells per time point. For the seven day time point, we infected two additional hMDM wells as “buffer” to compensate potential losses due to randomly occurring extramacrophagal yeast overgrowth. The additional value of multiple technical replicates can be questionable and must be weighed against possible disadvantages like e.g. prolonged “in-between”-incubation (time and steps between taking the sample and plating cfus) and working load.

1. Inoculum plating
    a. Prepare in sequential (~tenfold) dilution steps 10^3 yeast cells/mL dilution from original 1.5×10^6 yeast cells/mL solution used for hMDM infection
        i. We performed 2 dilution series each prior and after hMDM infection to check for stability of cfu counts
    b. Plate 200 µL from (each) 10^3 yeast cells/mL dilution per YPD agar plate (results in 4 plates in total for each biological replicate for one *C. glabrata* strain)

2. Plating after 3 hours *C. glabrata* infection of hMDMs
    a. Collection of supernatant
        i. Pipette whole supernatant from one well in a 50 mL falcon
        ii. Wash the respective well twice with sterile PBS and combine the washing-PBS with the supernatant (total volume: 3.1 mL)
        iii. Put falcon on ice to avoid yeast growth before plating (comment: requires fast further processing since cfu counts tend to be unstable in this setting)
    b. Collection of lysate
        i. Add 100 µL sterile 0.5% Triton-X-100 per well directly after collection of supernatant from this well
        ii. After collection of all supernatants and addition of 0.5% Triton-X-100: Incubate 24-well plate 15 min with light shaking (30 rpm)
        iii. Add 900 µL sterile dH_2O per well, resuspend and pipette in a 50 mL falcon
        iv. Wash each well twice with 1 mL dH_2O and combine the washing solution with the lysate (total volume: 3 mL)
        v. Store lysates at room temperature before plating
    c. Plating of lysate and supernatant
        i. Supernatant should be plated as directly as possible (e.g. organize a helper which takes care of this task while you collect supernatants and lysates)
        ii. Prepare serially 1:5 and 1:25 dilutions
        iii. Plate 200 µL from the 1:25 dilution on a YPD agar plate
3. Plating after one day *C. glabrata* infection of hMDMs
    a. Discard supernatant
    b. Add 100 µL sterile 0.5% Triton-X-100 per well
    c. After addition of 0.5% Triton-X-100 to all wells: Incubate 24-well plate 15 min with light shaking (30 rpm)
    d. Add 900 µL sterile dH_2O per well, resuspend and pipette in a 50 mL falcon
    e. Wash each well twice with 1 mL dH_2O and combine the washing solution with the lysate (total volume: 3 mL)
    f. Prepare serially 1:5 and 1:25 dilutions
    g. Plate 200 µL from the 1:5 dilution on a YPD agar plate
    h. Plate 200 µL from the 1:25 dilution on a YPD agar plate
4. Plating after seven days *C. glabrata* infection of hMDMs

   a. Identical to plating strategy after one day, but perform additionally the following step
   b. Plate 200 µL from the undiluted lysate solution on a YPD agar plate
5. Incubate YPD agar plates after plating for one day at 37°C and count cfu afterwards (you can store the plates at 4°C)

Optional: In case you want to test the influence of antimycotic addition to the assay, it might make sense to minimize the influence of the antimycotic during the cfu plating steps since you want to measure the effect of the antimycotic in your assay and not during the handling procedure. We therefore directly added 1 mL 0.05% Triton-X-100 (instead of 100 µL 0.5%Triton-X-100 first plus 900 µL dH_2O later) in the lysing steps, thereby lowering the concentration of remaining antimycotic in this step.

Method C

The method output for method C is cytokine measurement of supernatants. Therefore, supernatant - which would be discarded otherwise - can be collected at the time points of media exchange. For additional time points, additional hMDM wells specifically for these time points are needed; otherwise the standard procedure would be altered in subsequent time points. For calculation of total cytokine levels within a well, the total media volume within a well at a certain time point (changes during media exchange procedure) has to be taken into account.

We always collected and combined the supernatant from two *C. glabrata*-infected / control hMDM wells for one biological replicate to achieve enough volume for subsequent measurements.

After collection, supernatants were centrifuged 10 min at 1000 g to remove cellular debris, aliquoted and stored at -20°C until measurement (see method section in manuscript III).

Method D

For generation of model output in method D (*C. glabrata* transcriptome), fungal RNA has to be either directly isolated from samples or (pelleted) yeast cell samples need to be shock-frozen or otherwise secured for later RNA isolation. The most critical point in this procedure is to separate yeast cells at best into a pellet from the smear-forming macrophage cell debris from lysed hMDM monolayers. This can be achieved by e.g. a) using a high enough MOI to maximize yeast cell numbers in relation to macrophage numbers (but this comes with the disadvantage that extramacrophagal yeast growth had to be controlled with addition of an antimycotic), b) exerting strong shear stress on the lysate e.g. by pipetting up and down several times with a 200 - 1000 µL range pipette to disrupt smears and c) by aliquoting the lysate in 1.5 mL Eppendorf tubes and use these

for centrifugation instead of centrifuging the whole lysate within a falcon.
Perform the following steps for taking samples:

1. Aspirate supernatant
2. Wash twice with ice-cold PBS (e.g. 20 mL in 175 cm^2 flask, 10 mL in 75 cm^2 flask)
3. Add AE + 10% SDS (e.g. 5 mL in 175 cm^2 flask, 4 mL in 75 cm^2 flask) and scrape cell layer with cell culture scraper
4. Mix and pipette supernatant into several 1.5 mL Eppendorf tubes with a 200 – 1000 µL range pipette; mix the aliquoted sample with your pipette several times up and down to effectively destroy the smears; aliquot much less than the full volume per tube since you will need additional room for foam
5. Put processed tubes directly into a precooled cooling centrifuge
6. Centrifuge 2 min 12.000 g at 4°C
7. Remove supernatant without destroying your yeast cell pellet (the pellet can be very small especially after seven days)
8. Put processed tubes directly into liquid nitrogen for shock-frosting
9. Prior RNA isolation: Combine all samples of a biological replicate from one time point

Method E

Output for method E is (fluorescent) life cell imaging. Settings are highly dependent from the individual experiment, but should ensure that phototoxicity is minimized (could require to prepare several samples for several time points), and - if you aim for quantification - the location of picture acquisition within the hMDM layer is randomized and that enough pictures are taken.

5.2 Abbreviations

General

ABC	ATP binding cassette
ADP	adenosine-5'-diphosphate
AE buffer	acetate EDTA buffer (50 mM Na-acetate, 10 mM EDTA, pH 5.3, prepared with RNase free water or DEPC water)
AMB	amphotericin B
AspGD	*Aspergillus* Genome Database
ATP	adenosine-5'-triphosphate
Bar-Seq	barcode sequencing
BC	barcode
BLAST(P)	basic local alignment search tool (for proteins)
bp	base pairs
cAMP	cyclic adenosine monophosphate
CAS	caspofungin
Cdr	*Candida* drug resistance
CFU or cfu	colony forming unit
CFW	calcofluor white
CGD	*Candida* Genome Database
CLSI	Clinical and Laboratory Standards Institute
CLT	clotrimazole
CMC	critical micellar concentration
CSM	complete supplement mixture
CTAB	cetyltrimethylammonium bromide
CTP	cytidine triphosphate
CWI	cell wall integrity
Dhb	dehydrobutyrine
(d)dH_2O	(double) distilled water
DMEM	Dulbecco modified Eagle medium
DMSO	dimethyl sulfoxide
DNA	deoxyribonucleic acid
DOI	digital object identifier
DPBS	Dulbecco´s phosphate buffered saline
EDTA	ethylenediaminetetraacetic acid
e.g.	Latin for exempli gratia (“for example”)
EGTA	ethylene glycol-bis(β-aminoethyl ether)-N,N,N′,N′-tetraacetic acid
ELISA	enzyme-linked immunosorbent assay

ER	endoplasmic reticulum
ESCRT	endosomal sorting complexes required for transport
et al.	Latin for *et alia* (“and others”)
etc.	Latin for et cetera (“and so on”)
FAD	flavin adenine dinucleotide
FBS	fetal bovine serum
FCS	fetal calf serum
FDR	false discovery rate
FICI	fractional inhibitory concentration index
Fig.	figure
FITC	fluorescein isothiocyanate
FRT	flippase recognition target
Fura-2-AM	Fura-2-acetoxymethylester
FWER	family-wise error rate
g	gravity (centrifugal force in times gravity)
GI	gastrointestinal
Gln	glutamine
Gly	glycine
GO	gene ontology
GPI	glycosylphosphatidylinositol
GSEA	gene set enrichment analysis
GTP	guanosine-5'-triphosphate
HEK293T	human embryonic kidney cell line (293T expresses SV40 large T antigen)
HEPES	4-(2-hydroxyethyl)-1-piperazineethanesulfonic acid
hip	high persister
HIR (complex)	histone regulation (complex)
His	histidine
HIV	human immunodeficiency virus
HMA	β-hydroxymyristic acid
hMDM	human monocyte derived macrophages
HO endonuclease	**ho**mothallic switching endonuclease
HOG pathway	high-osmolarity glycerol pathway
HS	human serum
Hsp	heat shock protein
IC_{50}	half maximal inhibitory concentration
i.e.	Latin for id est (“that is to say”)

IL-6/IL-8	interleukin 6 / 8
Indel	term for **in**sertion or **del**etion of bases in the genome
kDa	kilodalton
LOH	loss of heterozygosity
LPS	lipopolysaccharide
MAMPs	microbe-associated molecular patterns
MAP(K)	mitogen-activated protein (kinase)
M-CSF	macrophage colony-stimulating factor
Mdr	Multi drug resistance
METs	macrophage extracellular traps
MIC	minimal inhibitory concentration
MOI	multiplicity of infection
mRNA	messenger ribonucleic acid
mTOR	mechanistic target of rapamycin
NAD(P)	nicotinamide adenine dinucleotide (phosphate)
NAT	nourseothricin N-acetyl transferase
NETs	neutrophil extracellular traps
nt	nucleotides
OD	optical density
ORF	open reading frame
P-body	processing body
PBS	phosphate buffered saline
PCR	polymerase chain reaction
PI	propidium iodide
PIP_2	phosphatidylinositol 4,5-bisphosphate
PKA	protein kinase A
PKC	protein kinase C
PSG	proteasome storage granule
RAM	regulation of Ace2 and morphogenesis
RNA	ribonucleic acid
ROS	reactive oxygen species
rpm	revolutions per minute
RPMI	Roswell Park Memorial Institute
SAGA complex	Spt-Ada-Gcn5-acetyltransferase complex
SAS (complex)	something about silencing (complex)
SC medium	synthetic complete medium
SD	standard deviation

SD medium	synthetic defined medium
SDS	sodium dodecyl sulfate
SGD	*Saccharomyces* Genome Database
Snf	sucrose non-fermenting
SNP	single nucleotide polymorphism
S phase	synthesis phase
spp.	species
Suppl.	supplement
$t_{1/2}$	half-maximal time
TCA cycle	tricarboxylic acid cycle
Thr	threonine
TNF-α	tumor necrosis factor α
TORC1	target of rapamycin complex 1
T6P	trehalose-6-phosphate
tRNA	transfer ribonucleic acid
t-SNARE	target synaptosome-associated protein receptor
Tyr	tyrosine
UDP	uridine-5'-diphosphate
UPR	unfolded protein response
UTR	untranslated region
vol/vol	volume/volume
WLIP	white line inducing principle
wt/vol	weight/volume
Wt / WT	wild type
yeGFP	yeast green fluorescent protein
Y(E)PD	yeast extract peptone dextrose
YNB	yeast nitrogen base

<u>*Species*</u>

A. nidulans	*Aspergillus nidulans*
C. albicans / *C. a.*	*Candida albicans*
C. auris	*Candida auris*
C. dubliniensis	*Candida dubliniensis*
C. glabrata / *C. g.*	*Candida glabrata*
C. krusei	*Candida krusei*
C. neoformans	*Cryptococcus neoformans*
C. parapsilosis	*Candida parapsilosis*

D. discoideum	*Dictyostelium discoideum*
J. agaricidamnosum	*Janthinobacterium agaricidamnosum*
L. sativum	*Lepidium sativum*
P. reactans	*Pseudomonas reactans*
P. tolaasii	*Pseudomonas tolaasii*
S. alba	*Sinapis alba*
S. cerevisiae	*Saccharomyces cerevisiae*
S. pombe	*Schizosaccharomyces pombe*

Species prefixes before gene names etc.

Ca	*Candida albicans*
Cg	*Candida glabrata*
Cp	*Candida parapsilosis*
Sc	*Saccharomyces cerevisiae*

5.8 Selbstständigkeitserklärung

Hiermit erkläre ich, dass ich die vorliegende Arbeit selbst verfasst habe und keine anderen als die angegebenen Quellen und Hilfsmittel verwendet habe. Mir ist die geltende Promotionsordnung der Fakultät für Biowissenschaften der Friedrich-Schiller-Universität Jena bekannt. Personen, die mich bei den Experimenten, der Datenanalyse und der Verfassung der Manuskripte unterstützt haben, sind als Ko-Autoren auf den entsprechenden Manuskripten verzeichnet. Personen die mich bei der Verfassung der Dissertation unterstützt haben, sind in der Danksagung der Dissertation vermerkt. Die Hilfe eines Promotionsberaters wurde nicht in Anspruch genommen. Es haben Dritte weder unmittelbar noch mittelbar geldwerte Leistungen für Arbeiten erhalten, die im Zusammenhang mit dem Inhalt der vorgelegten Dissertation stehen. Die vorliegende Arbeit wurde in gleicher oder ähnlicher Form noch bei keiner anderen Hochschule als Dissertation eingereicht und auch nicht als Prüfungsarbeit für eine staatliche oder andere wissenschaftliche Prüfung verwendet.

Jena, den 09.06.2021

Daniel Fischer

Daniel Fischer

5.9 Acknowledgements

First of all, my sincere thanks go to Prof. Bernhard Hube for giving me the great opportunity to be a part of the Microbial Pathogenicity Mechanisms Team to do my PhD, to participate in a lot of conferences and for being an excellent boss. I also want to thank the other referees of this thesis.

Moreover, special thanks go to our “iron man” or the “man whom you have to ask if you have any question (from repairing coffee machines etc. over personal advices to getting your wanted program script)” Dr. Sascha Brunke for his constant guidance, patience (especially with my usually over-long and over-detailed text drafts never coming to an end and containing the same message over and over again also it was already written plenty times before in the text draft which by following this writing style makes the text completely unreadable…) and encouragement, for all the helpful advice in the course of my PhD and for proof-reading this thesis.

Moreover, I´d like to thank all current and former members of my two offices, especially Nadja, Stephie, Daniela, Birgit and Dorothee for all scientific (technical) and non-scientific advices / discussions and their ability to separate lab conflicts from personal relationships (otherwise my sometimes absent-minded and over-motivated phases in the lab could have developed into real big problems) and Osama, Philipp, Volha and Sofía for the excellent working atmosphere and plenty of helpful advice.

Further, I would like to thank all other (former and current) MPM and MI members for being excellent colleagues and for provision of their help and advice, in and outside the lab. I cannot mention everyone separately, but want to point out some outstanding ones: first, our more or less constant “Mensa group” which was famous for entertaining the whole Mensa (especially during the time when Pim and Hasan did their best to support Nicole), but also daily ensured that I keep in connection with “normal life”. Besides the already named ones, I want to thank Melanie, Ann-Kristin, Annemarie, Karolin and Tony for great lunch times. Tony was also part of the “Washington state rainforest´s exploring group” together with Franzi, Bettina and Christine which I would like to thank for a nice and surprisingly rainless rainforest team time. However, seeing Washington´s forests burning again this year after an already hard fire season in 2017 makes me think whether it really was a good decision for the beautiful nature I´ve found to come there personally by flight (which extends of course to the meeting in Seattle I attended beforehand and the other meetings in Birmingham and Nice). This brings me to thank Osama, Bettina, Elena, Franzi, Melanie, Sarah, Mario, Sofía, Nicole and Marina, but also Prof. Ilse Jacobsen and Prof. Bernhard Hube, for all support and/or discussions at one or the other point when it comes to activism against racism and climate justice. Coming back to the lab, I want to thank our former Hiwi´s Ankido, Leon, Lucas, André and Maximilian, but

also Franzi, Volha, Osama, Philipp and our TA´s Nadja, Stephie and Daniela for making this work possible by supporting me again and again in the lab, especially with the time and energy consuming persistence screens and assays. A big thank goes also to our TA´s (including Birgit and Katja) for providing and fighting for excellent working conditions in the lab, and this again - and again - , and again – and for provision of hMDMs, for which I also want to thank the whole “macrophage crew” around Marcel, Annika and Dr. Lydia Kasper and of course all unknown blood donors.
Moreover, I want to thank Prof. Ilse Jacobsen, Dr. Lydia Kasper, Dr. Katja Graf and Dr. Silke Machata for their valuable input and all Co-Authors from the jagaricin publication for their excellent cooperation. I want to thank Dr. Jörg Linde for discussions around bioinformatical topics, Dr. Selene Mogavero for taking responsibility of a continuing project which was developed in cooperation and Fabrice Hille for his good cooperation during the time I had the pleasure to take part in his supervision.
Last but not least, I want to thank my family and non-lab friends for their love, moral support, encouragement and the little distractions from work that were greatly appreciated.